MAT-89-05

Radar Signal Enhancement for DART

Ontario

Ministry of Transportation

Research and Development Branch

Technical Report Documentation Page

Radar Signal Enhancement for DART

Author(s):	T. Chung and C. R. Carter, Communications Research Laboratory, McMaster University
Number:	MAT-89-05
Date of Publication:	June, 1989
Ministry Contact:	Dr. Tony Masliwec (416) 235-4689
Abstract:	Deck Assessment by Radar and Thermography (DART) i s a project involving the use of impulse radar for the remote sensing and evaluation of asphalt-covered bridge decks. Previous studies have shown that the DART system is capable of distinguishing between areas of good bridge deck and areas which suffer from one of several different forms of deterioration, such as, debonding, scaling and delamination. In this project, we show that both the antenna internal reflections and surface reflection can be cancelled from the reflected waveform using a subtraction process based on an adjusted fit thus enhancing system performance. This technique allows the reflection from the boundary of different layers of asphalt to be identified. Experiments on the properties of asphalt, membrane and concrete have shown that this method is quite accurate for thickness measurement of a single layer of asphalt. The new software package has been tested and checked with real data taken from three totally different bridge decks including structures with: two layers of asphalt over membrane over concrete; two layers of asphalt over concrete; and three layers of asphalt over concrete. The results are shown to agree quite closely with the actual conditions of the bridge decks.
Comments:	Final report of Research and Development Branch project 22175
Key words:	impulse radar deck assessment, structures, durability, deterioration, bridge decks
Distribution:	Internal and on request
Copyright Status:	Crown copyright © 1989 Ministry of Transportation

MAT-89-05

Radar Signal Enhancement for DART

T. Chung
Communications Research Laboratory
McMaster University

C.R. Carter
Communications Research Laboratory
McMaster University

Published by
The Research and Development Branch
Ontario Ministry of Transportation
Hon. Ed Fulton, Minister
D.G. Hobbs, Deputy Minister

Published without prejudice as to the application of the findings. Crown copyright reserved; however, this document may be reproduced for non-commercial purposes with attribution to the Ministry.

For additional copies, contact:
The Editor, Technical Publications
Room 320, Central Building
1201 Wilson Avenue
Downsview, Ontario
Canada M3M 1J8

Telephone: (416) 235-3480
CNCP Dialcom Electronic Mail: 23:MIN006
June 1989

Table of Contents

Executive Summary vii

1/ Introduction 1
1.1/ Previous Studies 1
1.2/ Objectives 1
1.3/ Overview 2

2/ Waveform Processing and Measurement Accuracy 4
2.1/ Internal Antenna Reflections 4
2.2/ Antenna Calibration 6
2.3/ Surface Waveform Cancellation 18
2.4/ Waveform Correlation 19
2.5/ Measurement Accuracy 27
2.5.1/ Reflection Coefficient Calculation 27
2.5.2 A/ Evaluation of Errors in Reflection Coefficient 29
2.5.2 B/ Waveform Distortion Due to the Lossy Property of Asphalt 35
2.5.2 C/ Waveform Variation Due to Motion of the Antenna in the Vertical Plane 35
2.5.2 D/ Distortion Produced by the Input Amplifier-Filter 35
2.5.2 E/ Precision of Analog to Digital Converter 39
2.5.2 F/ Intersample Spacing Errors 39
2.5.2 G/ Waveform Corruption Due to Receiver Noise 41
2.5.2 H/ Overall Effect on the Calculation of Reflection Coefficient 42
2.5.3/ Calculation of Dielectric Constant 43
2.5.4/ Calculation of Asphalt Thickness 45
2.5.5/ Averaging Per Metre, Per Line and Per Deck 47
2.6/ Summary of Results 47

3/ Properties of Asphalt, Membrane and Concrete 49
3.1/ Asphalt 49
3.2/ Membrane 55
3.3/ Concrete 59
3.3.1/ Concrete With No Rebars 60
3.3.2/ Single Layer of Rebars 60
3.3.3/ Two Layers of Rebars 71
3.4/ Summary of Results 78

4/ Cluster Analysis 80

5/ Field Evaluation 86
5.1/ Processing of Ninth Line Data 86
5.1.1/ Computer Analysis 86
5.1.2/ Asphalt Thickness 90
5.1.3/ Concrete Over Reinforcement 91
5.1.4/ Bridge Deck Conditions 98
5.1.5/ Summary 98
5.2/ Processing of Winston Churchill Data 108
5.2.1/ Computer Analysis 108
5.2.2/ Verifications of Computer Results 116
5.2.3/ Computer Results Versus Site Observations 120
5.2.4/ Summary 126
5.3/ Processing of Bloor Street Via Duct Data 126

Table of Contents
(continued)

5.3.1/ Core Sample 126
5.3.2/ Waveforms Comparison 5.3.3/
Data Processing Speed 136
5.3.4/ Data Analysis of Eastbound Deck 136
5.3.5/ Data Analysis of Westbound Deck 154
5.3.6/ Summary 172

6/ Conclusions and Recommendations for Further Research 188
6.1/ Conclusions 188
6.2/ Recommendations for Further Research 189
7/ References 191
Appendix A. The Data Acquisition System for the DART System using Impulse Radar 193
A.1/ System Configuration 195
A.2/ General Descriptions of the Data Acquisition System 195
A.2.1/ The Tape Recorder 195
A.2.2/ The TECMAR Interface System 197
A.2.3/ The Microcomputer System 198

Appendix B. Details of Interfaces for Dart 201
B.1/ Fifth Wheel Filter Interface 203
B.2/ Fifth Wheel Counter Circuit Interface 203
B.3/ Input Filter for High Video Interface 203
B.4/ Tape Recorder/Computer Control Interface 203

Appendix C. The Signal Processing Software 207
C.1/ General Descriptions of the Software Algorithms 209
C.2/ MTC87 Package 209
C.2.1/ Subroutine FPADC 209
C.2.2/ Subroutine FPVOLT 211
C.2.3/ Subroutine RESDUE 213
C.2.4/ Subroutine DIGSIG 216
C.2.5/ Subroutine SIGPRO 218
C.2.6/ Subroutine CONDIT 220
C.2.7/ Subroutine AVETHK 223
C.2.8/ Subroutine HIGSAM 223
C.2.9/ Subroutine TABPRN 224
C.3/ DECK87 Package 224

Appendix D. Cluster Analysis Results 229
D.1/ Ninth Line Data 231
D.2/ Winston Churchill Data 239
D.3/ Bloor Viaduct Data 246

Executive Summary

Background

Previous studies have shown that the Deck Assessment by Radar and Thermography system (DART) is capable of distinguishing between areas of good bridge deck and areas which suffer from one of several different forms of deterioration. Supported by theoretical analysis, it has been found that the parameters can be identified which characterize the different fault conditions.

Of considerable importance in making the measurements is the quality of the transmitted and reflected signals. Recently it has been shown that internal reflections in the antenna system can produce significant error in the processing of the radar waveforms. In addition, the processing of exposed concrete is significantly degraded by the strong surface reflection which occurs at the air-concrete interface. This effectively prevents waveform analysis and detection of cracks just below the surface of the concrete.

Objectives

The objectives of the present project are to develop new software packages, compatible with existing software, that will:

a) cancel the internal antenna reflections from the total reflected signal;

b) cancel the surface reflections from the total reflected signal;

c) be capable of testing the correlation technique of matched filtering for impulse detection;

d) identify variations in the amplitude and location of waveform peaks (employing cluster analysis or statistical variation of waveforms) and use this information to further improve the detection of deterioration;

e) evaluate end result specifications such as:

i) concrete thickness;

ii) asphalt thickness;

iii) cover over reinforcement.

f) detect deterioration under pavements (voids).

g) assess the precision and accuracy of the system.

h) prepare full documentation on system performance and operation.

Summary of Results

It has been shown that internal antenna reflections can be cancelled from the reflected waveform using a subtraction process based on an adjusted fit. However, there remains a residue which is one order of magnitude less than the original internal reflected signal.

Surface reflection cancellation has also been successfully accomplished using the same technique as employed for internal reflection cancellation. This technique now allows the reflection from the boundary of different layers of asphalt to be identified.

Waveform correlation has been tested but provides no new information; thus, no further study in this area is warranted.

A study of measurement accuracy shows that the system is capable of determining average asphalt thickness over one metre to within + 5 mm, assuming an asphalt thickness of 80 to 100 mm. For a deck, averaging reduces this number to less than 1 mm.

Experiments on the properties of asphalt, membrane and concrete have shown that the surface reflection technique presently employed with internal antenna reflections removed is quite accurate for thickness measurement of a single layer of asphalt. The measurements were checked by comparing the propagation time through the asphalt sample and the agreement in dielectric constant calculation was found to be within + 5%.

For the membrane, the measurement was not quite as precise due to what is thought to be the smaller size of the sample. The results do indicate that membrane has a dielectric constant about

half that of asphalt which may be useful in helping to identify the boundary with concrete. It is suggested that further work take place to more accurately categorize the material.

Measurements on the dielectric constant of concrete were quite revealing. It was found that the rebars imbedded in concrete reduce the dielectric constant value calculated from surface reflection meaurements. Further study in this area may be required.

Cluster analysis is useful in providing an indication of the variation in the location of peaks in the reflected waveform. The interpretation of these peaks requires further study in order to gain insight into relating the different reflecting surfaces i.e. each layer of asphalt, membrane, concrete and rebars, to the peaks observed. Developing a strategy based on known properties of deck construction may be useful. For example, information concerning the maximum probable change of asphalt thickness per metre along deck and across deck could be incorporated into the software in order to reduce the problems of absurd interpretations. Such inputs would also be useful for the membrane layer and the cover over reinforcement.

Field Evaluations

The results of field evaluations are provided for three totally different bridge decks. The decks analysed include: 1) Ninth Line bridge deck in Oakville, which is a new deck in excellent condition having two layers of asphalt over rubber membrane and a well defined membrane concrete interface; 2) Winston Churchill overpass across Highway 401 west of Pearson International Airport, which is a deck in poor condition with two layers of asphalt and little or no membrane material; and 3) Bloor Street Viaduct in Toronto, which is a deck having some damage with three layers of asphalt.

The Ninth Line bridge deck was found to be in good condition as expected with virtually no damage. This result is important since it provides an indication of the false alarm rate of the software package.

The Winston Churchill bridge deck was found to be in poor condition with a considerable amount of delamination. Close examination of the actual waveforms confirms this interpretation.

The Bloor Street Via Duct posed a new problem not previously encountered. The deck has three layers of asphalt each with a considerably different dielectric constant as witnessed by the strong

reflections from the different boundaries. One such reflection was unfortunately interpreted by the software as being an indication of delamination since the particular waveform was almost identical to the shape produced by serious delamination.

As a result, it is strongly recommended that at least one core sample should be taken from every bridge deck that is surveyed in order to ensure that the concrete surface is properly identified. Once identified, the software package provided a meaningful evaluation. In this case, the deck was found to be approximately 17% delaminated. A useful technique was also developed to further identify the concrete surface that relies on the reflections from any metal plates which might exist under the asphalt. However, there is really no substitute for a core sample.

1/ Introduction

1.1/ Previous Studies

Previous studies [1-6] have shown that the Deck Assessment by Radar and Thermography system (DART) is capable of distinguishing between areas of good bridge deck and areas which suffer from one of several different forms of deterioration. Supported by theoretical analysis, it has been found that the parameters can be identified which characterize the different fault conditions [6].

Of considerable importance in making the measurements is the quality of the transmitted and reflected signals. Recently it has been shown that internal reflections in the antenna system can produce significant error in the processing of the radar waveforms. In addition, with the present radar system (1 ns transmitter pulse) the processing of exposed concrete is significantly degraded by the strong surface reflection which occurs at the air-concrete interface. This effectively prevents waveform analysis and detection of cracks just below the surface of the concrete.

1.2/ Objectives

The project objectives are to develop new software packages, compatible with existing software, that will:

a) cancel the internal antenna reflections from the total reflected signal;

b) cancel the surface reflections from the total reflected signal;

c) be capable of testing the correlation technique of matched filtering for impulse detection;

d) identify variations in the amplitude and location of waveform peaks (employing cluster analysis or statistical variation of waveforms) and use this information to further improve the detection of deterioration;

e) evaluate end result specifications such as:

   i) concrete thickness;
   ii) asphalt thickness;
   iii) cover over reinforcement;

f) detect deterioration under pavements (voids);

g) assess the precision and accuracy of the system;

h) prepare full documentation on system performance and operation.

1.3/ Overview

In Section 2, the method for the removal of antenna internal reflections is discussed. It is shown that to a high degree of accuracy, these reflections remain constant provided that the orientation of the antenna to the van is not changed significantly. Further, it is shown that the surface reflection from different materials can be canceled leaving only a second order residue. This feature is useful in analysing bridge decks with thin asphalt overlays. Unfortunately, it is found that the method of waveform correlation is not effective in improving the performance of the system. Finally, a study of all the different forms of error that may enter the processing system are examined. The final results are provided in parametric form.

Section 3 examines the properties of asphalt, membrane and concrete. It is found that the dielectric constant of asphalt can be accurately measured from surface reflection measurements provided that the antenna internal reflections are first eliminated. The membrane is examined to determine its dielectric constant. The measurement of the properties of concrete was also successful; however, it is seen that rebars effect the surface reflection and have an influence on the measurement of dielectric constant. It is suggested that the determination of dielectric constant of concrete be studied in order to further bound the range of values.

Section 4 deals with sensitivity analysis using cluster analysis based on the histogram. It it shown that when peaks occur in the waveforms, they often cluster about a central point. However, certain exceptions also take place notably the cover over reinforcement being a case in point.

Section 5 provides the details of surveys for three different bridge decks namely: Ninth Line in Oakville, Winston Churchill west of Pearson International Airport and Bloor Street Via Duct in Toronto using the new software package containing the concepts developed in Sections 2, 3 and 4. It is seen that the new package does indeed provide improved performance over the previously developed software package. However, several problem areas are identified concerning the number of asphalt layers on a given bridge deck, the determination of dielectric constant for each of

these layers in order to determine overall asphalt thickness and the determination of dielectric constant for both membrane and concrete. In particular, detection of the concrete surface is identified as a problem requiring further study.

Section 6 provides conclusions and recommendations for further research and references are provided in Section 7.

2/ Waveform Processing and Measurement Accuracy

2.1/ Internal Antenna Reflections

It is important to receive true reflected waveforms for bridge deck assessment using impulse radar since the accuracy in measurement is affected by the quality of the received signals. It is observed that internal reflections in the antenna system produce significant error in the processing of the radar waveforms. The origin of this interference is due to complications in the design of the antenna system.

Figure 2.1 illustrates a transmitted radar waveform. The signal is obtained by positioning the radar antenna directly over a thin metal plate placed on the asphalt surface. We note that the entire waveform has a duration of 20 ms. Internal antenna reflections dominate the first 8 ms of the signal. The peak at point A represents the surface reflection from the metal plate and is also used to calibrate the system for reflection from the asphalt surface. However, in order to obtain a correct measurement of the surface reflection, we have to consider that this portion of the waveform is corrupted by the internal antenna reflections. In particular, for an ideal transmitted radar signal, both negative peaks at point P and Q are expected to have comparable magnitude. The waveform in Fig. 2.1 indicates that the difference between the two peaks exceeds 2 volts. It is, therefore, proposed that the internal antenna reflections be removed from the total reflected signal by means of signal processing.

This can be accomplished by recording the signal with the antenna at a 'suitable' height over a metal plate and feeding this signal into the computer. This recorded signal waveform is used for calibration since it contains only the internal antenna reflections.

One method to record the waveform containing only the internal reflections is to locate the MTO van on a ramp raising the antenna well above ground level. The measurement was conducted in mid-May 1987 at the MTO Brampton test site (near the intersection of Highways 10 and 401). The ramp was built such that the vertical height of the antenna over ground level exceeded 1.5 m. A metal plate was then adjusted to different heights above ground level giving different distances between the end of the antenna and the metal plate. Distances selected from antenna end to metal plate surface were: 1.45 m, 1.33 m, 1.20 m, 1.08 m, 0.94 m, 0.79 m, 0.66 m, 0.54 m, 0.42 m, 0.35 m, 0.28 m, 0.21 m, 0.14 m, 0.10 m, 7 cm, 2 cm and 1 cm. Samples of these reflected waveforms are given in Figs. 2.2, 2.3 and 2.4 for distances of antenna end to metal plate of 7 cm, 0.54 m and 1.45 m, respectively.

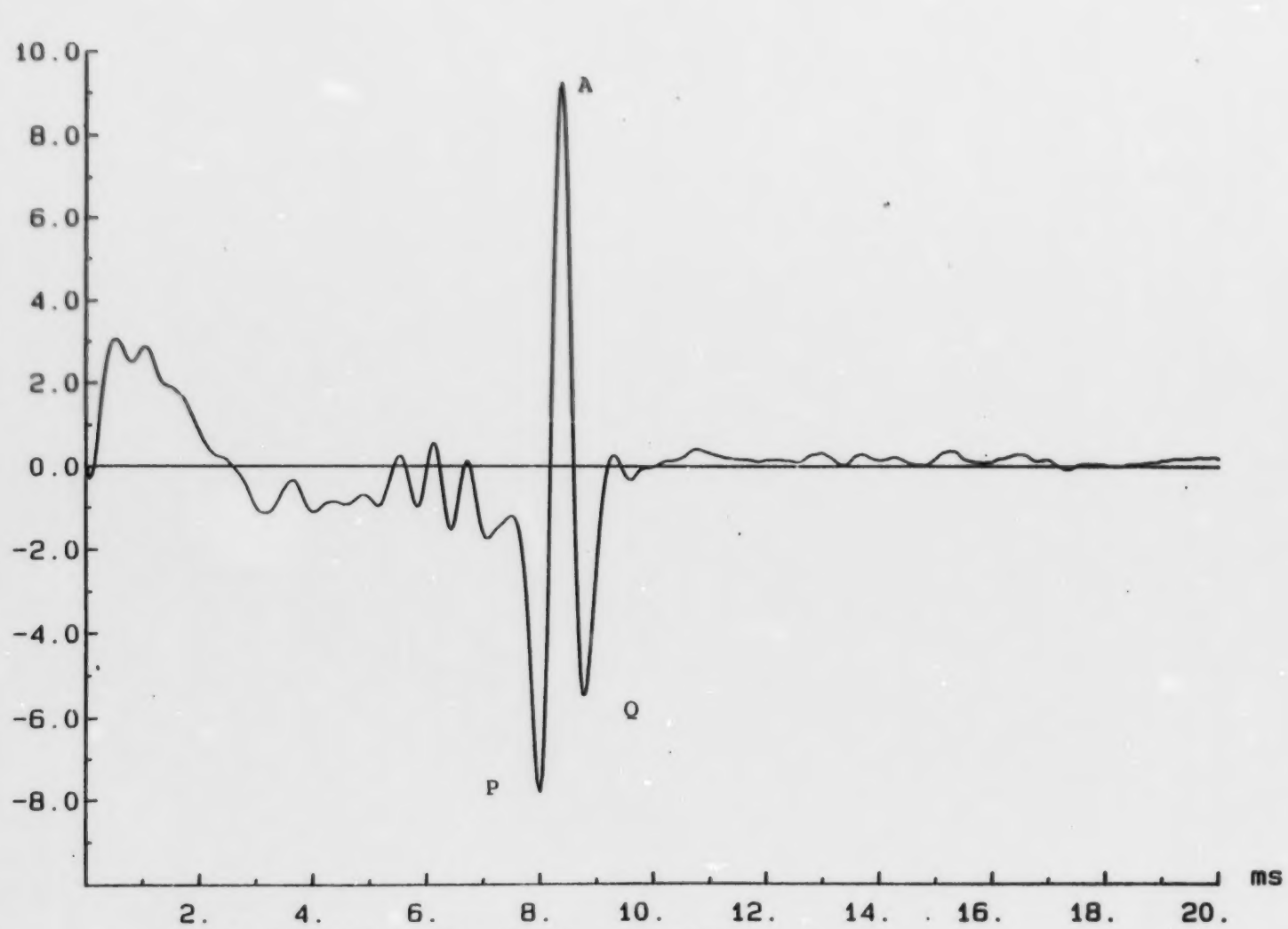

Fig. 2.1: Transmitted radar waveform.

At 7 cm, the reflected waveform is similar to the result obtained in Fig. 2.1. From the waveforms at 0.54 m and 1.45 m, we have two observations: (1) The surface reflection occurs at a later time along the waveform and the magnitude is reduced as the metal plate is moved away from the antenna. This is because the strength of the antenna system attenuates as the distance increases. (2) There is an exponentially shaped curve between the 8 ms and 10 ms duration on the waveform. This non-linearity affects the waveform measurement, since the surface reflection and reflection from asphalt-concrete interface frequently occur in this interval. This partially accounts for the unequal and changing magnitudes of peaks P and Q in Fig. 2.1. (A second but significant effect is the presence of the van itself. It has been found that the relative strength of the two negative peaks change when the antenna is mounted on a wooden base removed from metal object. Of course once mounted, the effect remains constant).

In practice, our investigations do not exceed 1 m depth in free space. Therefore, for our purpose Fig. 2.4 can be used as a representation of the internal antenna reflections of the system. Also, a duration of 16 ms waveform is sufficient for the signal processing. We provide this 16 ms view of the internal reflections waveform in Fig. 2.5.

One remark about the signature of the waveform given in Fig. 2.5 is that it is unique. If the radar antenna is not mounted to the MTO van or if the antenna is positioned in a different orientation, the signature of the internal reflections will not be the same. For this report, we employ the calibration depicted by Fig. 2.5.

2.2/ Antenna Calibration

A true reflected signal can now be obtained by simply removing the internal antenna reflections from the actual reflected waveform. The internal antenna reflection waveform, i(t), is stored in a data file (or memory) in the computer. The received signal, s(t), is fed into the computer and a first order subtraction is performed with the stored record of internal reflections yielding the true waveform or

$$r(t) = s(t) - i(t) \tag{2.1}$$

This procedure is quite simple, since both waveforms are already-time-aligned prior to being fed the computer by using the radar sync signal.

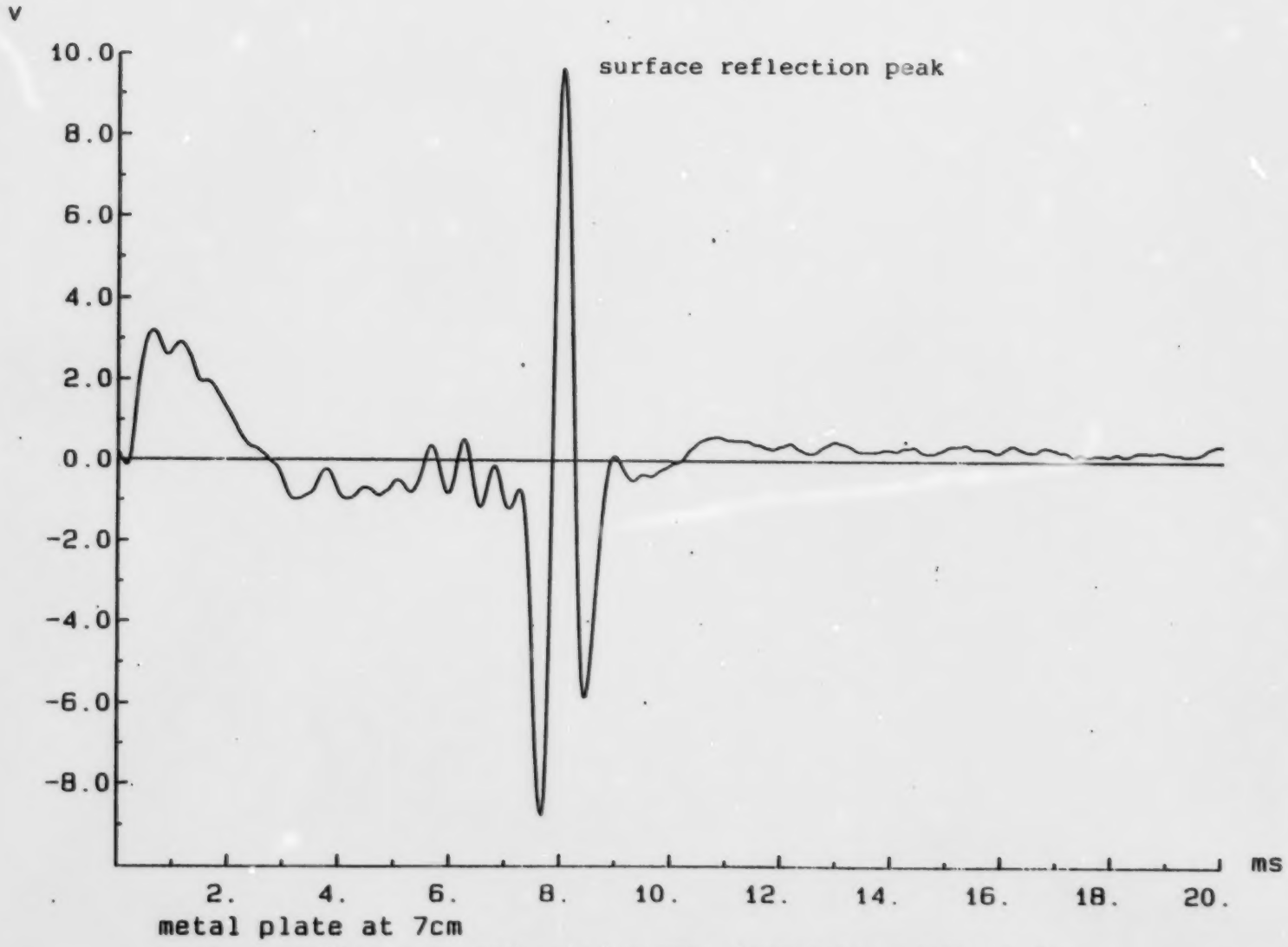

Fig. 2.2: Reflected signal from metal plate at 7cm.

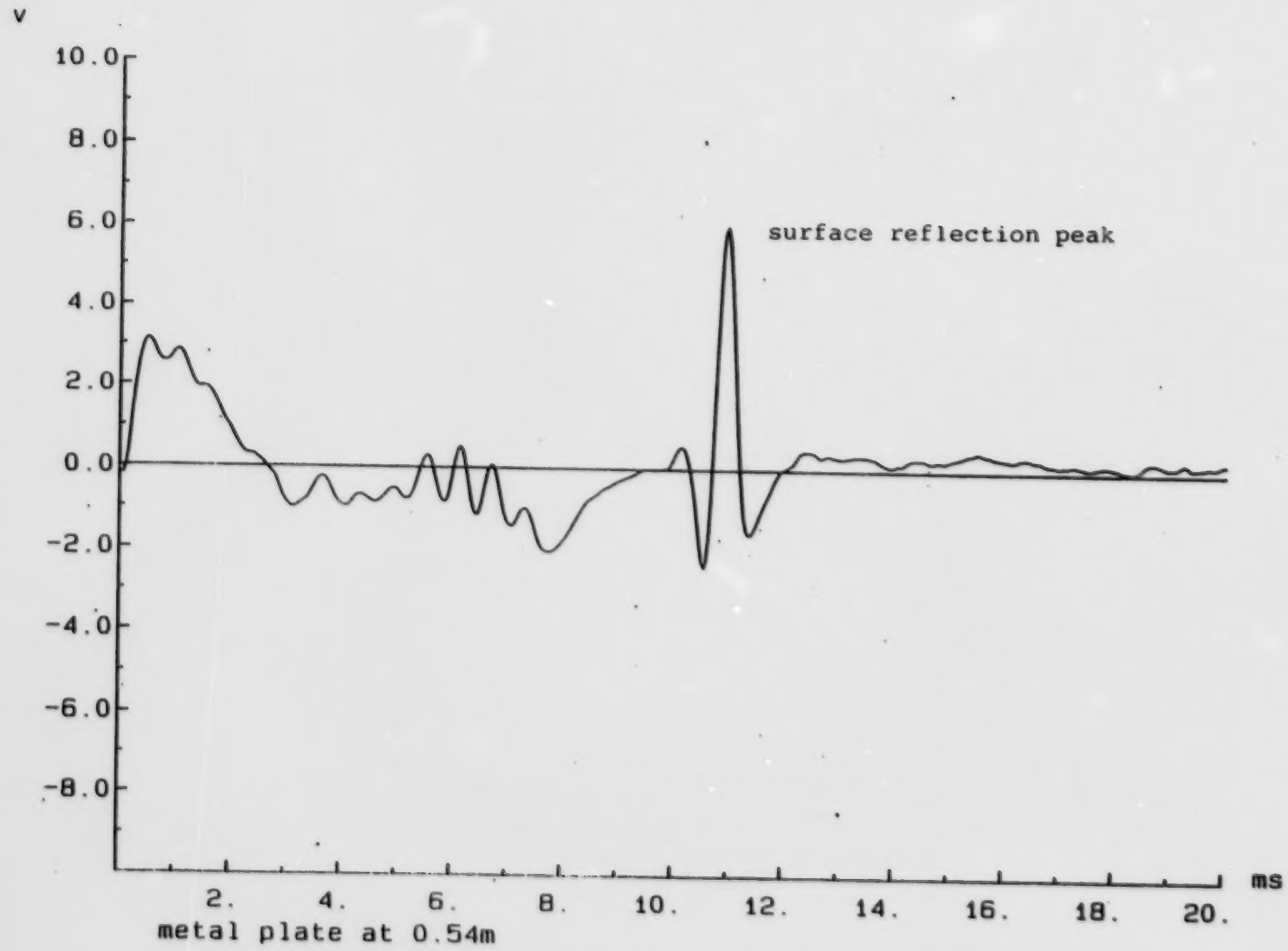

Fig. 2.3: Reflected signal from metal plate at 0.54m.

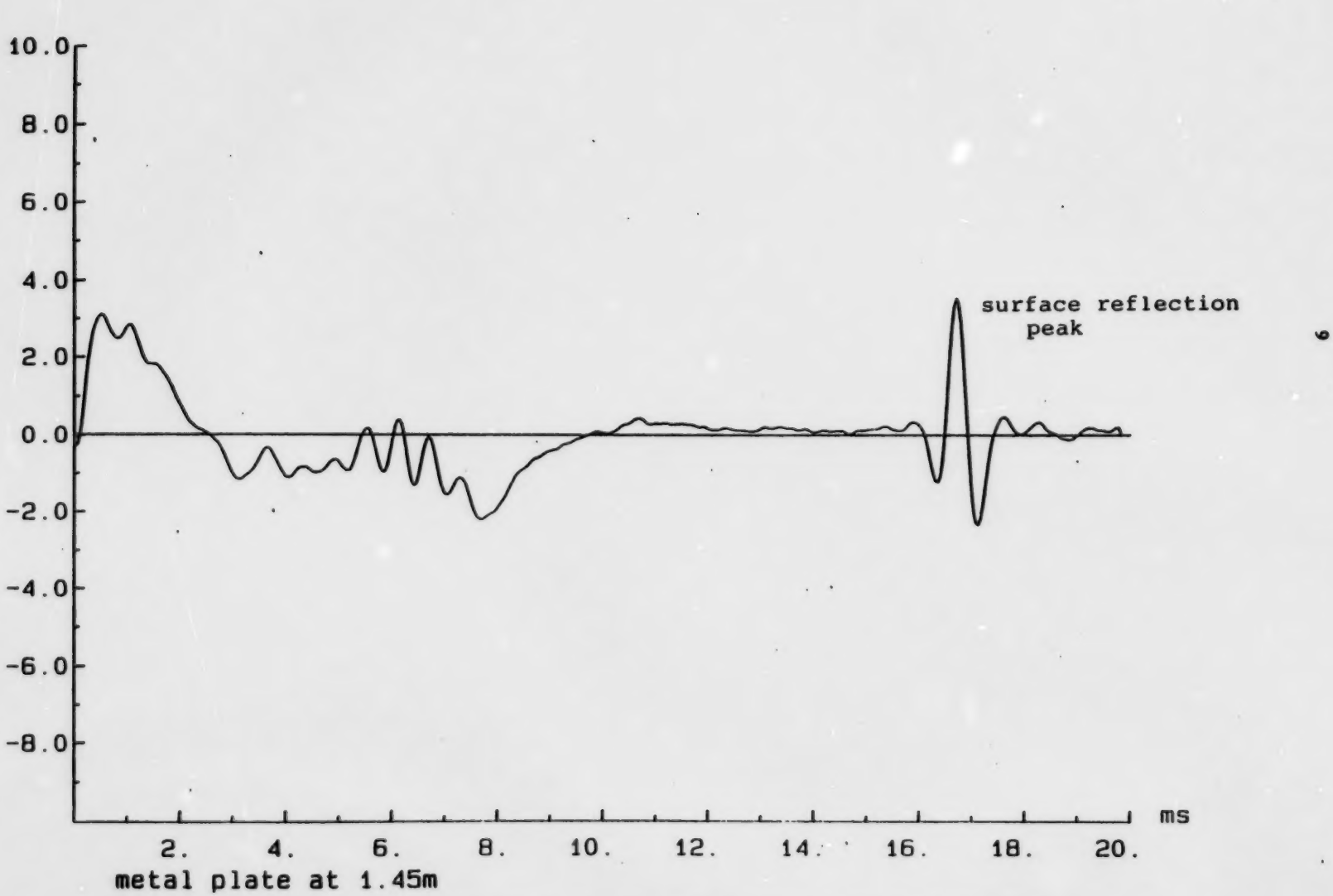

Fig. 2.4: Reflected signal from metal plate at 1.45m.

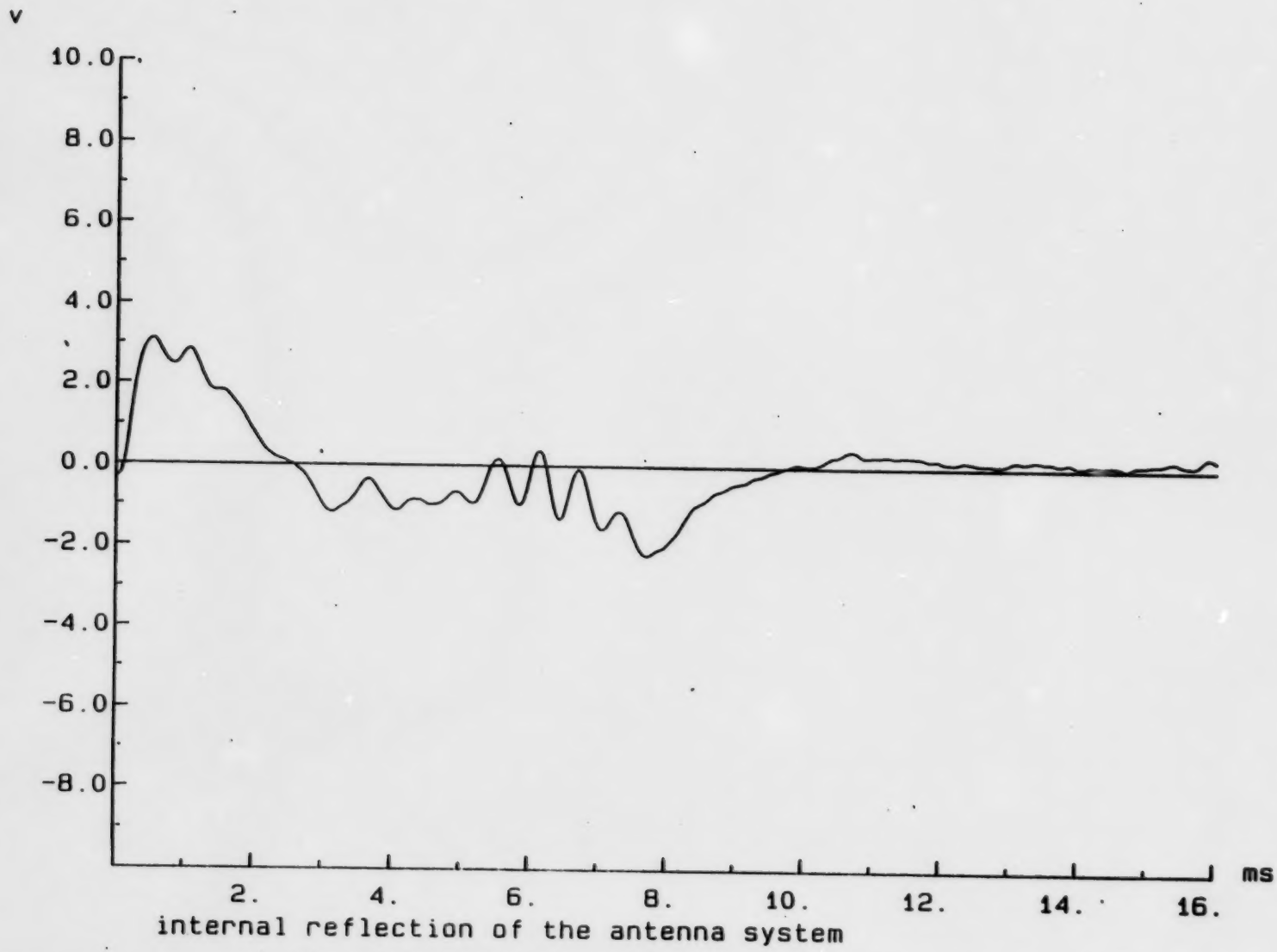

Fig. 2.5: Radar signature of internal antenna reflections.

In Fig. 2.6, the waveforms from both the internal antenna reflections and metal plate are provided on the same plot. Our intention is to minimize the amount of error generated by the internal reflections. Experiments show that improved results are obtained if both signals are aligned at point R instead of the radar sync signal.

Since the recorded signal is digitized into the computer, there are sampling time inaccuracies involved. Therefore, a direct subtraction of both waveforms does not necessary provide the true reflected waveform. However, this discrepancy can be reduced by performing the subtraction over a three sample set: (1) Exact case - no shift, (2) Left shift case- shift one sample of the received signal to the left with respect to point R, and (3) Right shift case - shift one sample of the received signal to the right with respect to point R. The magnitude of the residue is computed from point R to S and compared for the three cases. Waveform subtraction, using eq. (2.1), is then performed by selecting the case which has the minimum residue.

In Figs. 2.7, 2.8 and 2.9, residue waveforms are plotted for the waveform subtraction of Fig. 2.6 following the described procedures. The time reference of the residue signals has been adjusted for the convenience of signal processing. From Fig. 2.9 the portion between point R and S is noted to be relatively more 'quiet' than the waveforms obtained in Figs. 2.7 and 2.8. The magnitude of the three residue waveforms (between point R and S) is computed: (1) Exact case = 19.30 V (2) Left shift case = 28.97 V and (3) Right shift case = 11.97 V The measurement suggests that the 'right shift' case produces the best waveform of true reflected signal of the metal plate. It is recommended that this procedure of waveform subtraction should be carried out for each input waveform during signal processing.

The same procedure is applied to the waveform measurement of signal reflected from asphalt overlay surface. In Fig. 2.10, the received signal and the internal reflections waveform are given on the same plot. Only the portion after point R is plotted with the resulting subtraction given in Fig. 2.11. The magnitudes of the three comparisons are (1) Exact case = 6.99 V, (2) Left shift case = 16.41 V and (3) Right shift case = 12.49 V. In this case, residue waveform using the 'exact case' is selected. It is worth noting that the characteristic `W' [6] between point C and D is now more prominent than was previously obtained.

Three observations, from the residue waveforms of Fig. 2.7 to 2.9 and Fig. 2.11, can be reported: (1) The portion after point S of the three residue waveforms seem to have the same signature. Therefore, the comparison technique is robust. (2) The difference in magnitude between the two negative peaks at point P and Q, in Fig. 2.9 and 2.11, is reduced to about 1 volt and (3) the

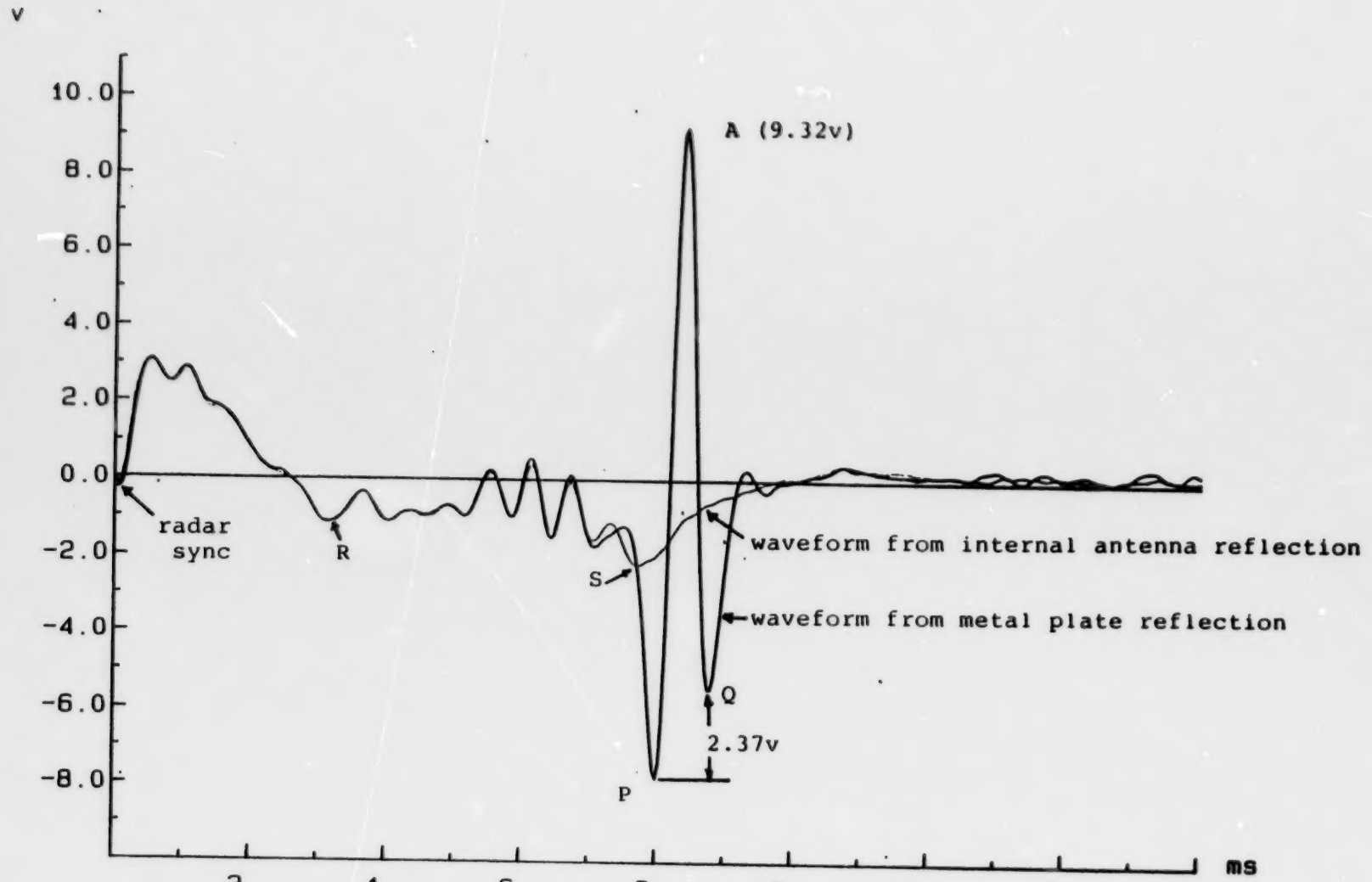

Fig. 2.6: Superimposed waveforms from internal antenna reflection and metal plate reflection.

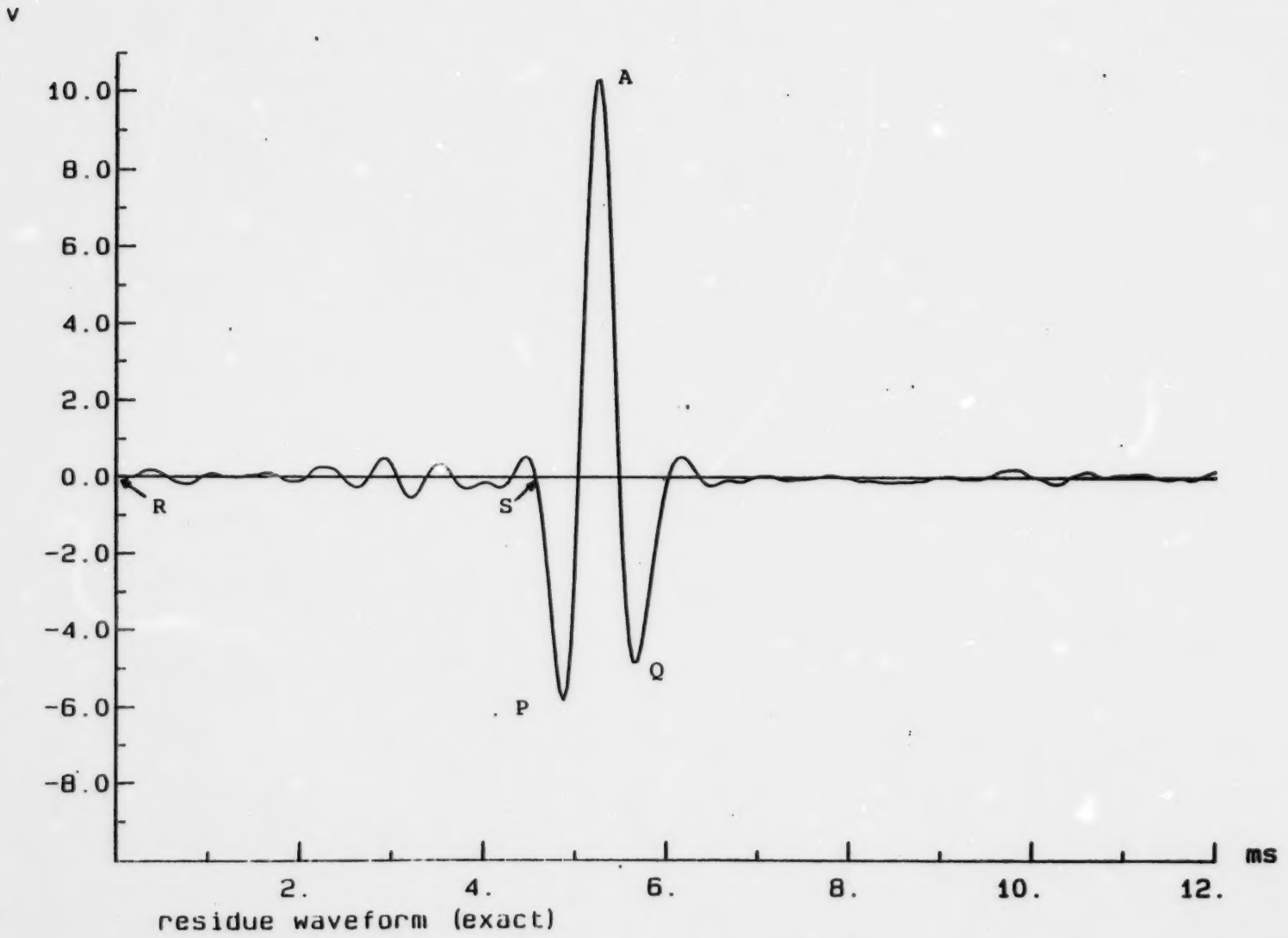

Fig. 2.7: Residue waveform from EXACT case

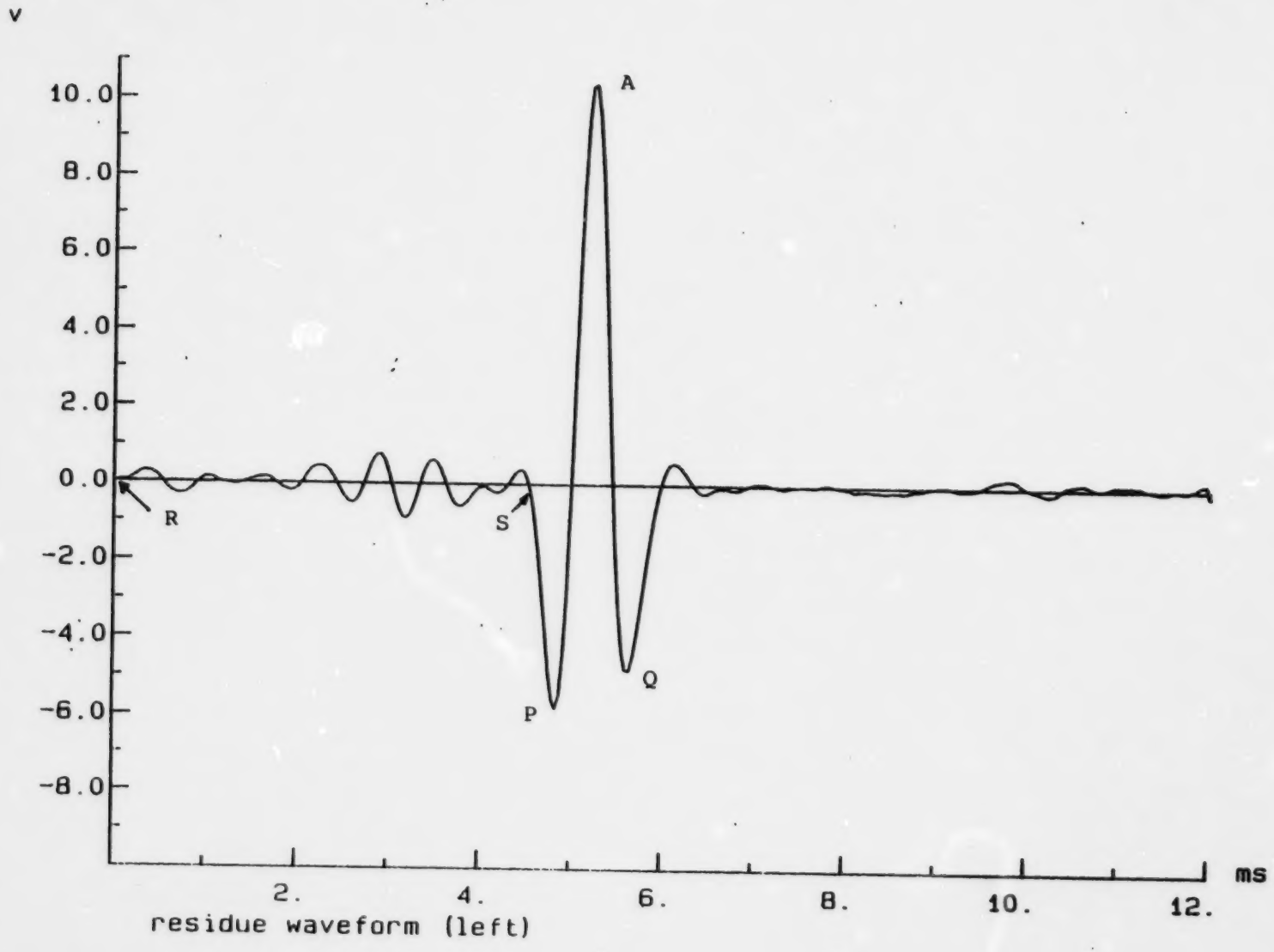

Fig. 2.8: Residue waveform from LEFT SHIFT case.

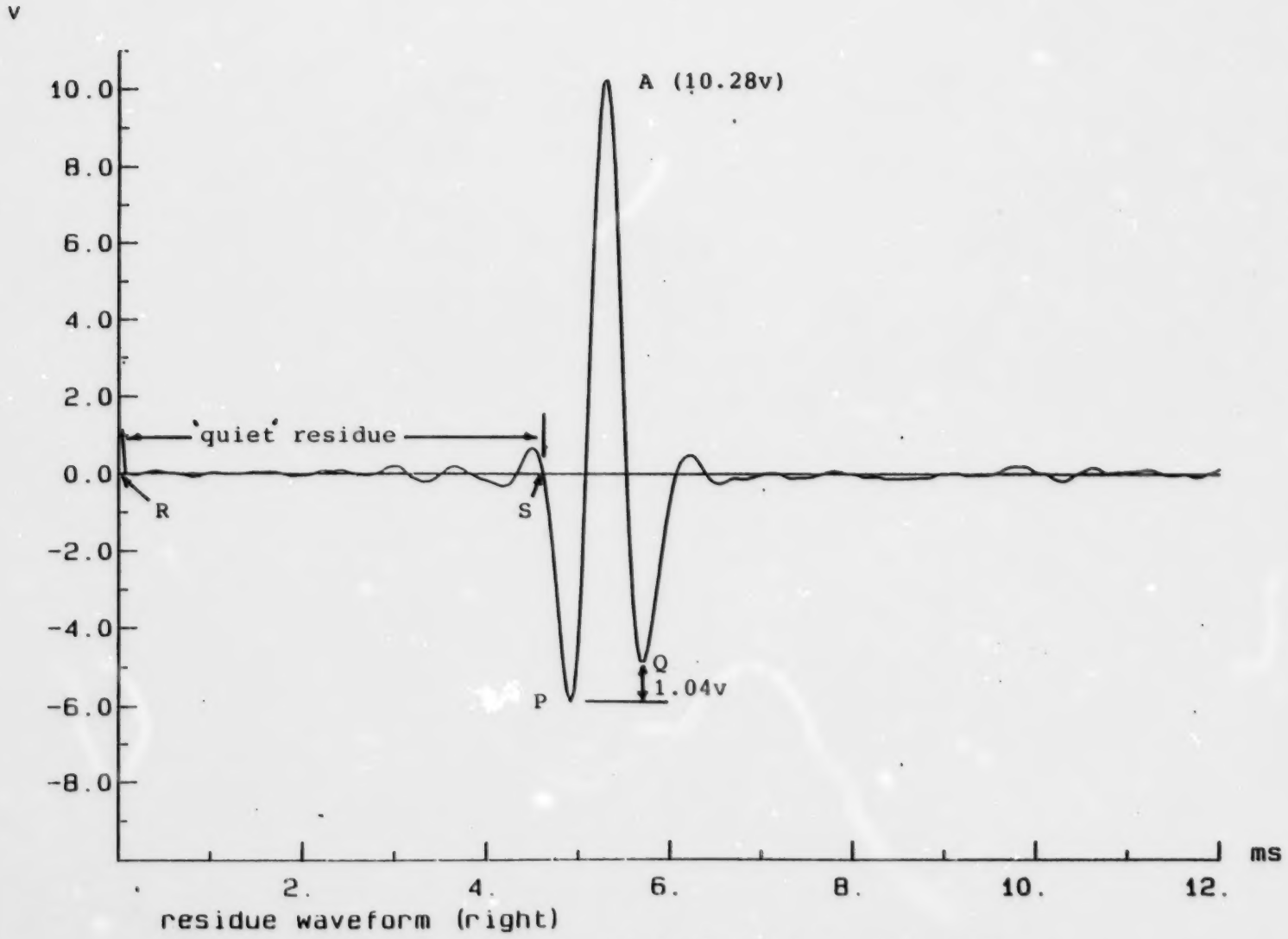

Fig. 2.9: Residue waveform from RIGHT SHIFT case.

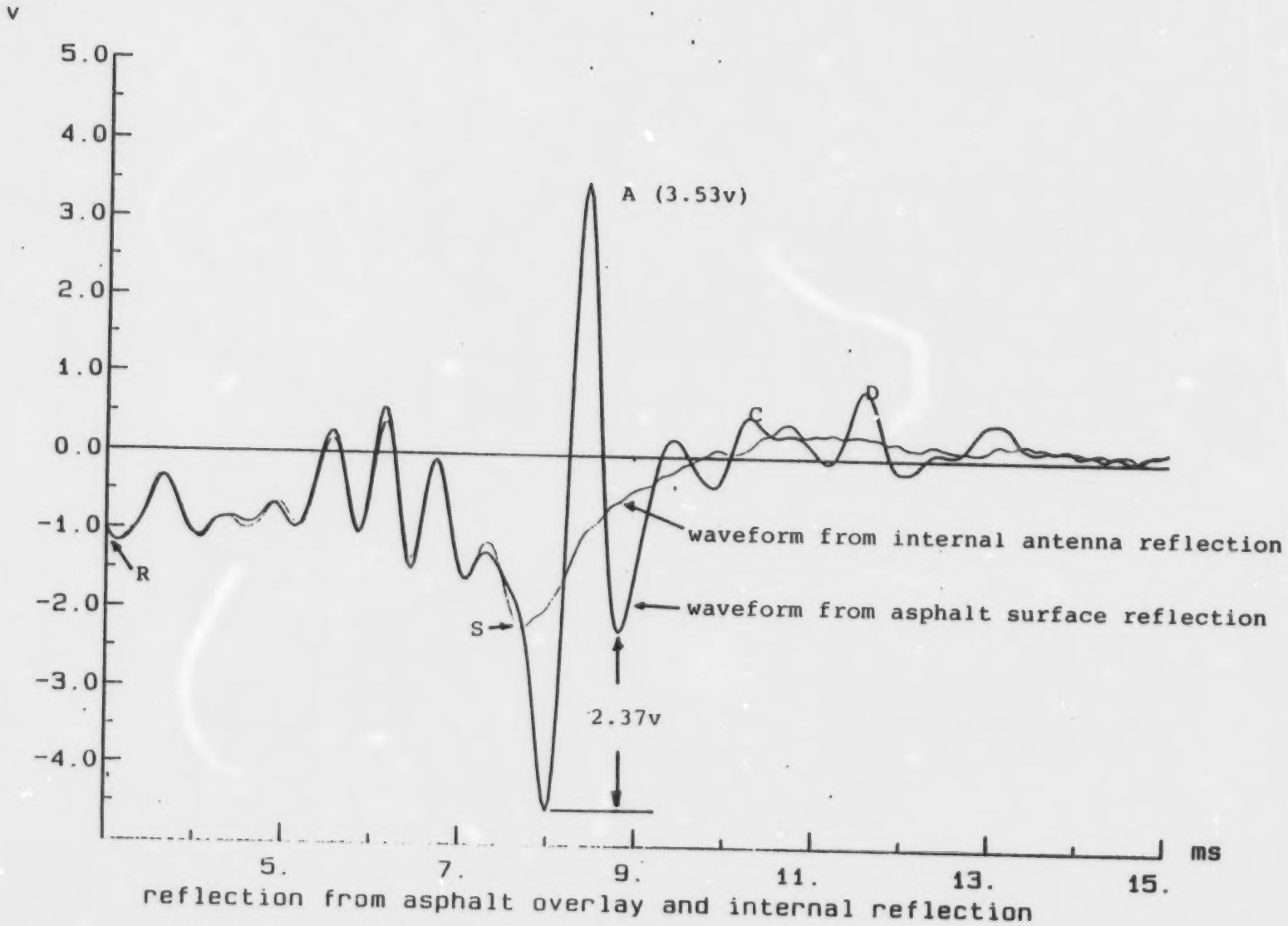

Fig. 2.10: Superimposed waveforms from internal antenna reflection and asphalt surface reflection.

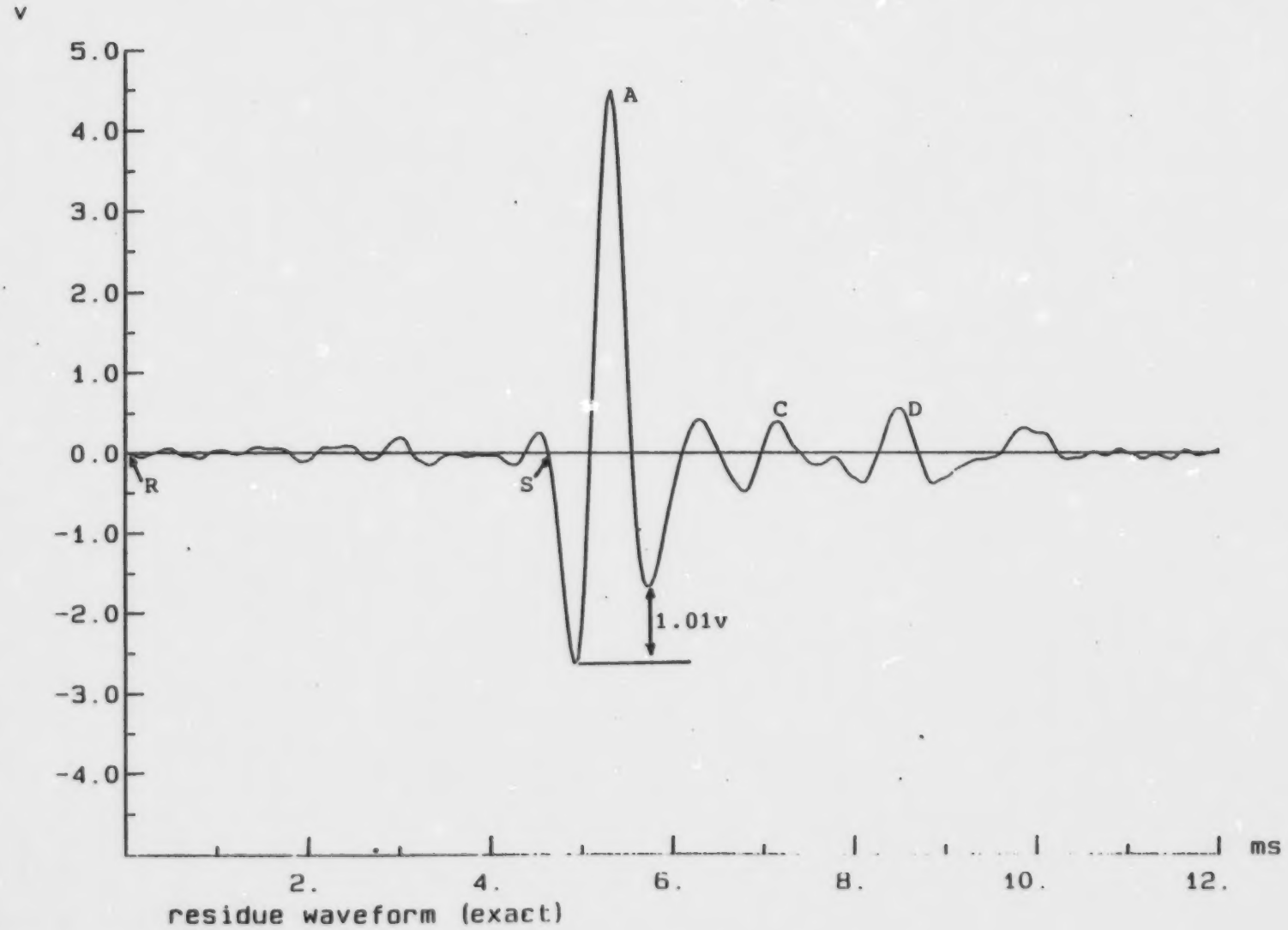

Fig. 2.11: Residue waveform from EXACT case

magnitude of the surface reflection peak at point A is increased by 10 percent in Fig. 2.9 relative to Fig. 2.6 and 20 percent in Fig. 2.11 relative to Fig. 2.10. The resulting waveform is seen to much more closely related to the expected reflected waveform than the actual received signal.

2.3/ Surface Waveform Cancellation

It is important to relate the actual structure of the bridge deck with the radar waveforms being received. The two most common features considered include: (1) Detection and identification of different layers of asphalt and (2) Detection and identification of the waterproofing membrane.

It has been reported that most bridge decks are covered by at least two layers of asphalt over the concrete surface. The different layers of asphalt do not have the same mix design. As a result, separate signal reflections are expected from the interface between the layers of asphalt. The waterproofing membrane, which is mostly a rubber material, is located between the asphalt and the concrete layers. Consequently, this added feature causes certain reflections as radar signals propagate through the asphalt-membrane-concrete interfacing layers.

We have seen from the previous results that the surface reflection occurring at the air-asphalt surface interface is very significant. It is of considerable concern that this strong positive peak may hamper reflections from the different asphalt layers and the asphalt-membrane-concrete interfaces. Using the similar method as outlined in Section 2.2, the surface reflection of each waveform can be removed by means of waveform subtraction. This then leaves a residue signal with all remaining information.

The steps in carrying out this procedure are (1) Record the surface reflection from the metal plate and subtract the internal antenna reflections by following the technique described in Section 2.2. This gives the true metal plate waveform. (2) Repeat step (1) for an actual reflected waveform. This provides the true reflected waveform. (3) The true metal plate waveform is 'scaled' to that of the true reflected waveform. The scaling factor is the ratio of the height of the surface reflection peak of the true reflected waveform to the true metal plate waveform. (4) Using the 'exact', 'right shift' and 'left shift' method with respect to the surface reflection peak, subtract both waveforms entirely and select the minimum residue.

The residue signal obtained in Fig. 2.11 is a true reflected waveform recorded from a bridge deck located at Ninth Line, Oakville. The deck has two layers of asphalt and a waterproofing membrane. Waveform analysis is performed on this signal employing the above procedures. In Fig. 2.12, the true reflected waveform and the true metal plate scaled waveform are given. The residue signal is

presented in Fig. 2.13. We note that the subtraction procedure is quite successful. The surface reflection peak is completely eliminated. The residue signal provides an extra positive peak at point Q', which has never been detected in any of the previous cases. This peak corresponds to the reflections at the interface between the first and second layer of asphalt. By knowing the speed of propagation for the transmitted signal into asphalt and calculating the time delay between point A' and Q', the thickness of the first layer of asphalt can be measured. The velocity of propagation in each material is defined by the velocity of light divided by the square root of the dielectric constant of the material. This issue will be discussed later in detail.

It has been found that the value of dielectric constant of the waterproofing membrane is close to that of rubber but it is less than that of asphalt. It is expected that the reflection at the interface between the second layer of asphalt and the membrane is a negative going peak. This is indicated by point M'. The thickness of the second layer of asphalt can be obtained by measuring the time separation between peak Q' and M' with the known value of dielectric constant of asphalt. The positive peak at point N' is due to the sum of the transient of both peaks at Q' and M'. The

membrane-concrete interface reflection is at peak C' and the rebar reflection is at peak D'. The thickness of the waterproofing membrane and the cover over reinforcement can then be identified respectively.

The same analysis is applied to a waveform which is recorded from Bloor Street Via Duct, Toronto. A photograph of a core sample obtained from the bridge deck is given in Fig. 2.14. This deck has three different layers of asphalt. Waveforms of the true reflected signal and the true metal plate reflection are plotted in Fig. 2.15. The reflections from each asphalt interfacing layer are identified and indicated from the residue signal depicted in Fig. 2.16. The thickness measurement of each layer of asphalt can then be evaluated.

2.4/ Waveform Correlation

The correlation process is a classical technique in the detection of radar signal in noise [7]. A correlation function measures the coherence between two signals. If the two waveforms are not equal, the process is called the cross-correlation. Otherwise, it is known as the autocorrelation.

In our study, it is required to detect signal reflections at the boundaries between asphalt-membrane-concrete surfaces. In order to measure signal reflections, the received signal is checked for the degree of similarity with the transmitted signal. This is actually a cross-correlation process. In Fig. 2.17, the true metal plate waveform (from Fig. 2.9) and the true reflected signal (from Fig. 2.11)

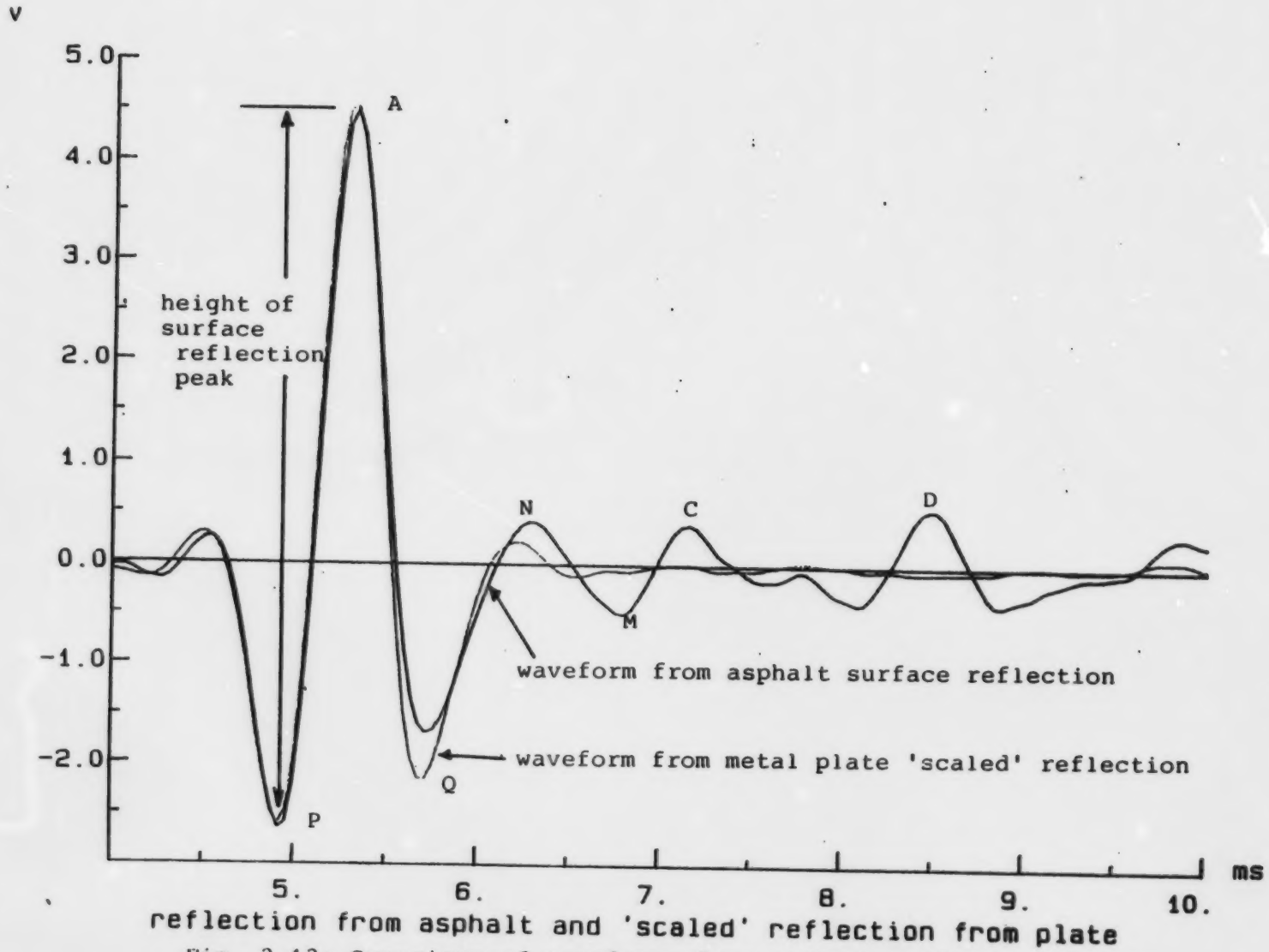

Fig. 2.12: Superimposed waveforms from asphalt surface reflection and metal plate 'scaled' reflection.

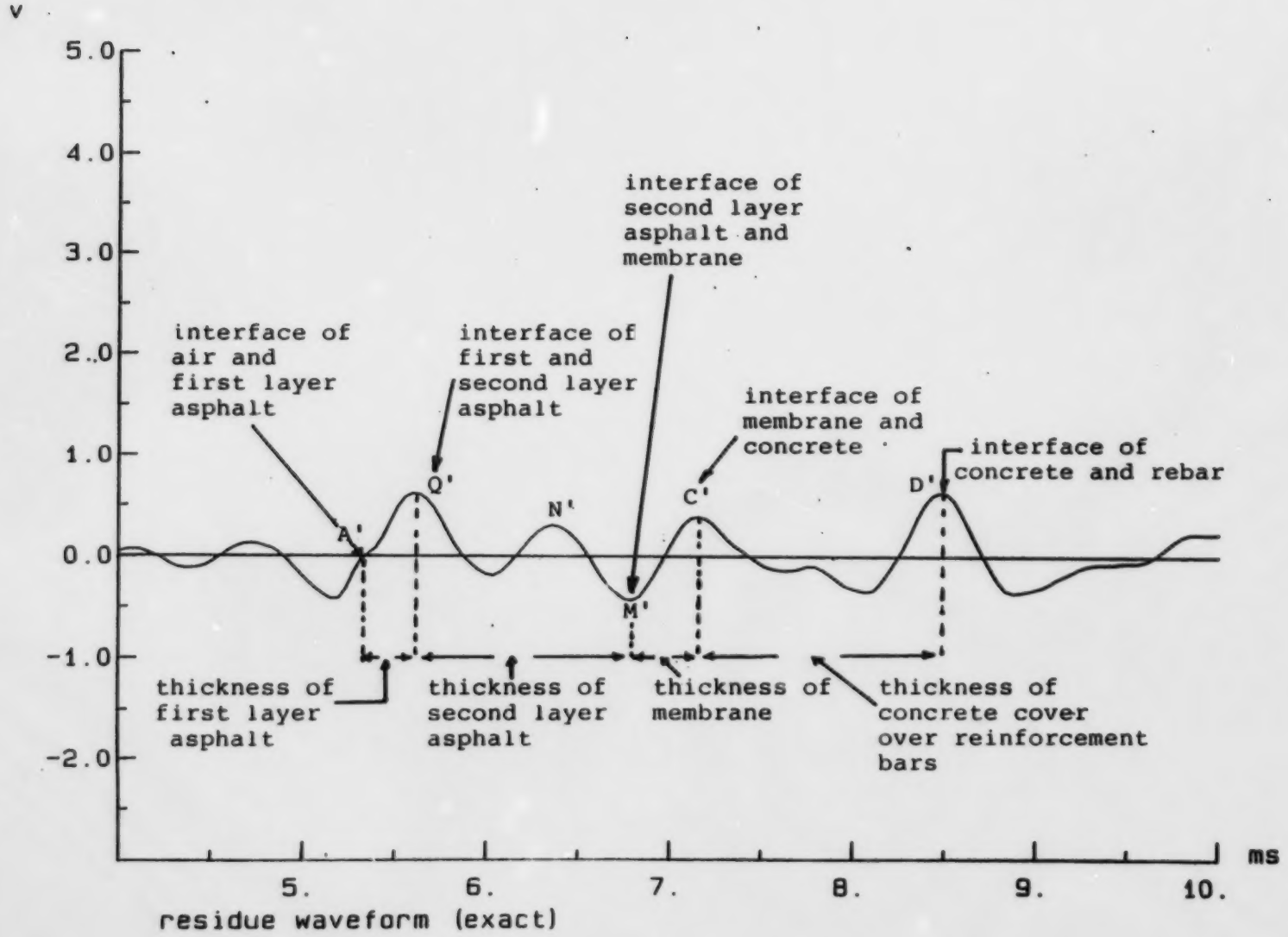

Fig. 2.13: Residue waveform from EXACT case.

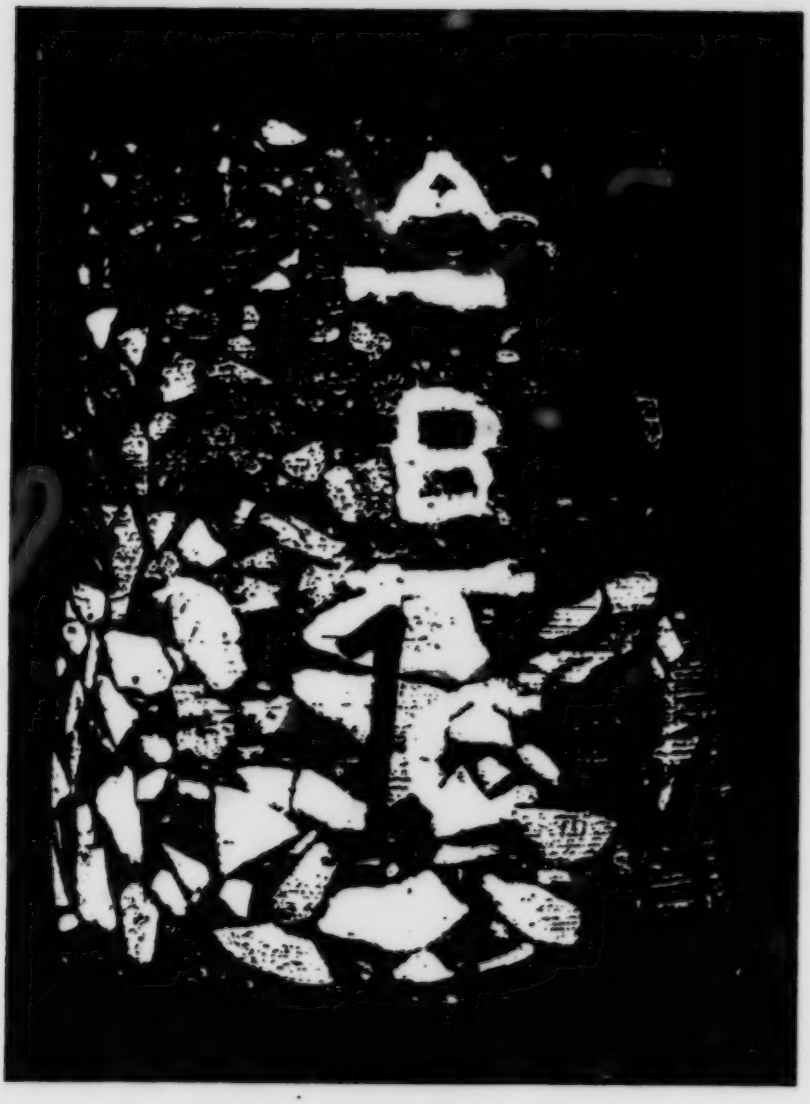

Fig. 2.14: Photograph of a core sample obtained from the Bloor Street bridge deck.

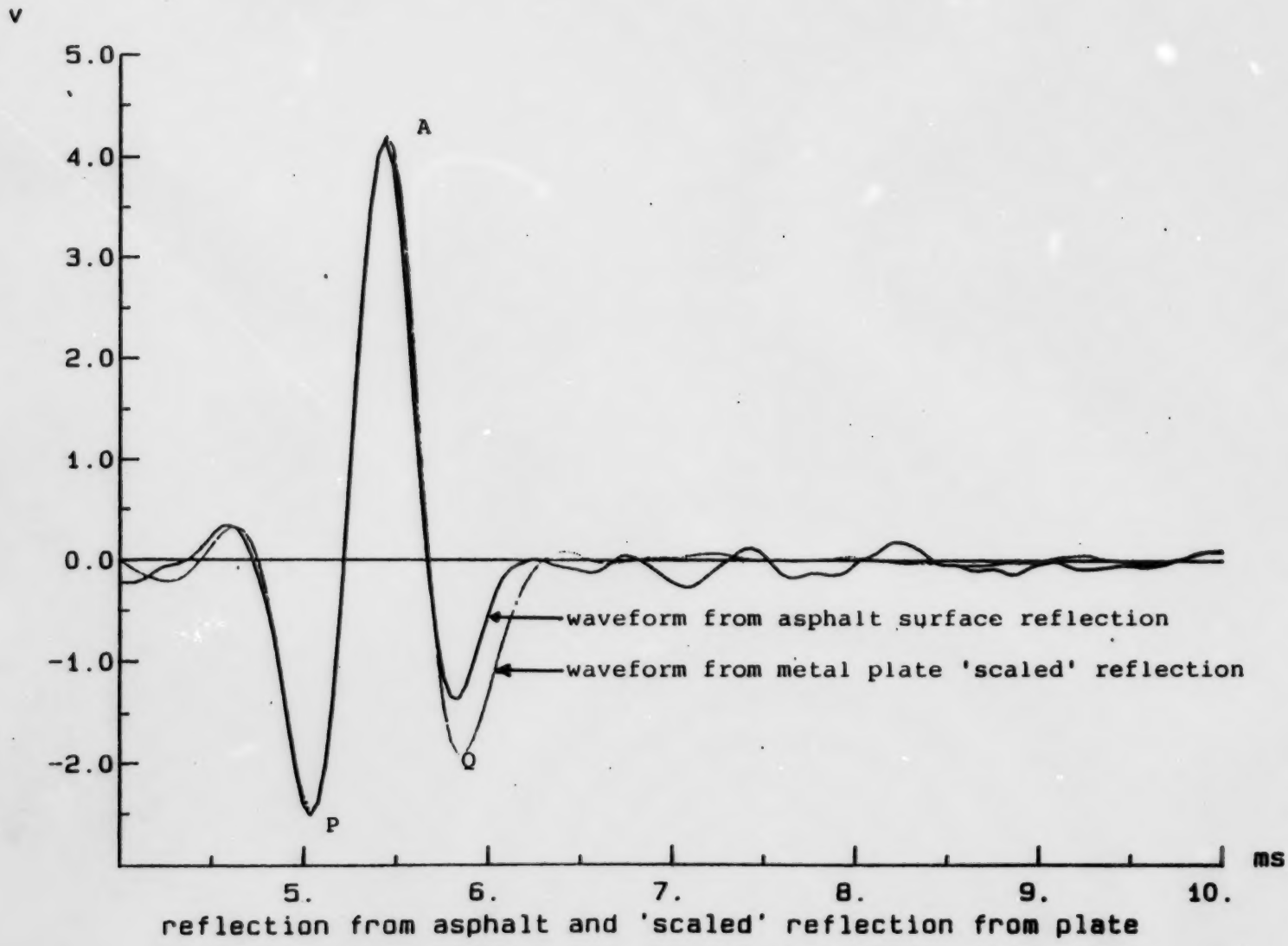

Fig. 2.15: Superimposed waveforms from asphalt surface reflection and metal plate 'scaled' reflection.

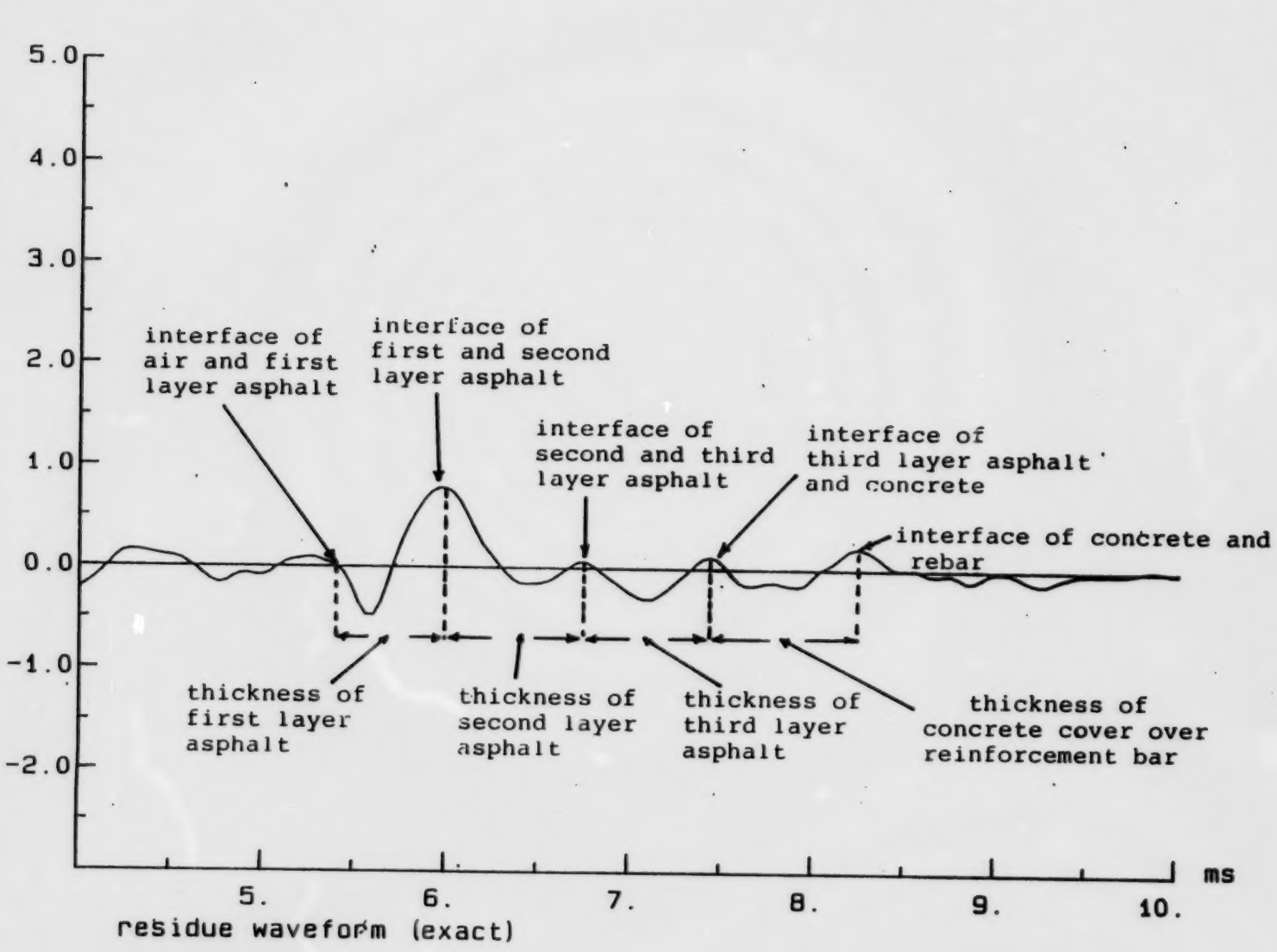

Fig. 2.16: Residue waveform from EXACT case

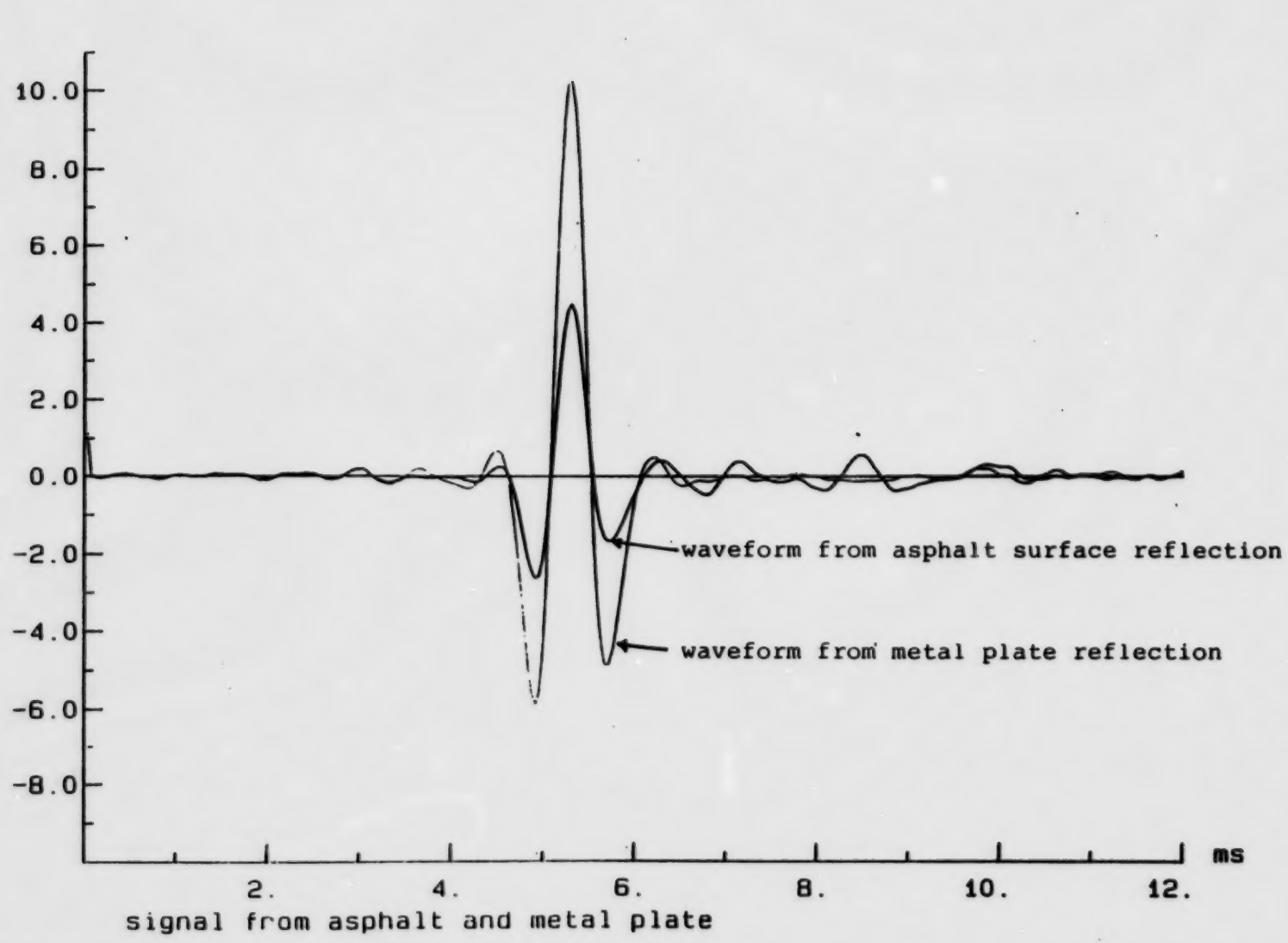

Fig. 2.17: Superimposed waveforms from asphalt surface reflection and metal plate reflection.

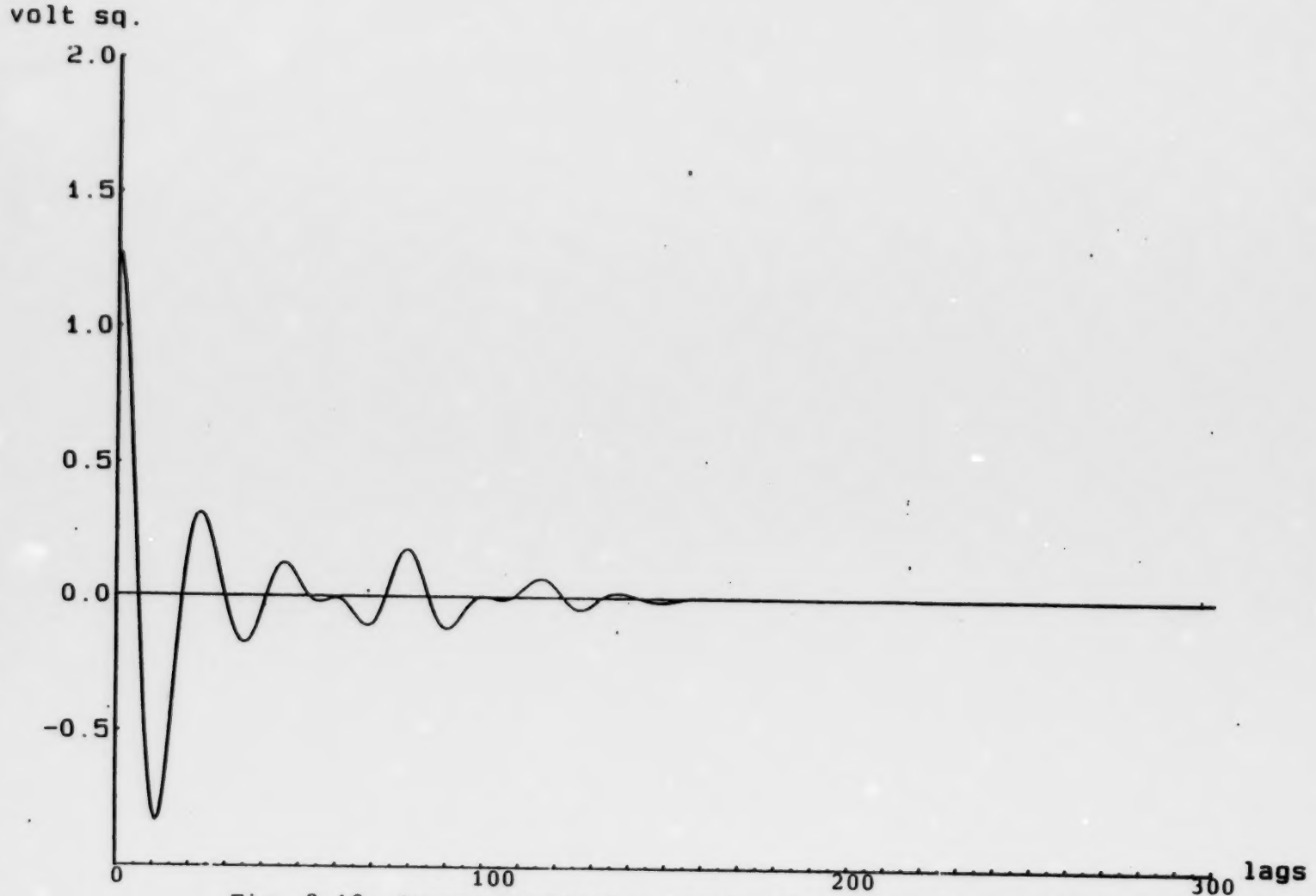

Fig. 2.18: Cross correlation result of signals from asphalt surface reflection and metal plate reflection.

of asphalt are given. A cross-correlation process, for N sample points, is performed according to the equation,

$$C_{MS}(k) = \frac{1}{N} \sum_{j=1}^{N} M(j)\, S(j+k) \qquad k=0,\ldots, N-1 \qquad (2.2)$$

where $C_{MS}(k)$ = the cross-correlation function at lag k

$M(.)$ = the true metal plate waveform

$S(.)$ = the true reflected signal from asphalt

The cross-correlation function defined by eq. (2.2) is computed and presented in Fig. 2.18. We note that the cross-correlation process produces a waveform signature which is similar to the true reflected waveform. The reason is that the transmitted pulse of the radar system is actually an impulse signal. During the cross-correlation procedure, the surface reflection peak from the metal plate waveform matches only to the peaks of the true reflected signal. The result is just a shifted replica of the true reflected waveform. Unfortunately, the correlation technique does not yield additional information for peaks detection.

2.5/ Measurement Accuracy

In order to determine a bound on the accuracy of the measurement of asphalt thickness, it is necessary to estimate the errors involved in the actual measurements and determine how these errors propagate through the calculations to the final result.

2.5.1/ Reflection Coefficient Calculation

We start by noting that the calculation of reflection coefficient is given by the negative of the ratio of two measured values, namely the reflection from asphalt, X_2 , and the reflection from the flat plate, X_1 , or

$$\rho = -\frac{X_2}{X_1} \qquad (2.3)$$

There are a number of sources of error which may affect the calculation of the reflection coefficient. These include:

1) waveform distortion due to the antenna internal reflections;

2) waveform distortion due to the lossy property of asphalt;

3) waveform variation due to motion of the antenna in the vertical plane;

4) waveform distortion produced by the interface amplifier- filter;

5) precision of the analog-to-digital converter;

6) intersample spacing due to the sampling rate; and,

7) waveform corruption due to receiver noise.

Each of these error sources is discussed in detail and the relative amounts of the errors estimated. Once the overall error in the reflection coefficient is determined, it is relatively straight forward to determine the error in the calculation of asphalt thickness.

There are several other factors which could affect the accuracy of the measurements but these are assumed to produce negligible effect on the results. These include:

1) waveform distortion due to variations in dielectric constant along the direction of travel. If the asphalt composition were to vary radically within the footprint of the antenna, then the measurement would be affected. In general, we assume that the asphalt is homogeneous.

2) waveform distortion due to the roughness of the asphalt surface. Normally, this is important when the dimensions of the roughness are comparable to 1/10 of a wavelength. In the present case, the wavelength at centre frequency (1 GHz) is 300 mm which indicates that surface roughness should be less than 30 mm. Normally, this is true.

3) waveform corruption due to thin layers of foreign material on the asphalt surface such as sand, water, dirt and the like. Normally, the asphalt surface is clean; however, measurements should be made on dry surfaces in order to avoid an error due to water layer or water permeating the asphalt.

4) size of the reflecting plate used for flat plate measurement. The main requirement is that the flat plate should be at least twice the extent of the antenna footprint in each dimension.

5) effect of having a large metal object such as the van in close proximity to the antenna. Since all measurements are affected in a similar manner, it is thought, at present, that the antenna internal reflection cancellation procedure also cancels the effect of the van.

2.5.2/ Evaluation of Errors in Reflection Coefficient

A. Waveform Distortion Due to Antenna Internal Reflections

The main problem here is that the antenna internal reflections add an error term to all parts of the waveform. This error waveform, shown in Fig. 2.19, varies in a non- predictable way from - 1V to + 0.3V over the range of the required measurements. Since the error is not flat, there are two effects. First, the amplitude at each point of the reflections is no longer accurate; and second, the waveforms are actually skewed in shape depending on height. Thus, simple waveform subtraction of the transmitted signal cannot be accomplished.

Figure 2.20 illustrates the super position of the flat plate measurement and the antenna internal reflection waveform. It is seen that the error is quite significant. Figure 2.21 illustrates the subtraction of the two waveforms which results in the true flat plate measurement. The trace is nearly nulled except in the region of the impulse itself. Ideally, of course, the null portion would be exact.

Figure 2.22 shows the super position of the surface reflection from asphalt measurement and the antenna internal reflection waveform. Again, we see that the error waveform is very significant. Figure 2.23 demonstrates the true surface reflection waveform. We note that the true flat plate waveform and the true surface reflection waveform are not exactly the same shape. This factor will be discussed in Part B.

The main sources of error in subtracting the antenna internal reflection waveform is in determining this waveform. The only attractive method found to date is to raise the entire vehicle with the antenna attached so that the surface reflection from the ground is effectively moved out of range. This signal is then recorded using the tape recorder. Whether this changes with time is yet to be determined.

From Fig. 2.23, it appears that the rms uncancelled voltage waveform is of the order of 50 mV. Taking this value, and noting that the flat plate reflection is 10V and the surface reflection is 4V, we then find that the resulting errors in X_1 and X_2 are:

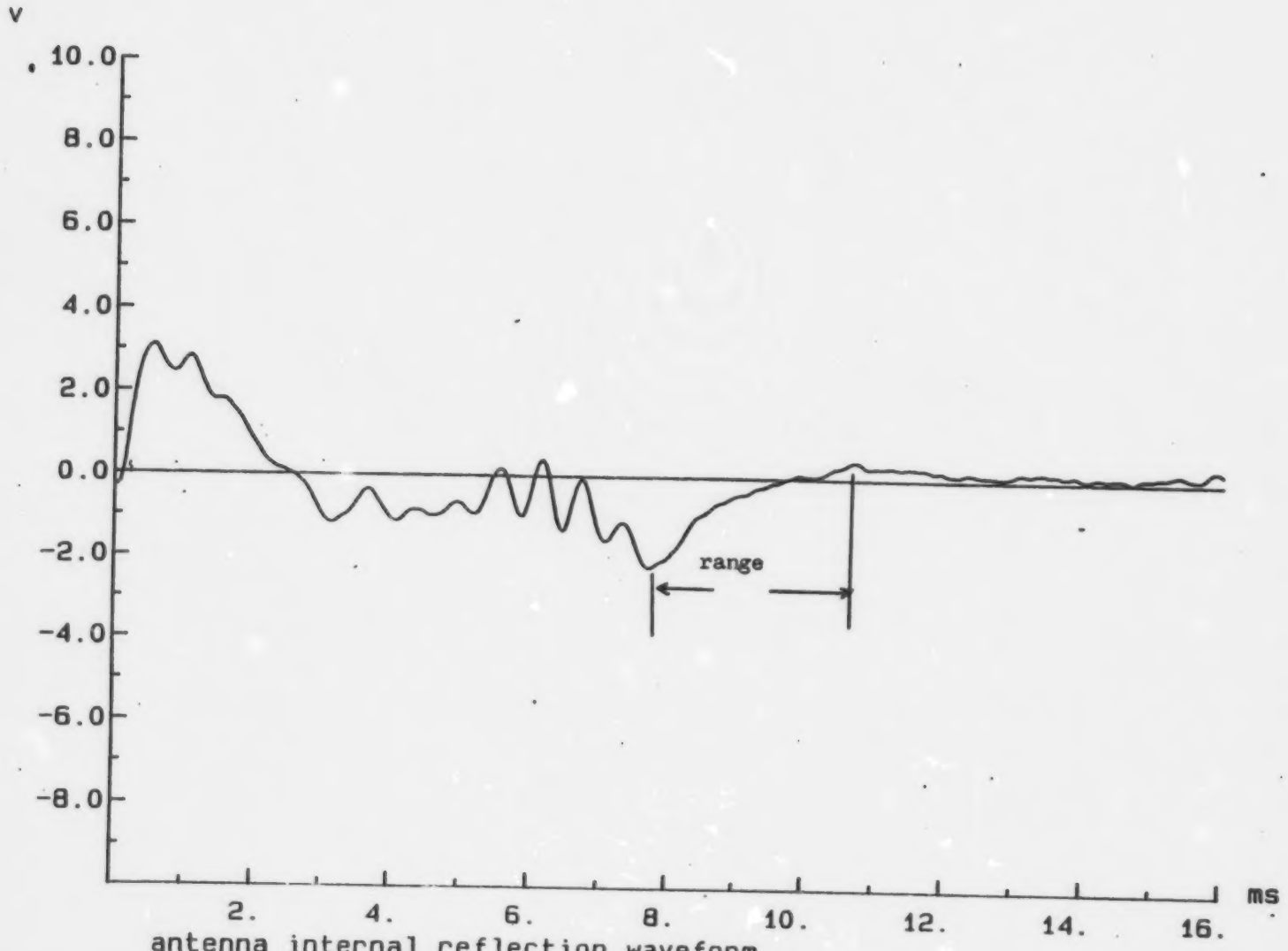

Fig. 2.19: Reflection generated inside the antenna.

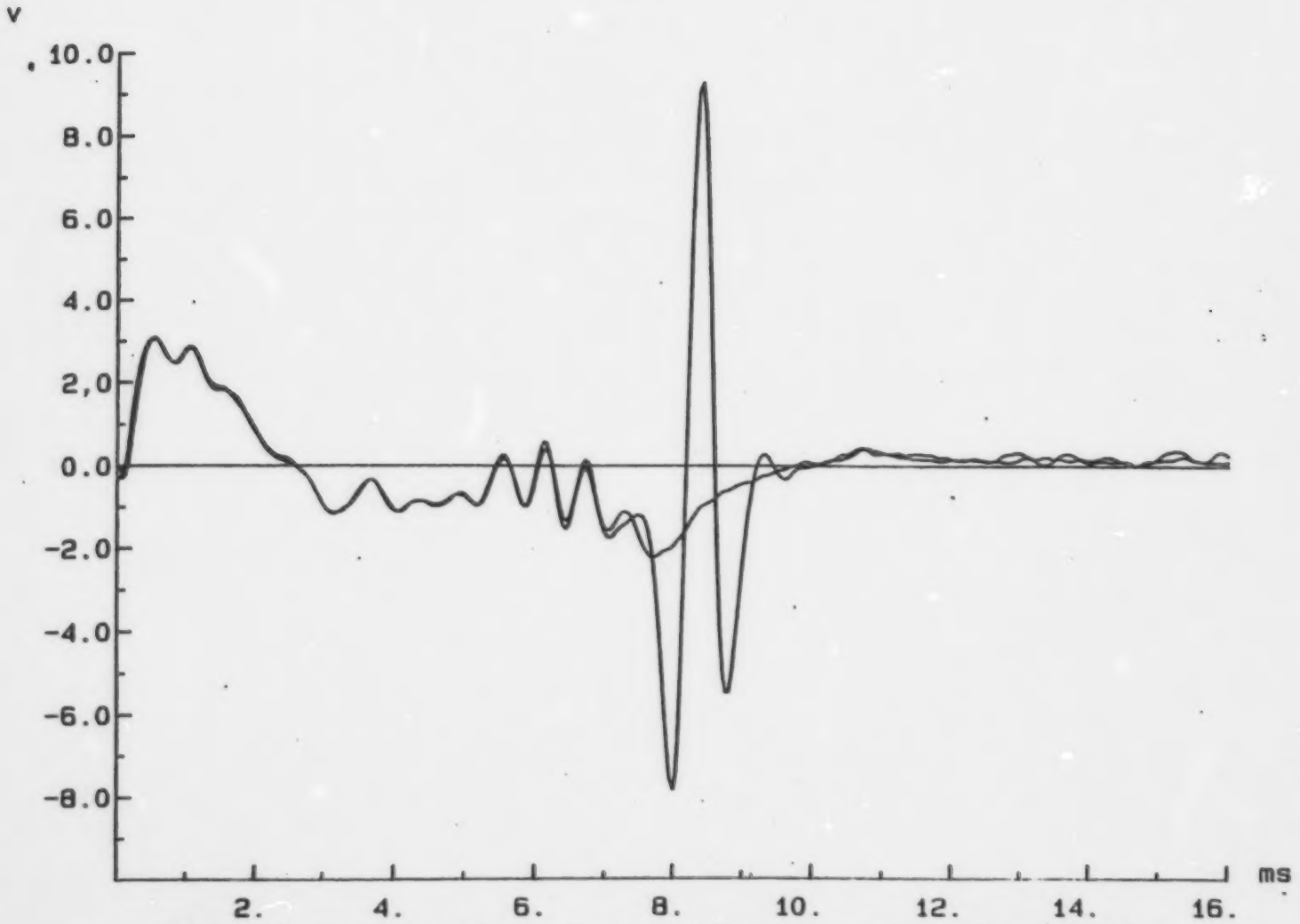

Fig. 2.20: Superposition of the metal plate waveform and the internal reflection.

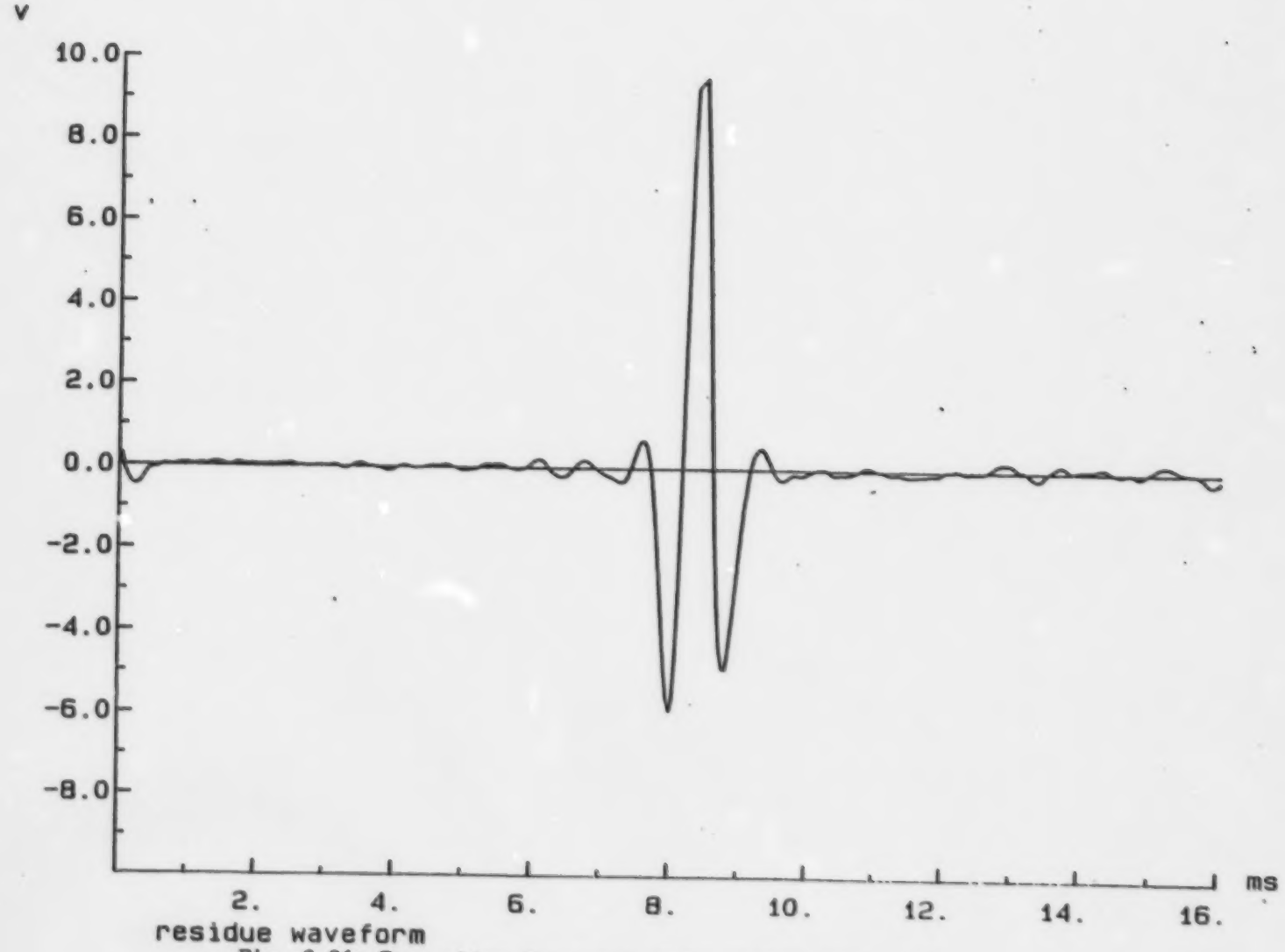

Fig. 2.21: True video for metal plate reflection.

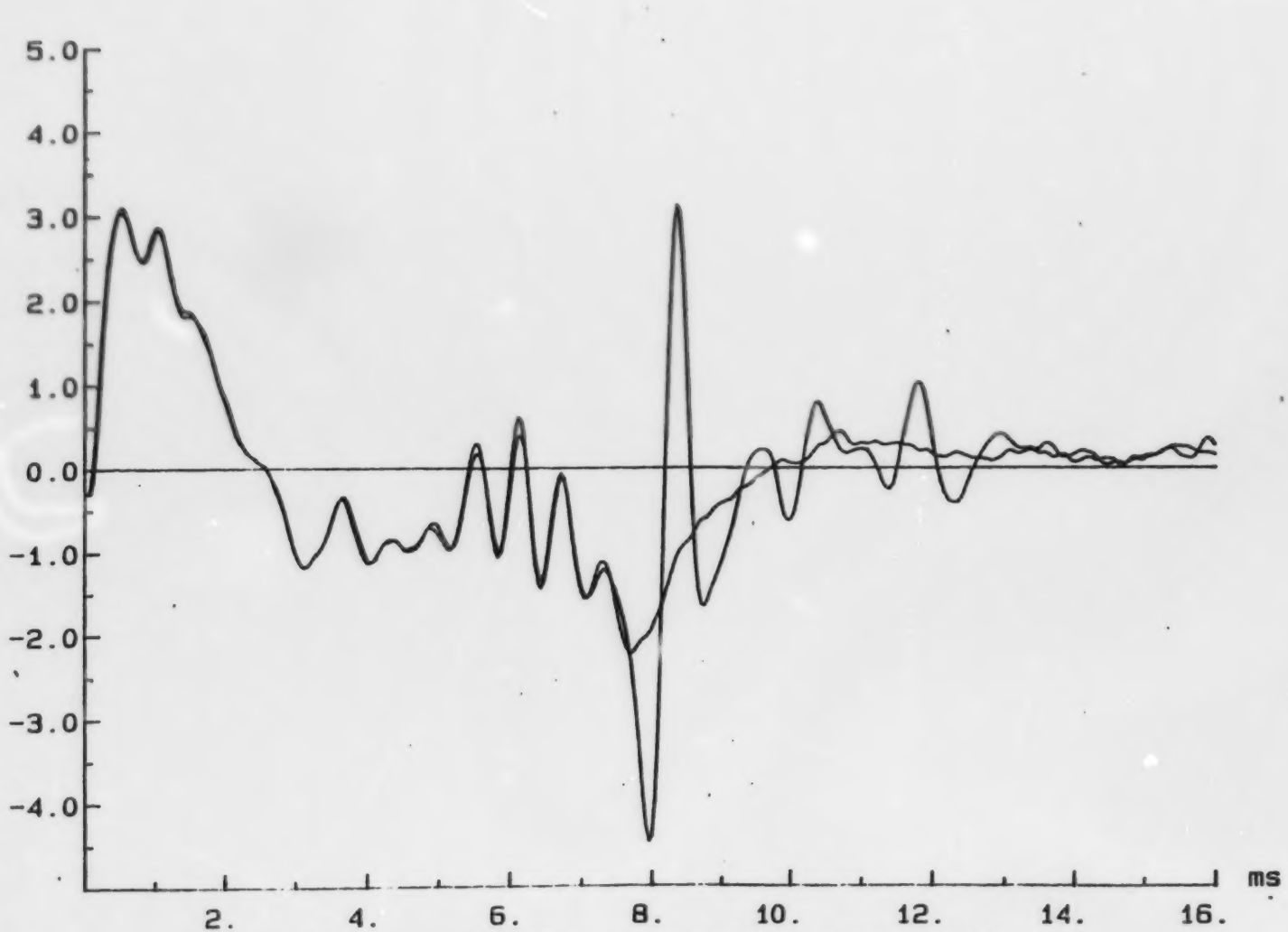

Fig. 3.22: Superposition of asphalt reflection and internal reflection.

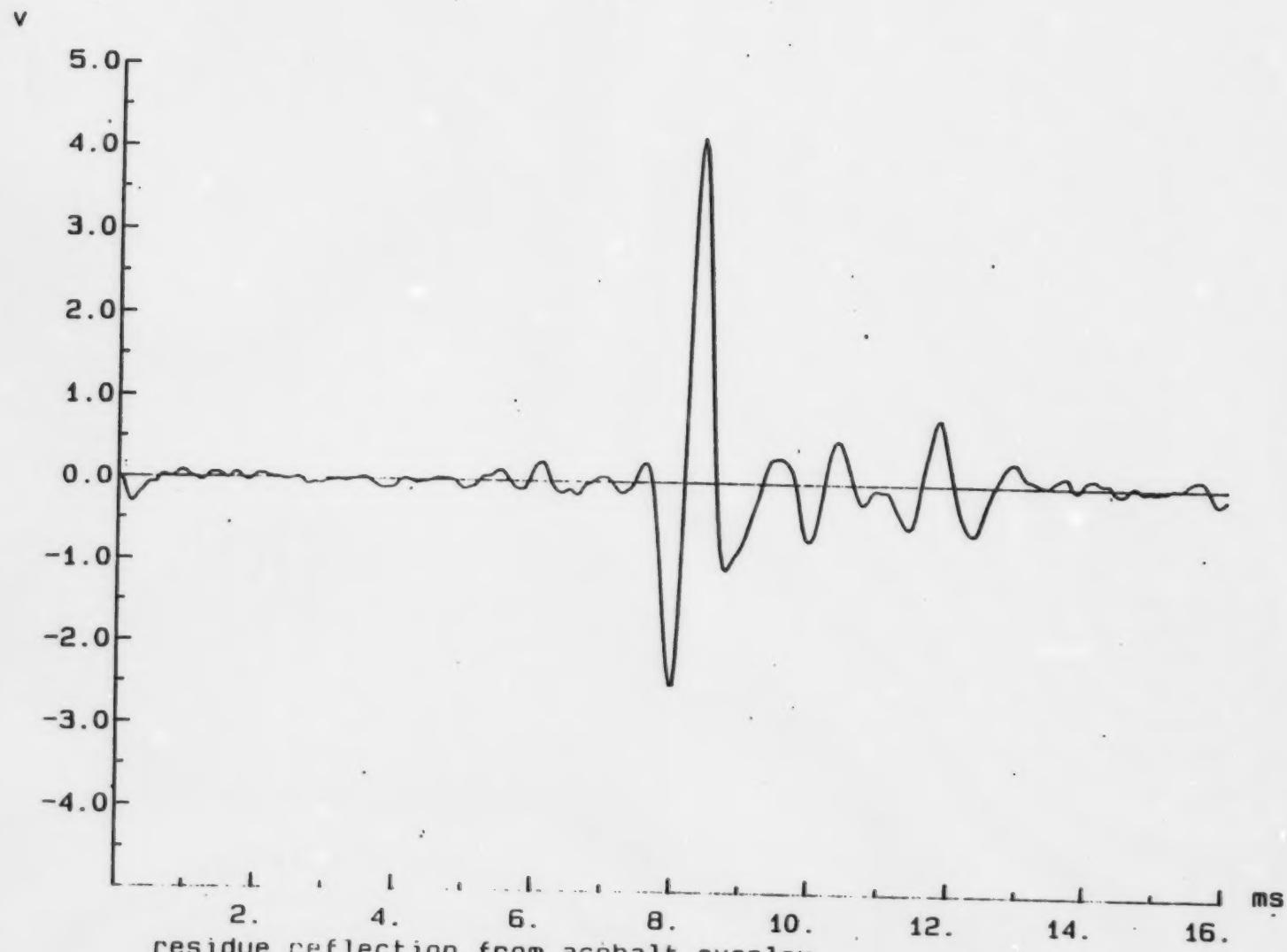

Fig. 2.26: True video for asphalt overlay.

flat plate error (EFP1) = 0.5%

surface reflection error (ESR1) = 1.25%

We note that the error in both cases is in the same direction; thus, overall error is simply the difference or 0.75%.

B. Waveform Distortion Due to the Lossy Property of Asphalt

Comparing Fig. 2.21 and Fig. 2.23, we note that there is distortion in the surface reflected waveform. This is presently being investigated and results of reflections of waveforms from concrete will provide an indication of the effect of loss. Also note that the metal van causes waveform distortion.

C. Waveform Variation Due to Motion of the Antenna in the Vertical Plane

Motion of the antenna in the vertical plane can occur when the vehicle is in motion due to the suspension of the vehicle. Thus, this is an error which would affect the amplitude of the surface reflection but not the flat plate reflection. In order to estimate this error, it is necessary to determine

the extent of the motion of the antenna about the mean height above asphalt. Then, knowing the calibration of the antenna field strength versus height, given in Fig. 2.24, it is possible to estimate the error.

For the nominal height above asphalt of 150 mm, it is seen from Fig. 2.24 that the variation of amplitude versus height is approximately 2.9 V/m. If it is assumed that the antenna height varies by 5 mm, then the error is approximately 15 mV. Normally, the amplitude being measured is of the order of 2 to 3 V for the surface reflection; thus the error is

surface reflection error (ESR3) = 0.5%

D. Distortion Produced by the Input Amplifier-Filter

There are two possible sources of distortion which can be produced by the amplifier-filter interface; namely the amplifier effects and the filter effects. These two effects are essentially

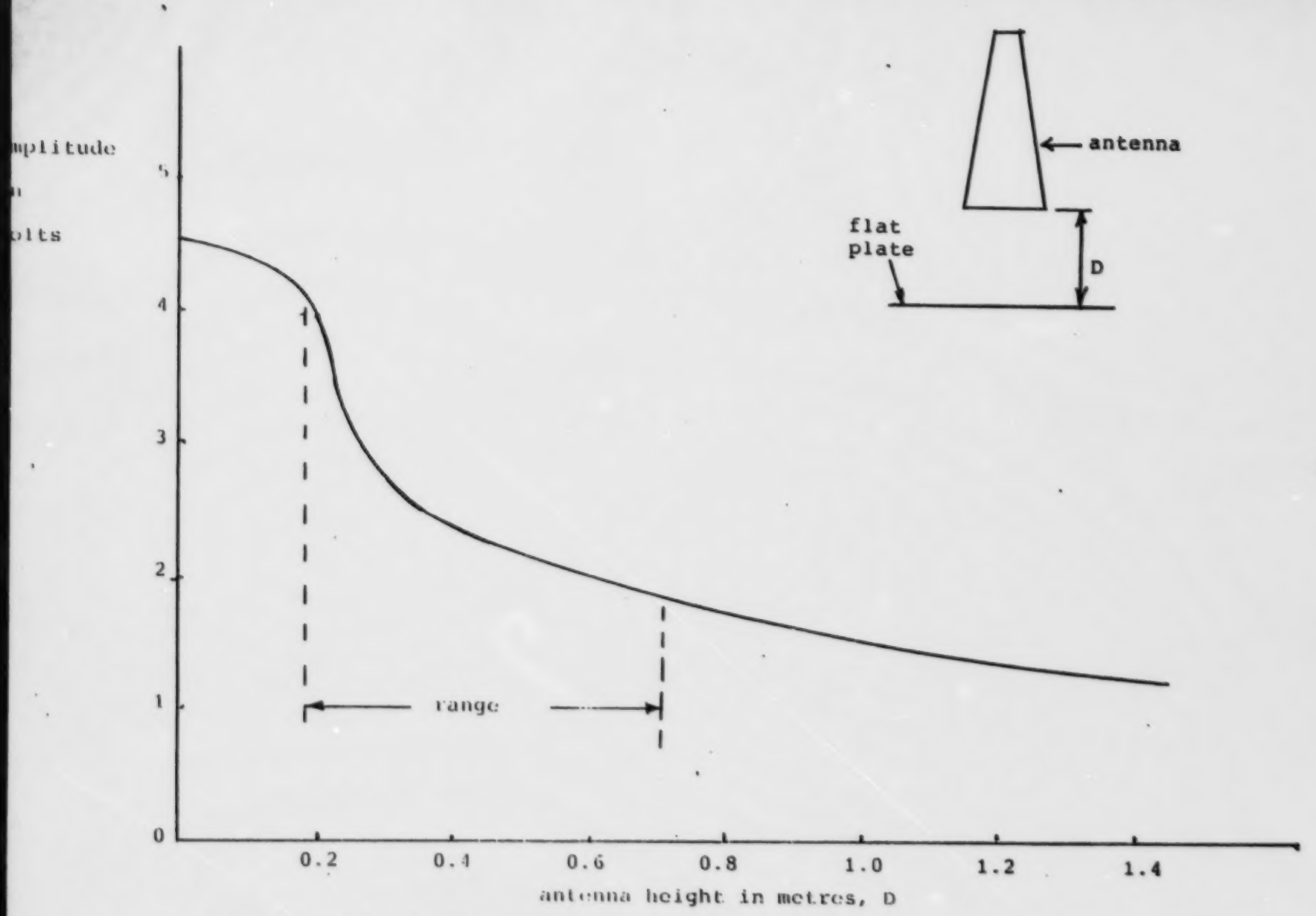

Fig. 2.24: Reflection amplitude from metal plate at different heights.

independent since the amplifier has a band width greatly in excess of the filter band width and the filter is linear.

1. *Amplifier Effects*

The main problem of the amplifier is the gain non-linearly. In our case, this should be negligible since the input from the radar to the operational amplifier is of the order of one volt and the maximum differential voltage to the operational amplifier is of the order of 0.1 mV. Thus, the maximum error is approximately 0.01%.

The only other possibility of distortion which can arise due to the amplifier is if the output signal attempts to exceed the limits of the power supply voltages. Since power supply voltages of + 15V and - 15V are employed and the output voltage is in the range of - 10V to + 10V, this source of error is negligible.

Thus, the errors in flat plate measurement and surface reflection measurement are:

flat plate error (EFP4A) = 0.01%

surface reflection error (ESR4A) = 0.01%

2. *Filter Effects*

The second factor which can cause distortion is the effect of the filtering on the signal. Two processes can alter the signal. The first is the amplitude characteristic of the filter and the second is the phase characteristic of the filter. The filter chosen is the third order Butterworth with cutoff of 5 KHz, illustrated in Fig. 2.25. Since almost all of the components of the signal lie in the range from 0 to 2 KHz, it is unlikely that the amplitude response of the filter causes any deleterious effects on the signal.

The phase response of the filter may cause some waveform distortion since there is considerable non-linearity beyond 2.5 kHz frequency. However, this distortion will mainly effect the fast time-change features of the signal such as cusps and sharp transitions. At present, the signal processing analysis does not rely on these features. Thus, we assume the error to be of the same order as that produced by the amplifier or

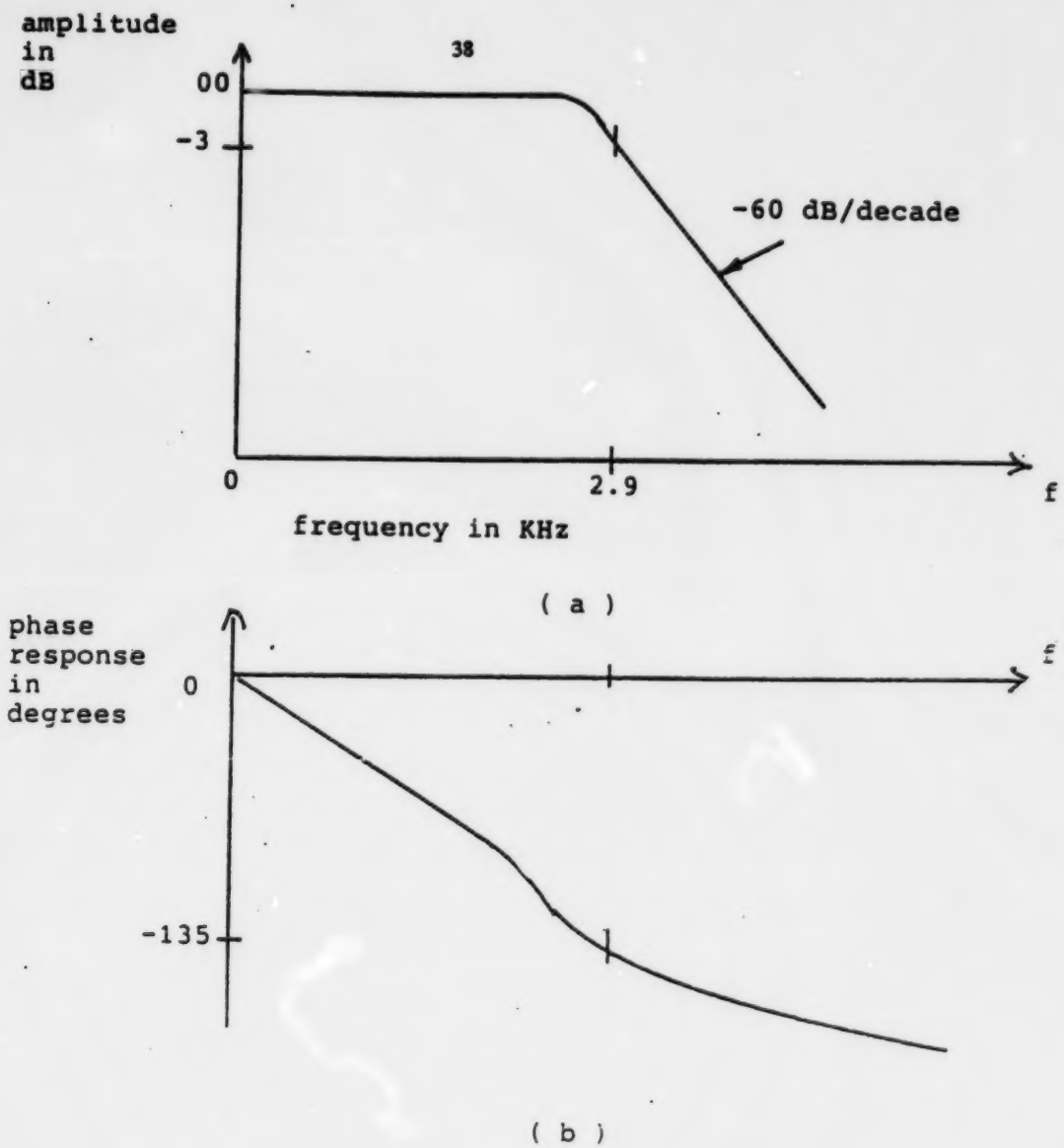

Fig. 2.25: (a) Amplitude response of a third order Butterworth filter.

(b) Phase response of a third order Butterworth filter.

flat plate error (EFP4B) = 0.01%

surface reflection error (ESR4B) = 0.01%

E. Precision of Analog-to-Digital Converter

The analog-to-digital converter used in the interface has 12 bits of resolution and a total voltage range from - 10V to + 10V. Thus, the step size of the converter is given by 20V/4096 or 4.88 mV. In practice, the input voltage levels to the ADC of the reflections from the flat plate and the surface reflection are approximately 8V and 3V, respectively. Thus, the errors due to the step size are:

flat plate error (EFP5) = 0.06%

surface reflection error (ESR5) = 0.163%

F. Intersample Spacing Errors

Since the input waveform is analog, it is necessary to provide a sampling technique in order to convert the waveform into a digital format. Unfortunately, the sampled waveform is exactly equal to the actual waveform only at the sample points. The problem produced by this effect becomes clear when we note the variation in amplitude of a peak, such as that produced by the flat plate reflection or the surface reflection. In both cases we note, from Fig. 2.26, that it is possible to miss the actual peak value due to the time between samples.

In our case, this error can be estimated by noting that with a sampling rate of 25000 samples per second, the time between samples is 40 microseconds. The peak of the reflected waveforms can be modeled as a half cosine wave, as illustrated in Fig. 2.27, with the time between zero-crossings being 1 ms. This gives the equation

$$s(t) = A \cos(\pi t / T) \qquad (2.4)$$

where t is the time and T is time between zero-crossings. The true amplitude is A and the maximum error due to sampling is the amplitude at half the sampling spacing, we get the error to

Fig. 2.26: (a) Sampling at the true peak.
(b) Sampling error of ½ sample.

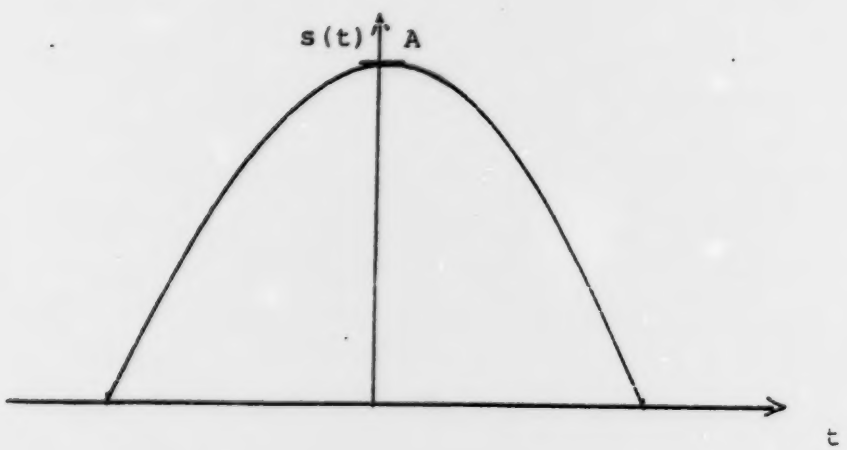

Fig. 2.27: Peak of the reflected waveform modelled as a cosine waveform.

be $[1- \cos (\pi T_s /2T)]*100\%$, where T_s is the sampling time. For the above mentions values, this is approximately 0.02%. Therefore, the errors due to sampling are:

flat plate error (EFP6) = 0.02%

surface reflection error (ESR6) = 0.02%

Note that the error is considerably more in the region of zero-crossings; however, these values are not used in the calculations.

G. Waveform Corruption Due to Receiver Noise

In this system, the level of receiver noise has not been observed. A simple calculation can confirm this result. It is well known that the level of receiver noise is -114 dBm/ MHz for a receiver with 0 dB noise figure. For the actual system, it could be assumed that the receiver has a noise figure of 20 dB (or 100 times). If it is further assumed that output bandwidth is 2.5 KHz, then the total noise power P is -68 dBm or 1.59E-10 Watts. The resulting rms noise voltage is then given by

$$V_n = [P Z]^{\frac{1}{2}} \qquad (2.5)$$

$$= 0.24 \text{ mV}$$

Assuming that the signal voltage entering the receiver the voltage level entering the receiver is at least 20 mV, the noise voltage is 70 times lower than the signal. This corresponds to an error given by:

flat plate error (EFP7) = 1.4%

surface reflection error (ESR7) = 1.4%

H. Overall Effect of Errors on the Calculation of Reflection Coefficient

The overall effect of the errors in determining the values of the flat plate reflection and the surface reflection can now be considered. We see that for the worst case situation,

$$\rho \pm \Delta\rho = - \frac{X_2 + \Delta X_2}{X_1 - \Delta X_1}$$

$$= - \frac{X_2 (1 + \frac{\Delta X_2}{X_2})}{X_1 (1 - \frac{\Delta X_1}{X_1})}$$

By multipling the numerator and denominator of the above equation by $(1 + \frac{\Delta X_1}{X_1})$, and since $(\frac{\Delta X_1}{X_1})^2$ is very much less than 1. The expression is reduced to

$$\rho \pm \Delta\rho = - \frac{X_2}{X_1} (1 + \frac{\Delta X_2}{X_2}) (1 + \frac{\Delta X_1}{X_1})$$

By expanding the terms in the equation and neglecting small terms, we have

$$\rho \pm \Delta\rho = - \frac{X_2}{X_1} [1 + (\frac{\Delta X_2}{X_2} + \frac{\Delta X_1}{X_1})] \qquad (2.6)$$

where

$\frac{\Delta X_1}{X_1}$ = sum of EFP values

$\frac{\Delta X_2}{X_2}$ = sum of ESR values

Using the values of EFP and ESR deduced from the above analysis, we find:

$$\frac{\Delta X_1}{X_1} = (EFP1^2 + EFP4A^2 + EFP4B^2 + EFP5^2 + EFP6^2 + EFP7^2)$$

$$= (0.5^2 + 0.01^2 + 0.01^2 + 0.06^2 + 0.02^2 + 1.4^2)^{\frac{1}{2}}$$

$$= 1.5\%$$

$$\frac{\Delta X_2}{X_2} = (ESR1^2 + ESR3^2 + ESR4A^2 + ESR4B^2 + ESR5^2 + ESR6^2 + ESR7^2)^{\frac{1}{2}}$$

$$= (1.25^2 + 0.5^2 + 0.01^2 + 0.01^2 + 0.16^2 + 0.02^2 + 1.4^2)^{\frac{1}{2}}$$

$$= 2\ \%$$

Therefore, the total error in ρ is the sum of these two values or 3.8%.

2.5.3/ Calculation of Dielectric Constant

Once the reflection coefficient is calculated, it is possible to determine the dielectric constant of the asphalt. We note that the expression for asphalt thickness varies inversely as the square root of the dielectric constant. This is given by

$$\sqrt{\varepsilon_A} + \sqrt[4]{\varepsilon_A} = \frac{1 - (\rho + \Delta\rho)}{1 + (\rho + \Delta\rho)}$$

$$= \frac{[1 - \rho]}{[1 + \rho]} \left[1 \pm \frac{2\Delta\rho}{1 - \rho^2}\right] \qquad (2.7)$$

The results of the analysis are plotted in parametric form in Fig. 2.28 for values of reflection coefficient ranging from -0.1 to -0.6. We see that for the value of $2\Delta\rho = 0.076$, the percent error in root dielectric constant ranges from about 8% to 12.5% as the reflection coefficient varies from of -0.1 to -0.6. Usually, the reflection coefficient is of the order of -0.3 which corresponds to an error of 8.8%.

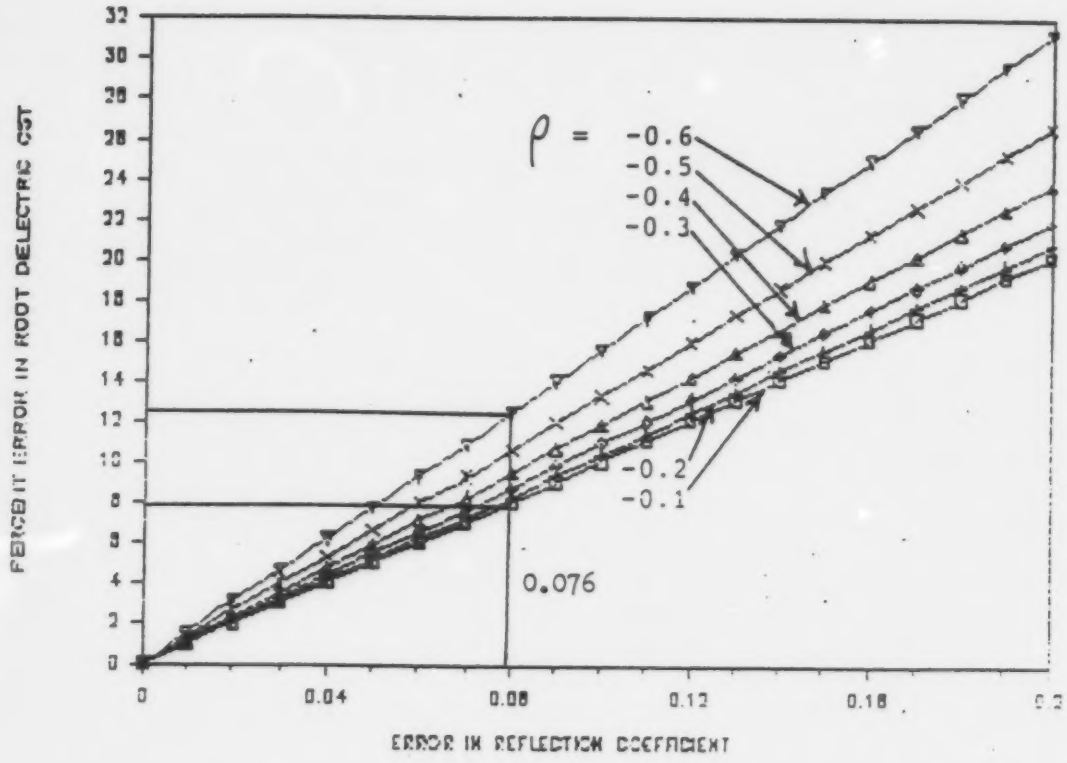

Fig. 2.28: Percent error in root dielectric constant in terms of error in reflection coefficient for different values of reflection coefficient.

2.5.4/ Calculation of Asphalt Thickness

The asphalt thickness is simply given by the product of the time delay T_A between the surface reflection and the asphalt-concrete interface reflection, and the velocity of light c divided by the square root of the dielectric constant or

$$d = \frac{T_A c}{\sqrt{\varepsilon_A}} \tag{2.8}$$

Now, the time delay between peaks is measured in terms of the digitized samples and each peak could be in error by plus or minus half an intersample spacing time delay. Thus, the total error is equal to one intersample spacing delay, T_s.

The time between peaks is normally 1 to 2 ms and the time between samples is 40 microseconds. Thus, the error in determining the peaks is approximately

timing error between peaks (EPK) = 4%

The error in the velocity of light is negligible in comparison to all other errors and neglected. Thus, the remaining error in root dielectric constant is given by eq. (2.6). Thus, we find that the overall error in deducing the thickness of asphalt based on a single measurement is

$$d + \Delta d = \frac{T_A c}{\sqrt{\varepsilon_A}} \left[1 + \frac{\Delta T_A}{T_A} + \frac{2\Delta\rho}{1 - \rho^2} \right] \tag{2.9}$$

This results in a percentage error of

$$\text{ERROR} = \left[\frac{\Delta T_A}{T_A} + \frac{2\Delta P}{1 - P^2} \right] \times 100\,\% \tag{2.10}$$

$$= 4\% + 8.8\% = 12.8\%$$

Of course, this result applies to the single shot measurement. In practice, five such measurements are made per metre of travel which then reduces the error as discussed next.

* ASPHALT *

metre	mini	maxi	AVE (all in mm)	
1	60	126	94	*
2	115	127	122	*
3	114	125	119	←112
4	114	125	119	
5	102	117	109	
6	99	105	102	
7	95	100	97	
8	94	106	101	
9	93	103	96	
10	94	104	97	
11	96	105	100	
12	93	101	98	
13	92	98	94	
14	93	95	94	
15	93	97	94	
16	93	97	94	
17	96	98	96	
18	99	103	100	←105
19	95	97	95	
20	92	99	94	
21	97	102	98	
22	94	99	96	
23	95	102	98	
24	94	103	99	←100
25	95	107	99	
26	96	103	99	
27	95	100	97	
28	93	100	96	
29	93	99	95	
30	95	99	97	
31	94	100	96	
32	92	98	95	
33	94	100	96	
34	95	100	96	
35	98	99	98	
36	98	101	99	
37	98	101	99	
38	94	99	97	
39	90	95	92	
40	92	101	96	
41	94	98	96	
42	95	99	96	
43	93	98	96	
44	95	100	97	
45	97	101	99	

Fig. 2.29: Table of minimum and maximum asphalt thickness measurements for the Ninth Line bridge deck in Oakville.

2.5.5/ Averaging Per Metre, Per Line and Per Deck

Normally, it is not required that the thickness of asphalt be determined with a single measurement. In most cases, five measurements are made per metre and the thickness is averaged over the one metre length. This reduces the error in a Gaussian distributed random variable by a factor of N assuming all errors have the same distribution, which in this case is 2.23. Consequently, the error for the 1 metre measurement is approximately 6%. Relating this to the nominal asphalt thickness of 80 mm (or 100 mm), we see that the error is about 5 mm (or 6 mm).

When an entire line is averaged, the average of the one metre averages are averaged. For a 100 m long bridge deck in which the asphalt is nearly uniform in thickness, the error is further reduced by a factor of 10 resulting in the overall error of 1 mm.

2.5.6/ Comparison with Actual Measurement

Since the results of this study relate directly to the measurement of asphalt thickness in a new deck, we present some data taken from the Ninth Line bridge in Oakville. Minimum and maximum asphalt values over 1 m segments are listed in Fig. 2.29 for one line. Dismissing the outliers (marked with an asterisk *), we see that the variation from metre to metre ranges from approximately + 3 mm to + 6 mm for much of the data. At the start of the line, there is considerably more variation indicating, perhaps, a water layer at the asphalt membrane interface. However, this is speculative.

As indicated on the chart, actual measurements of combined asphalt and membrane thickness were made at the 3 metre, the 18 metre and 24 metre points. The radar measured values averaged over 1 metre lengths were found to be 119 mm, 100 mm and 99 mm, respectively. By driving a spike into the asphalt, the actual values for the same points were found to be 112 mm, 105 mm and 100 mm. The corresponding errors for the three points are +7 mm, -5 mm and -1 mm. Thus, we see that the error estimate of 5.8 mm deduced through analysis is reasonably close.

2.6/ Summary of Results

It has been shown that internal antenna reflections can be cancelled from the reflected waveform using a subtraction process based on an adjusted fit. However, there remains a residue which is one order of magnitude less than the original internal reflected signal.

Surface reflection cancellation has also been successfully accomplished using the same technique as employed for internal reflection cancellation. This technique now allows the reflection from the boundary of different layers of asphalt to be identified. Further studies in this area should be conducted to fully exploit the capabilities of the radar.

Waveform correlation has been tested but provides no new information; thus, no further studies in this area is warranted.

A study of measurement accuracy shows that the system is capable of determining average asphalt thickness over one metre to within + 5 mm, assuming an asphalt thickness of 80 to 100 mm. For a deck, averaging reduces this number to less than 1 mm.

3/ Properties of Asphalt, Membrane and Concrete

3.1/ Asphalt

The thickness of an asphalt layer from a bridge deck is evaluated by first measuring the one-way time delay between the surface reflection and the asphalt-concrete interface reflection, T ; second, multiplying this time delay by the speed of light, c; and third, dividing the product by the square root of the dielectric constant of asphalt, ε_a. This equation has been discussed in the previous chapter and is repeated here for convenience,

$$d = \frac{T_A c}{\sqrt{\varepsilon_A}} \tag{3.1}$$

The value of the dielectric constant has yet to be determined. The first step to obtain the dielectric constant of asphalt is to measure the reflection coefficient of air-asphalt interface. This is defined by the negative ratio of the amplitude of the surface reflection from asphalt X_2 to the amplitude of the surface reflection from metal plate X_1

$$\rho A = - \frac{X_2}{X_1} \tag{3.2}$$

Once the value of ρA is known, the dielectric constant of asphalt can be deduced by

$$\varepsilon_A = \frac{(1 - \rho A)^2}{(1 + \rho A)^2} \tag{3.3}$$

and the asphalt thickness can be measured by eq. (3.1).

In order to verify the measurement of the dielectric constant of asphalt based on this method, we employed an asphalt sample with known dimensions. First, we follow the above procedures to determine the reflection coefficient of air-asphalt interface, and calculate the dielectric constant and

the thickness of the asphalt. Second, we use direct measurement of the asphalt thickness to calculate its dielectric constant. Both results are compared and checked for accuracies.

The asphalt sample was found to have dimensions of 49.53 cm in length, 38.10 cm in width and 8.26 cm in thickness. The antenna was at 99.06 cm above ground and 24.13 cm from the asphalt surface. The distance between the base of asphalt and ground is, therefore, approximately 66.68 cm.

The surface of the asphalt was found to be relatively smooth on one side and rough on the other side. Measurement is carried out for three separated cases: (1) Asphalt over a metal plate with smooth surface facing top, (2) Asphalt over a metal plate with rough surface facing top and (3) Rough surface facing top without metal plate. The reflection waveform from metal plate over the asphalt surface is given in Fig. 3.1 and the reflections from the three cases are provided in Fig. 3.2 to Fig. 3.4, respectively. The purpose of putting a metal plate directly underneath the asphalt is intended to mark the asphalt-metal interface boundary. Reflections from air-asphalt, asphalt-metal, asphalt-air and air-ground interface are indicated on each plot.

The amplitudes of the surface reflection from metal plate X_2 and asphalt X_1 , as well as the propagation time (T_A) through asphalt are measured from each waveform. The dielectric constant can be evaluated using either eq. (3.1) or eq. (3.2) since the reflected waveforms are available and the thickness of the sample and the related propagation delay are measured. These results are presented in Table 3.1.

Table 3.1/ Calculated values of the dielectric constant

Case	dielectric constant eq. 3.2	dielectric constant eq. 3.1
1	8.03	6.85
2	7.01	6.11
3	6.22	6.11
averaged value	7.09	6.36

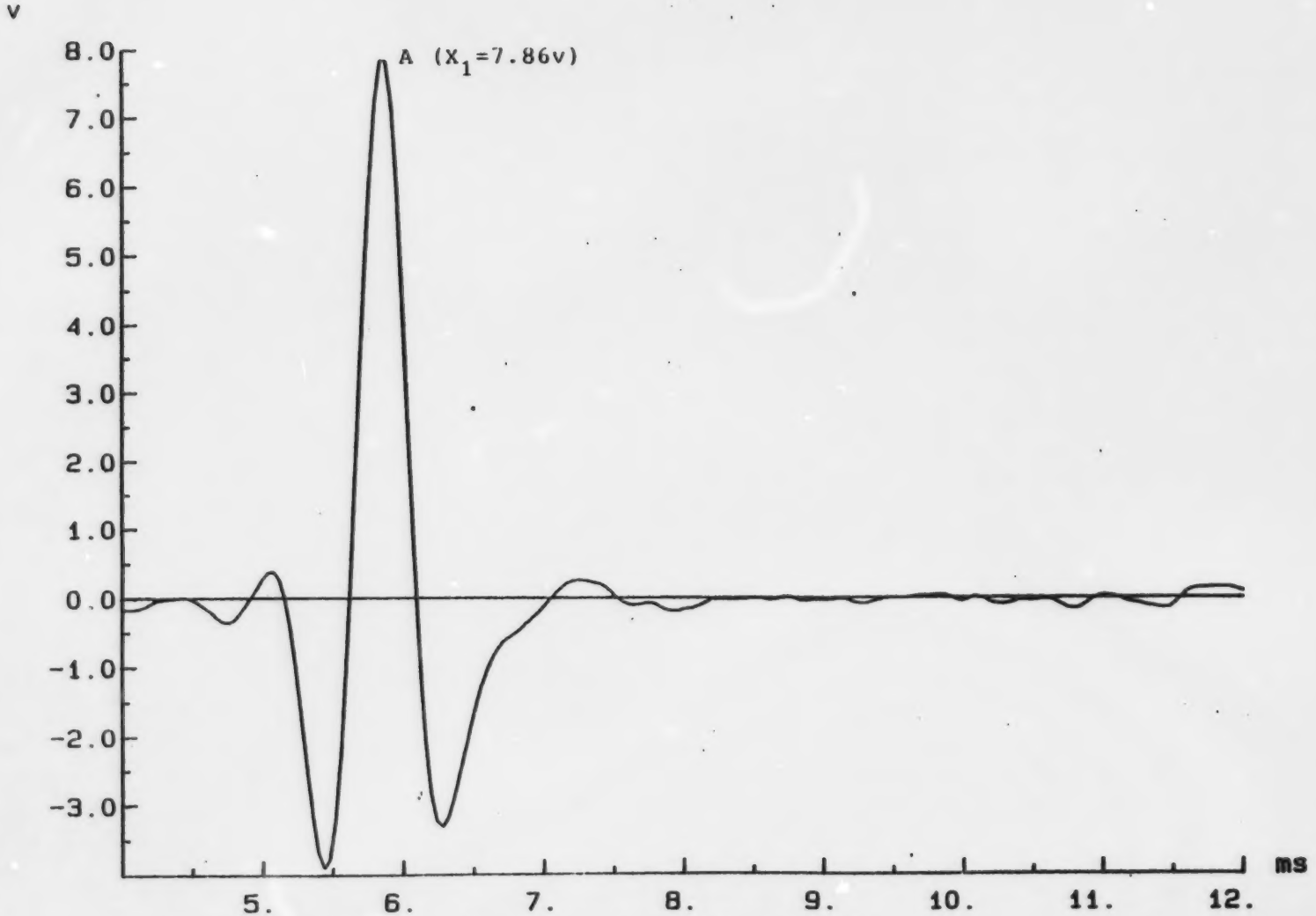

Fig. 3.1: Reflection waveform from metal plate over the asphalt surface.

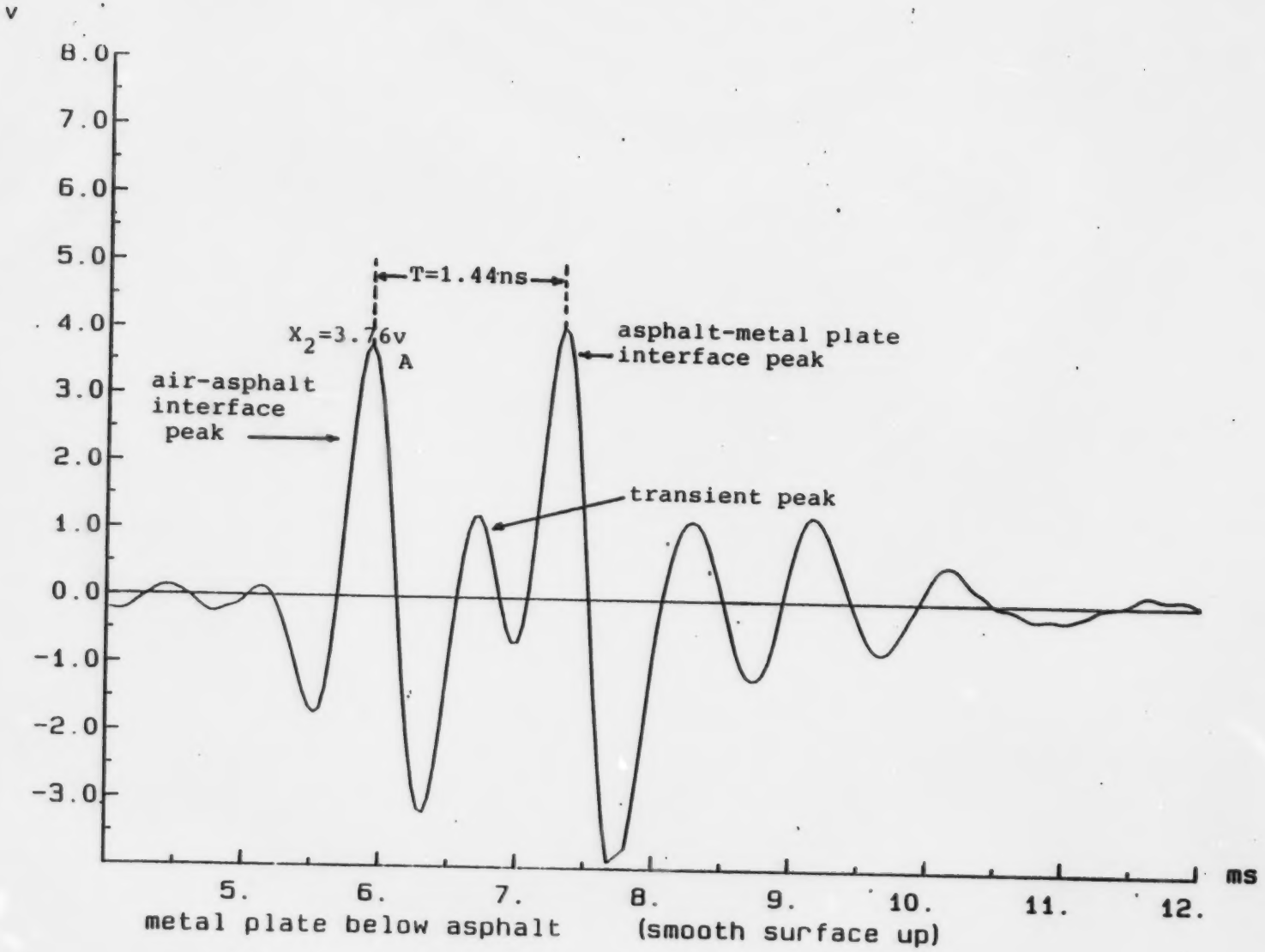

Fig. 3.2: Waveform from asphalt (smooth surface up) over a metal plate. (case 1)

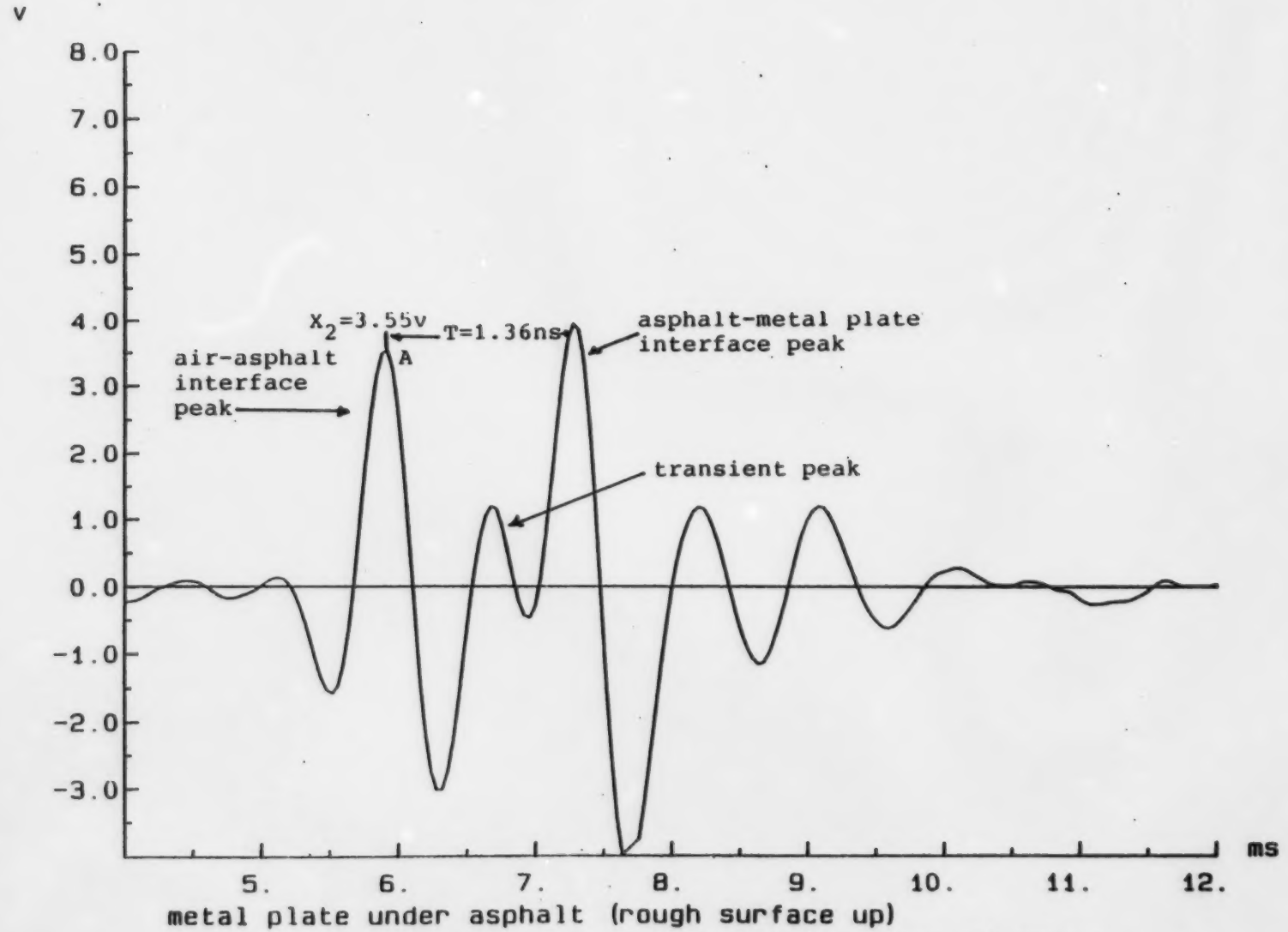

Fig. 3.3: Waveform from asphalt (Rough surface up) over a metal plate.(case 2)

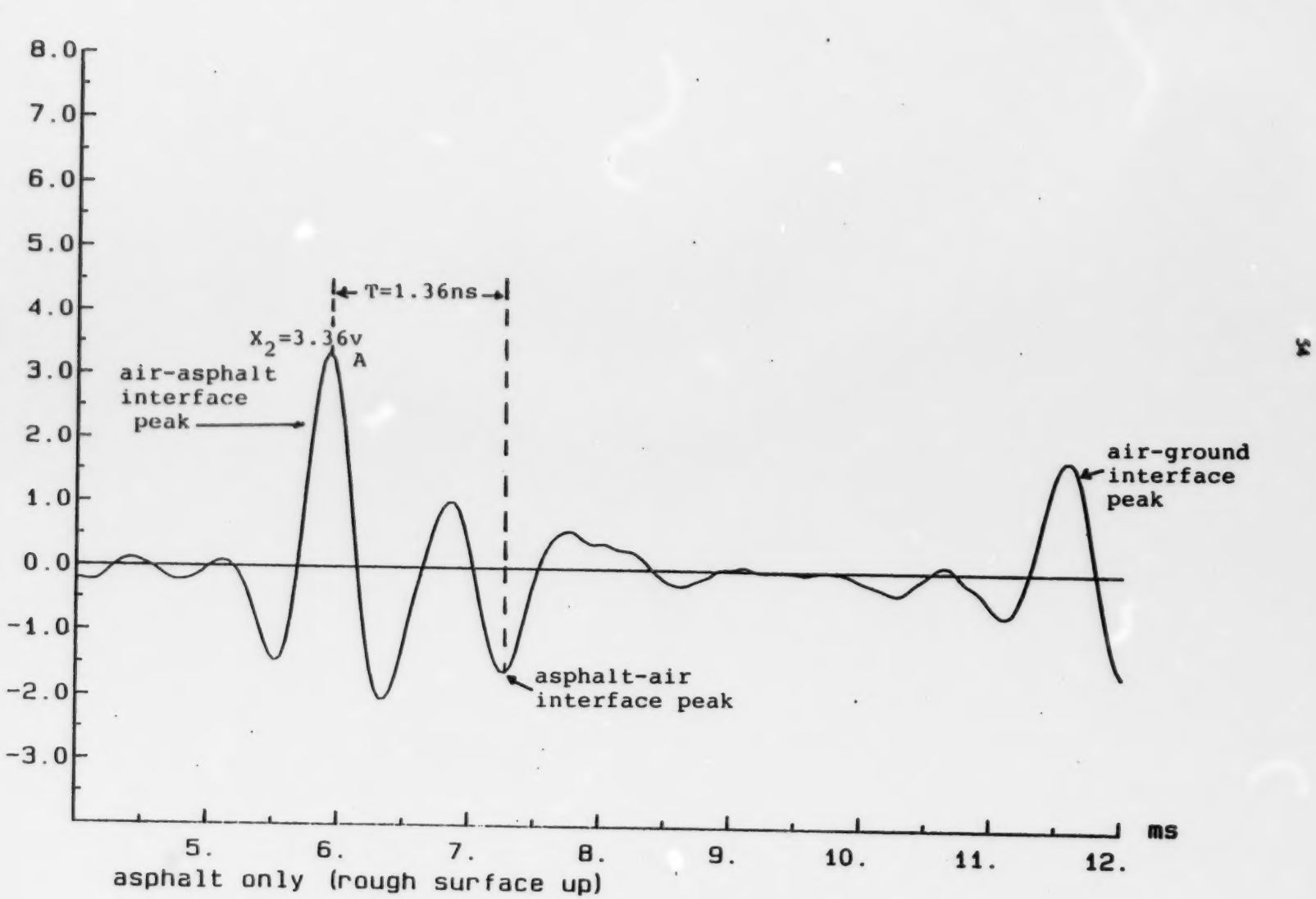

Fig. 3.4: Waveform from asphalt (rough surface up) sample. (case 3)

The larger values of dielectric constant of asphalt for Case 1 and Case 2 using eq. (3.2) in Table 3.1 are thought to be primarily due to the metal plate placed underneath the asphalt. The asphalt-metal interface produces a very strong reflection. The transient response from this reflection distorts the surface reflection peak. As a result, the amplitude of the surface reflection is affected by an amount which propagates through the calculations of air-asphalt reflection coefficient and dielectric constant of asphalt. Note that this distortion does not affect the location of the peaks in time to such a serious extent; thus, the time delay measurement is more accurate. (Of course, in practice, the metal plate is not normally present at the asphalt- concrete interface so this error does not occur).

In case (3), the actual asphalt-concrete interface is replaced by asphalt-air interface. The calculated dielectric constant of asphalt using eq. (3.1) and eq. (3.2) are in close agreement with the difference being only about 1.8%. Thus, we conclude that the asphalt sample has a dielectric constant of around 6.1 to 6.2 and the surface reflection method is indeed accurate to within + 1%.

3.2/ Membrane

For many newer bridge decks, a waterproofing membrane is installed between the asphalt and concrete surface. This extra layer of material produces certain reflections at the asphalt- membrane and membrane-concrete interfaces. The polarity of reflection peak is determined by the difference in dielectric constant between these materials. Assuming that the waterproofing membrane has dielectric constant lower than that of asphalt, then the reflection peak is negative going and vice versa. This identification provides a means of differentiate boundaries of the asphalt-membrane-concrete interface.

In Section 3.1, we calculated the dielectric constant of asphalt. The same method is applied to determine the dielectric constant of waterproofing membrane.

It is found that the major components of waterproofing membrane are rubber, tar, oil and limestone filler. The membrane used in our measurement has dimensions of 44.45 cm in length, 30.48 cm in width and 9.53 cm in thickness. The radar antenna is 22.86 cm above the membrane and 99.06 cm from ground. Figure 3.5 provides the surface reflection waveform from the metal plate which is placed on the surface of the membrane. The metal plate is then placed below the sample and the resulting waveform is given in Fig. 3.6. In Fig. 3.7, the waveform is shown with the metal plate removed.

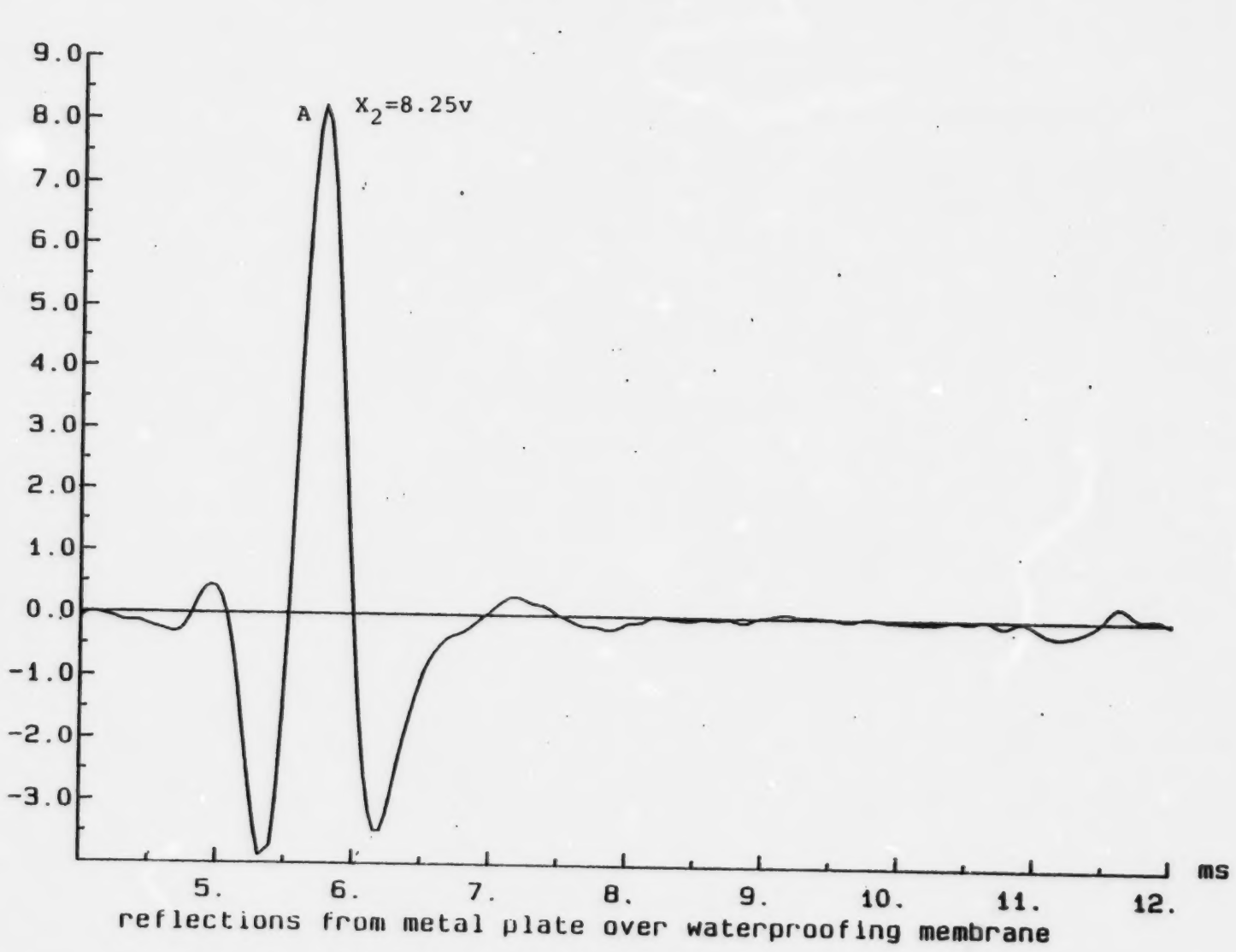

Fig. 3.5: Waveform from metal plate over a membrane sample.

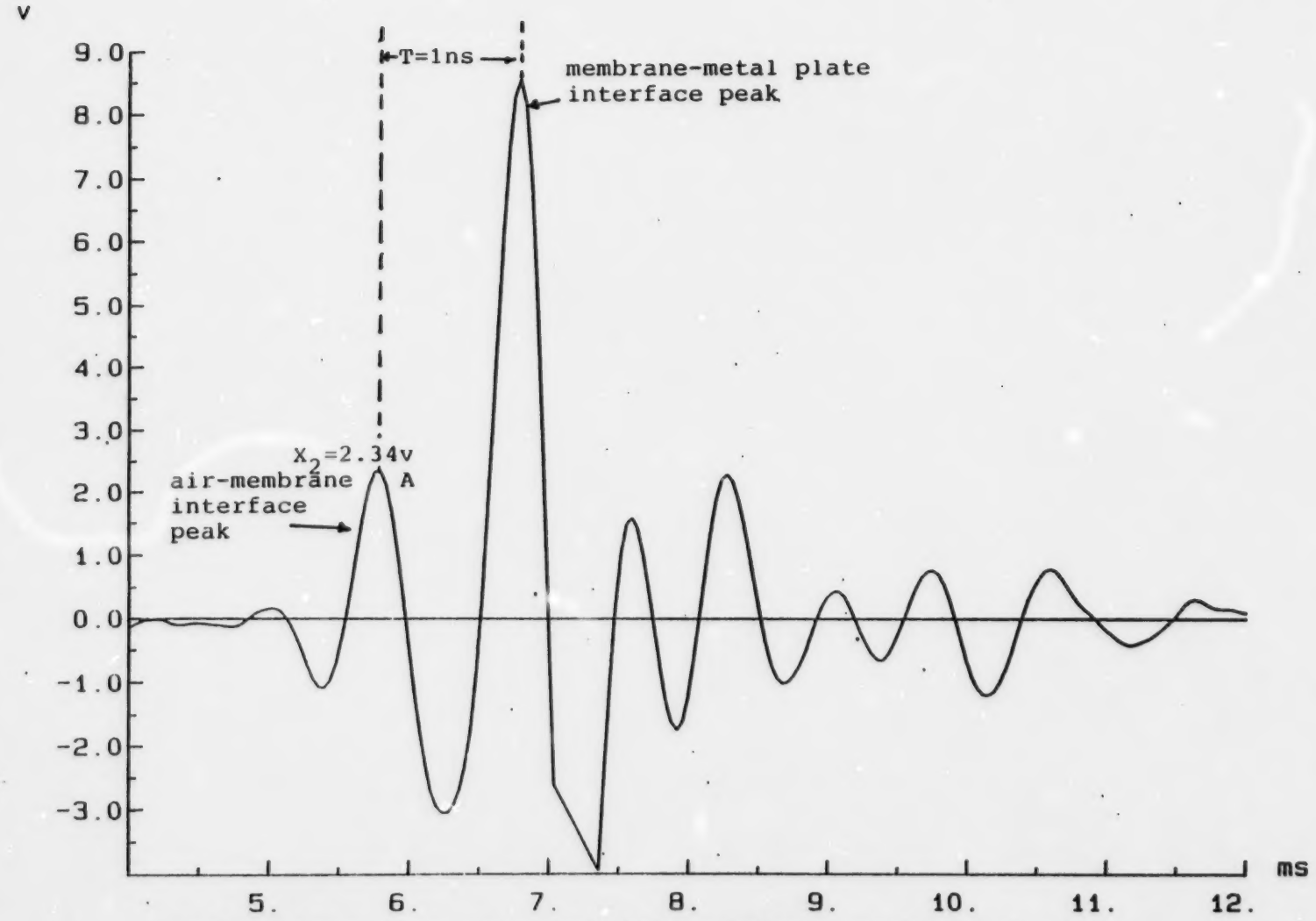

Fig. 3.6: Waveform from membrane sample over a metal plate.

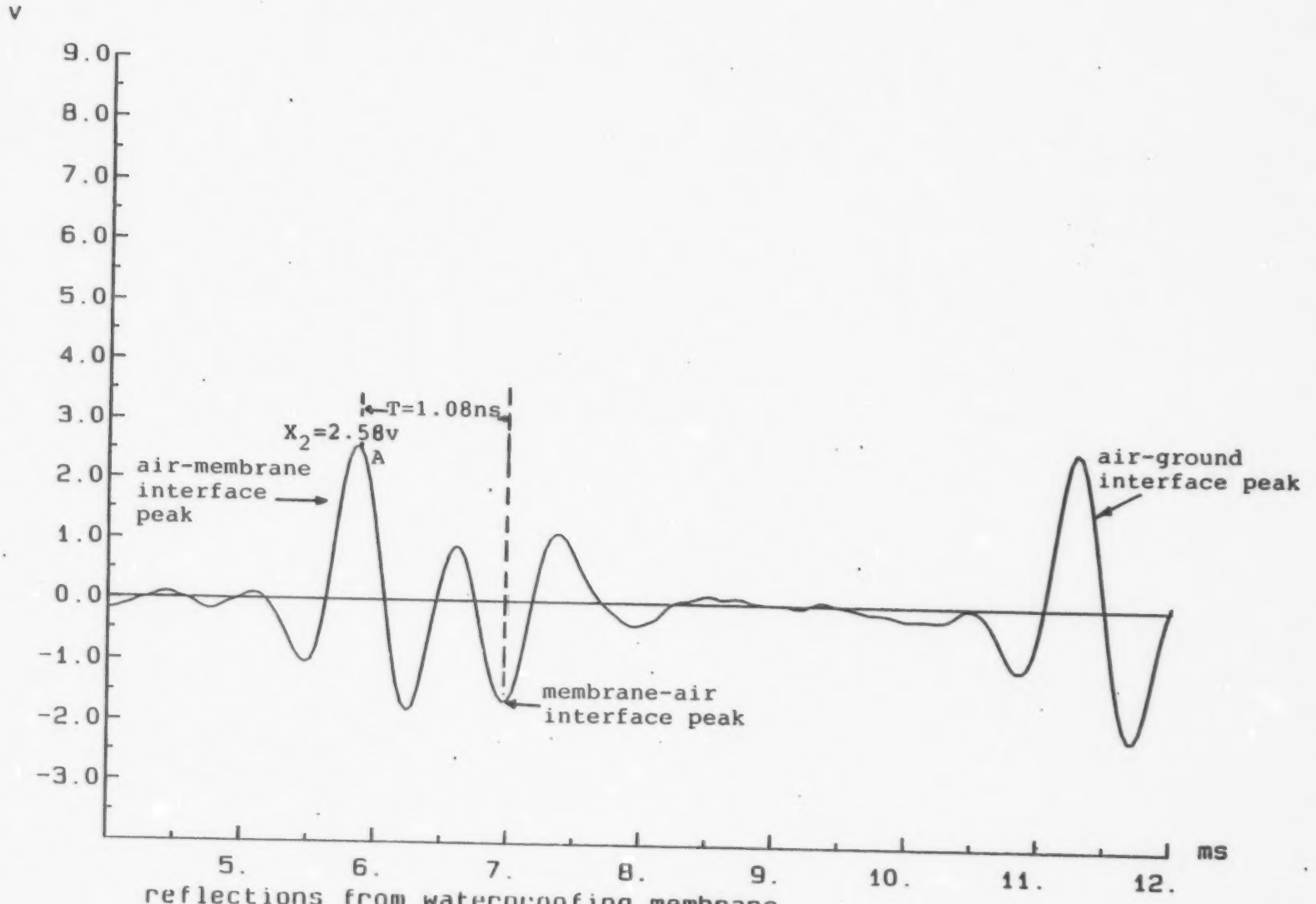

Fig. 3.7: Waveform from membrane sample.

The value of dielectric constant of membrane obtained by calculation using reflection coefficient and exact measurement are compared in Table 3.2. Results from the exact measurement are indicated by brackets,

Table 3.2/ Dielectric constant of waterproofing membrane

	dielectric consultants	
	surface reflections	time delay
membrane over metal plate	3.21	2.48
membrane with no metal plate	3.65	2.89
average	3.43	2.69

The results behave somewhat differently from the asphalt measurement which we have discussed in the previous section. The membrane has a higher value of dielectric constant when the metal plate is removed. However, the reverse was found from the asphalt measurement. Explanations for this behaviour have not yet been verified; however, it is thought that the horizontal crossection of the sample is involved since the waterproofing membrane was only marginally larger than the footprint size of the antenna.

Nevertheless, the value of 2.89 is believed to be reliable for the dielectric constant of the waterproofing membrane since this measurement was performed with no metal plate and employs the time delay technique. Further measurements in this area appear to be highly desirable.

3.3/ Concrete

In this section our objectives are (1) to measure the dielectric constant of concrete, (2) to identify the interface between concrete and ground and (3) to determine the location of reinforcing bars (rebars). The experiments are performed on three different concrete slabs. Each of the test slab has dimension of 82 cm in length, 89 cm in width and an averaged thickness of approximately 16.5 cm.

The first test slab is concrete with no rebars. This is used for the purpose of measuring the dielectric constant of concrete with no rebar influence. The second test slab contains a single layer of parallel rebars centred at 18 cm intervals, 6 cm below the concrete surface. Each rebar has a diameter of 1.27 cm. The third test slab has two layers of rebars forming a cross-hatch matte with interbar spacing of 18 cm. The two layers of rebars are 6 cm and 12 cm below the surface, respectively. When the incident RF wave propagates through the concrete to a layer of rebars, a signal reflection occurs at the boundary. Each measurement is now discussed.

3.3.1/ Concrete with No Rebars

Reflection waveforms recorded from metal plate and concrete surface are given in Fig. 3.8 and 3.9, respectively. The reflection coefficient is about -0.48 as determined by measuring the ratio in amplitude of the two surface reflections. The dielectric constant of concrete is calculated to have value of 8.21.

From Fig. 3.9, it is rather difficult to locate the concrete-ground (soil) interface boundary. The strong surface reflection from the air-concrete interface significantly degrades concrete subsurface detection. One of the effective methods is to subtract the surface reflection from the waveform as has been discussed in Section 2.3. In Fig. 3.10, we show the superimposed waveforms from the concrete and the metal plate (scaled reflection). The residue waveform is presented in Fig. 3.11. We note that there is a residue peak in the time frame of 5.5 to 6 ms. Since, the test slab contains no rebars, this residue peak does not represent a reflection from boundary between different materials. Furthermore, the reflection between the bottom of the concrete and the ground is expected to occur at a later time along the waveform.

It is necessary to amplify the waveform in Fig. 3.11 in order to provide more detailed information. An enlarged view of the waveform is provided in Fig. 3.12. Using eq. (3.1) and giving that the concrete thickness is about 16.5 cm, the concrete-ground reflection is calculated to be at around 8.6 ms. The reflection is a negative going peak which indicates that soil has a lower dielectric constant than the concrete slab. However, this is not always the case. Depending on the soil moisture, the dielectric constant of soil can range from 4 to 20.

3.3.2/ Single Layer Of Rebars

Rebars imbedded in the concrete slab can be identified using impulse radar. In this measurement, we are interested in analysing the radar signatures from one layer of rebars. The concrete slab has

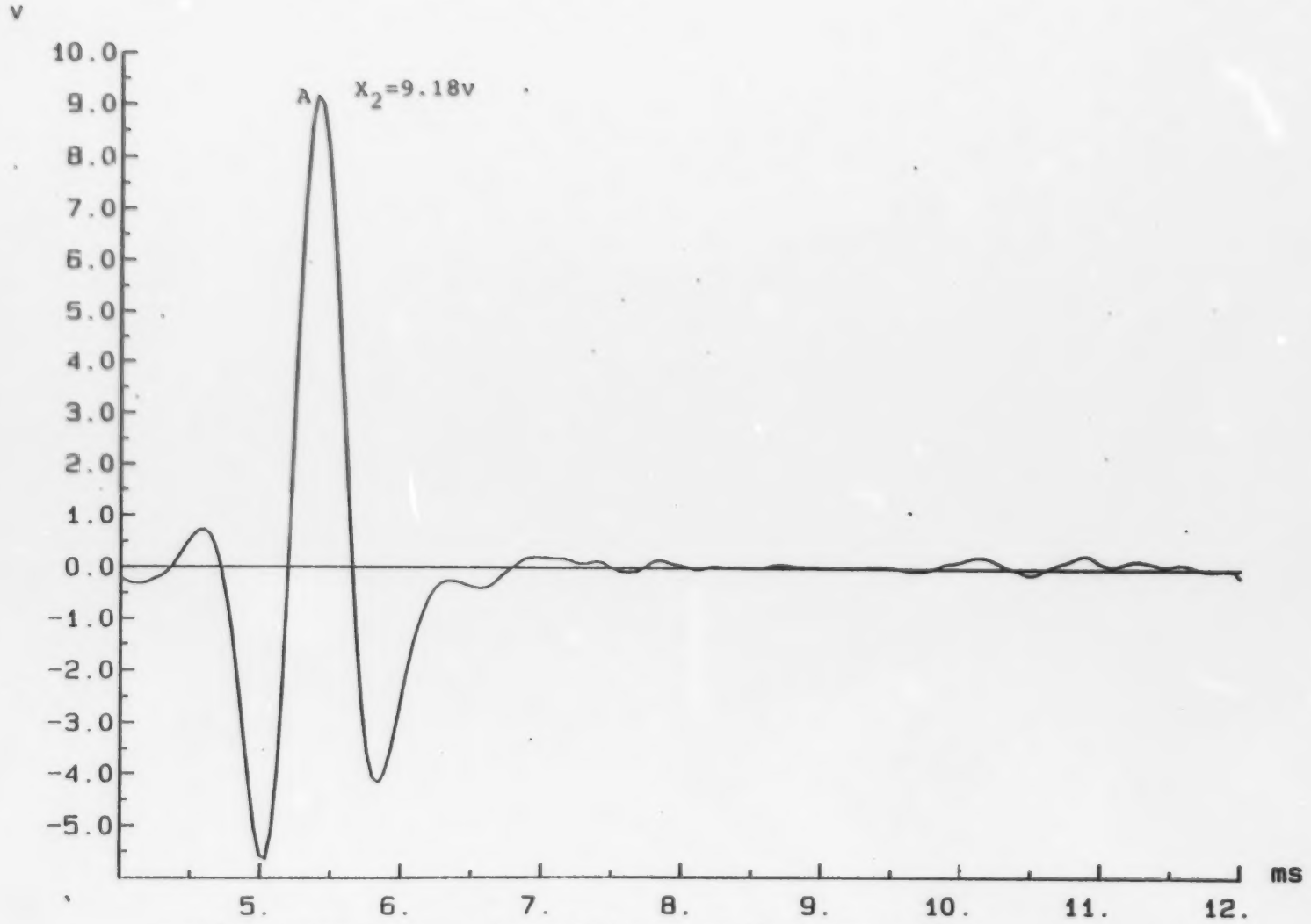

Fig. 3.8: Waveform from metal plate over a concrete slab without rebars.

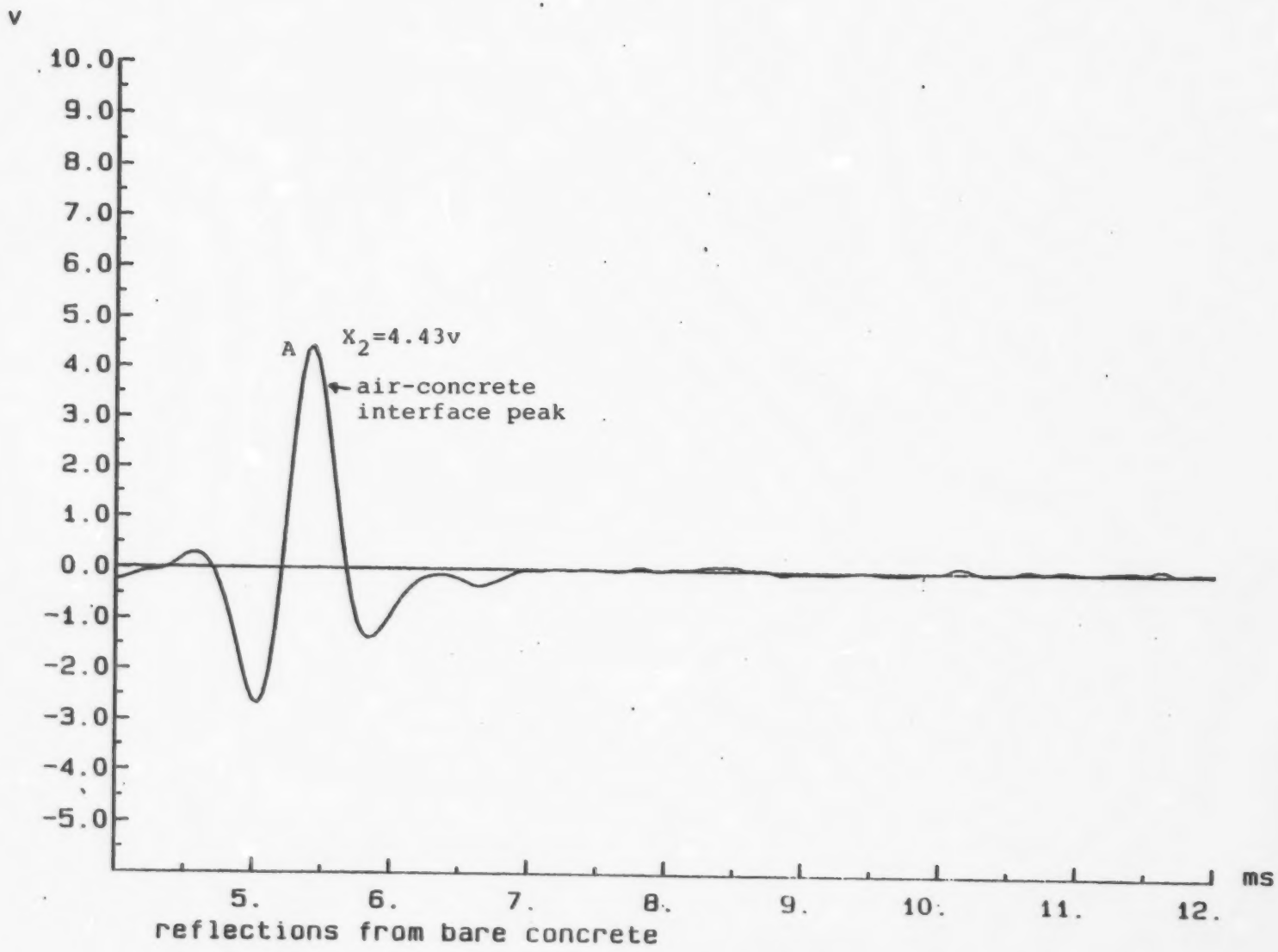

Fig. 3.9: Waveform from concrete slab without rebars.

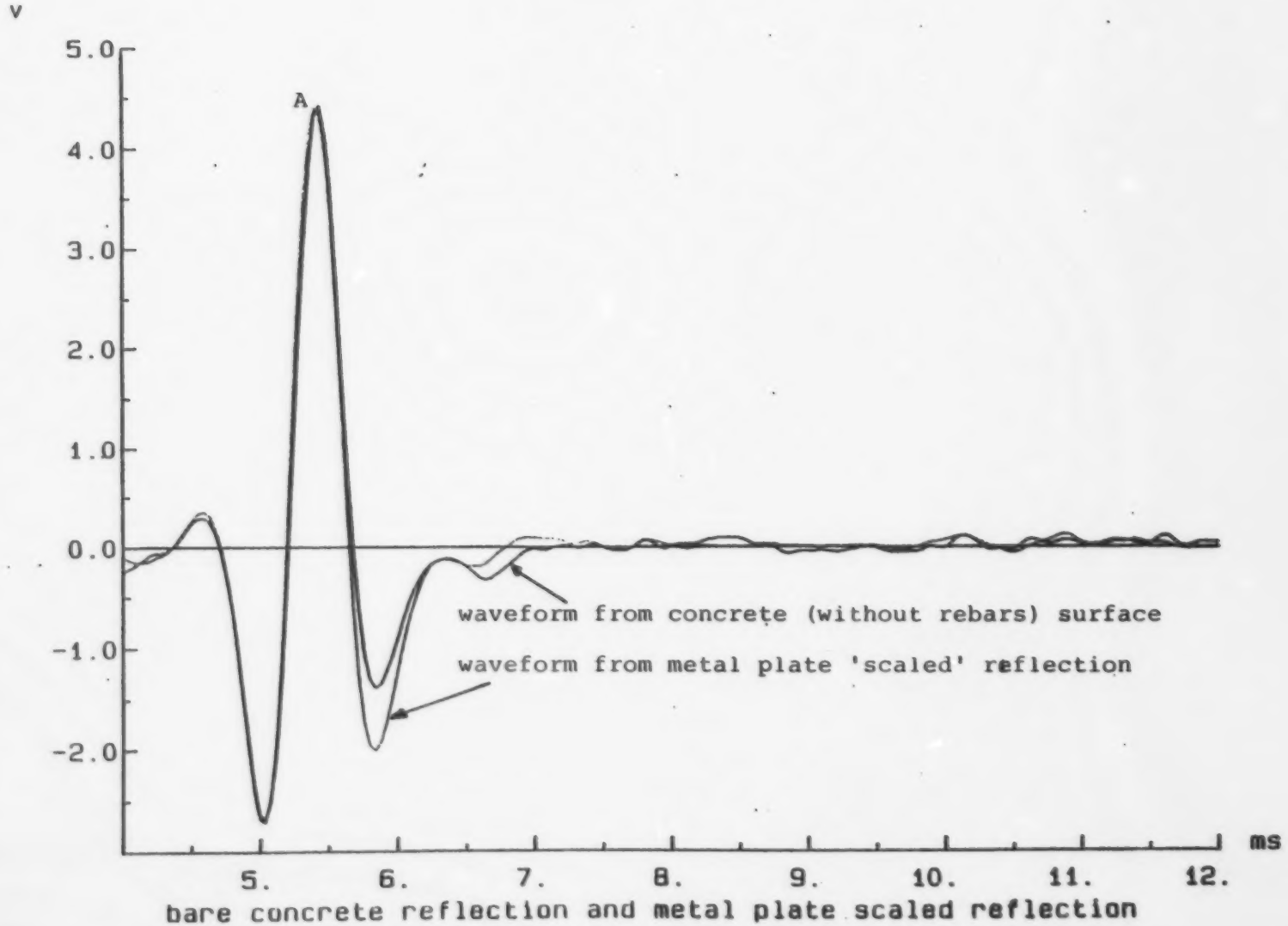

Fig. 3.10: Superimposed waveforms from concrete surface and metal plate.

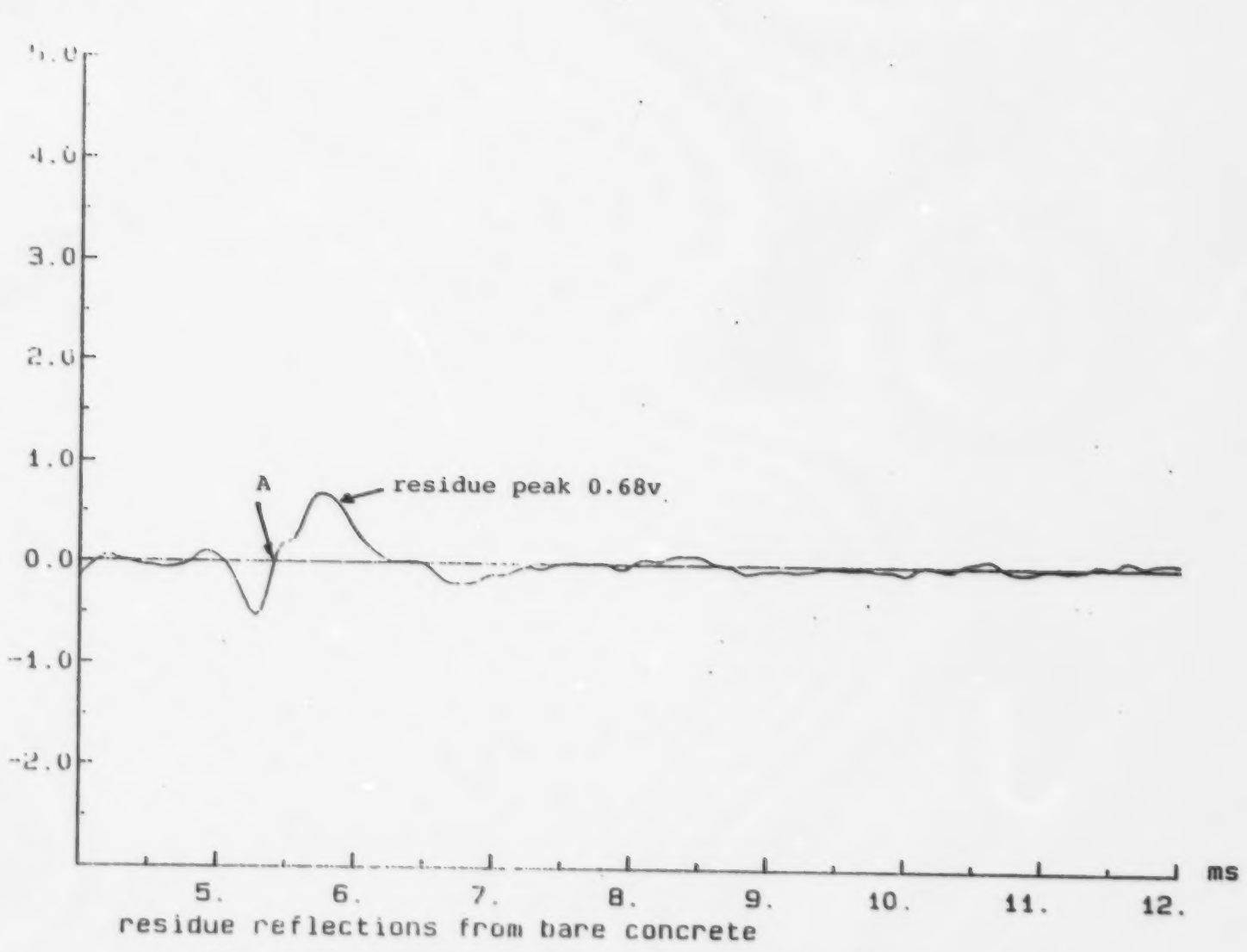

Fig. 3.11: Residue waveform from concrete slab (no rebars).

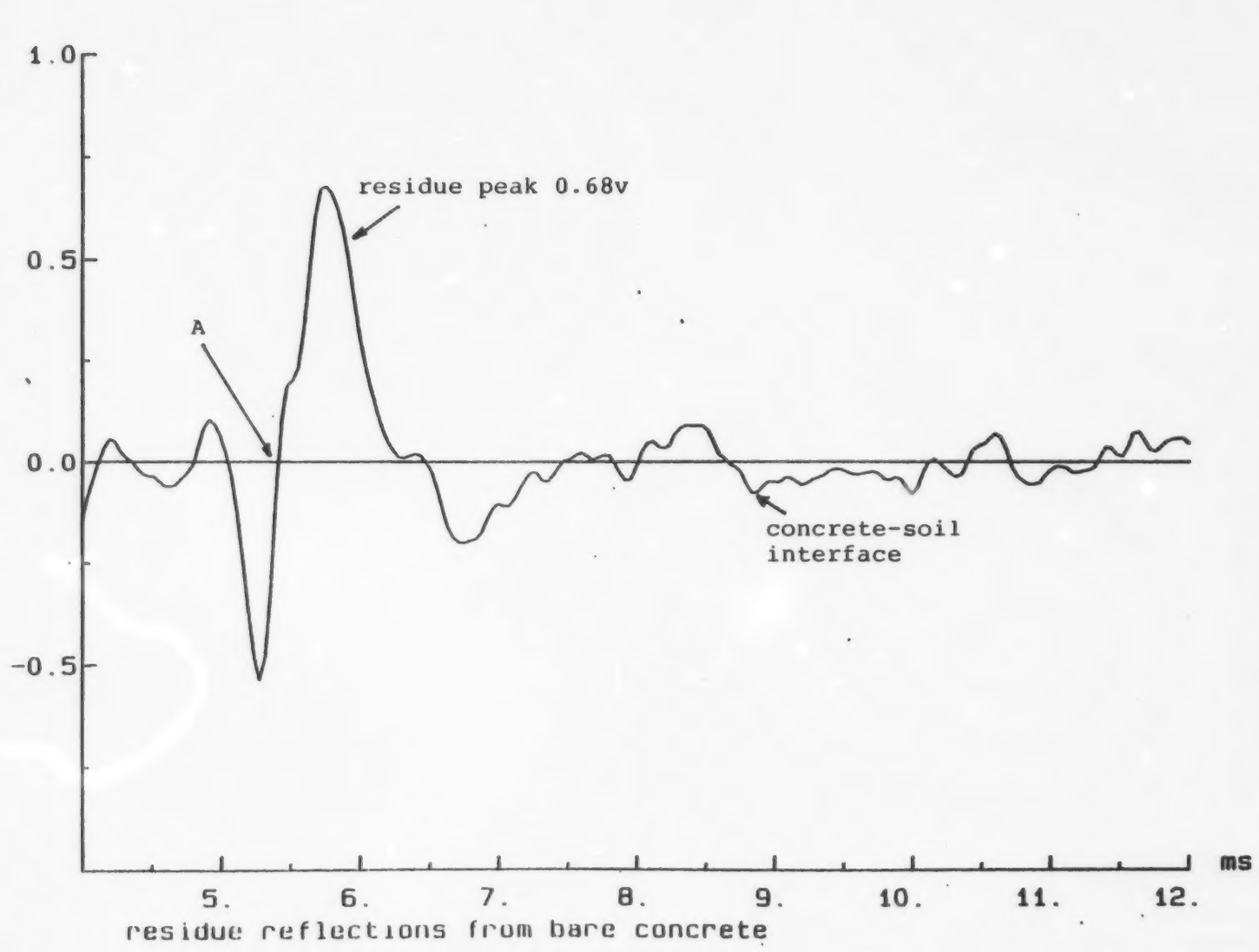

Fig. 3.12: Expanded view of the residue waveform from concrete slab.

four rebars placed horizontally with separation of 18 cm between centres, 6 cm below the surface. Two experiments are conducted on the concrete slab: (1) Measurement is carried out by recording radar waveforms directly over the one rebar and (2) Waveforms are recorded directly between two rebars. These tests are to determine the difference between these two cases.

In Fig. 3.13, the reflected waveform of case (1) is given together with the metal plate scaled reflection. The superimposed waveforms are used for the purpose of surface reflection subtraction. The dielectric constant of concrete is calculated to have value of 6.73 which is lower than that obtained from concrete with no rebars. It is believed that the transient response from the concrete-rebar interface overlaps the surface reflection. As a result, the reflection coefficient is affected. For case (1), the reflection coefficient is determined to be -0.44 (whereas for concrete with no rebars the value is -0.48). After waveforms subtraction, we obtain the residue signal. An enlarged view of this waveform is given in Fig. 3.14. From the plot, we note that there are two prominent positive peaks being indicated as peak B' and C. Peak C is identified to be the reflection from the concrete-rebars interface. The depth of the rebar is computed to be at 6.7 cm below the concrete surface when 6.73 is used as the dielectric constant of concrete and is 6.1 cm if 8.21 is used as the value of dielectric constant giving a total variation of + 5%. The latter figure reflects the actual measurement.

The residue at peak B' belongs to the uncancelled portion, from the waveform subtraction, of the surface reflections from concrete surface and metal plate. This erroneous peak provides misleading information and causes a major concern for the identification process. Therefore, it is necessary to seek a more sophisticated method in order to enhance the waveform analysis.

The superimposed waveforms from the two rebars case and the scaled metal plate reflection are given in Fig. 3.15. The reflection coefficient is determined to be -0.45 and the dielectric constant of concrete is 6.92. The residue waveform is provided in Fig. 3.16. Using the dielectric constants of 6.92 and 8.21, the depth of the rebars is calculated to be at 6.6 and 6.1 cm, respectively. In terms of waveform signatures, there is no significant difference between the cases of reflections from one rebar and reflections from two rebars. It is proposed that, at this stage, that differences between rebar configurations not be considered to be an important factor in our measurements.

It is of particular interest in locating the bottom of the concrete slab. However, due to the changes in the percentage of moisture in soil, it is not that easy to identify the concrete- soil interface. Nevertheless, using the given thickness of the slab and the dielectric constant value at 8.21, reflection at the concrete-soil boundary can be approximated and this is indicated on both plots (Fig. 3.14 and 3.15) for reference purposes.

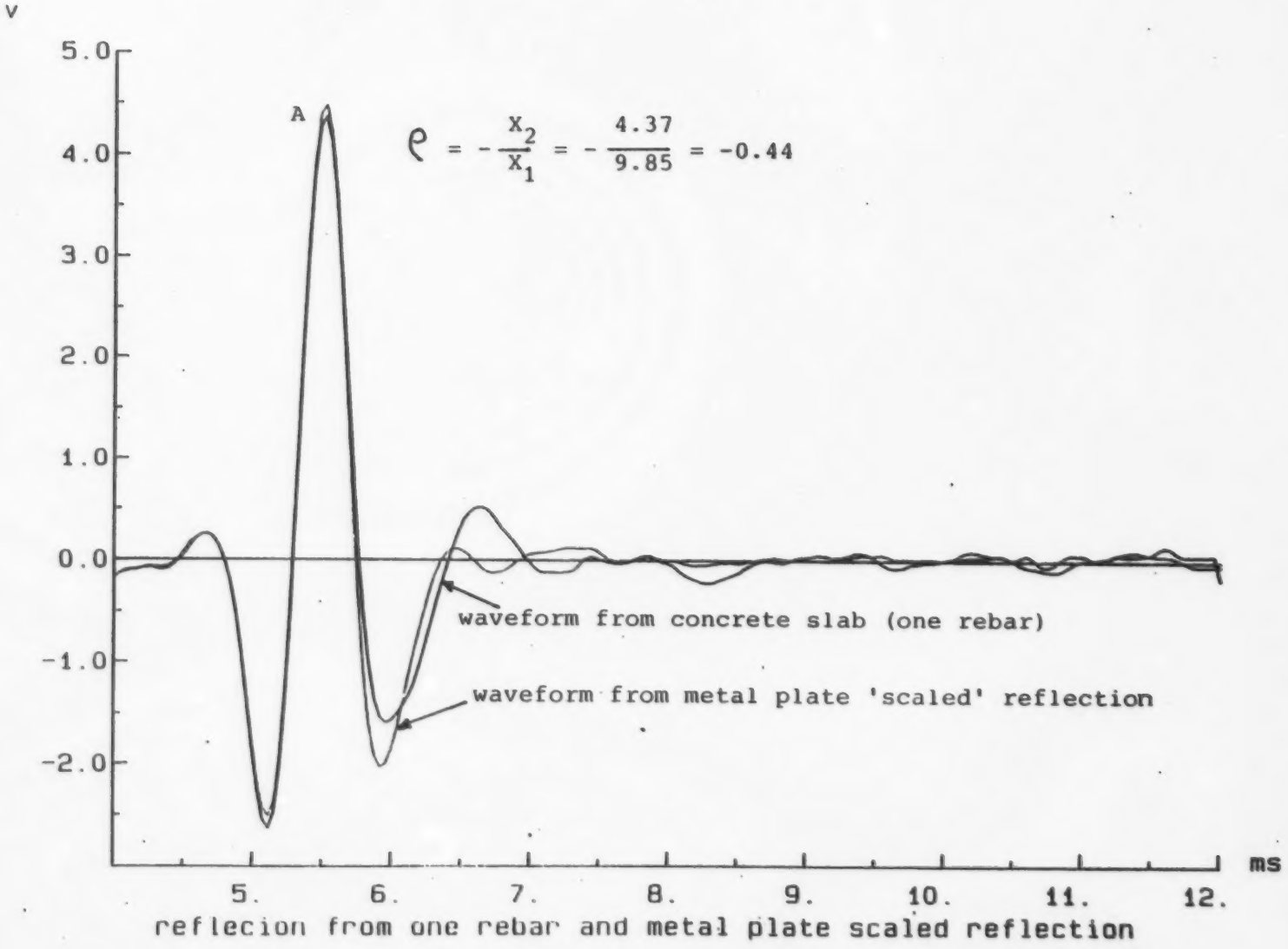

Fig. 3.13: Case 1- superimposed waveforms from metal plate and directly over one rebar.

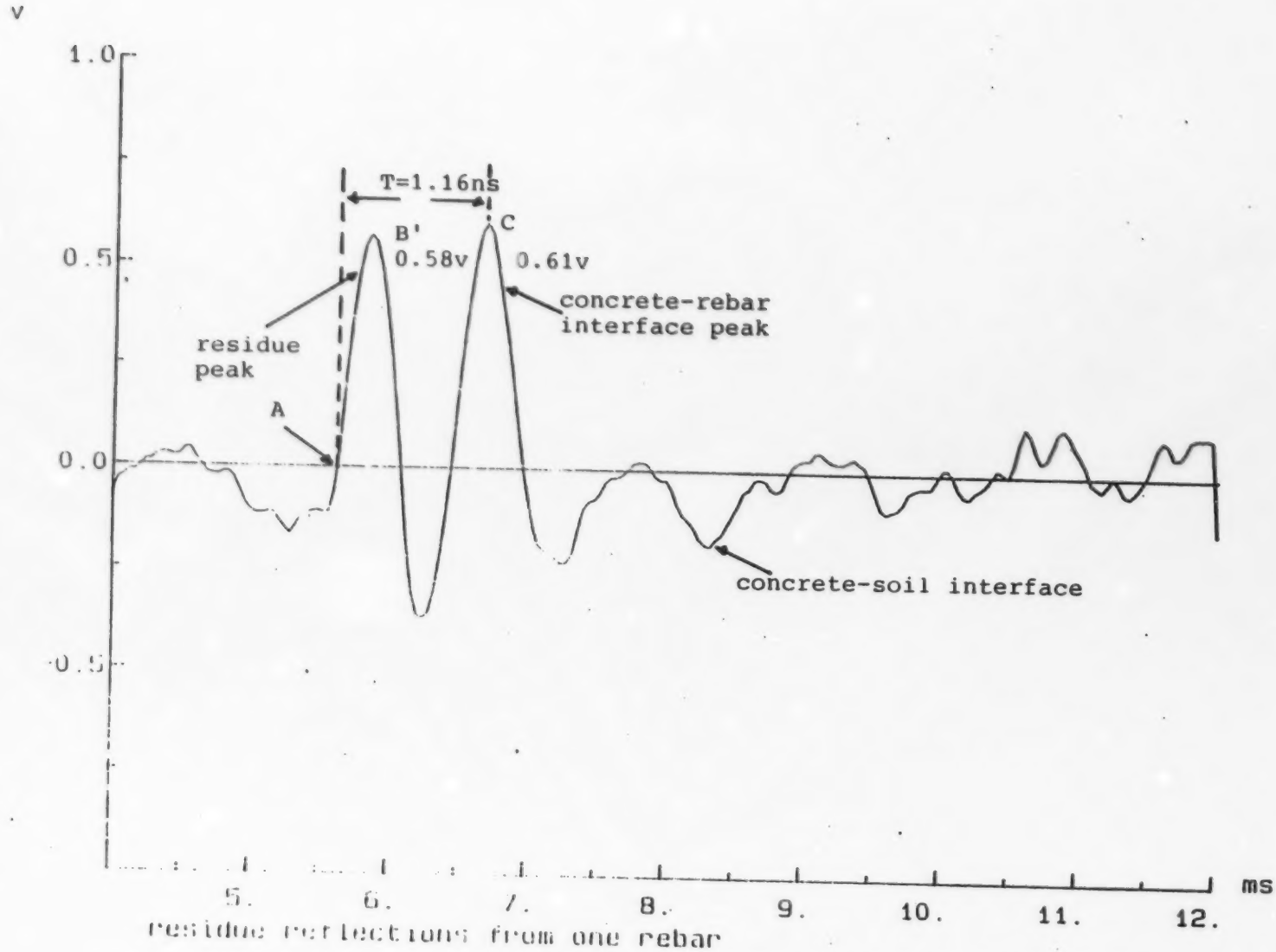

Fig. 3.14: Residue reflections from waveform directly over one rebar.

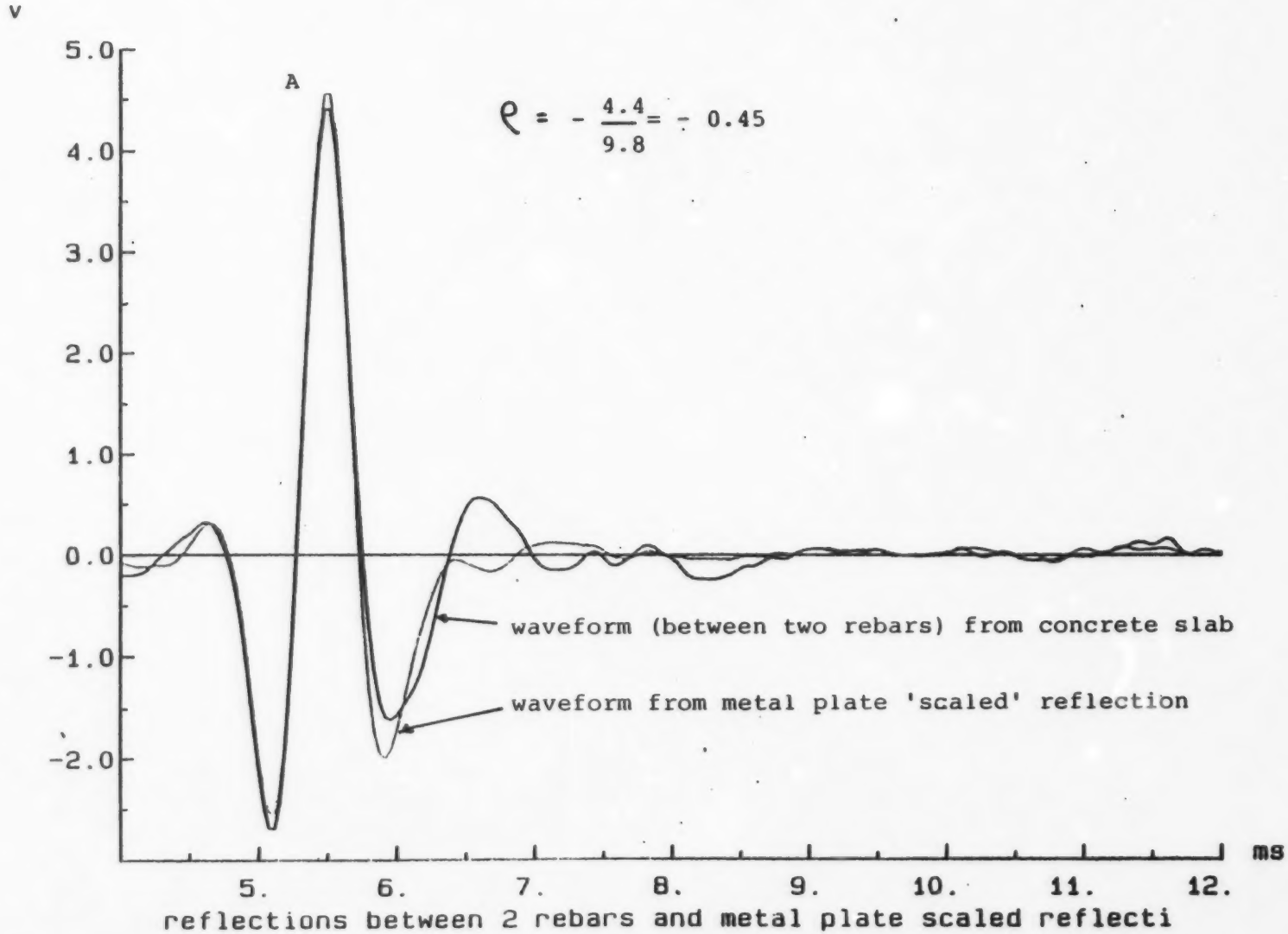

Fig. 3.15: Case 2- superimposed waveforms from metal plate and directly between two rebars .

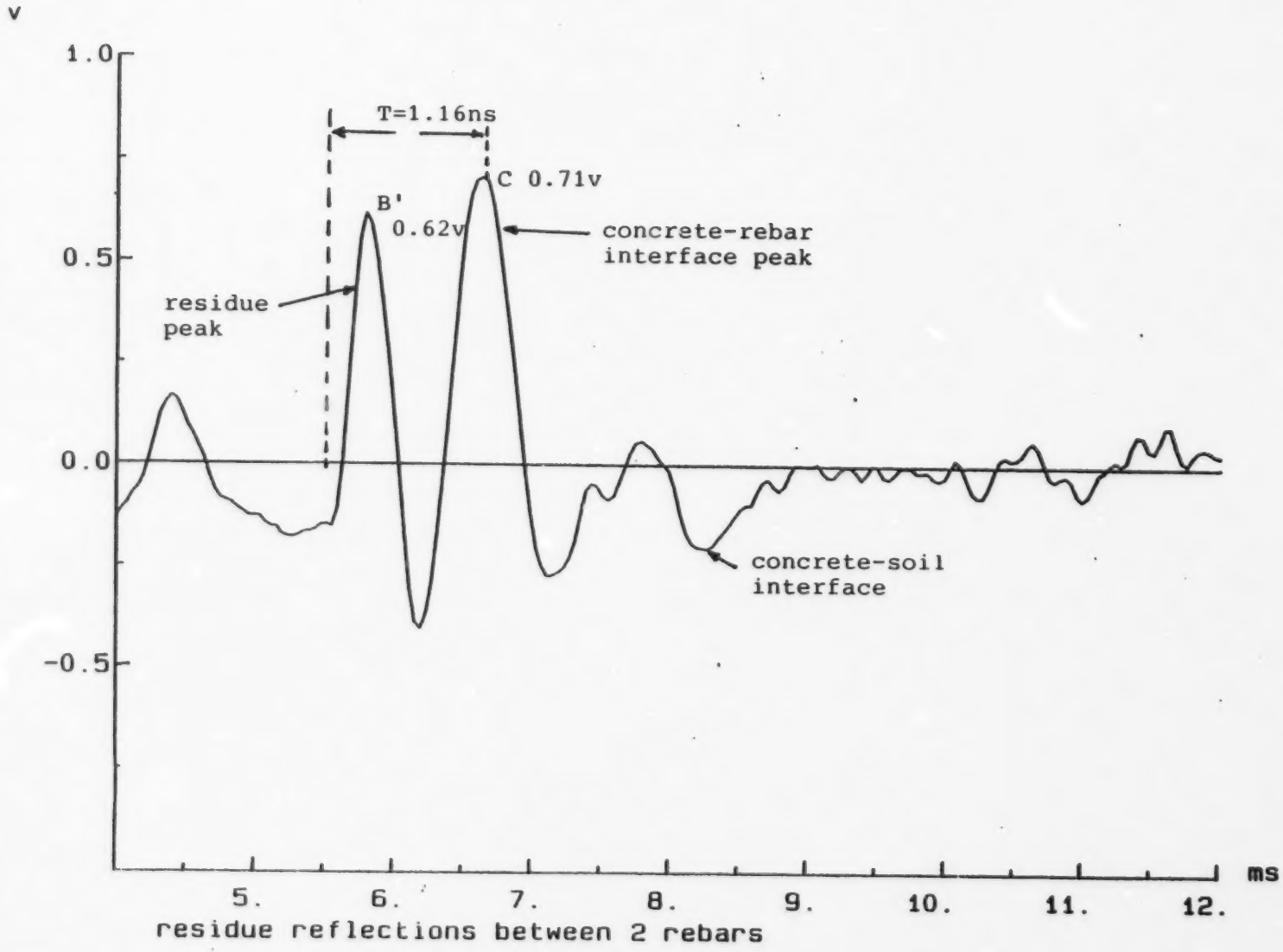

Fig. 3.16: Residue reflections from waveform between two rebars.

3.3.3/ Two Layers Of Rebars

Rebars normally form a cross-hatch matte. Depending on whether the radar antenna is over the cross of the bars or over a space between bars. In either case, most of the signal power passes through the matte but there are still changes in the effective reflection coefficient. In this section, we examine the waveform signatures from three different locations of the matte. These are (1) Over the cross of the two layers of rebars. This is represented by the symbol '+', (2) Between two bars of the top layer and over one bar at the second layer. This is represented by the symbol 'H', and (3) Over the space of the two layers of rebars. This is given by the symbol '#'. Figures 3.17 to Fig. 3.22 are the reflected and residue waveforms of the three cases. The reflection coefficients at the air-concrete interface and the resulting dielectric constant determinations of concrete from the three measurements are reported in Table 3.3,

Table 3.3/ The calculated values of the reflection coefficient at air-concrete interface and the dielectric constant of concrete from the three measurements of two layers rebars

case	+	H	#
reflection coefficient	-0.44	-0.45	-0.42
dielectric constant	6.62	6.99	6.07

We note that the dielectric constant of concrete varies accordingly with the reflection coefficients.

The residue waveforms from Fig. 3.18, 3.20 and 3.22 show that reflections from the concrete-rebars at the top and bottom layers are indicated by peak C and D. The residue peak at B' is still comparable in amplitude with peak C. The depth of the two layers of rebars are measured using the dielectric constant of concrete obtained from each individual case in Table 3.3. In Table 3.4, the results are compared with the calculations which use the dielectric constant of concrete with no rebars. (Note that from actual measurements, the top layer of rebars is 6 cm below the surface and the second layer of rebars is 12 cm below the surface).

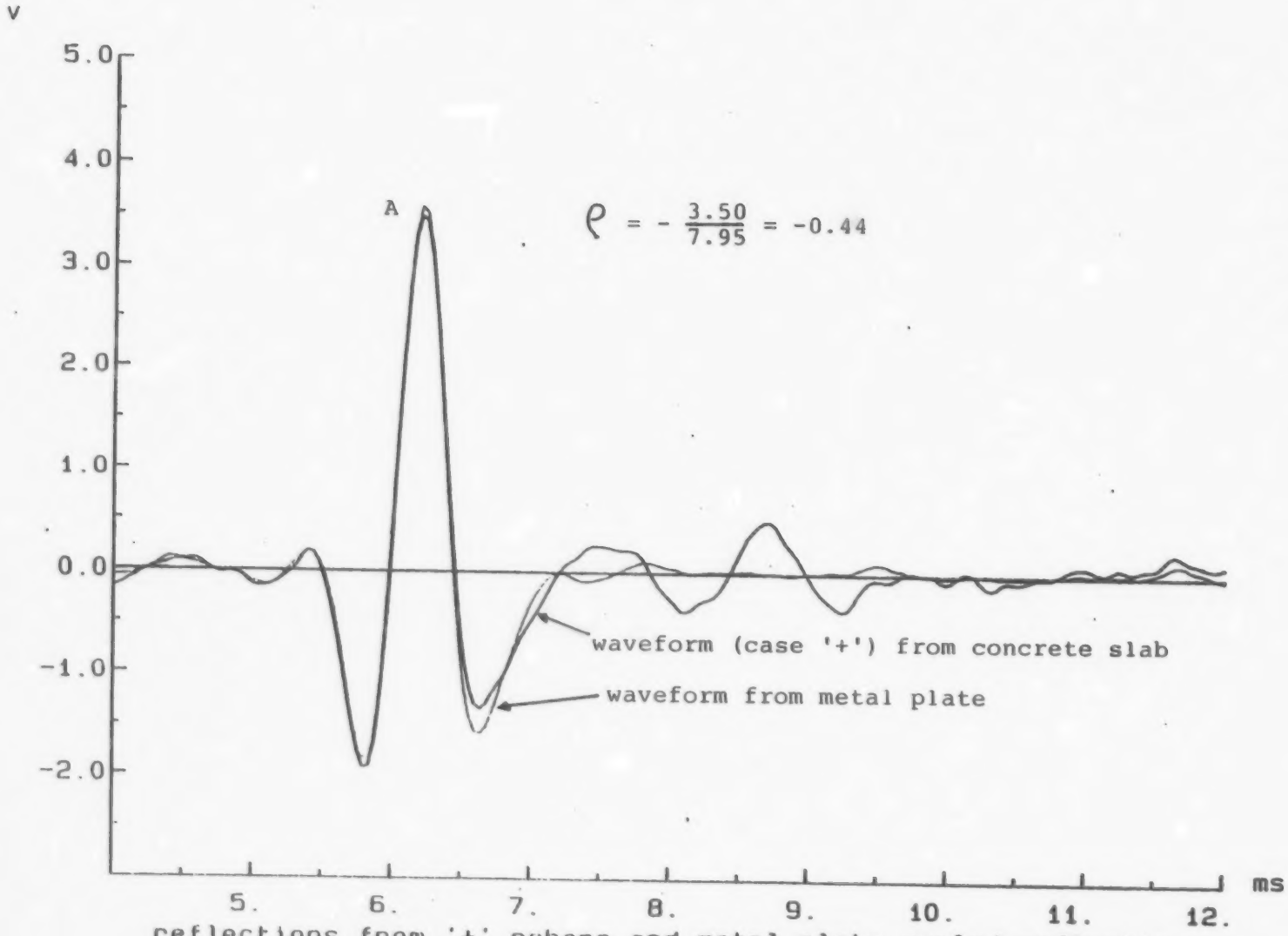

Fig. 3.17: Case '+' - superimposed waveform from metal plate and directly over '+' rebars configuration.

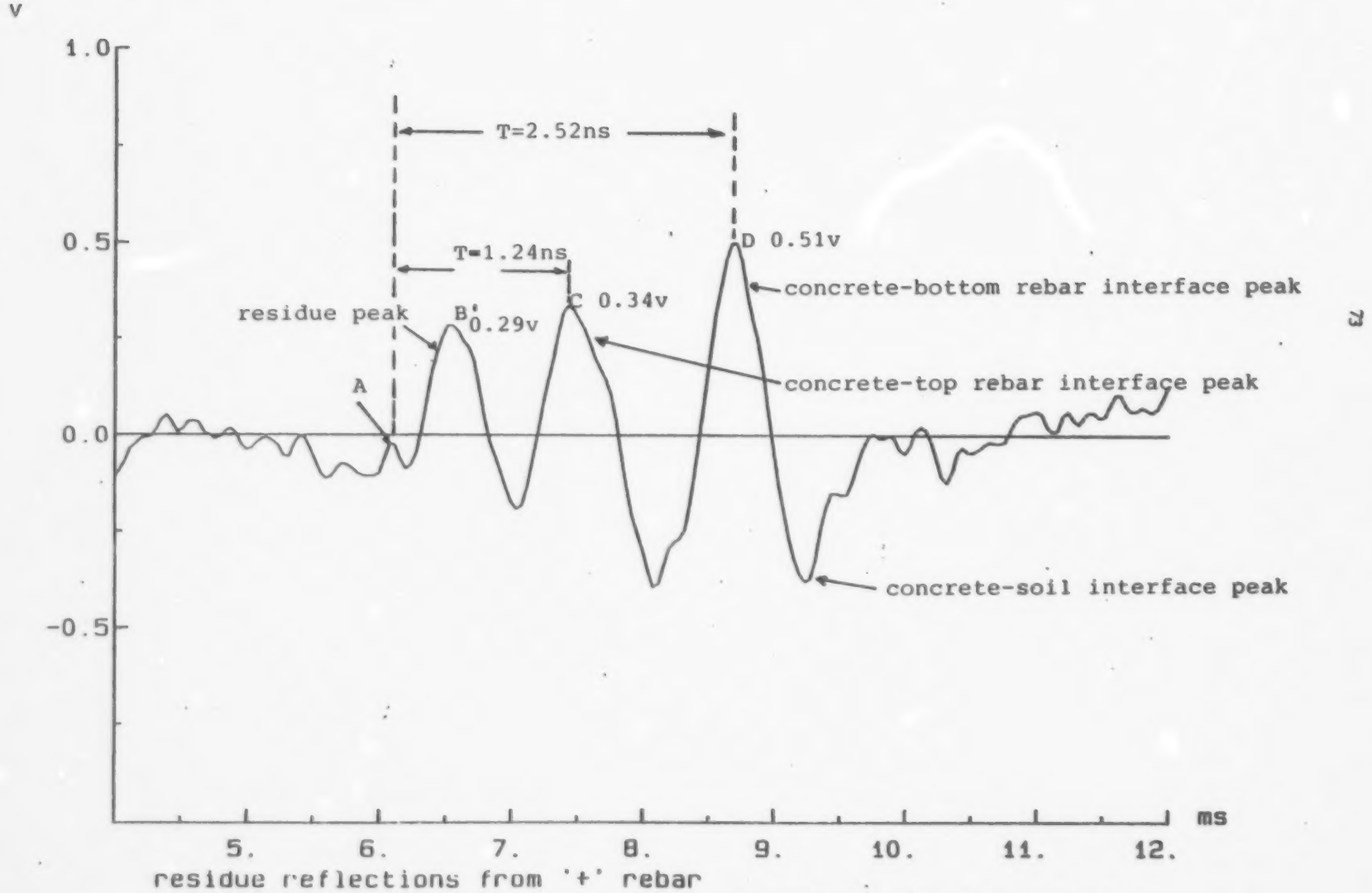

Fig. 3.18: Residue reflections from waveform directly over the cross of the two layers of rebars.

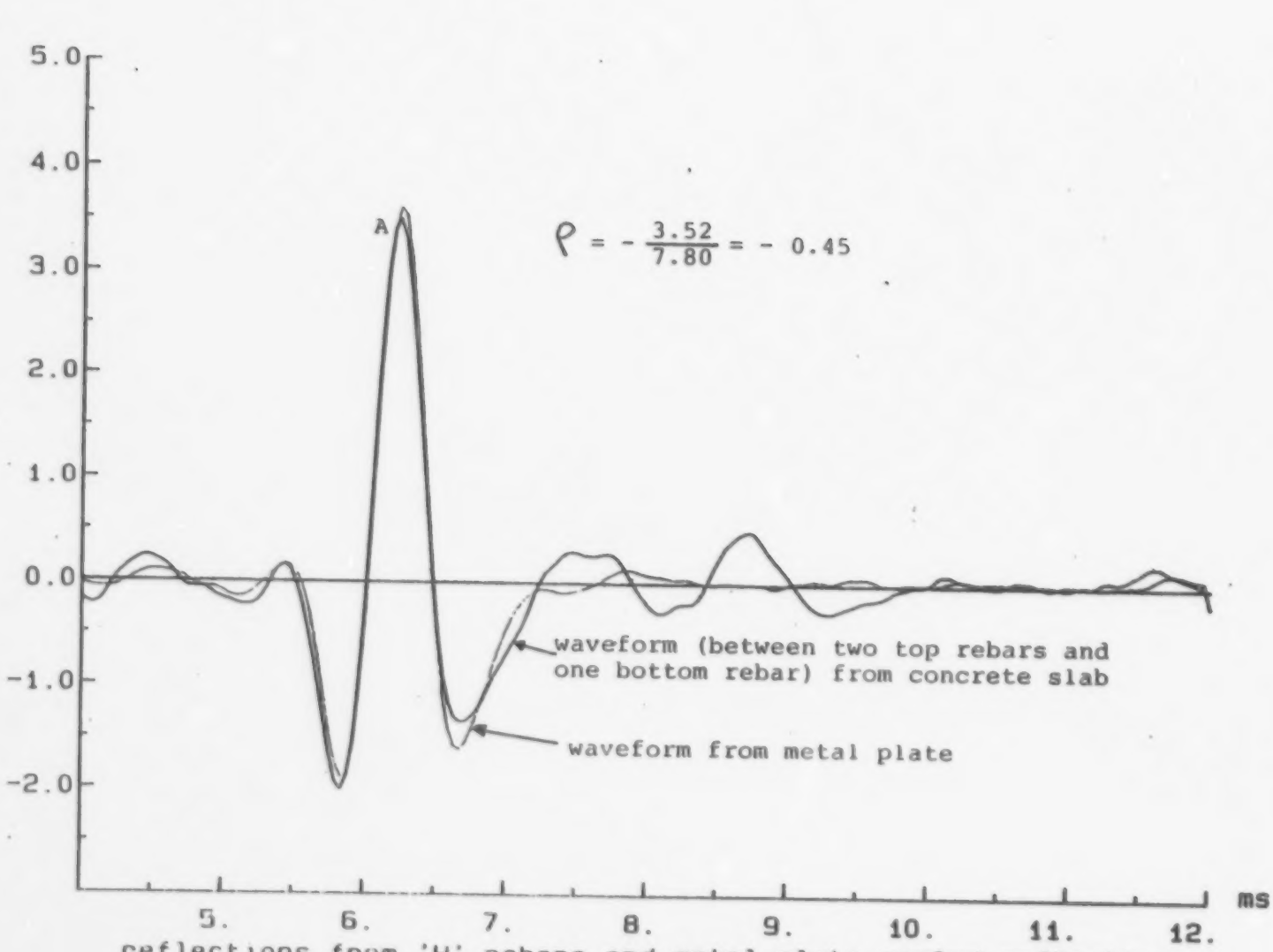

reflections from 'H' rebars and metal plate scaled reflectio

Fig. 3.19: Case 'H'- superimposed waveforms from metal plate and directly over 'H' configuration.

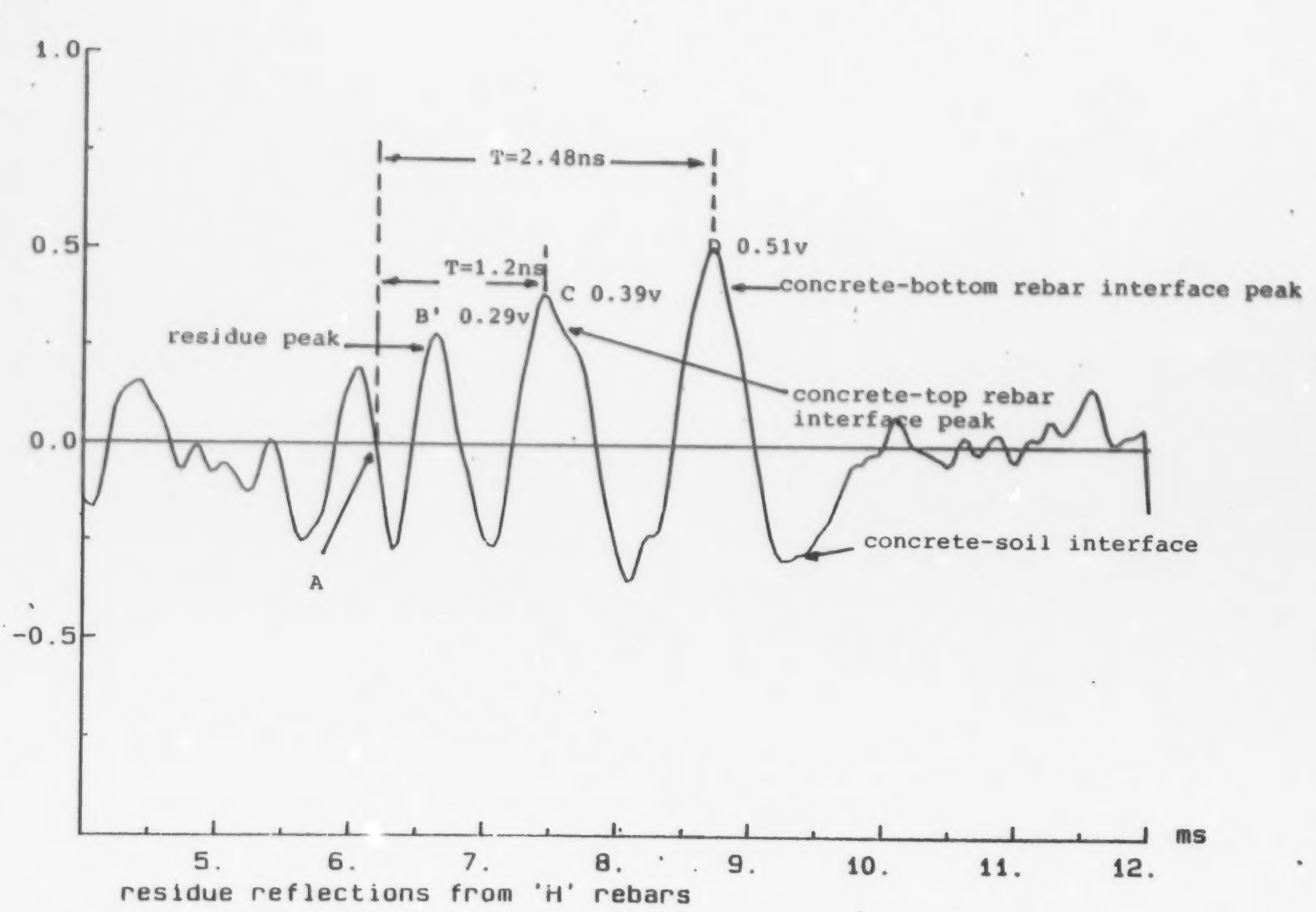

Fig. 3.20: Residue reflections from waveform between two top rebar and one bottom rebar.

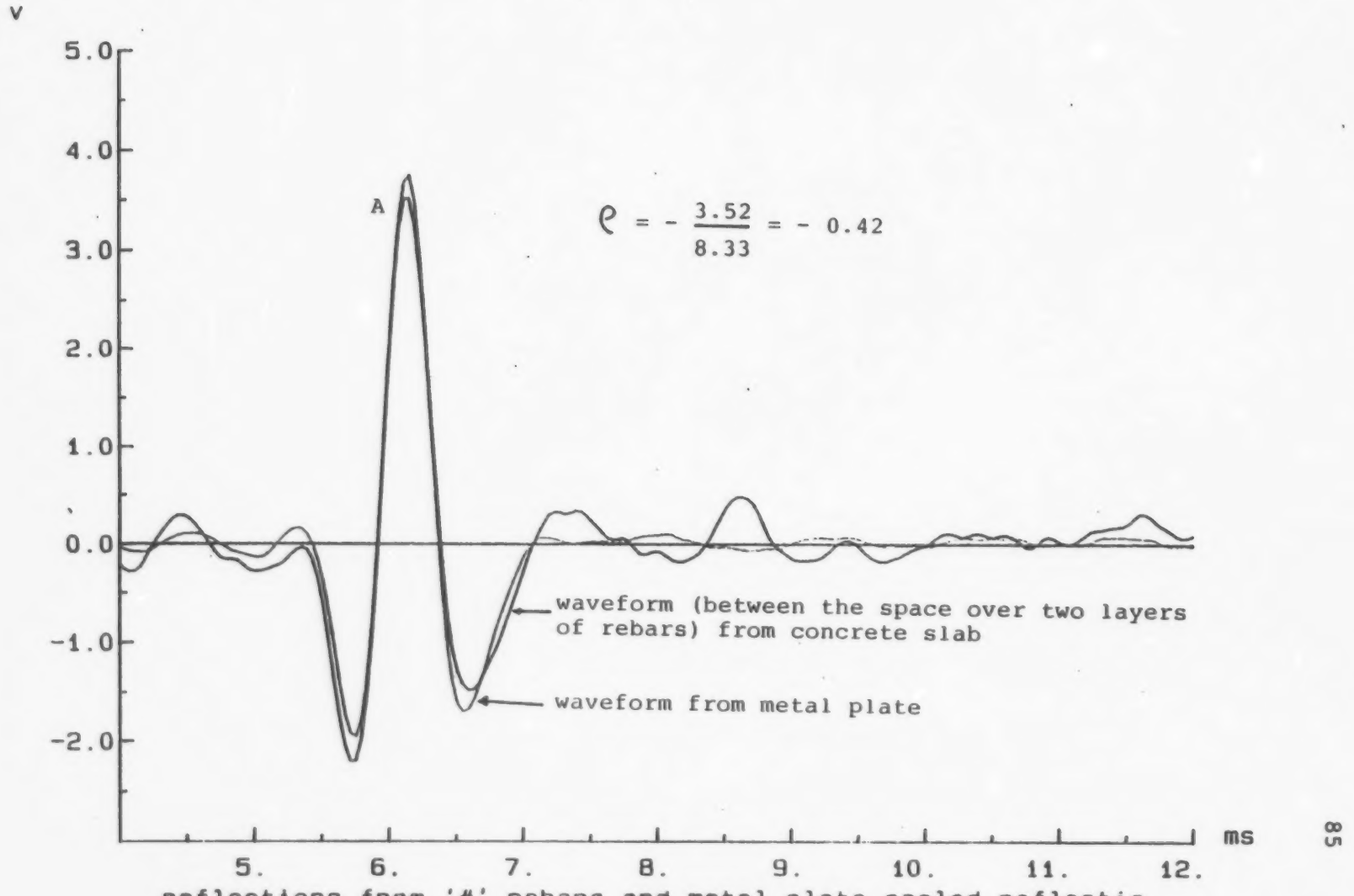

Fig. 3.21: Case '#' - superimposed waveforms from metal plate and directly over the '#' configuration.

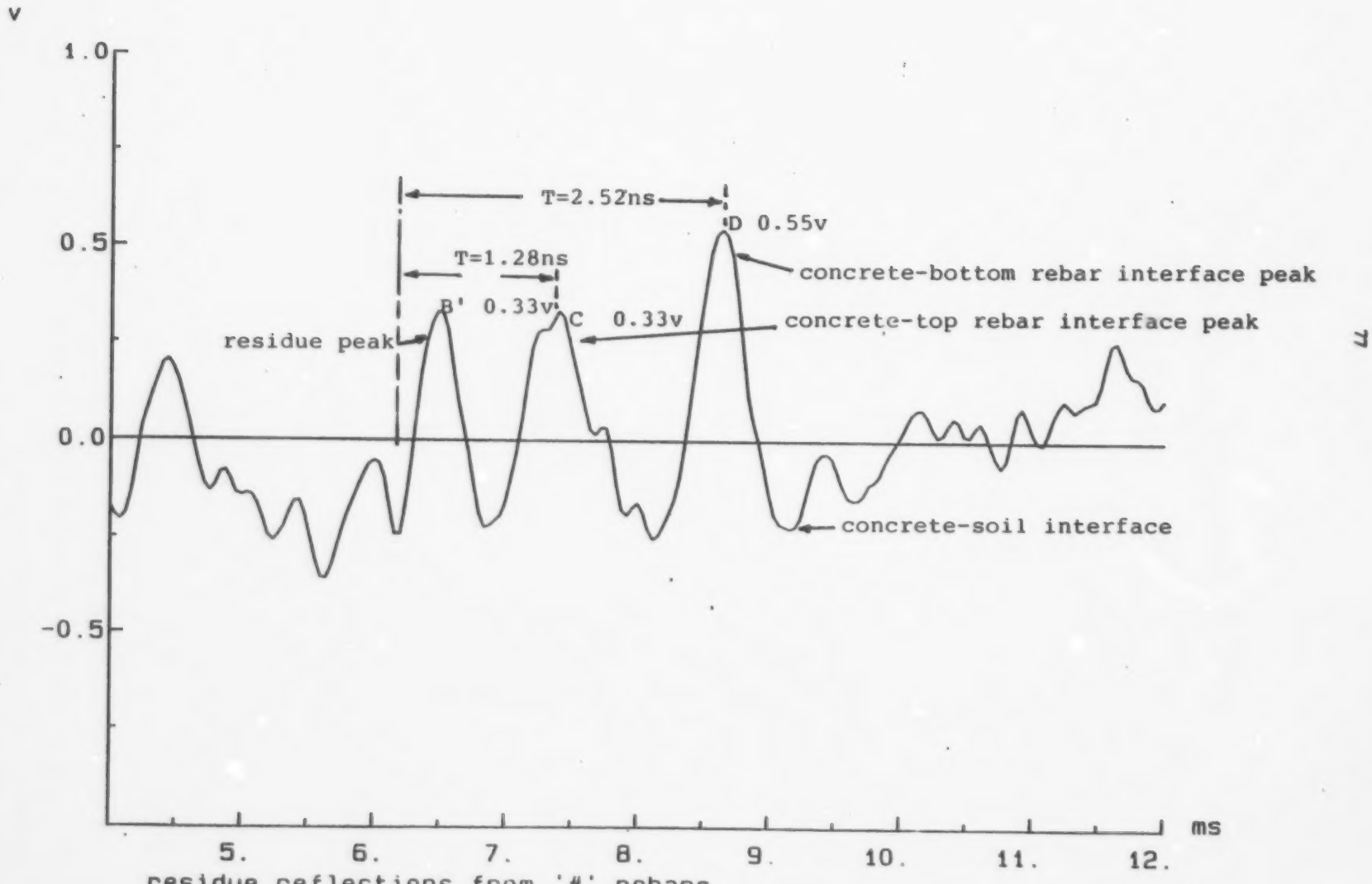

Fig. 3.22: Residue reflections from waveform directly over the space of the two layers of rebar.

Table 3.4 / The depth of the two layers of rebars

case	dielectric constant	Top	Bottom	dielectric constant	Top	Bottom
+	6.62	7.23	14.69	8.21	6.49	13.19
H	6.99	6.80	14.07	8.21	6.28	12.98
#	6.07	7.79	15.34	8.21	6.70	13.01
averages		7.27	14.7		6.49	13.06

From the table, we note that the measured cover over reinforcement using the dielectric constant measured with rebars present is in error by 21% and 22.5% for the upper and lower layers, respectively. For the case of dielectric measurement using concrete with no rebars to deduce the dielectric constant, the corresponding errors are 8% and 8.8%. Since in practice it is difficult to determine the actual dielectric constant of concrete under asphalt, it may be more appropriate to use an averaged value obtained by collecting data on different concrete mixes.

Finally, we see that the concrete-soil boundary is indicated on each plot. Again, this negative peak is far from distinct suggesting that further analysis and measurements are desirable.

3.4/ Summary of Results

Experiments on the properties of asphalt, membrane and concrete have shown that the surface reflection technique presently employed with internal antenna reflections removed is quite accurate for asphalt. The measurements were checked by comparing the propagation time through the asphalt sample and the agreement in dielectric constant calculation was found to be within + 1%.

For the membrane, the measurement was not quite as precise due to what is thought to be the smaller size of the sample. The results do indicate that membrane has a dielectric constant about half that of asphalt which may be useful in helping to identify the boundary with concrete. It is suggested that further work take place to more accurately categorize the material.

Measurements on the dielectric constant of concrete were quite revealing. It was found that the rebars imbedded in concrete upset the dielectric constant deduced from surface reflection measurements. Further study in this area may be required.

4/ Cluster Analysis

The problem of collecting reliable information on the condition of asphalt-covered bridge deck is particular acute in waveform processing. It has been demonstrated that boundaries between different materials can be determined by observing phase shifts from the reflected waveforms.

Using a simple bridge deck structure as shown in Fig. 4.1, a transmitted radar signal travels from air into asphalt into concrete and reflects off the rebars. When the incident signal reflects from the asphalt surface, the waveform experiences a 180 degree phase shift since the dielectric constant of asphalt is higher than that of air. The incident wave propagates through the asphalt resulting in another reflection at the asphalt-concrete interface again with 180 degree phase shift relative to the incident wave since the dielectric constant of concrete is higher than that of asphalt. The incident wave continues to propagate through the concrete to the layer of rebars where a third reflection occurs, also with 180 degree phase shift relative to the incident wave. The three reflections are sketched in Fig. 4.2 where we see that the peak at A represents the reflection from asphalt; the peak at C is produced by the asphalt-concrete interface and the reflection at D is from the rebars. The negative peak at B is the transient portion of the waveform. With peak A, C and D being identified, the thickness of asphalt and cover over reinforcement bars can be measured using eq. 3.1.

We note that the well-defined features of the three peaks definitely facilitate any peak detection algorithms. Since the antenna is at a fixed distance above the asphalt surface, it is expected that the locations of both peaks A and B are relatively stationary with respect to time or sample point number. The location of peak C depends on the thickness of asphalt layer which may not be uniform over a given bridge deck. Also, the layer of rebars may not be aligned properly. As a result, the locations of peaks C and D vary among waveforms. It is envisaged that some knowledge about the spread of these peaks would benefit the reliability of system performance. Cluster analysis is the most convenient method in measuring such variations.

For a given set of data, the mean, variance and standard deviation are the three basic measurements in cluster analysis. The mean yields the averaged value of a data set. This is defined by

$$\bar{m} = \frac{1}{N} \sum_{i=1}^{N} x\ i \qquad (4.1)$$

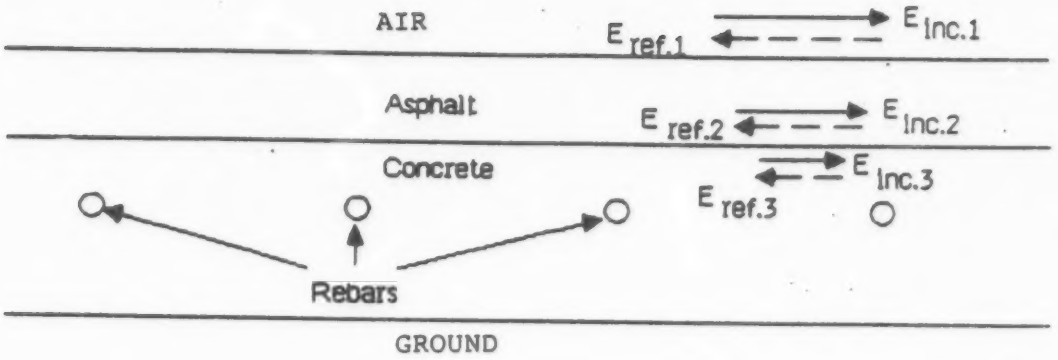

Fig. 4.1: Transmission and reflection of the radar signal from the bridge deck structure. Note that the reflected waves are all 180 degree out of phase with the incident waves.

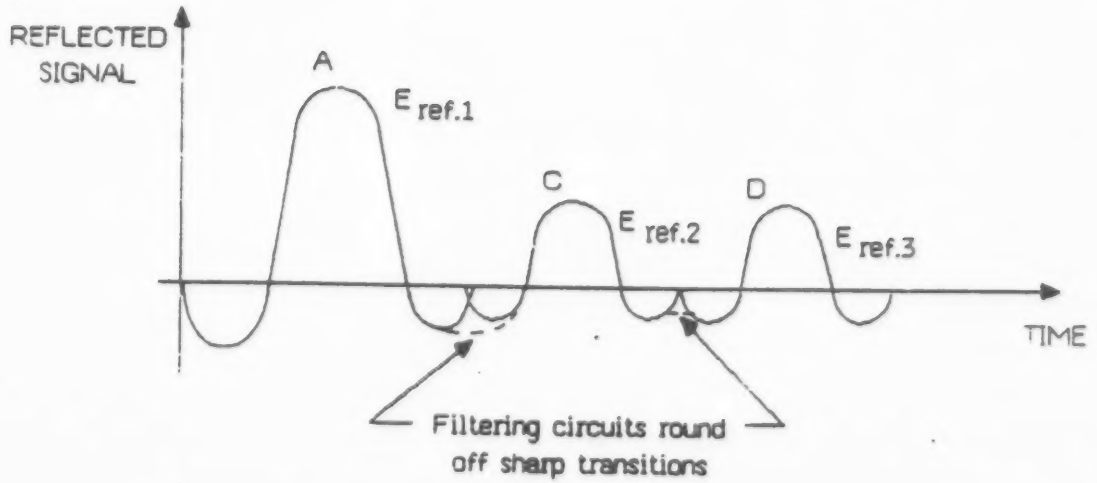

Fig. 4.2: Signal received from the bridge deck structure. Note the peaks A, C and D are all well defined.

where N is the total number of observations and x_i (at the ith observation) can be any one of the following parameters:

1) the sample point number of each peak location

2) the amplitude voltage of each peak

3) the thickness of asphalt layer

4) the thickness of cover over reinforcement bars

The variance is a measure of the spread or variation of the value of x_i

$$\sigma^2 = \sum_{i=1}^{N} (x_i - \bar{m})^2 \qquad (4.2)$$

The square root of the variance gives the standard deviation. We can also calculate the percentage of variation using the mean value and standard deviation

$$e = \frac{\sigma}{\bar{m}} * 100\% \qquad (4.3)$$

In Fig. 4.3, a sample output of cluster analysis is produced for a set of bridge deck data (320 waveforms). Statistical measurements are provided for peaks A,B,C and D. The first entry inside the bracket is related to the sample point number of the peak and the second entry is related to the amplitude voltage. From Fig. 4.3, peak A is on the average located at sample point number 133 with an averaged amplitude of 4.328483 V; the variance of the sample point is 0.7 and variance of the amplitude voltage is .058327 V^2 ; the standard deviation of the sample point is 0.8 and the standard deviation of the amplitude voltage is .24151 V; the variation in sample point is .63% and the variation in the amplitude voltage is 5.58 %.

The statistical values of asphalt thickness and cover over reinforcement bars are indicated by THK(.) and COR(.) respectively. Both measurements are given in mm.

Ninth Line (Oakville): Feb 18, 1988
LINE : 2, CLUSTER ANALYSIS REPORT

*** MEAN values ***

A(133 4.328483) B(143 -1.476318) C(174 .784546) D(211 .414782) THK(97) COR(76)

*** VARiances ***

A(.7 .058327) B(.8 .011303) C(8.8 .093513) D(11.6 .020542) THK(66) COR(41)

*** STandard DEViations ***

A(.8 .241510) B(.9 .106315) C(3.0 .305799) D(3.4 .143326) THK(8) COR(6)

*** % of VARIATions ***

A(.63 5.58) B(.63 7.20) C(1.70 38.98) D(1.61 34.55) THK(8.25) COR(7.89)

*** HISTogram (PEAKs) ***

[Point SAMPle]	Numbers of NOVEform at PEAK A	B	C	D
100 to 105 :	0.	0.	0.	0.
105 to 110 :	0.	0.	0.	0.
110 to 115 :	0.	0.	0.	0.
115 to 120 :	0.	0.	0.	0.
120 to 125 :	0.	0.	0.	0.
125 to 130 :	0.	0.	0.	0.
130 to 135 :	306.	0.	0.	0.
135 to 140 :	17.	0.	0.	0.
140 to 145 :	0.	302.	0.	0.
145 to 150 :	0.	21.	0.	0.
150 to 155 :	0.	0.	0.	0.
155 to 160 :	0.	0.	0.	0.
160 to 165 :	0.	0.	0.	0.
165 to 170 :	0.	0.	4.	0.
170 to 175 :	0.	0.	174.	0.
175 to 180 :	0.	0.	121.	0.
180 to 185 :	0.	0.	18.	0.
185 to 190 :	0.	0.	6.	0.
190 to 195 :	0.	0.	0.	0.
195 to 200 :	0.	0.	0.	0.
200 to 205 :	0.	0.	0.	2.
205 to 210 :	0.	0.	0.	88.
210 to 215 :	0.	0.	0.	191.
215 to 220 :	0.	0.	0.	38.
220 to 225 :	0.	0.	0.	3.
225 to 230 :	0.	0.	0.	1.
230 to 235 :	0.	0.	0.	0.
235 to 240 :	0.	0.	0.	0.
240 to 245 :	0.	0.	0.	0.
245 to 250 :	0.	0.	0.	0.

*** HISTogram (THICKness) ***

[THICKness]	Nos. of NOVEform asphalt	C/o RIFmant
0 to 10 :	0.	0.
10 to 20 :	0.	0.
20 to 30 :	0.	0.
30 to 40 :	0.	0.
40 to 50 :	0.	3.
50 to 60 :	1.	0.
60 to 70 :	2.	33.
70 to 80 :	2.	195.
80 to 90 :	9.	89.
90 to 100 :	212.	3.
100 to 110 :	77.	0.
110 to 120 :	11.	0.
120 to 130 :	9.	0.
130 to 140 :	0.	0.
140 to 150 :	0.	0.
150 to 160 :	0.	0.
160 to 170 :	0.	0.
170 to 180 :	0.	0.
180 to 190 :	0.	0.
190 to 200 :	0.	0.
200 to 210 :	0.	0.
210 to 220 :	0.	0.
220 to 230 :	0.	0.
230 to 240 :	0.	0.
240 to 250 :	0.	0.
250 to 260 :	0.	0.
260 to 270 :	0.	0.
270 to 280 :	0.	0.
280 to 290 :	0.	0.
290 to 300 :	0.	0.

Fig. 4.3: A sample output of cluster analysis for a set of bridge deck data.

The distributions of peak locations and thickness measurements can also be presented in a histogram format.

Using the histogram, observations for peak locations are confined to the region between sample point number 100 and 250 with 5 sample points being declared as one bin. The first bin is assigned for sample point number 100 to 105 and the last bin is for sample point number 245 to 250. From Fig. 4.3, we note that for peak A there is a total of 306 waveforms collected in the bin 130-135 and 17 waveforms recorded in the bin 130-135. This implies that the majority of waveforms (in this example) have peak A located within the sample point number 130 to 135. This agrees with the mean value which is 133. For thickness measurement each bin is set for 10 mm. The first bin is from 0 to 10 mm and the last bin is from 290 to 300 mm. From Fig. 4.3, we note that there are 212 waveforms measured having asphalt thickness about 90 mm to 100 mm and 195 waveforms have cover over reinforcement bars about 70 to 80 mm.

The histogram provides useful information for determining the asphalt-concrete interface layer. The centralization of peak C around a bin indicates uniformity in the thickness of asphalt layer. The result given in Fig. 4.3 illustrates a relatively uniform asphalt-covered bridge deck where peak C varies over four adjacent bins with the bin at 170-175 having the largest number of entries (174 waveforms in this bin). However, a histogram for a non-centralized situation can take the form of

100-105	0
.	.
.	.
155-160	0
160-165	2
165-170	55
170-175	64
175-180	0
180-185	38
185-190	51
190-195	12
195-200	1
200-205	1
205-210	0
.	.
.	.
225-230	0

In this example, the peaks are concentrated around two different bins: bin 170-175 and 185-190. As a result, two possible observations can be given related to the asphalt-concrete layer: (1) It is possible that the asphalt thickness varies significantly over a bridge deck or (2) It is possible that within the searching window of the peak detection algorithm there exists two competitive peaks in which one of the peak represents the true asphalt-concrete interface and the other does not. In order to minimize this ambiguity, it is suggested that a few core samples be taken as part of the data collection in the field. This is to be discussed in the following chapter.

In summary, we note that cluster analysis is useful in providing an indication of the variation in the location of peaks in the reflected waveform. The interpretation of these peaks requires further study in order to gain insight into relating the different reflecting surfaces i.e. each layer of asphalt, membrane, concrete and rebars, to the peaks observed. Developing a strategy based on known properties of deck construction may be useful. For example, information concerning the maximum probable change of asphalt thickness per metre along deck and across deck could be incorporated into the software in order to reduce the problems of absurd interpretations. Such inputs would also be useful for the membrane layer and the cover over reinforcement.

5/ Field Evaluation

The results of field evaluations are now presented for three totally different bridge decks. The software modifications discussed in Sections 2, 3 and 4 were incorporated into the processing package in order to determine evaluate system performance.

The three decks presented include: 1) Ninth Line bridge deck in Oakville, which is a new deck in excellent condition having two layers of asphalt over rubber membrane and a well defined membrane concrete interface; 2) Winston Churchill overpass across Highway 401 west of Pearson International Airport, which is a deck in poor condition with two layers of asphalt and little or no membrane material; and 3) Bloor Street Via Duct in Toronto, which is a deck having some damage with three layers of asphalt.

5.1/ Processing of Ninth Line Data

A site visit to Ninth Line, Oakville, near 403 Highway was conducted in mid-May of 1987. Eight different lines were recorded and the site plan is sketched in Fig. 5.1. The bridge deck is expected to be in good condition since it is built just several years ago. It is also known that beneath the asphalt surface there is a layer of waterproofing membrane. The purpose of processing Ninth Line data is that it is important to test the reliability of the software in measuring both the asphalt and concrete cover over reinforcement.

A second site visit was conducted several weeks later. This time measurements of the asphalt thickness were obtained at selected locations. By piercing through the asphalt surface to the 'believed' concrete surface, a rough measurement of asphalt thickness was obtained. Three spots on each of line 1 and line 2 were chosen. On line 1 the thickness at the 3 m, 18 m and 24 m locations were found to be, respectively, 115 mm, 102 mm and 107 mm. On line 2 the same distances have measured thickness of 112 mm, 105 mm and 100 mm. We note that these measurements are approximation. A core sample is more accurate in providing the actual asphalt thickness. Beside the asphalt measurement, a survey of the concrete cover over reinforcement was also obtained from the MTO. These two sets of data can be compared with the computer results.

5.1.1 Computer Analysis

The recorded data were processed using the MTC87 package. One of the input required by the software is the asphalt thickness of core sample. Since we do not have core samples from Ninth

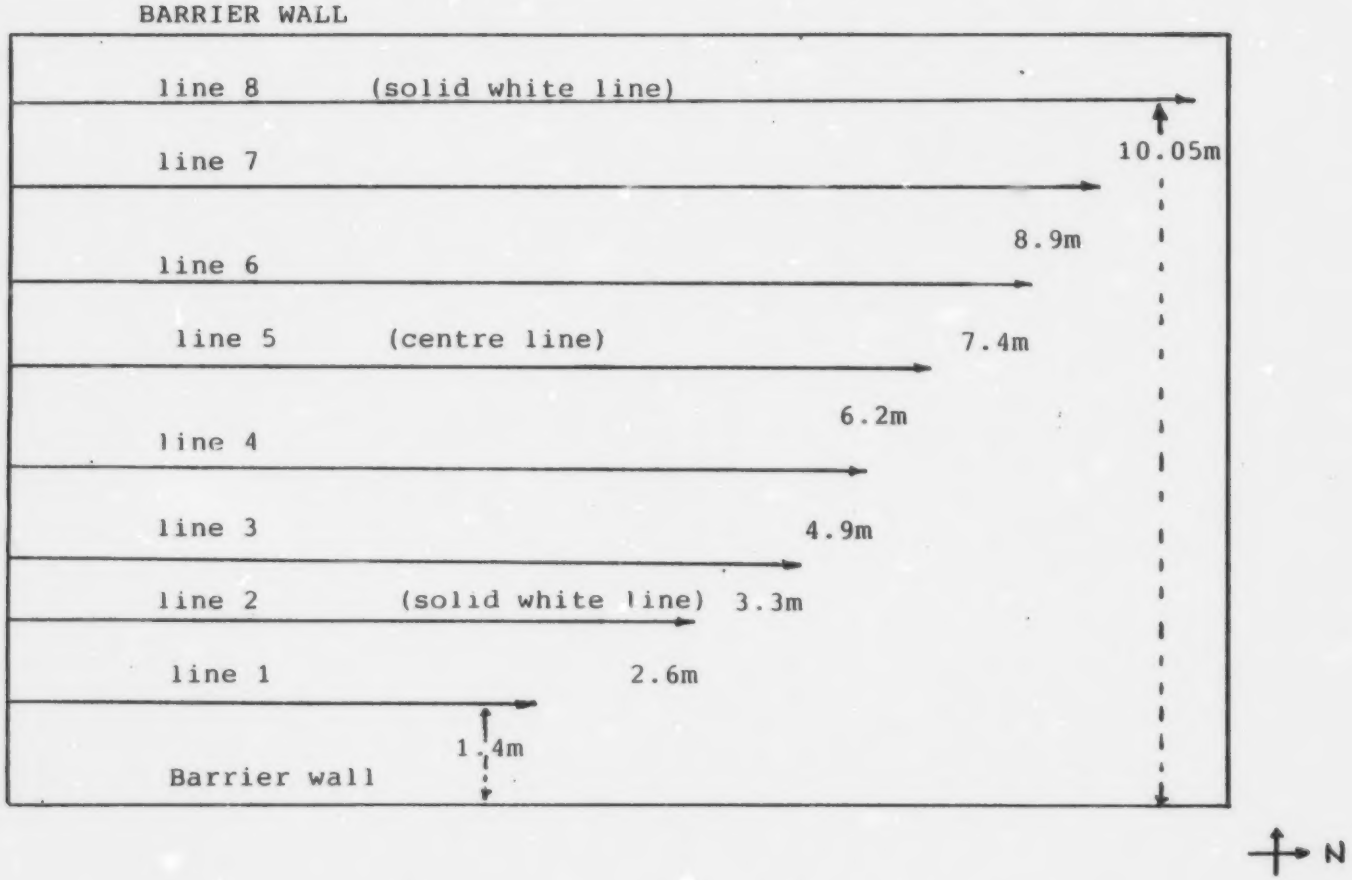

Fig. 5.1: A sketched site plan of Ninth Line Birdge Deck.

Ninth Line (Oakville): line 1 to 8 (Feb 18, 1988)
AVEraged THICKness SUMMARY

(AVEraged THICKness (mm))
line number

metre	1	2	3	4	5	6	7	8
1	109 (66)	94 (64)	87 (62)	85 (38)	92 (62)	87 (47)	92 (58)	90 (58)
2	127 (83)	122 (73)	106 (69)	110 (90)	110 (99)	116 (82)	108 (71)	106 (79)
3	134 (80)	119 (74)	112 (72)	116 (90)	109 (104)	91 (99)	109 (71)	109 (78)
4	121 (88)	119 (75)	114 (71)	113 (94)	106 (104)	112 (72)	111 (73)	111 (75)
5	120 (86)	109 (81)	110 (77)	115 (86)	111 (104)	111 (91)	113 (71)	110 (74)
6	116 (81)	102 (80)	107 (73)	111 (87)	110 (103)	115 (86)	111 (71)	113 (72)
7	114 (82)	97 (83)	101 (77)	110 (90)	103 (106)	11[illegible] (82)	111 (69)	110 (70)
8	113 (93)	101 (80)	103 (70)	110 (90)	102 (105)	112 (80)	111 (67)	108 (66)
9	113 (91)	96 (80)	104 (69)	108 (88)	101 (108)	109 (82)	111 (63)	110 (68)
10	114 (90)	97 (82)	104 (68)	105 (90)	103 (107)	108 (82)	108 (64)	112 (66)
11	111 (80)	100 (73)	105 (66)	106 (94)	106 (105)	107 (78)	114 (66)	110 (76)
12	114 (75)	98 (71)	108 (61)	105 (91)	106 (102)	106 (74)	80 (96)	111 (79)
13	114 (77)	94 (72)	100 (63)	104 (86)	100 (100)	107 (74)	71 (101)	110 (80)
14	115 (77)	94 (75)	95 (66)	105 (79)	95 (103)	102 (80)	74 (96)	108 (75)
15	109 (81)	94 (73)	94 (69)	98 (86)	93 (102)	102 (77)	77 (85)	112 (64)
16	109 (79)	94 (79)	93 (73)	98 (91)	91 (102)	97 (78)	109 (64)	108 (74)
17	111 (80)	96 (79)	93 (76)	99 (87)	93 (100)	77 (94)	110 (58)	111 (70)
18	113 (79)	100 (73)	96 (71)	103 (81)	95 (96)	65 (110)	112 (54)	111 (64)
19	110 (83)	95 (79)	91 (71)	100 (82)	93 (98)	101 (77)	110 (56)	111 (63)
20	111 (84)	94 (79)	91 (71)	100 (84)	95 (100)	105 (77)	110 (57)	111 (69)
21	112 (87)	98 (78)	93 (70)	103 (78)	97 (96)	106 (71)	109 (55)	110 (64)
22	113 (89)	96 (79)	94 (67)	101 (79)	96 (98)	105 (69)	109 (58)	111 (70)
23	117 (83)	98 (78)	92 (70)	97 (109)	90 (101)	101 (104)	106 (62)	113 (67)
24	118 (73)	99 (70)	97 (65)	99 (101)	88 (111)	92 (114)	103 (63)	106 (71)
25	116 (72)	99 (72)	95 (68)	100 (109)	85 (118)	88 (115)	100 (65)	104 (76)
26	105 (75)	99 (73)	99 (68)	104 (101)	89 (116)	92 (118)	104 (63)	112 (67)
27	110 (74)	97 (73)	101 (64)	107 (104)	86 (133)	92 (116)	109 (60)	121 (64)
28	111 (77)	96 (78)	101 (63)	109 (108)	87 (131)	95 (115)	110 (65)	114 (74)
29	111 (79)	95 (76)	107 (62)	102 (114)	85 (134)	93 (115)	106 (73)	108 (79)
30	110 (79)	97 (75)	105 (59)	103 (116)	87 (112)	97 (98)	107 (75)	100 (89)
31	110 (79)	96 (74)	102 (56)	95 (123)	86 (112)	94 (109)	105 (74)	108 (81)
32	106 (78)	95 (74)	97 (70)	93 (124)	91 (103)	97 (93)	106 (72)	107 (79)
33	103 (76)	96 (71)	97 (70)	98 (122)	91 (103)	98 (113)	107 (64)	111 (74)
34	107 (76)	96 (73)	96 (70)	99 (114)	90 (100)	98 (116)	107 (66)	113 (63)
35	106 (76)	98 (74)	97 (69)	102 (74)	93 (100)	98 (116)	116 (61)	115 (67)
36	106 (79)	99 (73)	101 (67)	100 (70)	94 (103)	99 (117)	111 (69)	117 (77)
37	111 (74)	99 (69)	96 (67)	100 (119)	92 (120)	96 (118)	77 (98)	114 (80)
38	110 (75)	97 (66)	93 (58)	94 (123)	90 (113)	92 (118)	102 (76)	110 (86)
39	112 (73)	92 (69)	86 (63)	92 (110)	89 (115)	89 (98)	93 (81)	109 (79)
40	110 (69)	96 (64)	88 (61)	92 (86)	90 (104)	86 (91)	94 (82)	125 (77)
41	115 (66)	96 (64)	90 (61)	94 (87)	89 (102)	89 (113)	101 (78)	115 (79)
42	106 (73)	96 (71)	88 (68)	95 (86)	92 (99)	90 (114)	112 (69)	117 (78)
43	103 (79)	96 (75)	92 (72)	94 (87)	90 (102)	88 (106)	109 (68)	114 (74)
44	99 (81)	97 (77)	96 (76)	94 (95)	92 (94)	87 (117)	113 (66)	109 (79)
45	98 (80)	99 (77)	99 (76)	95 (91)	90 (92)	89 (115)	107 (68)	111 (81)
46	98 (82)	93 (81)	97 (78)	94 (93)	87 (102)	88 (125)	108 (64)	112 (73)
47	92 (88)	94 (81)	96 (75)	91 (96)	87 (107)	89 (122)	111 (67)	116 (82)
48	93 (87)	90 (83)	93 (76)	90 (92)	87 (109)	91 (122)	105 (75)	112 (85)
49	93 (87)	91 (83)	93 (78)	91 (90)	87 (101)	92 (126)	103 (81)	116 (86)
50	92 (87)	90 (84)	93 (77)	92 (88)	89 (97)	94 (121)	111 (76)	124 (79)
51	96 (87)	92 (85)	94 (73)	94 (86)	90 (99)	94 (130)	101 (92)	116 (81)
52	94 (93)	93 (81)	94 (74)	94 (89)	92 (102)	94 (133)	98 (77)	113 (82)
53	93 (96)	92 (90)	96 (79)	91 (89)	93 (104)	95 (106)	96 (81)	113 (79)
54	96 (84)	93 (77)	97 (75)	95 (83)	94 (99)	91 (128)	93 (85)	110 (82)
55	99 (81)	97 (79)	99 (77)	96 (87)	92 (102)	87 (126)	79 (97)	108 (79)
56	100 (82)	98 (78)	100 (72)	96 (75)	91 (96)	87 (123)	70 (101)	108 (73)
57	103 (85)	103 (79)	100 (73)	96 (76)	89 (95)	84 (120)	153 (576)	109 (72)
58	99 (88)	102 (76)	101 (70)	96 (91)	87 (98)	86 (121)	120 (585)	107 (75)
59	101 (91)	101 (80)	99 (72)	95 (75)	85 (95)	88 (118)	34 (625)	107 (73)
60	104 (98)	101 (83)	99 (75)	95 (78)	84 (99)	83 (118)	116 (601)	105 (67)
61	106 (88)	104 (79)	99 (74)	89 (83)	83 (100)	94 (110)	92 (603)	96 (72)
62	100 (88)	98 (79)	103 (71)	96 (77)	82 (97)	91 (113)	85 (585)	92 (75)
63	93 (86)	96 (76)	100 (67)	97 (77)	84 (103)	95 (116)	79 (602)	91 (73)

Table 5.1: The thickness measurement of asphalt and concrete cover of Ninth Line data.

Ninth Line (Oakvill): line 1 to 8 (Feb 18, 1988)
BRIDGE deck CONDition SUMMARY

[ASPhalt AVERaged THICKness]

	line number 1	2	3	4	5	6	7	8
mm	107	97	97	99	92	95	103	109
in	4.21	3.82	3.82	3.90	3.62	3.74	4.06	4.29
ave dielect	6.14	6.38	6.56	6.42	6.26	5.81	5.89	6.15

[C/O REINFORCEment AVEraged THICKness]

	line number 1	2	3	4	5	6	7	8
mm	81	76	70	91	104	103	72	74
in	3.19	2.99	2.76	3.58	4.09	4.06	2.83	2.91

[LINE DISTRIBUTion (%)]

	line number 1	2	3	4	5	6	7	8
GOOD	98.76	98.14	94.39	98.13	93.46	98.44	97.50	99.07
DEBONDed	.93	.31	1.87	.93	6.23	.62	.00	.00
SCALEd	.00	.00	.00	.00	.00	.00	.00	.00
DELAMINATed	.31	1.55	3.74	.93	.31	.93	2.14	.31
BAD data	.00	.00	.00	.00	.00	.00	.36	.62
TOTAL	100.00	100.00	100.00	100.00	100.00	100.00	100.00	100.00

metal PLATE AMPlitude is: 9.948553 v

OVERALL AVEraged DIELECTric constant of asphalt is 6.2010

OVERALL AVERaged ASPhalt THICKness is 99 mm, [3.90 in]

OVERALL AVEraged C/O REINFORCEment THICKness is 83 mm, [3.27 in]

[OVERALL bridge deck CONDITION]

GOOD	97.24 %
DEBONDED	1.36 %
SCALed	.00 %
Delaminated	1.28 %
BAD data	.12 %
Total	100.00 %

Table 5.2: Summarized reports on the averaged thickness and bridge deck conditions of each line.

Line, the six measurements obtained from the site visit was averaged. The averaged thickness is 107 mm and this is used as the input to the software. (In a later section, we will show that core sample thickness is used as a benchmark for indicating the asphalt-concrete interface).

In Table 5.1, the thickness measurement of asphalt and concrete cover of Ninth Line are presented for every one metre interval. The number within the bracket is for concrete cover thickness. On line 7, from 57 to 63 m, the entries are all registered as 999's (999 represents bad data). This is because we encountered end of tape at 56 m so there are no data available for the rest of that line.

In Table 5.2, summarized reports on the averaged thickness and bridge deck conditions of each line are given. Also the overall averaged information is included. For the overall conditions, Ninth Line is found to be 97.24% good with a possible 1.28% delamination and 1.36% debonding (although these could simply be anomalies or false alarms in the processing). The averaged asphalt thickness is 99 mm and averaged concrete cover is 83 mm.

Results of the histogram calculation (described in Chapter 4) are given for each line. This is provided in Appendix D.

5.1.2/ Asphalt Thickness

Waveforms are sampled from the data set where the six locations of asphalt measurements are known. In Table 5.3 we compare the actual measurements with the computer results.

Table 5.3/ actual asphalt thickness vs computer results

LOC m	Line 1 actual mm	Line 1 computer mm	Line 1 error %	Line 2 actual mm	Line 2 computer mm	Line 2 error %
3	115	134	16.52	112	119	6.25
18	102	113	10.78	105	100	4.76
24	107	118	10.28	100	99	1.00

The comparison shows that there is about 12% error for line 1 and only 4% error for line 2 in measuring the asphalt thickness.

In order to justify the computer results, sample waveforms from these locations are examined. First, we obtain the metal plate reflection which is shown in Fig. 5.2. The surface echo amplitude is 9.95 V. Then according to the method described in Section 3.1, the asphalt thickness of each waveform is determined once the asphalt interface layer can be identified. Figures 5.3 and 5.4 provide waveforms corresponding to the 3 m, 18 m and 24 m locations along line 1 and 2, respectively. The peaks labeled A, C and D are the interface boundaries which are identified by the software. From calculations, the asphalt thickness related to each waveform are 132 mm, 115 mm and 117 mm for line 1 at 3 m, 18 m and 24 m; and 119 mm, 100 mm and 104 mm for line 2 at 3, 18 and 24 m. We note that the computer results from Table 5.3 arise from waveform averaging (5 waveforms) whereas in Fig. 5.3 and 5.4 the measurements involve single waveform. It is expected that there is a minor difference between the results.

From the waveform analysis, we see that the computer results are quite accurate. However, it is important to note that the asphalt thickness calculated here is actually a combined thickness of asphalt cover and waterproofing membrane.

5.1.3 Concrete Over Reinforcement

A survey of the concrete cover measurement of Ninth Line has been obtained from MTO. The survey provided data for the centre line (line 5) and the two outside lines 1 m away from both barrier walls (line 1 and 8). The measurement is given at every 3 m interval. Table 5.4 compares the survey results with the computer findings.

By comparing both results, on the average, there is a 13% error in calculating the concrete cover for line 1 and 8. However, the magnitude of this error increases to 25% for the centre line. We note that from Table 5.4, the computer results for the centre line have much thicker measurement than the survey. By referring back to the averaged thickness summary given in Table 5.1, we also see that line 4, 5, and 6 have concrete cover thicker than the rest of the lines. In view of this, waveforms from a section of northbound deck (lines 1 to 5) are examined. Figure 5.5 to 5.9 are the waveforms between 23 to 27 m. On each figure, we have plotted 20 consecutive waveforms and their average.

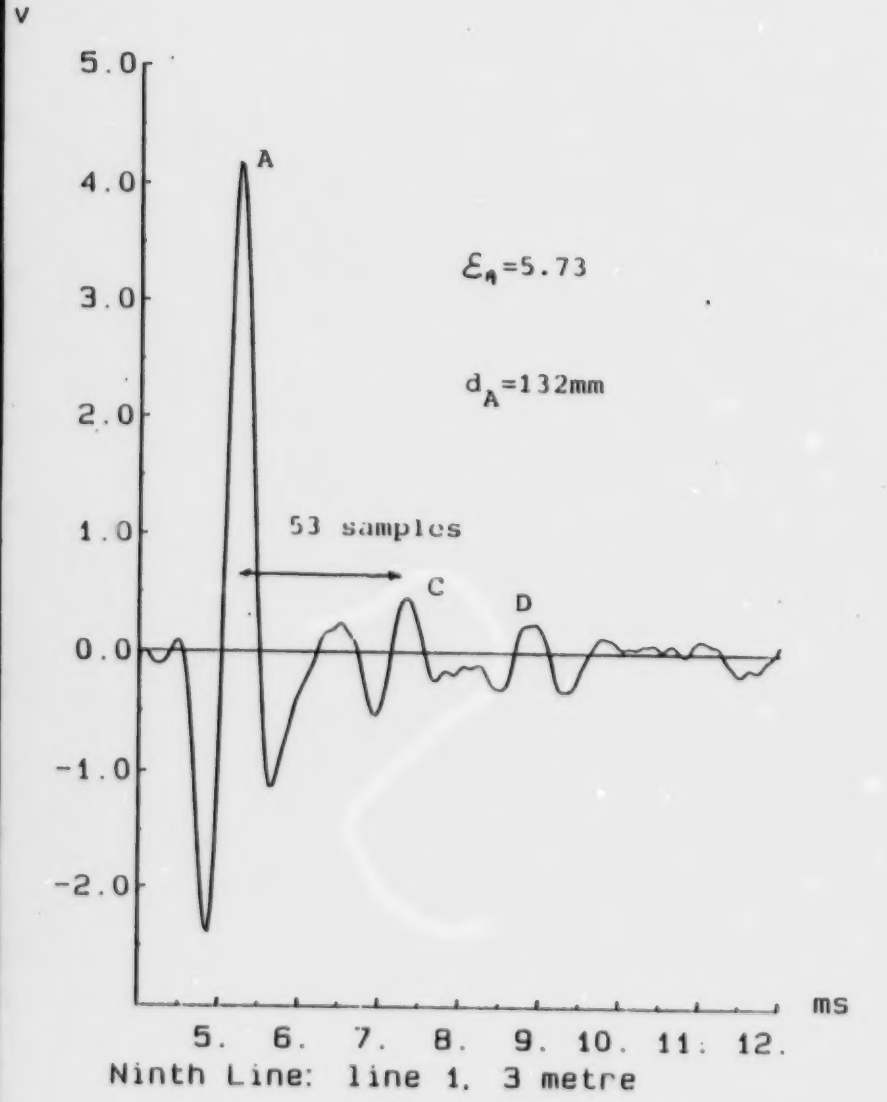

Fig. 5.3: (a)-waveform from line 1 at 3m

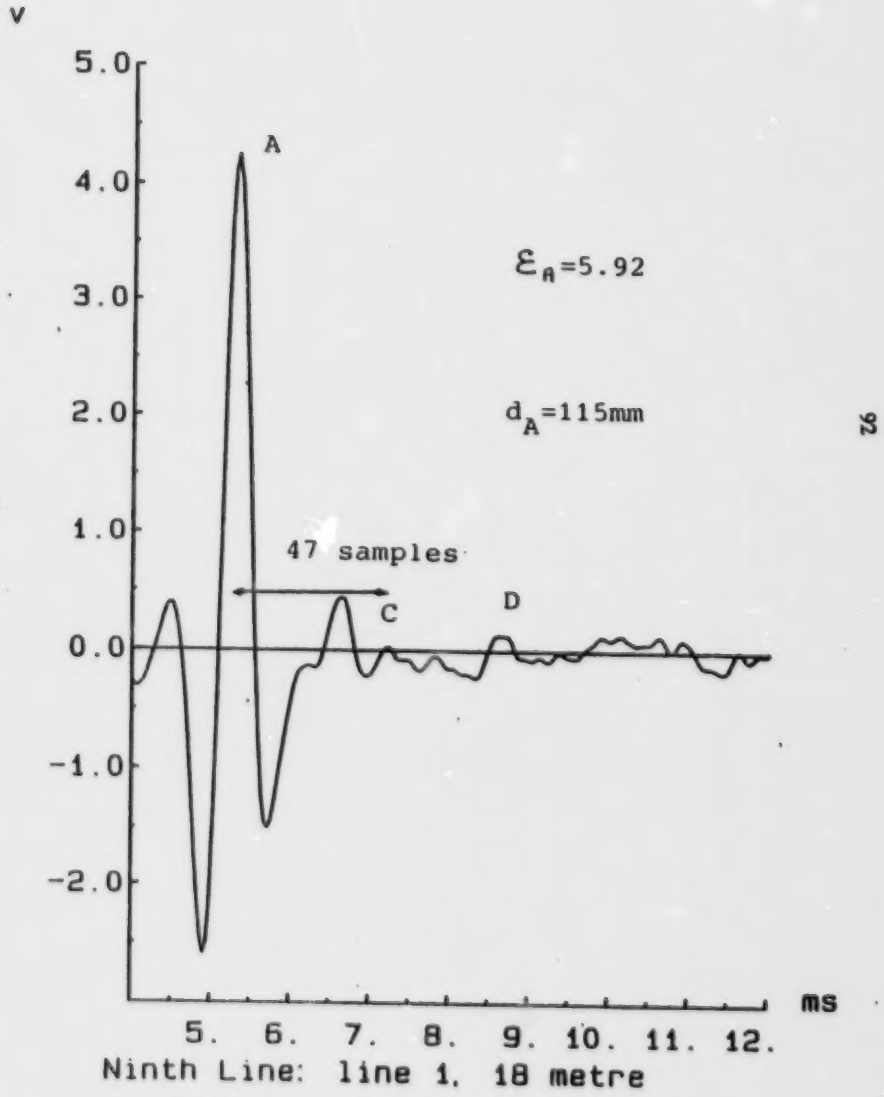

Fig. 5.3: (b)-waveform from line 1 at 18m

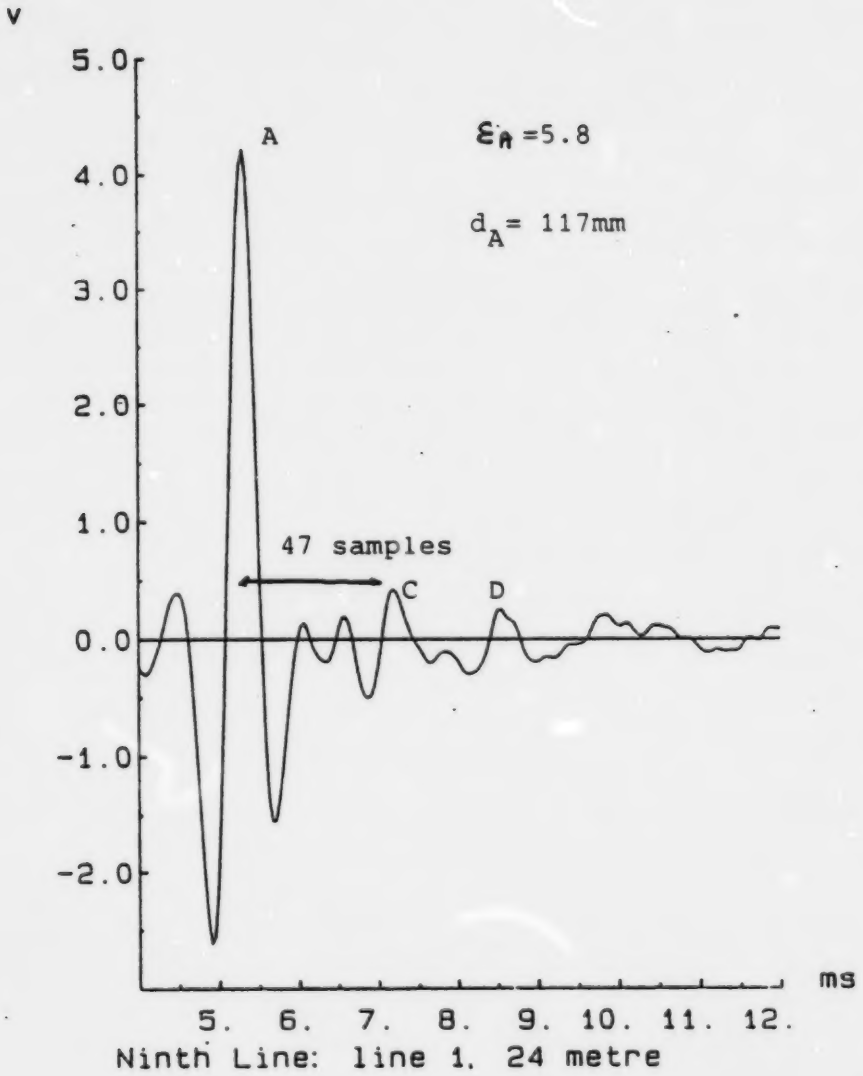

Fig. 5.3: (c)- waveform from line 1 at 24m.

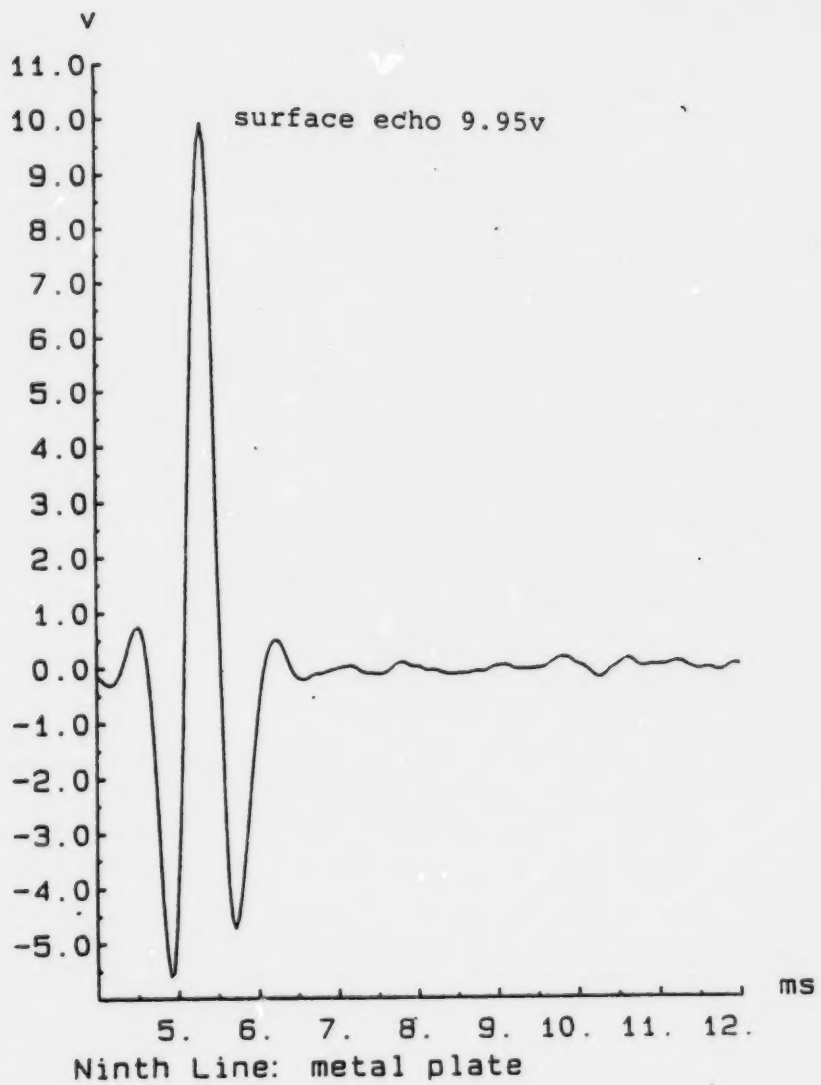

Fig. 5.2: metal plate reflection from Ninth Line.

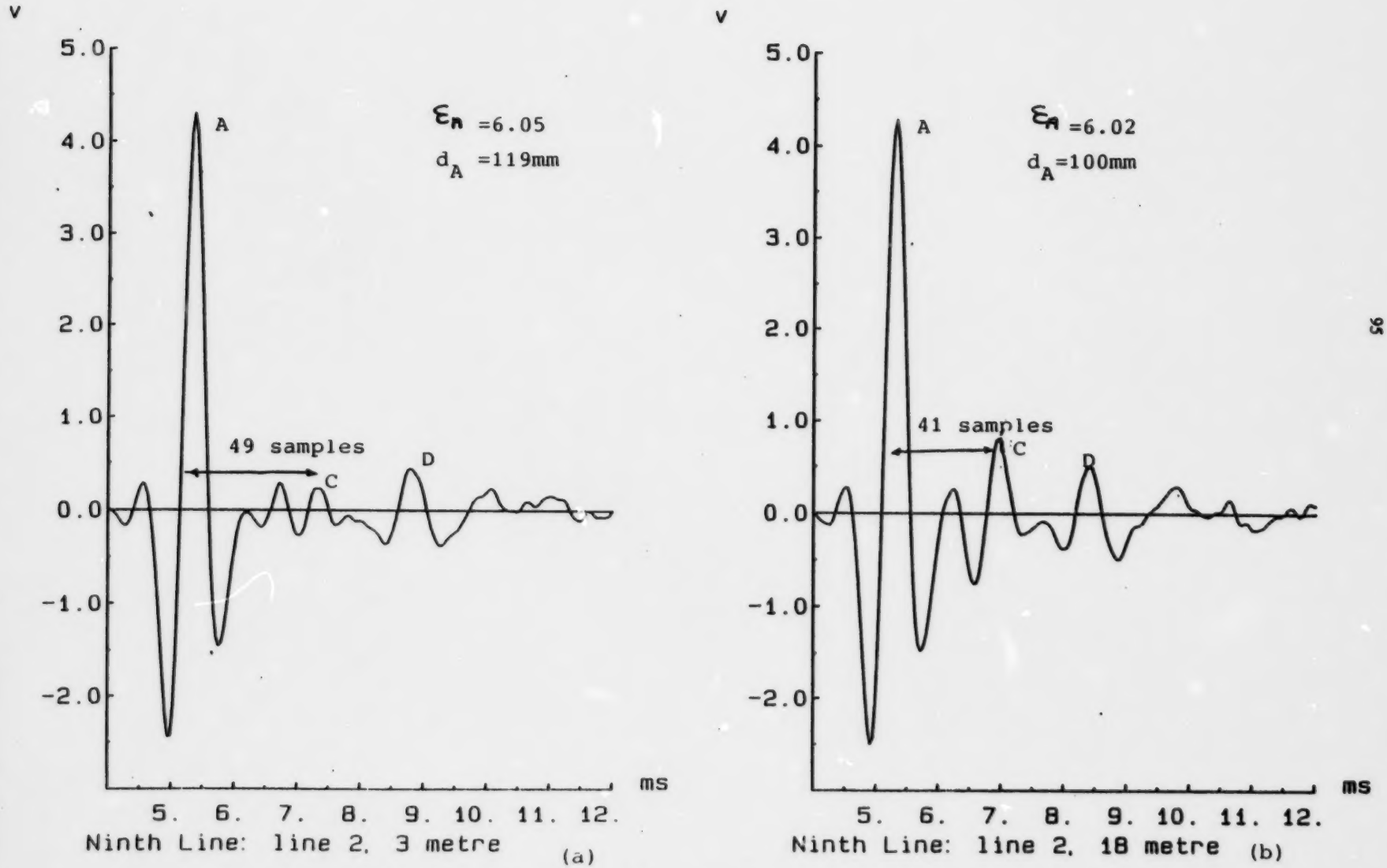

Fig 5.4: (a)-waveform from line 2 at 3m, (b)-waveform from line 2 at 18m

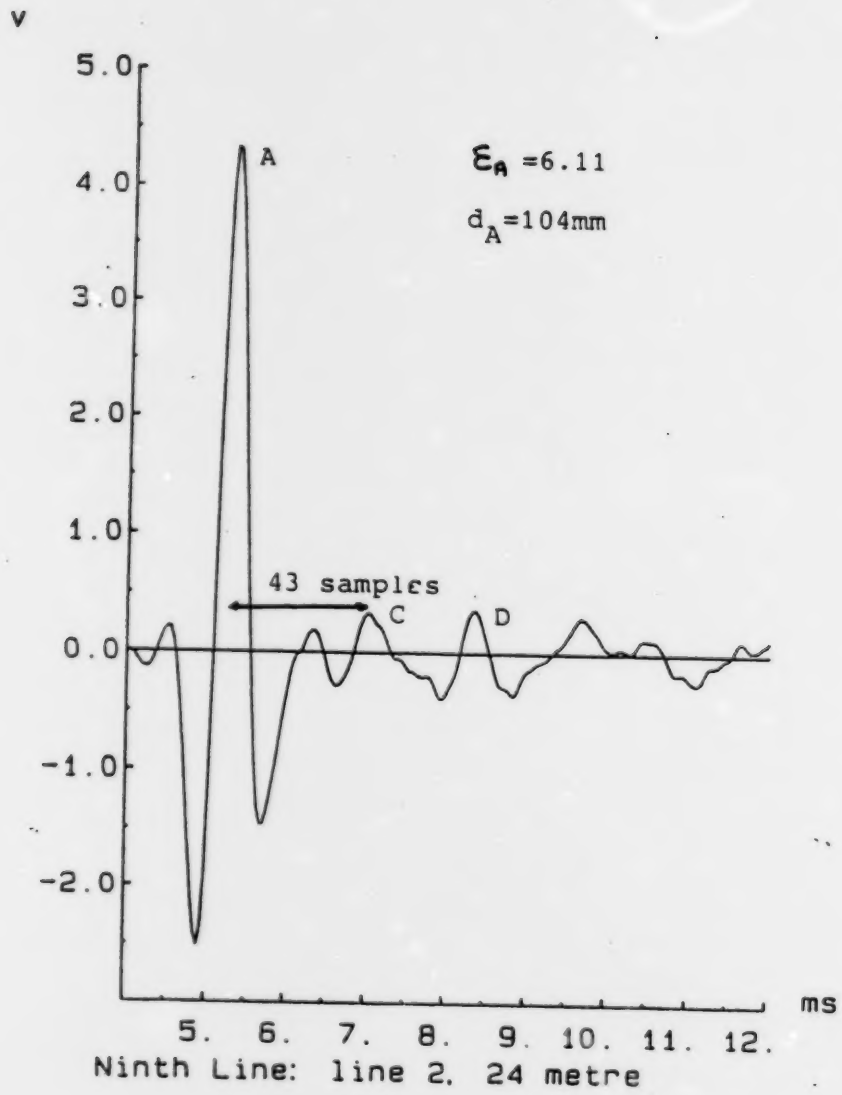

Fig. 5.4(c): waveform from line 2 at 24m.

Table 5.4/ Survey of concrete cover vs computer results

	line 1		line 5		line 8	
Loc m	survey mm	computer mm	survey mm	computer mm	survey mm	computer mm
1	82	66	120	62	72	58
3	80	80	82	104	64	78
6	90	81	87	103	63	72
9	82	91	88	108	80	68
12	89	75	80	102	90	79
15	94	81	70	102	85	64
18	89	79	77	96	74	64
21	79	87	90	96	82	64
24	92	73	75	111	62	71
27	89	74	80	133	80	64
30	78	79	85	112	82	89
33	85	76	85	103	89	74
36	89	79	80	103	81	77
39	78	73	85	115	73	79
42	57	73	90	99	73	78
45	83	80	100	92	80	81
48	73	87	87	109	77	85
51	73	87	92	99	85	81
54	79	84	90	99	60	82
57	84	85	90	95	68	72
60	70	98	92	99	65	67

By observation, we see that across the deck there is a significant variation in the concrete cover from line 1 to 5. In particular, the separation of peaks C and D in line 4 (Fig. 5.8) is increased compared to those appearing in Fig. 5.5 to 5.7. Also, from line 5 (Fig. 5.9) the peak from the layer of rebars is very difficult to locate. Nevertheless, the characteristic W can be identified from most of the waveforms. This is a strong indication that the bridge deck is in good condition.

5.1.4 Bridge Deck Conditions

A grid formatted layout of the bridge deck together with the indication of deterioration at each location is plotted using the package DECK87. According to the analysis of package MTC87, there are two forms of deterioration existing for Ninth Line. These are delamination and debonding. Areas of both deteriorations are marked in Fig. 5.10 and 5.11 respectively.

In order to support the computer results, we also provide waveforms where the map shows deteriorations. Figure 5.12 illustrates the waveforms for line 3 at 11 to 15 m and 30 to 34m. These two sections of line 3 indicate delamination. An asterisk is marked beside the waveform which might possess the delamination characteristic - i.e. absent or weak appearance of the characteristic W between peak C and D. In Fig. 5.13, the waveforms are from line 5 at section 33 to 37 m. This area is declared to have debonding. This set of waveforms does not have the distinct characteristic W but the reflection from the membrane-concrete interface (peak C) has comparable high amplitude (but not exceeding the value for scaling). This situation can also be found in Fig. 5.9.

5.1.5 Summary

We note that with sample waveforms, the computer results can be justified by performing waveform analysis. Using Ninth Line as an experimental deck, the reliability of the software in measuring asphalt thickness and cover over reinforcement can be evaluated. We have shown that there is a strong agreement of the waveform analysis with the computer findings, although the results differ from the actual measurement and survey.

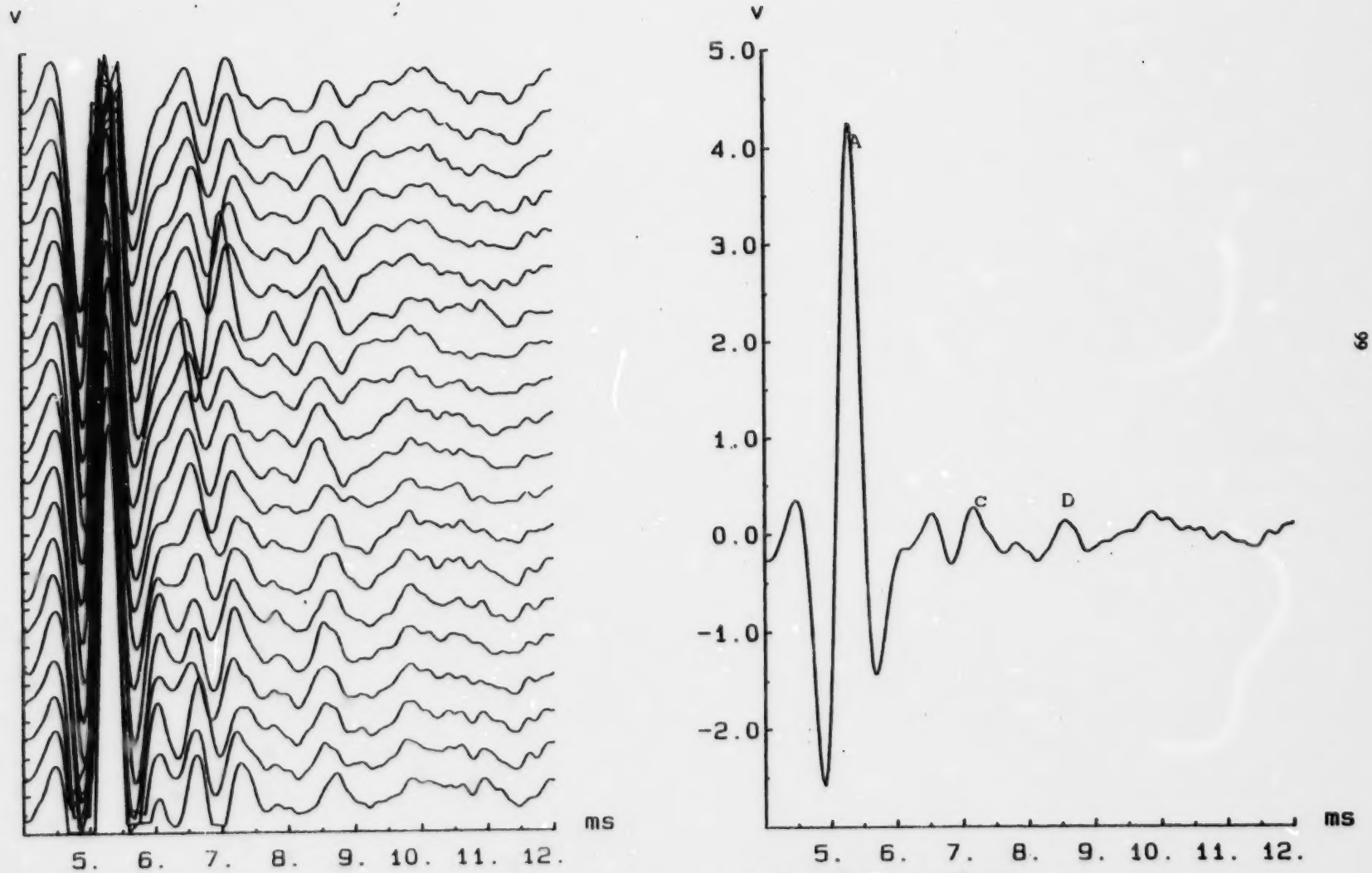

Ninth Line: Line 1, 23 to 27 metre (a) averaged waveform (b)

Fig. 5.5: (a) waveforms from line 1 between 23 to 27m, (b) averaged waveform of (a)

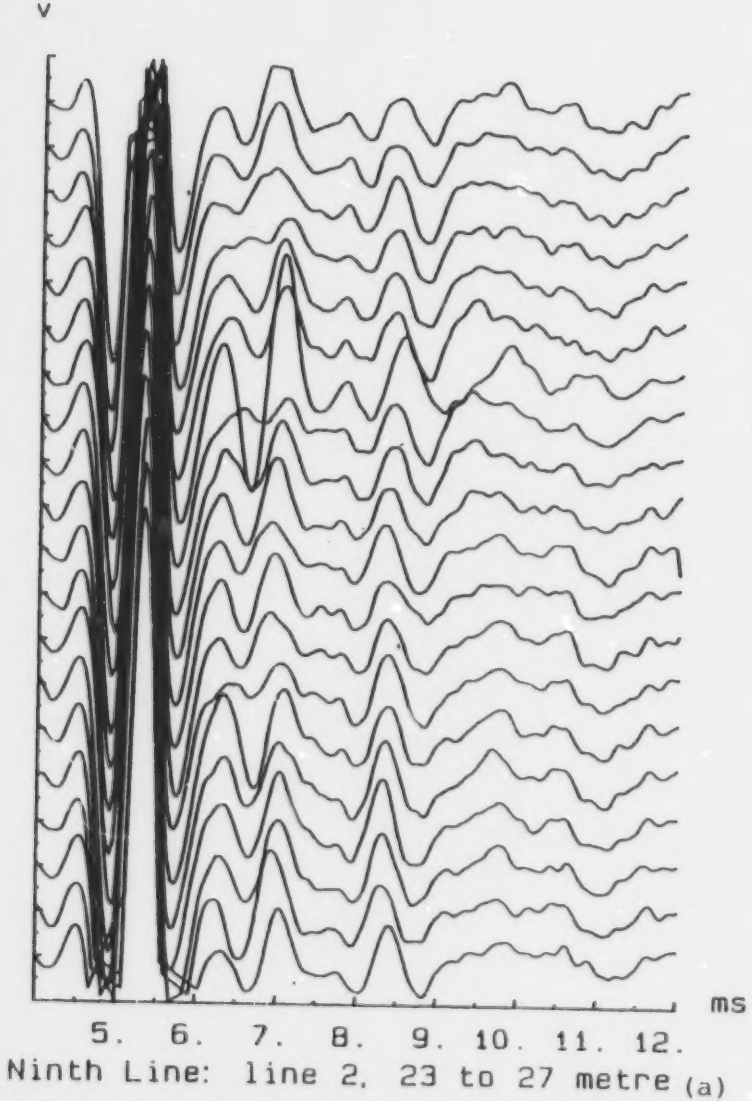

Ninth Line: line 2, 23 to 27 metre (a)

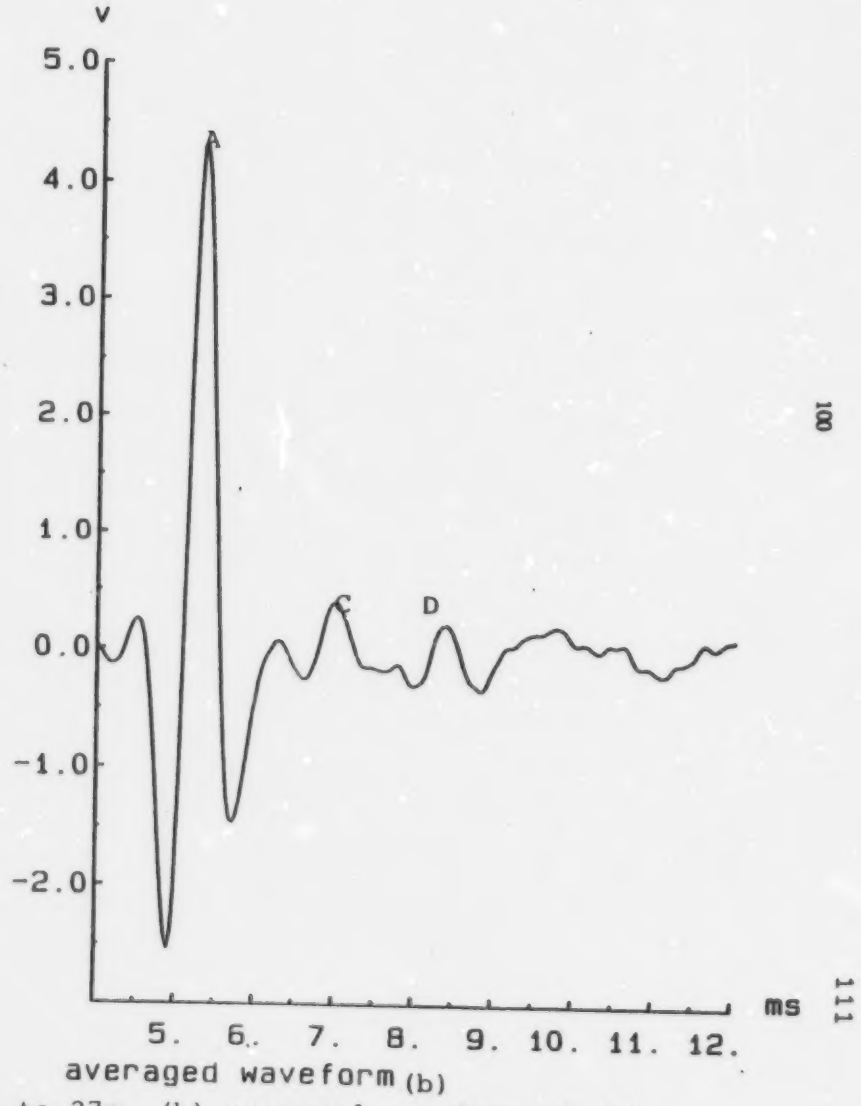

averaged waveform (b)

Fig. 5.6: (a) waveforms from line 2 between 23 to 27m, (b) averaged waveform of (a)

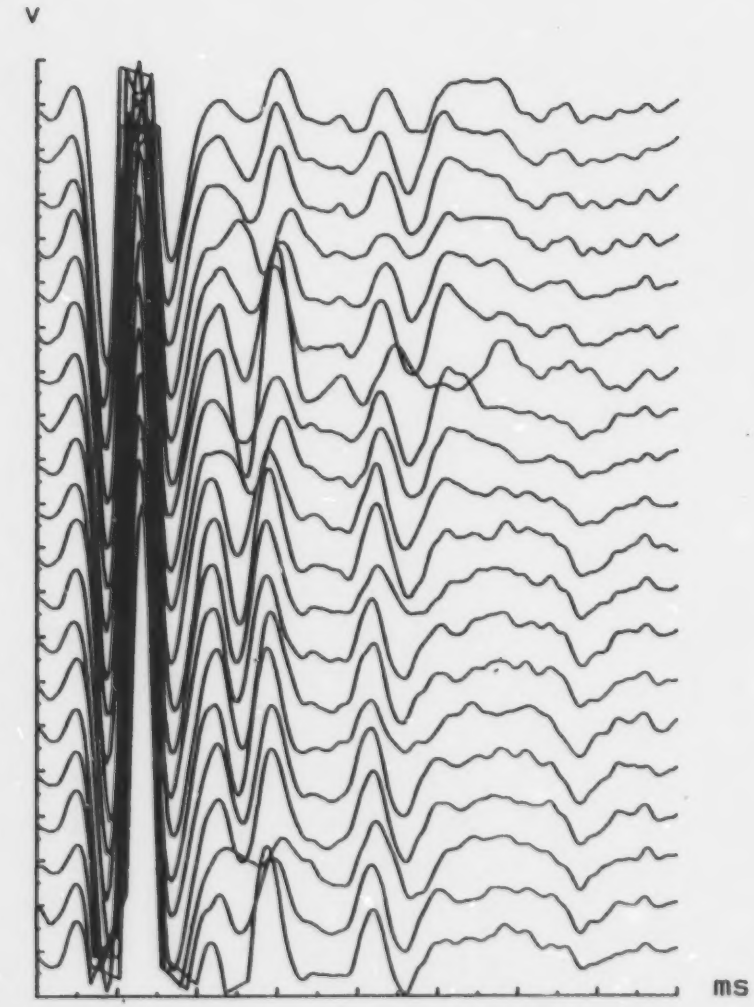

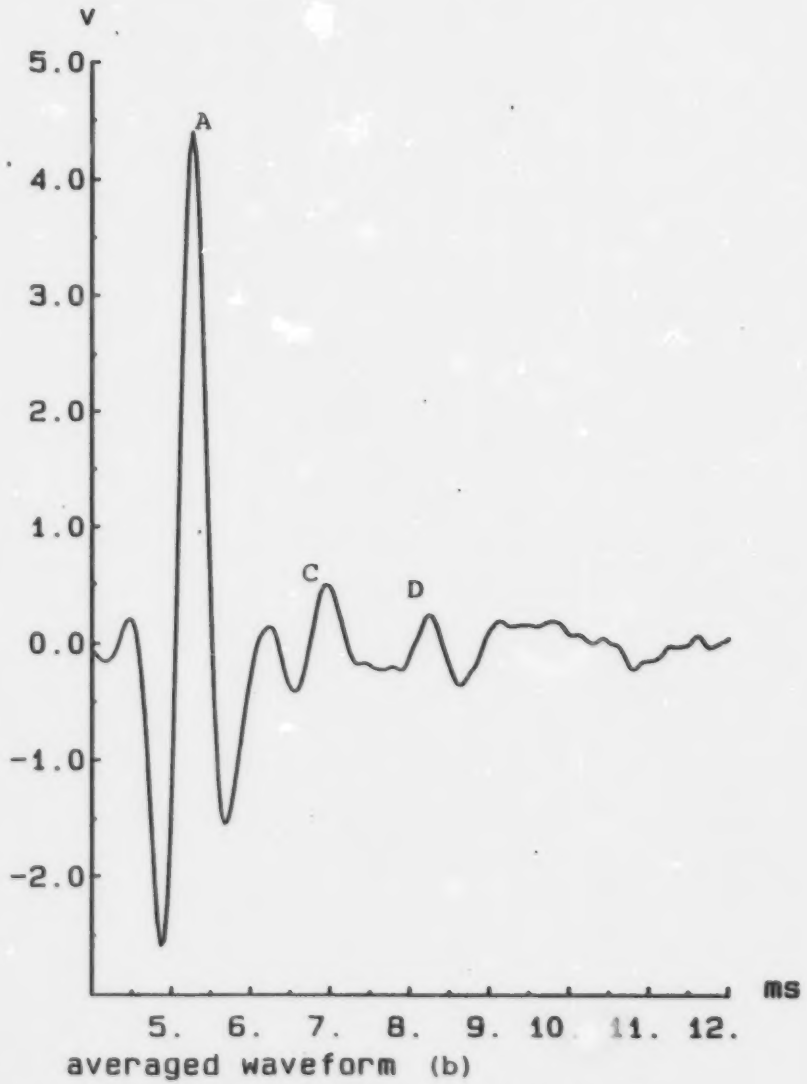

Fig. 5.7: (a) waveforms from line 3 between 23 to 27m, (b) averaged waveform of (a)

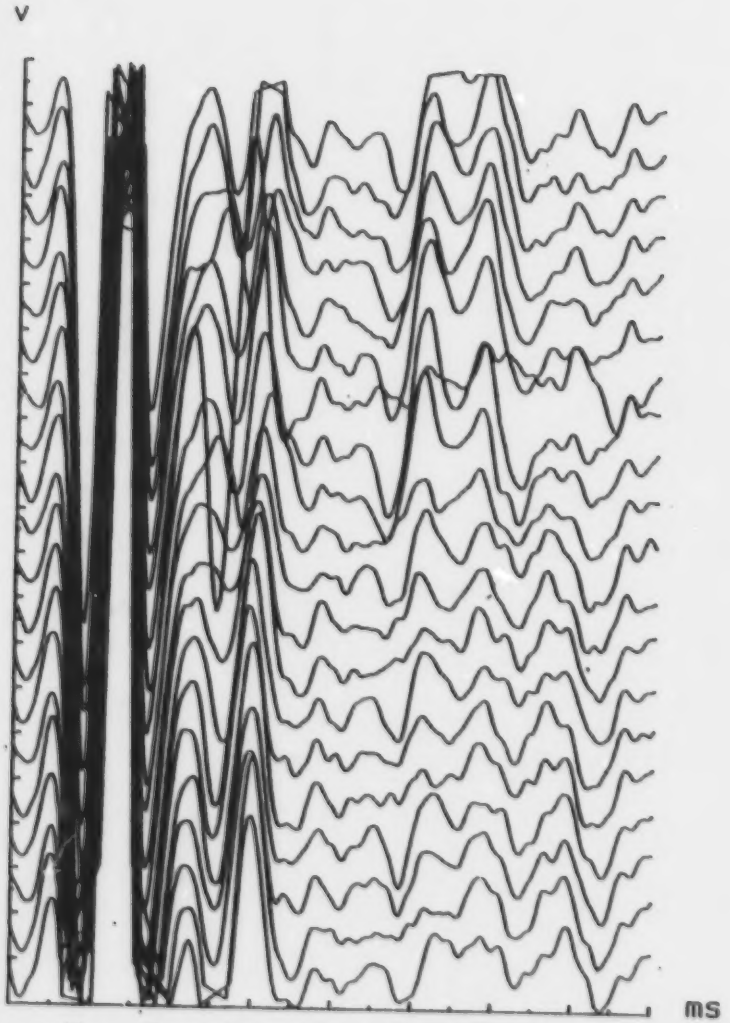

Ninth Line: line 4, 23 to 27 metre(a)

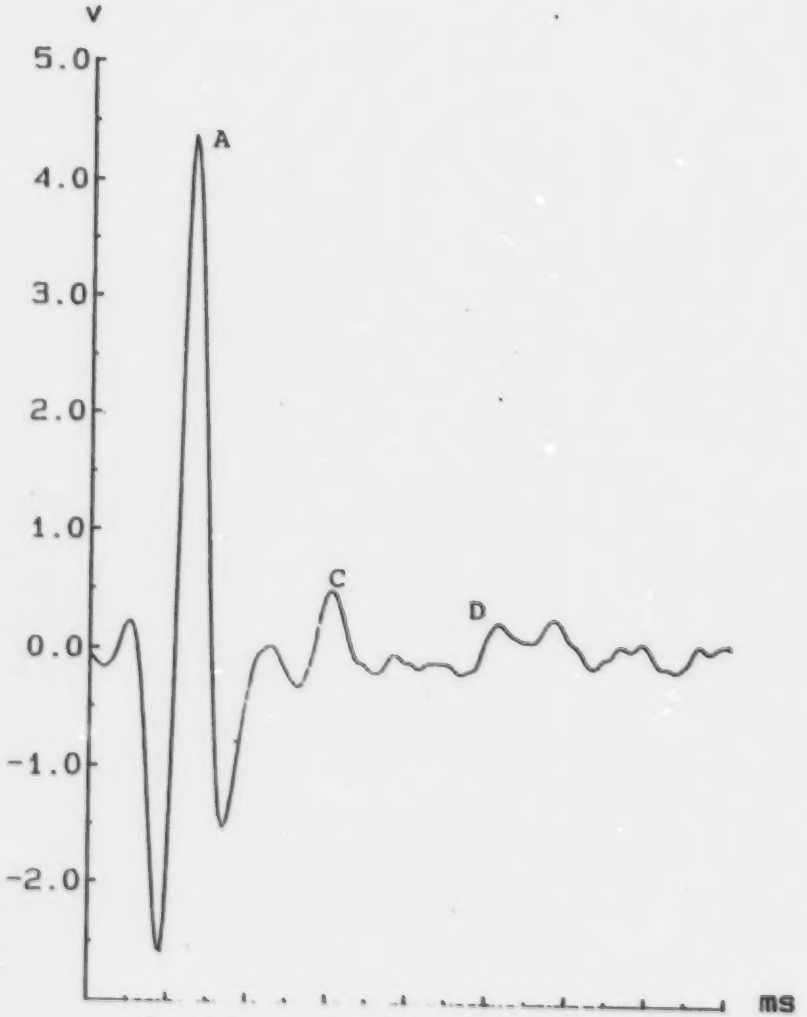

averaged waveform (b)

Fig. 5.8: (a) waveforms from line 4 between 23 to 27m,
(b) averaged waveform of (a)

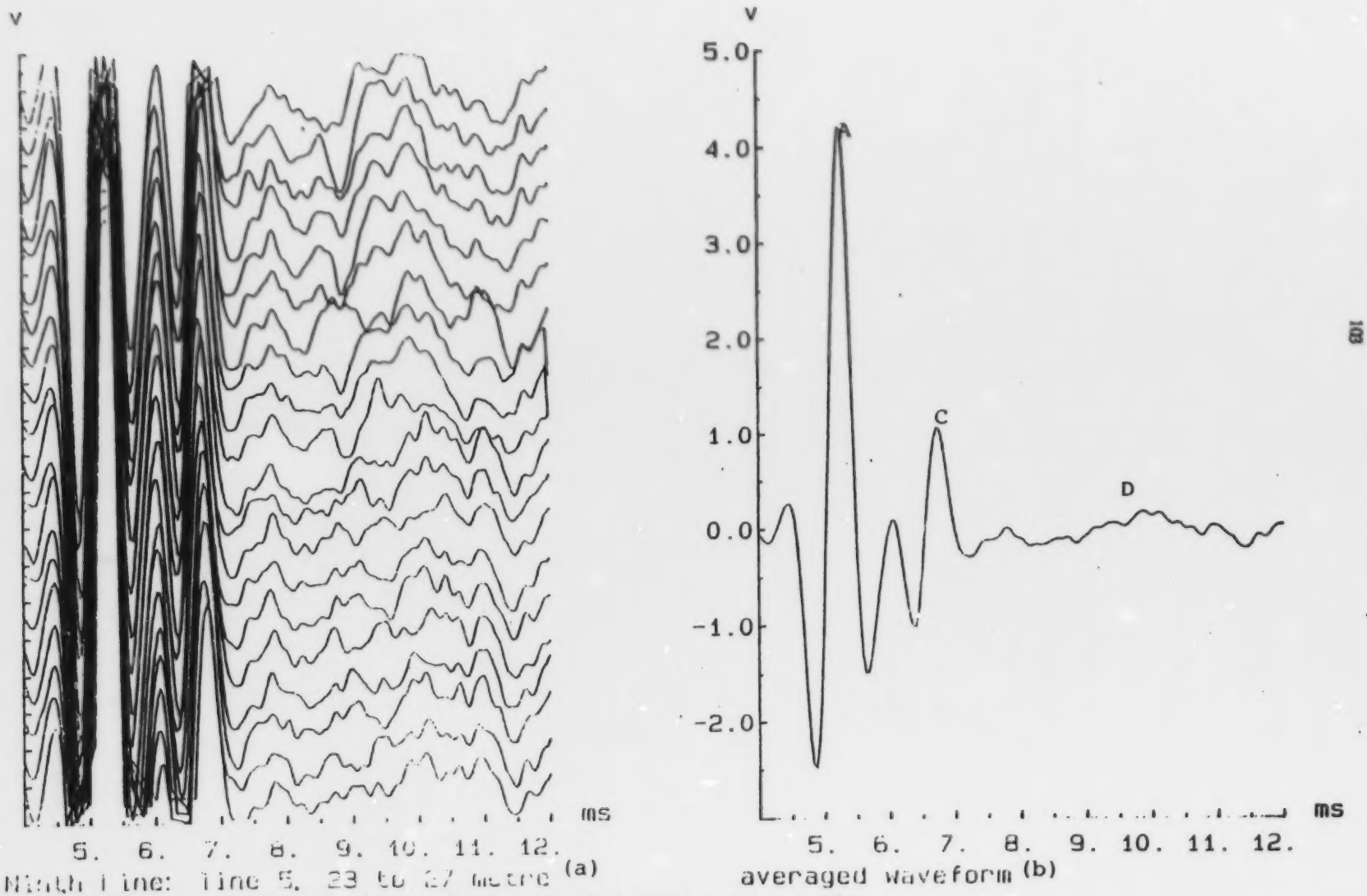

Fig. 5.9: (a) waveforms from line 5 between 23 to 27m,
(b) averaged waveform of (a)

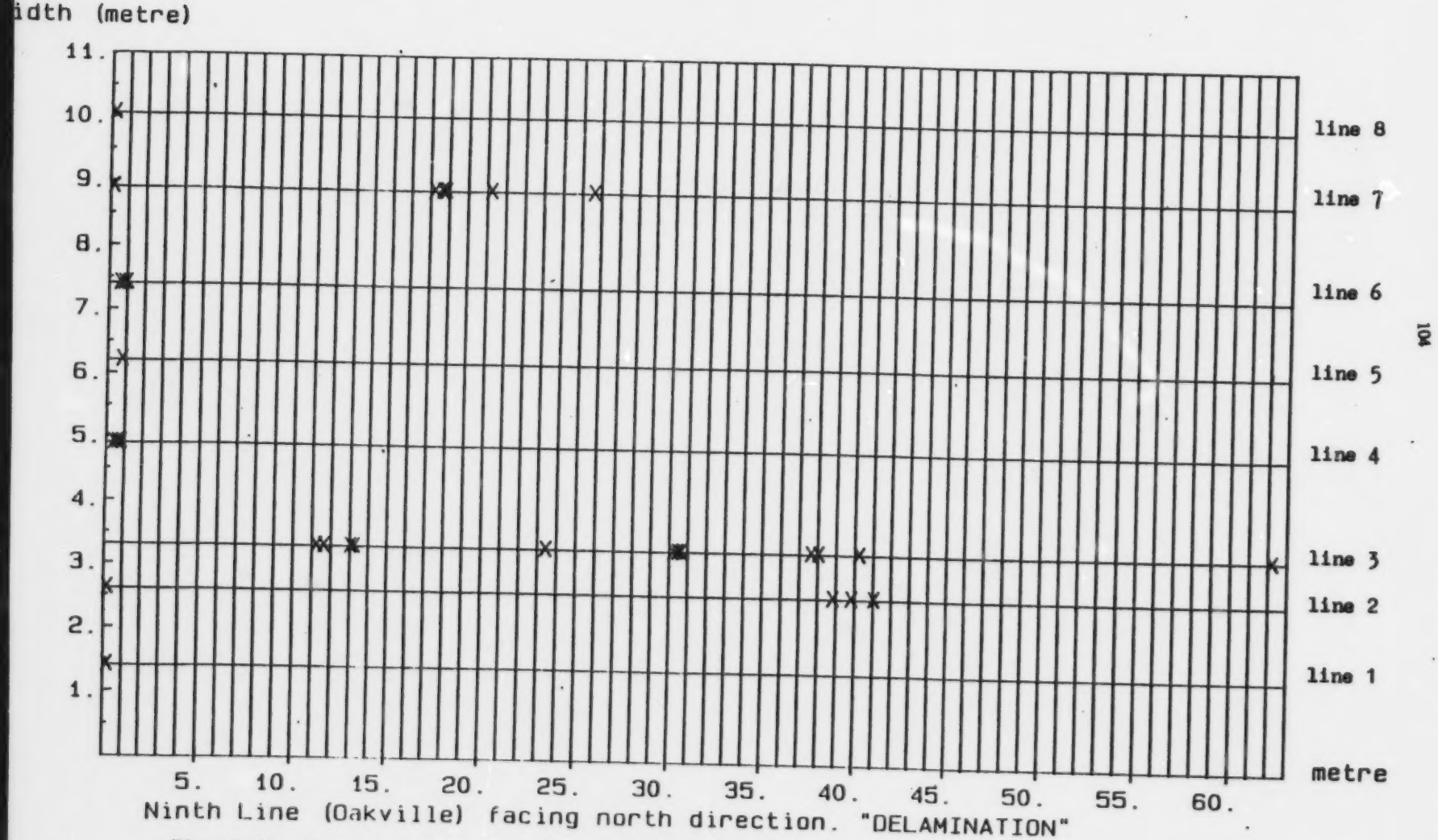

Fig. 5.10: Grid map indicates areas of delamination on Ninth Line bridge deck.

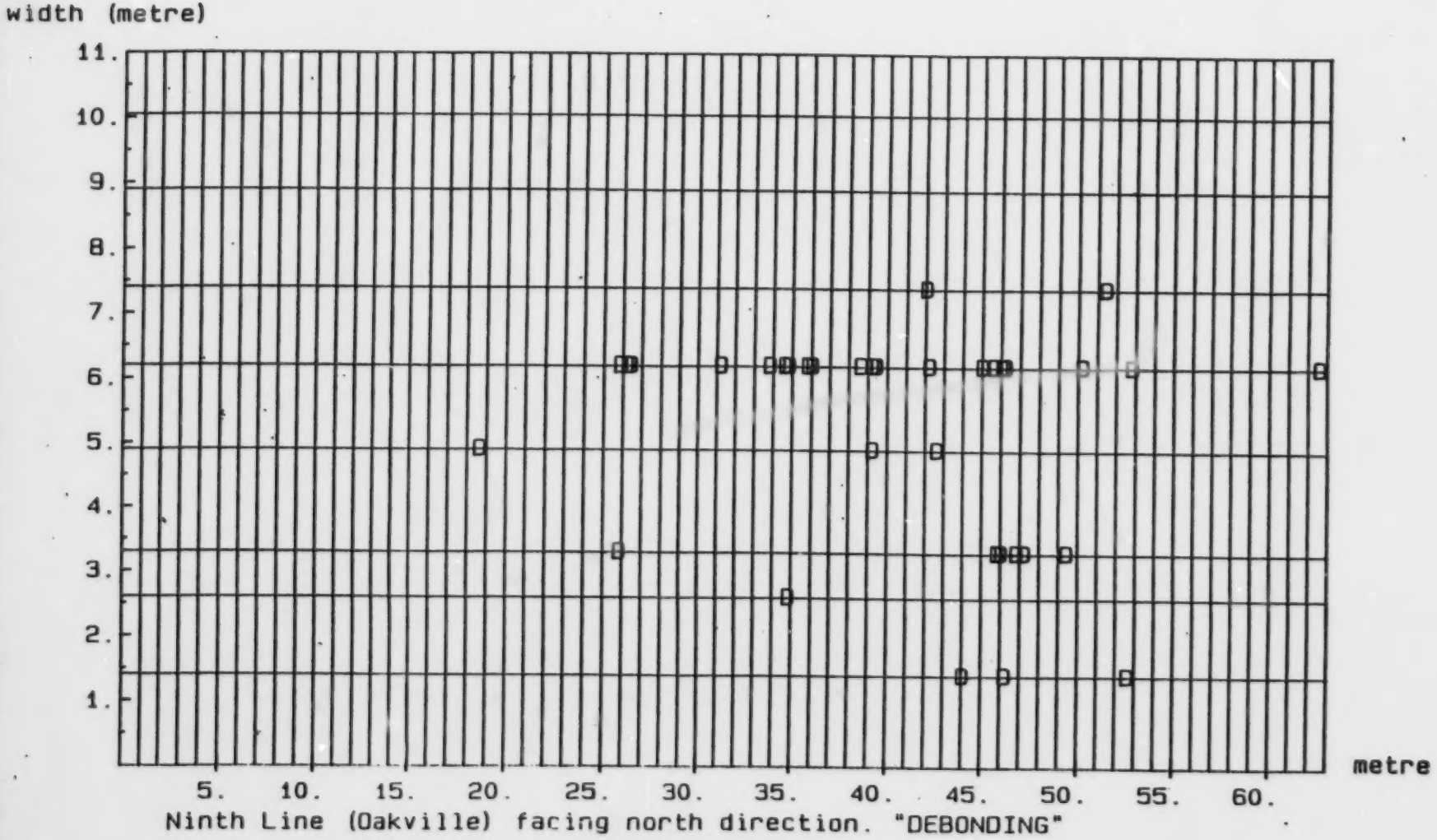

Fig. 5.11: Grid map indicates areas of debonding on Ninth Line bridge deck.

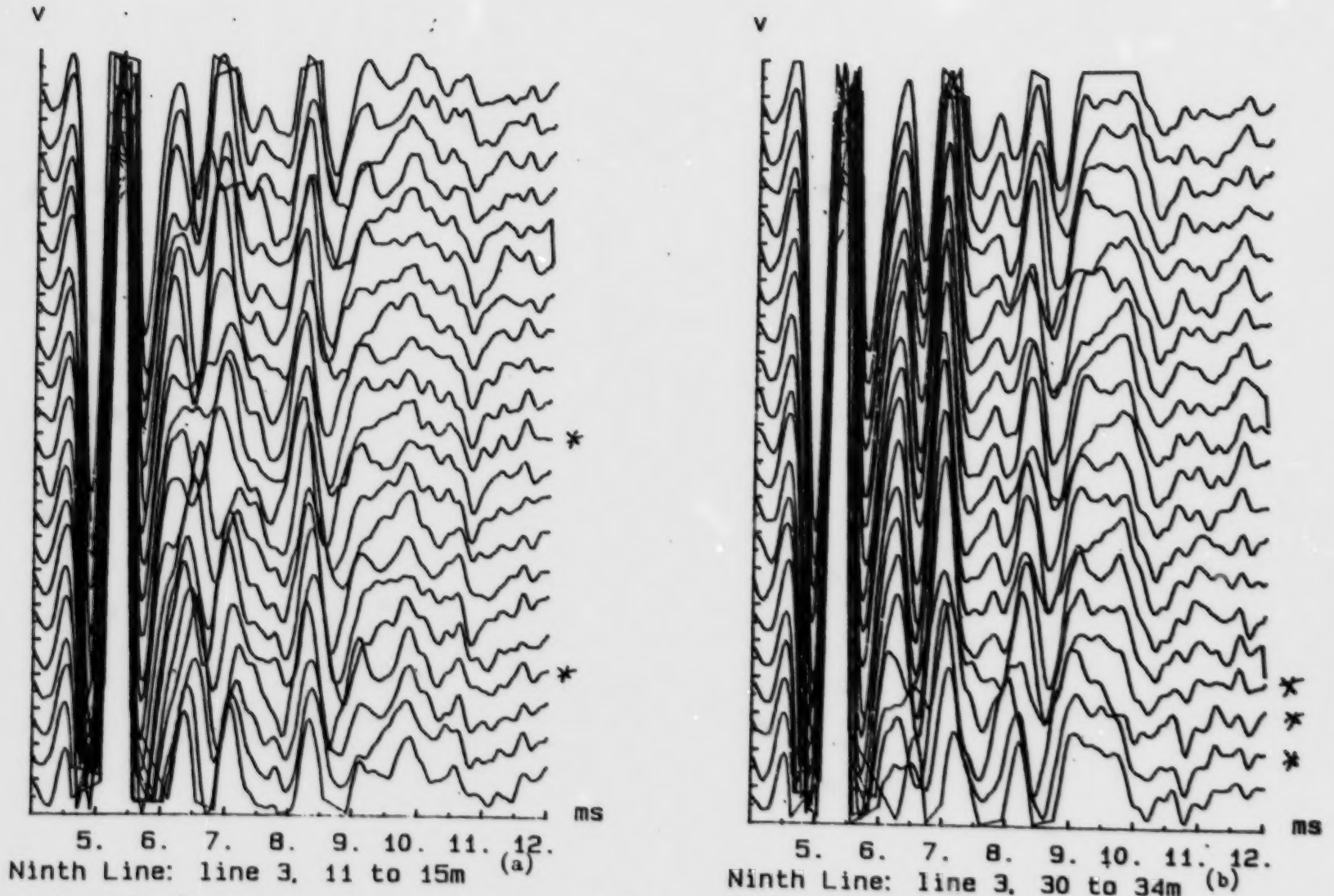

Fig. 5.12: (a) waveforms from line 3 between 11 to 15m and (b) between 30 to 34m.

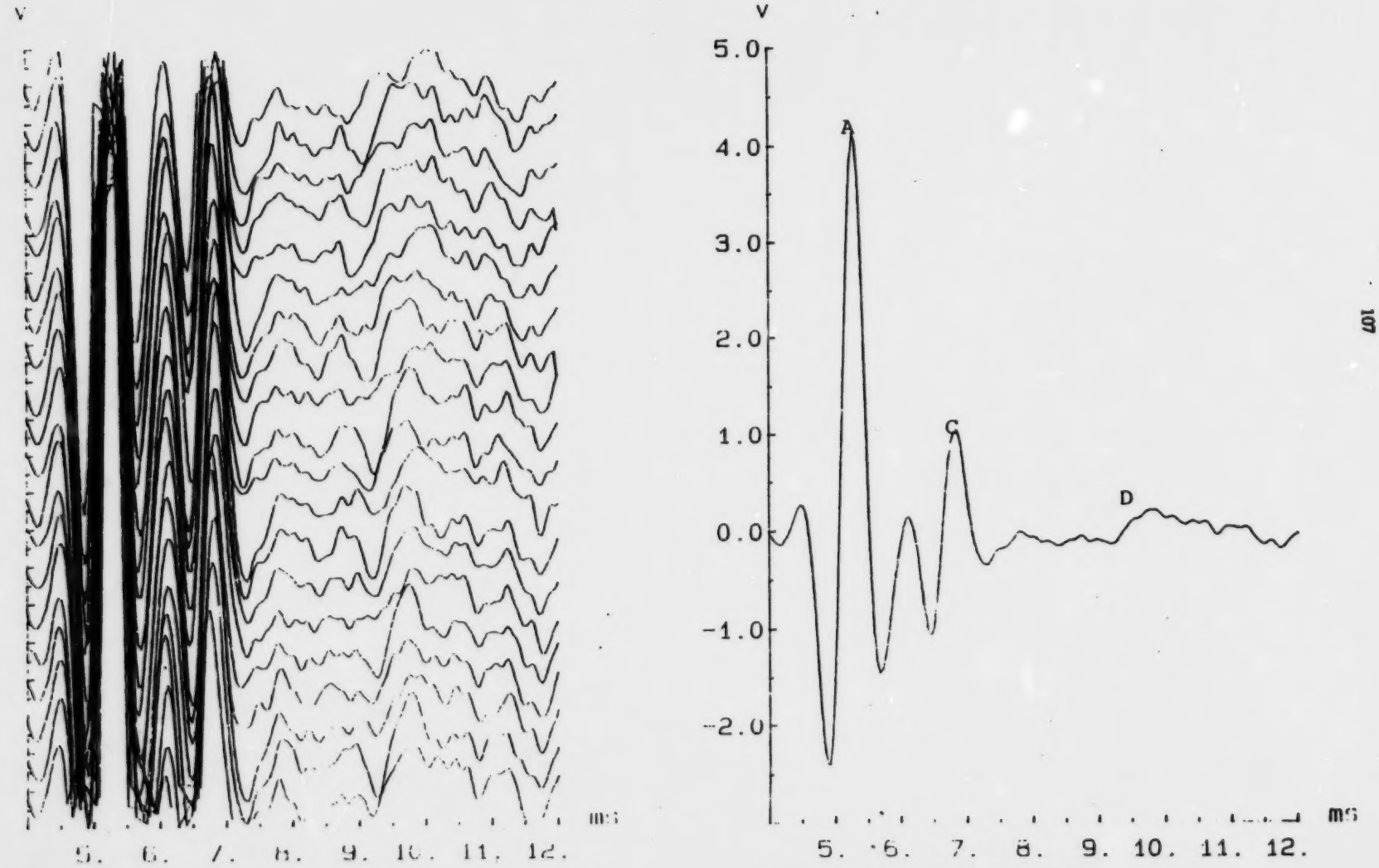

Fig. 5.13: (a) waveforms from line 5 between 33 to 37m
(b) averaged waveform of (a)

5.2 Processing of Winston Churchill Data

Data for Winston Churchill overpass at Highway 401 were collected in the mid-May 1987. The bridge deck spans 76 m and the surface is strictly asphalt covered with no waterproofing membrane. The traffic travels in a north-south direction with a single lane each way. By visual inspection, there are numerous locations where damaged asphalt surface and exposed concrete surface can be seen. Also in some areas, rusted reinforcement bars were noted.

Three lines were recorded on the traveling portion of each lane and one line was recorded along the east curb. The site plan is sketched in Fig. 5.14

A second site visit was conducted in the early August of the same year. The purpose of the trip was to verify the preliminary results obtained from computer analysis.

5.2.1 Computer Analysis

Three different sets of waveforms which cover the area from 16.2 to 21 m at lines 2, 3, and 4 are examined. The waveforms are plotted in Figs. 5.15, 5.16 and 5.17. From the site visit, we observed that thickness of the asphalt and concrete cover over reinforcement are relatively thin. We correlate this information with the waveforms provided.

The surface reflection (peak A) is seen to be very well defined in all waveforms. Since the deck is solely asphalt overlay, it is believed that the second positive peak (peak C) that follows the surface echo may be a reflection from the asphalt-concrete interface.

Once having obtained the value of the dielectric constant of asphalt, the thickness of asphalt is estimated by measuring the time delay between the two reflections. The averaged magnitude of surface echo from the waveforms is about 4.12 V and the metal plate reflection (Fig. 5.18) is found to have amplitude 9.99 V. By evaluating eqs. (3.2) and (3.3), the dielectric constant of asphalt is equal to 5.77. The averaged time delay between peaks A and C is about 0.96 ms (24 samples). Thus, from eq. (3.1) the depth of asphalt is estimated to be 60 mm.

The next positive peak (peak D) after the asphalt-concrete interface peak is believed to be the reflection from the rebars. We have shown in the previous discussion that the dielectric constant of concrete is 8.22. From the waveforms, the averaged time delay between peaks C and D is .80 ms or 20 samples. Using these values, the concrete cover is estimated to be 42 mm.

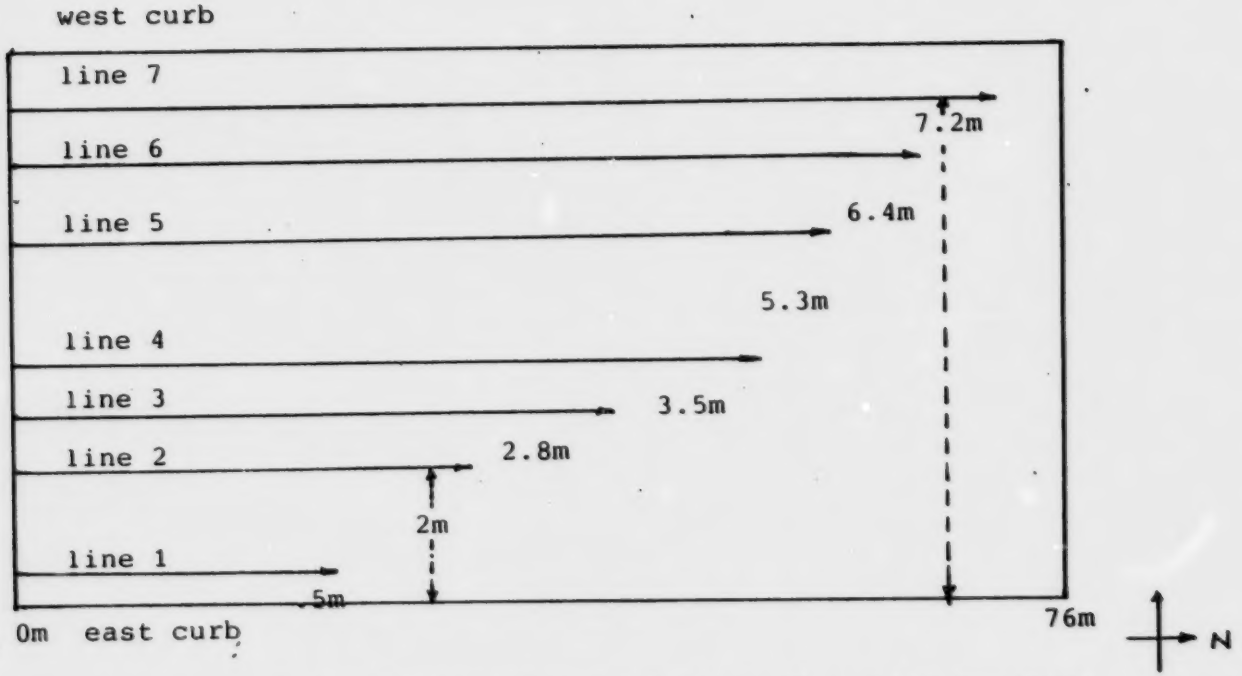

Fig. 5.14: A sketched site plan of Winston Churchill Overpass

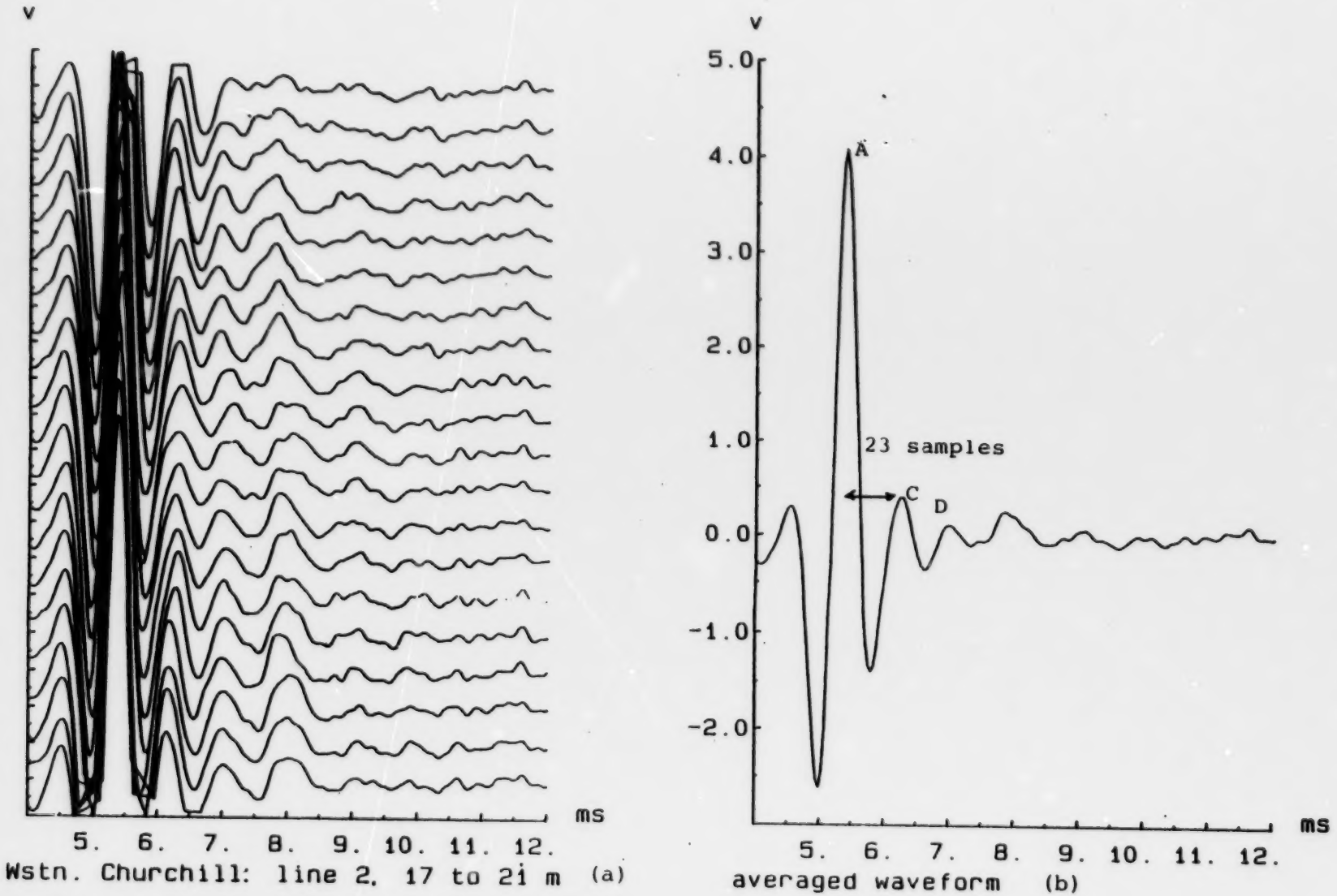

Fig. 5.15: (a)-waveform from line 2 between 16.2 to 21m
(b)-averaged waveform from (a)

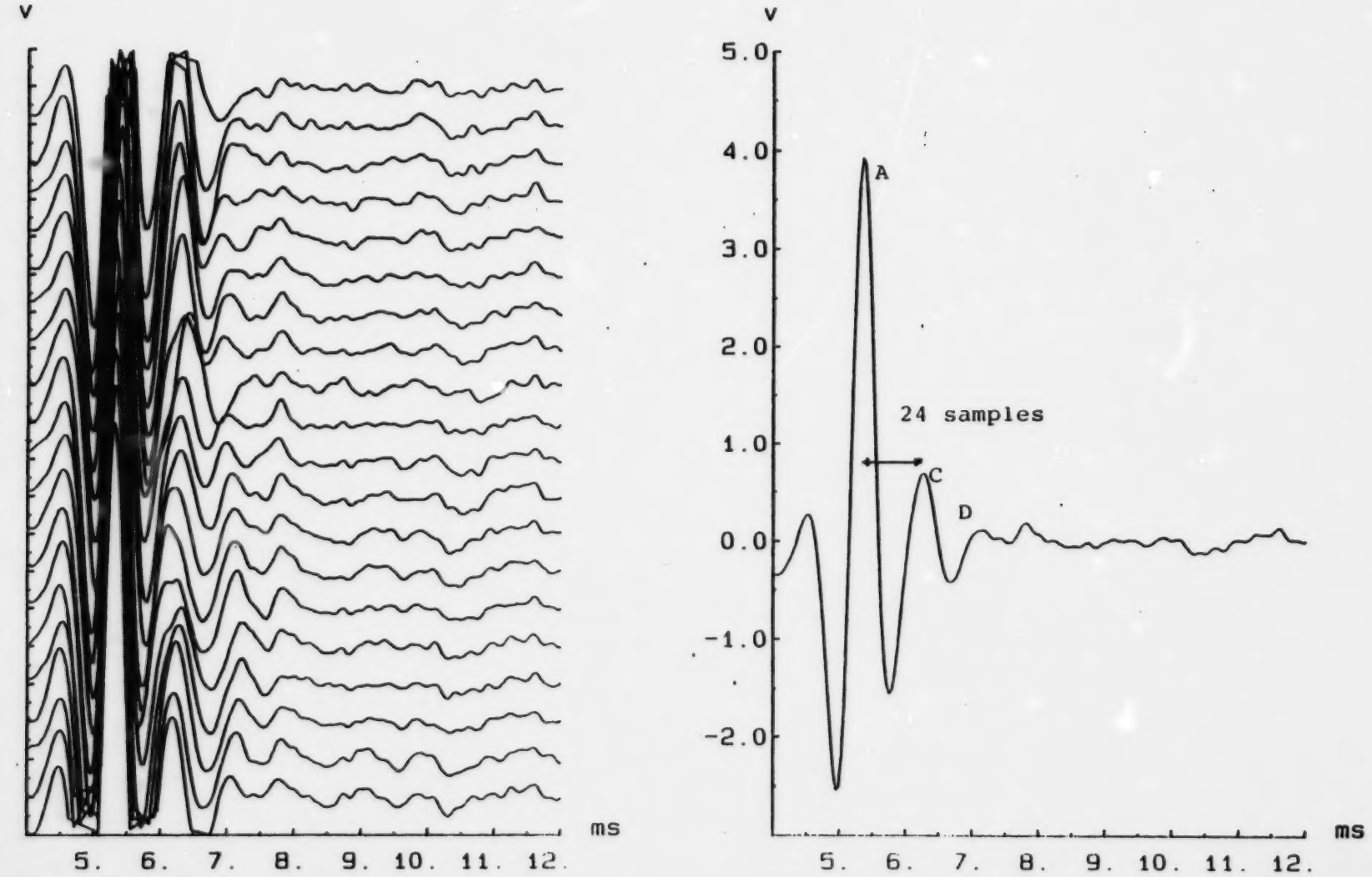

Fig. 5.16: (a) waveforms from line 3 between 16.2 to 21m
(b) averaged waveform from (a)

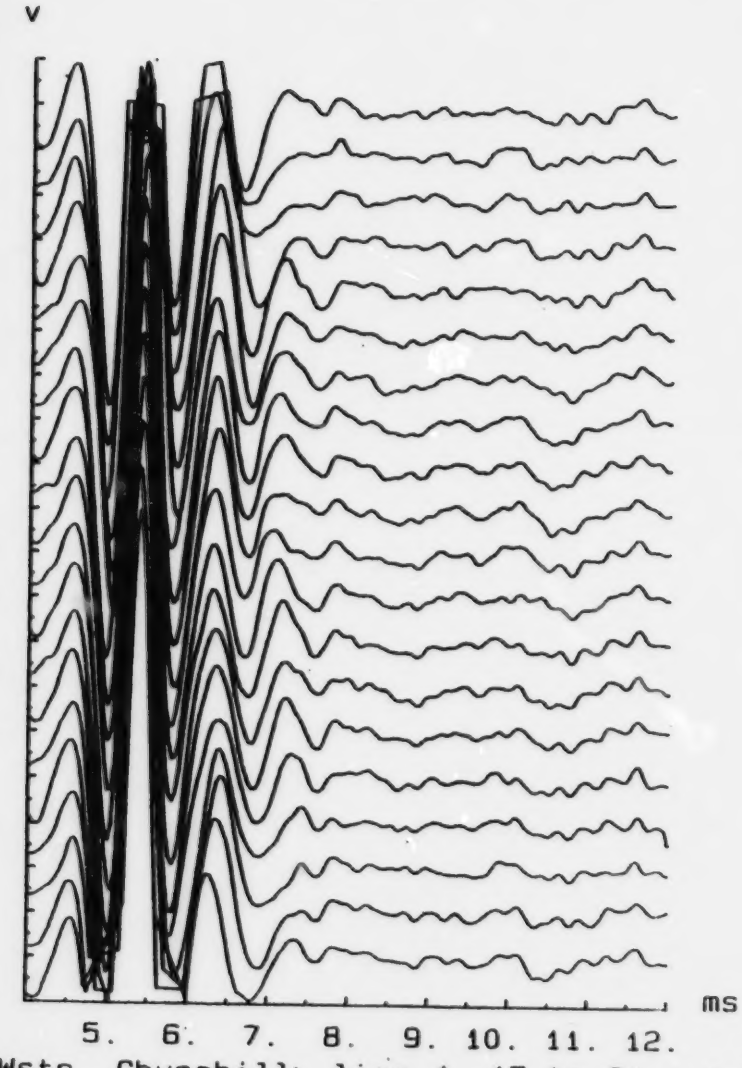

Wstn. Churchill: line 4, 17 to 21 m (a)

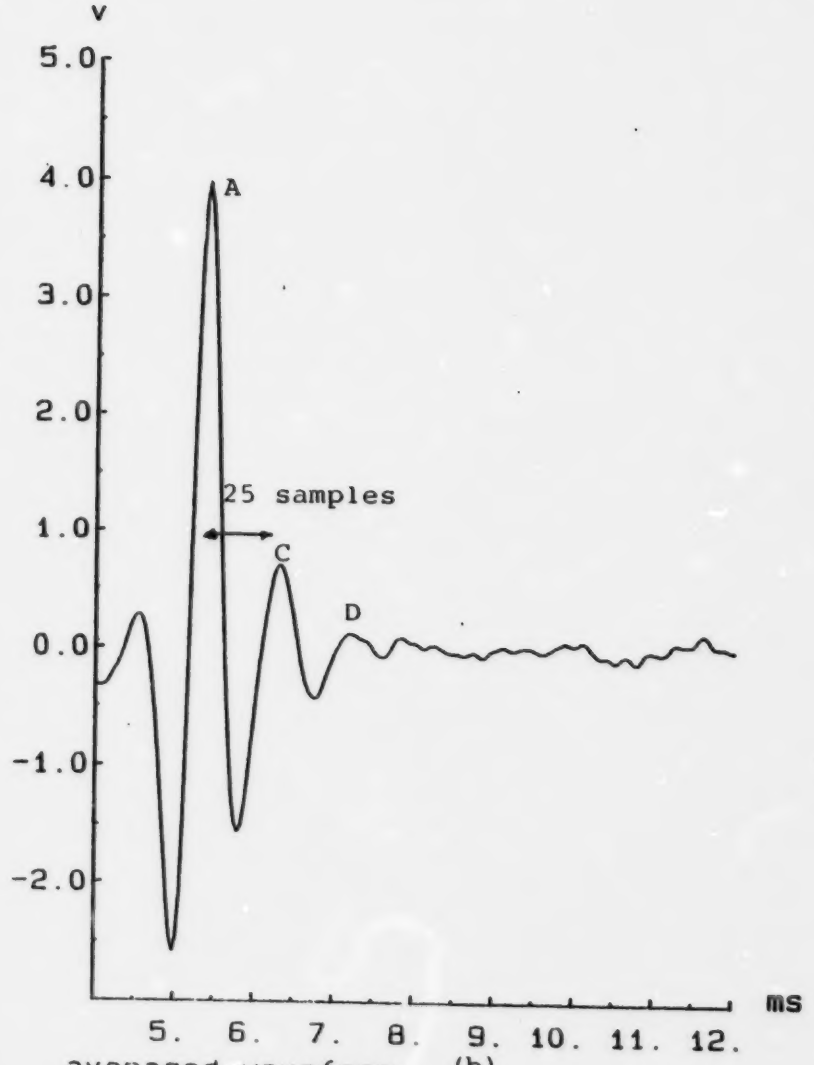

averaged waveform (b)

Fig. 5.17: (a) waveforms from line 4 between 16.2 to 21m
(b) averaged waveform from (a)

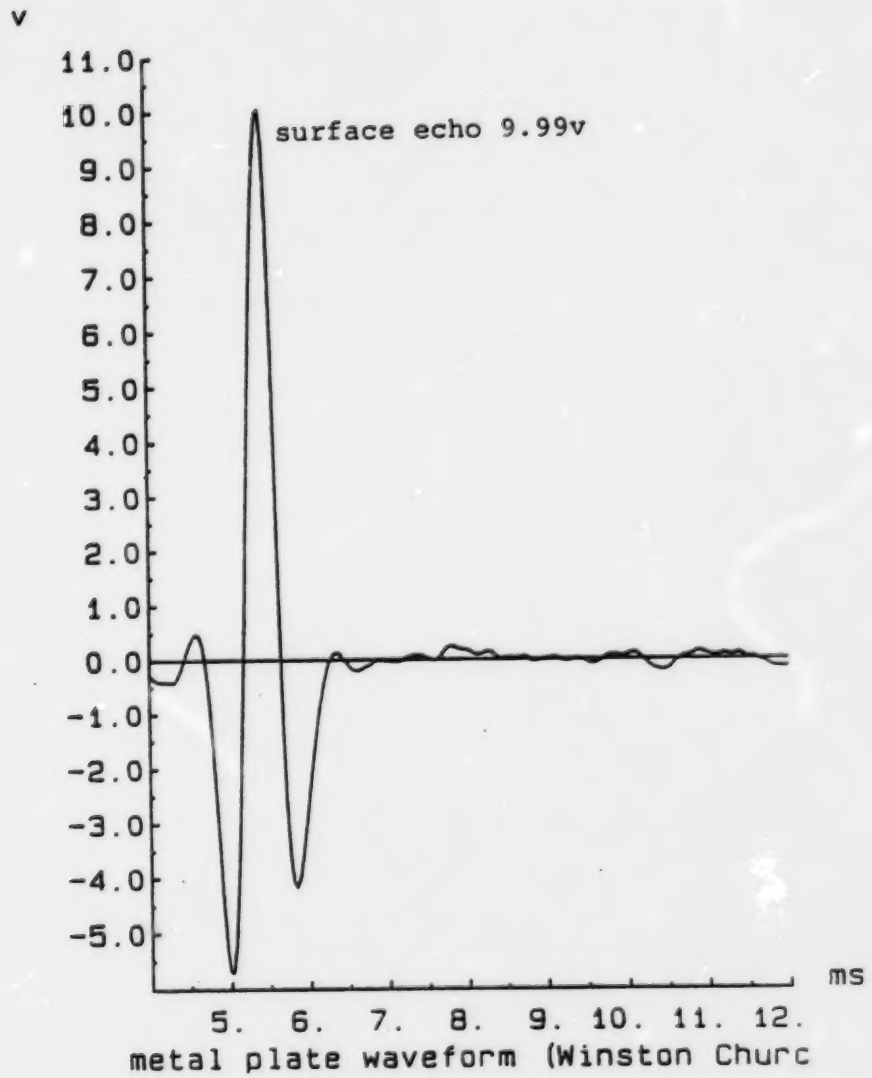

Fig. 5.18: metal plate from Winston Churchill

AVEraged THICKness SUMMARY

[AVEraged THICKness (mm)]

line number

114

metre	1	2	3	4	5	6	7
1	999 (999)	41 (53)	63 (36)	36 (38)	45 (56)	45 (55)	41 (38)
2	48 (40)	76 (51)	61 (53)	58 (66)	59 (68)	67 (53)	60 (47)
3	78 (38)	73 (42)	66 (46)	66 (50)	59 (64)	74 (47)	66 (39)
4	91 (33)	77 (39)	65 (43)	55 (48)	55 (55)	60 (47)	54 (46)
5	80 (34)	65 (40)	49 (43)	48 (49)	49 (45)	52 (40)	50 (44)
6	59 (35)	66 (36)	57 (46)	40 (59)	45 (43)	49 (33)	46 (32)
7	61 (33)	60 (53)	82 (41)	44 (52)	47 (40)	46 (51)	50 (51)
8	44 (41)	65 (39)	81 (35)	40 (45)	41 (47)	44 (33)	43 (30)
9	41 (45)	56 (43)	92 (32)	40 (44)	94 (39)	42 (35)	77 (46)
10	47 (43)	51 (67)	40 (60)	41 (41)	42 (42)	46 (39)	44 (41)
11	39 (39)	72 (50)	81 (33)	44 (39)	44 (39)	49 (38)	46 (46)
12	29 (44)	78 (47)	70 (42)	42 (42)	46 (38)	47 (44)	47 (48)
13	31 (41)	89 (35)	98 (39)	47 (41)	47 (46)	53 (37)	46 (34)
14	33 (46)	89 (46)	85 (46)	44 (49)	50 (39)	48 (37)	46 (37)
15	28 (42)	79 (43)	44 (47)	48 (42)	47 (42)	54 (37)	51 (37)
16	31 (40)	50 (47)	51 (43)	53 (40)	56 (47)	58 (49)	50 (42)
17	38 (45)	47 (57)	54 (53)	57 (51)	53 (41)	56 (35)	83 (52)
18	29 (50)	49 (50)	57 (47)	61 (51)	53 (33)	54 (34)	52 (34)
19	37 (45)	56 (51)	54 (43)	57 (43)	56 (44)	54 (41)	52 (39)
20	40 (45)	53 (41)	60 (41)	57 (41)	54 (54)	57 (44)	55 (42)
21	44 (54)	50 (49)	55 (47)	55 (50)	53 (41)	59 (42)	53 (41)
22	46 (48)	51 (49)	51 (44)	47 (46)	54 (38)	52 (37)	49 (34)
23	45 (48)	46 (41)	49 (60)	44 (71)	48 (39)	52 (38)	51 (48)
24	42 (47)	43 (48)	45 (49)	47 (51)	47 (39)	51 (40)	52 (40)
25	43 (47)	42 (42)	48 (40)	47 (46)	51 (43)	50 (35)	47 (33)
26	41 (46)	44 (39)	48 (44)	50 (42)	47 (39)	50 (38)	46 (35)
27	41 (48)	45 (42)	49 (41)	51 (44)	47 (36)	56 (38)	48 (35)
28	42 (52)	47 (46)	51 (47)	51 (51)	51 (39)	53 (47)	49 (39)
29	40 (53)	48 (45)	50 (46)	51 (47)	50 (61)	52 (65)	50 (47)
30	43 (47)	48 (38)	49 (41)	49 (43)	51 (62)	55 (56)	48 (43)
31	40 (44)	44 (89)	51 (47)	49 (44)	50 (49)	49 (40)	46 (41)
32	38 (49)	46 (38)	58 (42)	55 (48)	47 (37)	53 (38)	48 (37)
33	43 (50)	49 (37)	53 (43)	55 (48)	50 (33)	50 (40)	48 (38)
34	40 (48)	47 (35)	56 (37)	55 (36)	47 (39)	52 (44)	50 (42)
35	42 (54)	50 (39)	52 (38)	48 (37)	47 (47)	52 (60)	49 (53)
36	45 (45)	50 (46)	52 (39)	47 (38)	49 (54)	52 (42)	45 (41)
37	59 (46)	50 (64)	48 (67)	45 (42)	46 (41)	51 (48)	47 (45)
38	65 (39)	51 (41)	46 (50)	61 (28)	44 (63)	52 (49)	46 (52)
39	50 (41)	44 (50)	44 (44)	45 (45)	47 (42)	47 (53)	43 (45)
40	55 (44)	45 (37)	44 (45)	94 (36)	94 (29)	92 (41)	75 (29)
41	59 (39)	49 (48)	44 (43)	44 (42)	97 (36)	88 (36)	43 (34)
42	48 (47)	49 (42)	47 (48)	45 (49)	97 (42)	48 (32)	43 (34)
43	52 (38)	51 (42)	46 (53)	44 (61)	46 (39)	90 (32)	70 (37)
44	69 (47)	49 (39)	45 (41)	43 (44)	94 (32)	90 (36)	43 (37)
45	71 (49)	51 (42)	44 (46)	42 (40)	94 (29)	48 (37)	44 (39)
46	71 (53)	51 (47)	46 (44)	45 (47)	98 (43)	48 (39)	45 (33)
47	45 (32)	50 (46)	47 (46)	55 (40)	99 (43)	90 (42)	45 (31)
48	80 (43)	51 (37)	47 (39)	51 (40)	61 (42)	94 (44)	44 (39)
49	77 (47)	49 (37)	47 (41)	58 (41)	43 (89)	94 (50)	45 (35)
50	48 (79)	52 (35)	50 (39)	48 (80)	97 (41)	46 (60)	49 (40)
51	45 (78)	55 (29)	46 (43)	50 (82)	50 (43)	51 (41)	53 (43)
52	47 (75)	52 (30)	45 (43)	59 (43)	45 (87)	56 (43)	58 (45)
53	89 (44)	50 (35)	49 (52)	57 (42)	46 (88)	53 (38)	56 (37)
54	73 (53)	45 (45)	47 (47)	63 (38)	46 (86)	50 (39)	52 (37)
55	76 (46)	47 (40)	49 (45)	46 (49)	98 (42)	51 (43)	51 (33)
56	49 (76)	49 (37)	46 (50)	41 (42)	92 (46)	50 (35)	51 (33)
57	77 (36)	50 (54)	43 (62)	73 (39)	90 (51)	50 (39)	52 (37)
58	71 (39)	44 (34)	39 (62)	70 (49)	93 (48)	50 (36)	52 (36)
59	68 (39)	42 (40)	36 (37)	71 (43)	97 (47)	55 (38)	52 (41)
60	73 (44)	41 (38)	87 (29)	85 (40)	81 (29)	53 (47)	51 (40)
61	86 (47)	44 (45)	40 (54)	91 (34)	71 (26)	50 (53)	51 (46)
62	77 (42)	43 (45)	41 (60)	62 (65)	44 (71)	50 (56)	52 (42)
63	75 (50)	44 (40)	42 (58)	42 (53)	51 (41)	52 (39)	55 (40)
64	61 (44)	44 (38)	44 (44)	43 (36)	48 (85)	54 (54)	56 (46)
65	54 (51)	44 (32)	45 (38)	44 (40)	52 (76)	57 (52)	56 (46)
66	63 (55)	47 (57)	46 (39)	47 (87)	51 (81)	56 (49)	48 (53)
67	64 (54)	49 (35)	50 (39)	47 (67)	55 (74)	49 (39)	45 (45)
68	61 (52)	50 (39)	53 (44)	55 (40)	58 (54)	60 (27)	46 (54)
69	69 (57)	49 (35)	49 (46)	50 (85)	57 (67)	71 (44)	52 (31)
70	73 (51)	51 (37)	49 (52)	49 (49)	57 (69)	52 (56)	47 (52)
71	74 (52)	57 (41)	56 (40)	62 (42)	62 (61)	90 (35)	54 (36)
72	74 (35)	79 (38)	86 (41)	71 (31)	69 (64)	92 (48)	82 (39)
73	49 (79)	81 (44)	51 (37)	91 (50)	74 (54)	92 (38)	94 (33)
74	26 (77)	88 (44)	51 (31)	52 (63)	92 (45)	48 (38)	62 (39)
75	19 (51)	47 (34)	86 (42)	62 (66)	47 (71)	999 (999)	47 (43)
76	39 (41)	81 (46)	82 (41)	67 (67)	80 (58)	999 (999)	83 (43)

Table: 5.5: The averaged thickness of asphalt and concrete cover

BRIDGE deck CONDition SUMMARY

[ASPhalt AVERaged THICKness]

	line number 1	2	3	4	5	6	7
mm	51	54	54	58	63	58	52
in	2.01	2.13	2.13	2.28	2.48	2.28	2.05
ave dielect	7.83	6.16	5.56	5.59	5.42	5.58	6.58

[C/O REINFORCEment AVEraged THICKness]

	line number 1	2	3	4	5	6	7
mm	49	46	44	48	50	42	40
in	1.89	1.81	1.73	1.89	1.97	1.65	1.57

[LINE DISTRIBUTion (%)]

	line number 1	2	3	4	5	6	7
GOOD	33.07	20.67	21.19	28.50	43.34	23.86	15.18
DEBONDed	.00	.26	.00	.00	.00	.00	.00
SCALEd	.00	.26	2.33	.78	.52	.00	.00
DELAMINATed	65.63	77.78	75.45	69.95	55.87	76.14	84.29
BAD data	1.29	1.03	1.03	.78	.26	.00	.52
TOTAL	100.00	100.00	100.00	100.00	100.00	100.00	100.00

metal PLATE AMPlitude is: 9.899971 v

OVERALL AVEraged DIELECTric constant of asphalt is 6.1029

OVERALL AVERaged ASPhalt THICKness is 55 mm, [2.17 in]

OVERALL AVEraged C/O REINFORCEment THICKness is 45 mm, [1.77 in]

[OVERALL bridge deck CONDITION]

GOOD	26.54 %
DEBONDED	.04 %
SCALed	.56 %
Delaminated	72.16 %
BAD data	.70 %
Total	100.00 %

Table 5.6: A summary of deck assessment for Winston Churchill Overpass.

For the computer analysis, we now normally provide the computer with the thickness measurement of a core sample obtained from the site in order to initiate a searching window for the asphalt-concrete interface peak. Since both of our site visits to Winston Churchill were conducted at an early date, core sampling was not exercised. The bridge deck was evaluated using the MTC87 package. In Table 5.5, the averaged thickness of asphalt and concrete cover over reinforcement for each 1 m interval are given. A summary of deck assessment is provided in Table 5.6. The overall thickness of asphalt is 55 mm and the overall concrete cover is 45 mm.

From the analysis, it is reported that the deck has 72.16% delamination, 0.56% scaling and 0.04% debonding. There is only 26.54% good area. The maps shown in Figs. 5.19 to 5.21 are computer generated results which indicate locations where delamination, scaling and debonding are detected. In Appendix D, results from cluster analysis are given for reference purposes.

5.2.2 Verifications Of Computer Results

The sampled waveforms collected in Figs. 5.15 to 5.17 can be used to verify the computer survey. In order to compare the computer results with the waveforms, the measurements from lines 2, 3 and 4 are averaged from 17 to 21 m. According to Table 5.5, we have the following results:

Computer results showing the thickness measurements and terface peak locations. Peak C is asphalt-concrete interface and peak D is rebar. The dielectric constant of asphalt is obtained from Table 5.6.

Line	Fig	dielectric	asphalt	peak C	concrete	peak D
2	5.15	6.16	51 mm	6.20 ns	50 mm	7.15 ns
3	5.16	5.56	56	6.16	46	7.04
4	5.17	5.59	57	6.26	47	7.16

The asphalt-concrete and rebar interface peaks are estimated from the averaged thickness measurements. We note that there is a good correlation of the calculated locations with the reflections from averaged waveforms.

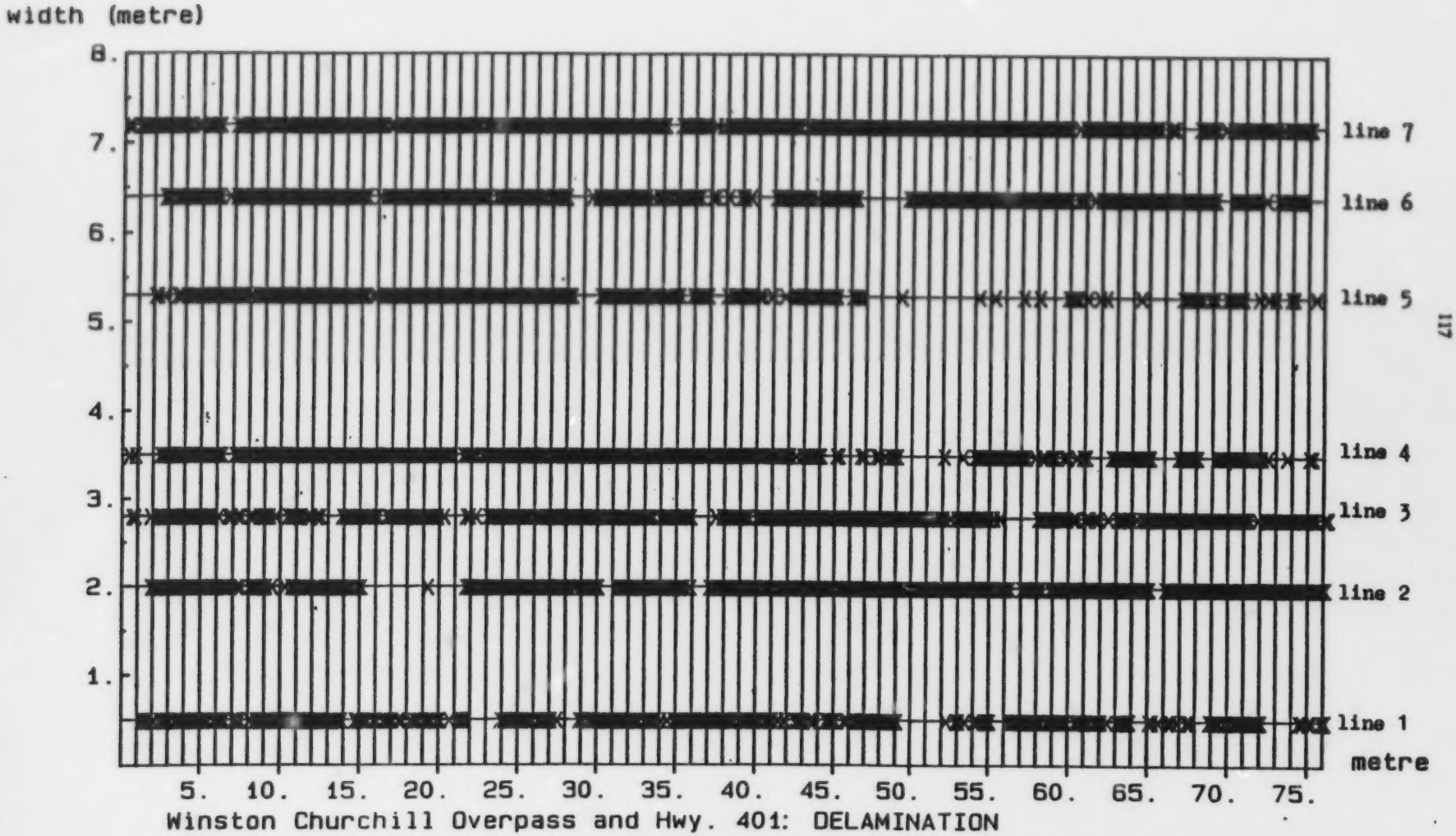

Fig. 5.19: Grid map indicates areas of delamination on Winston Churchill Overpass.

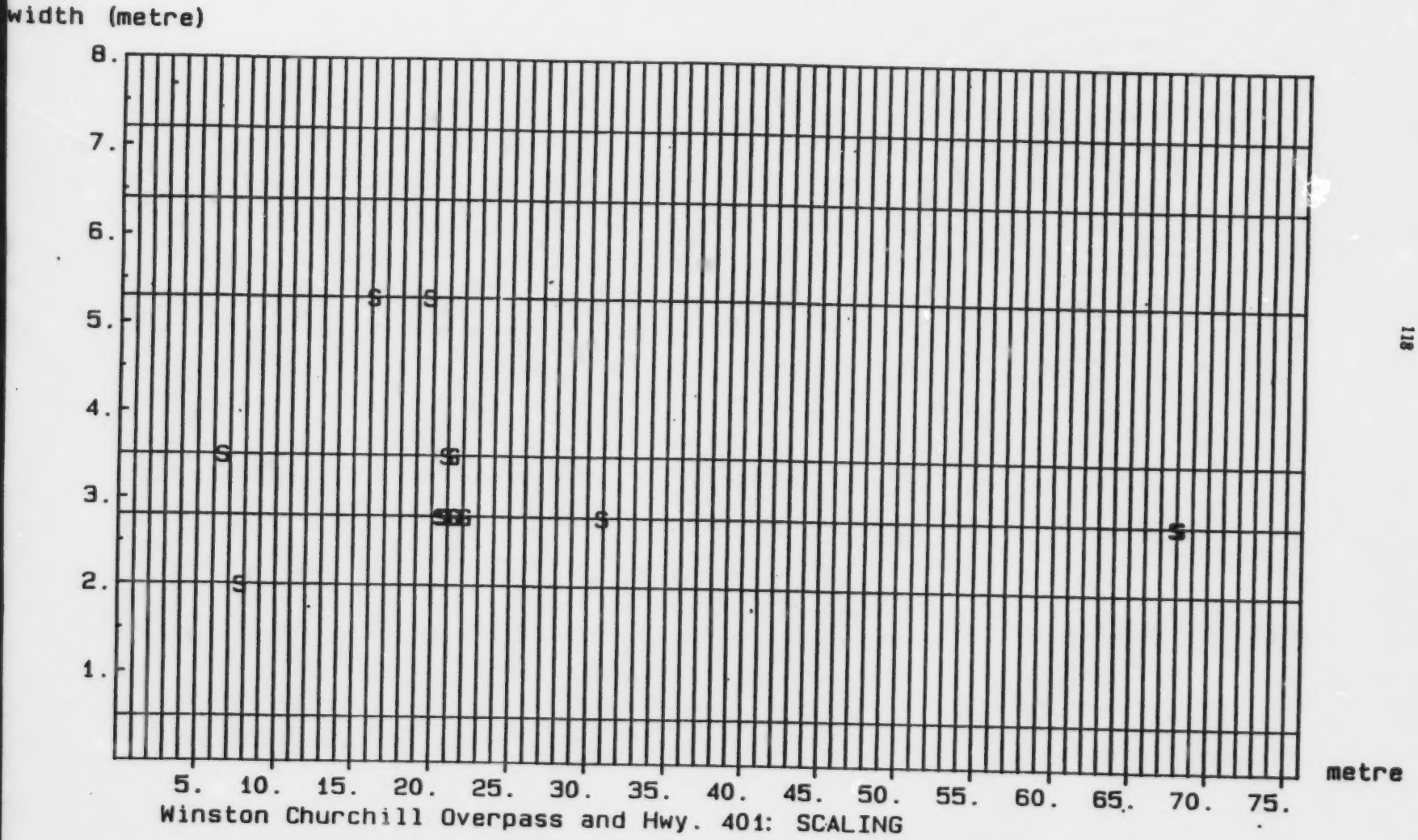

Fig. 5.20: Grid map indicates areas of scaling on Winston Churchill Overpass.

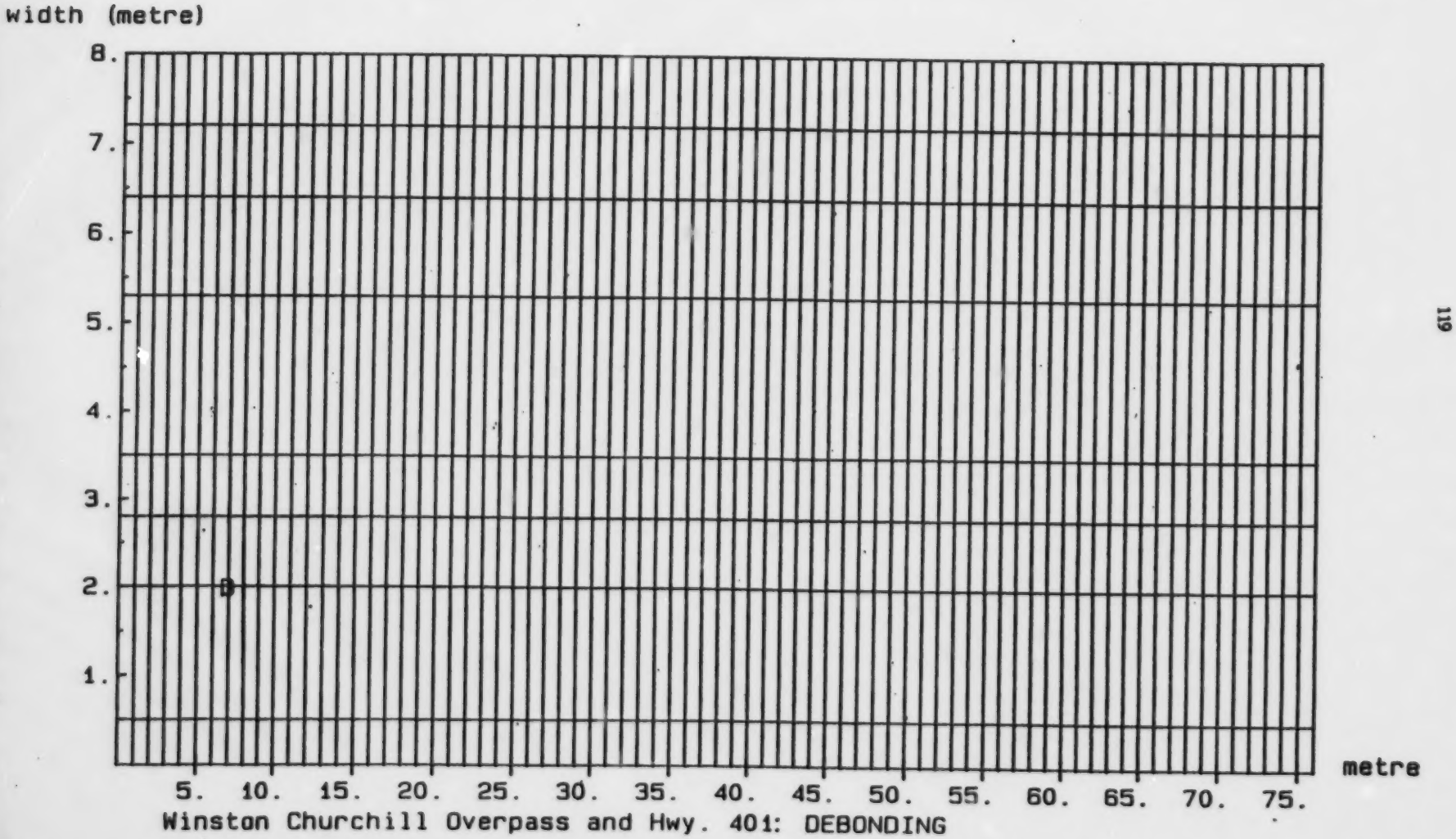

Fig. 5.21: Grid map indicates areas of debonding on Winston Churchill Overpass.

5.2.3/ Computer Results Versus Site Observations

On the second site visit, two areas where the maps (Figs. 5.19 and 5.20) are marked with deteriorations are examined. The selected areas are in the neighbourhood of 20 m and 40 m on line 3. These areas are declared scaled and delaminated.

The asphalt surface of the two areas was removed and the thickness measured. A sketch of the stripped areas is given in Fig. 5.22. At the 20 m location, we found that the asphalt- concrete interface layer was badly disintegrated. There was a mixture of coarse sand and loose gravel in the vicinity. This is the characteristic of scaling. By removing the loose substances, the rebars were found to be exposed and found to be rusty in several spots. The depth of four stripped pieces of asphalt were measured. They all had an averaged thickness of about 55 mm. The rebars were estimated to be 35 mm down from the asphalt-concrete boundary.

These observations are compared with the computer results. From Table 5.5, the averaged thickness of asphalt bounded by the area from 19 to 20 m at lines 2, 3, and 4 is 56 mm. The instantanenous thickness at line 3-20 m is 60 mm. For concrete cover measurement, the averaged depth of the rebars is 45 mm and the instantanenous depth is 41 mm from the asphalt-concrete interface. Sampled waveforms from 20 m at line 2, 3, and 4 were plotted in Fig. 5.23. We note that in Fig. 5.23(b) and (c) the reflection is quite prominent from the asphalt-concrete interface peak. Experience from previous studies have shown that only a waveform from an area of scaling produces this kind of signature. Our computer survey, in fact, gives the same results.

Around the 40 m location on line 3, the averaged thickness measured from several pieces of stripped asphalt was 50 mm. We observed that the concrete surface was still intact. The delamination test (based on the chain drag) was exercised in the area and the result showed a positive response. The concrete cover was later removed. It was found that rebars, which were about 35 mm from the asphalt-concrete boundary, also had a few rusty spots.

From Table 5.5, the nearby area (39-40 m lines 2,3,4) is calculated to have an averaged depth of 52 mm for asphalt and 38 mm for concrete cover. The instantaneous measurements at line 3-40 m are 44 mm and 45 mm respectively for the asphalt and concrete. Sampled waveforms are also provided for the 40 m location on lines 2, 3 and 4. These are shown in Fig. 5.24. We note the absent of the characteristic W between the asphalt-concrete interface peak and the rebars peak. From previous studies, it has been found that often delamination occurs when waveforms display has this property. Field observations agree quite well with the computer findings.

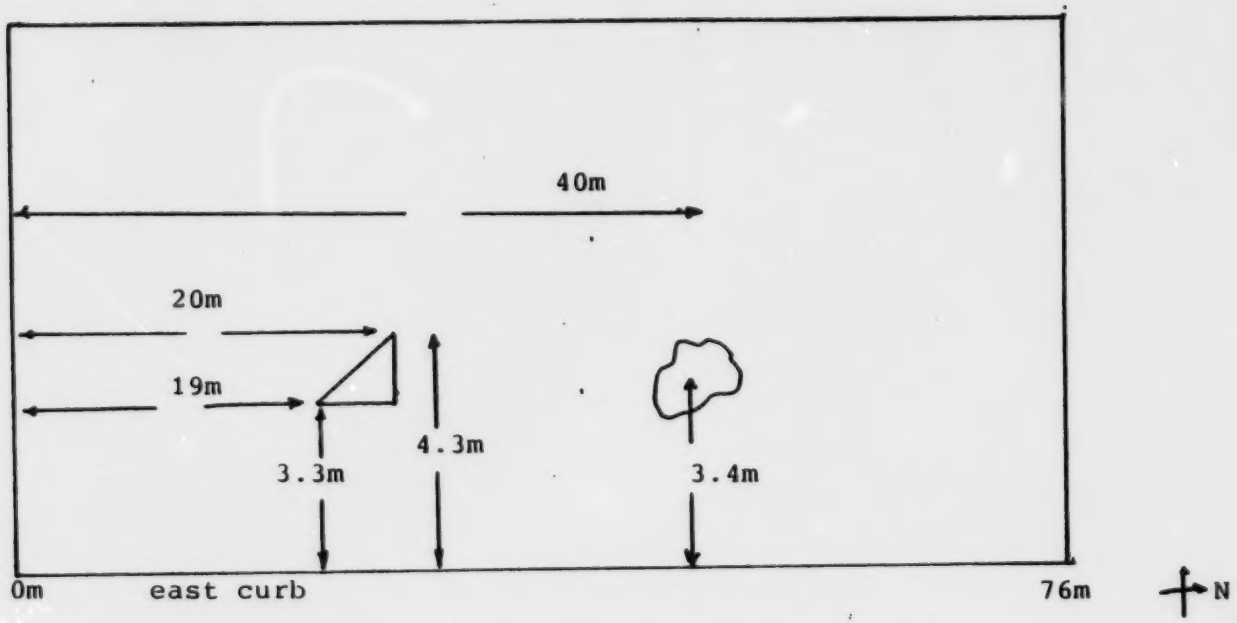

Fig. 5.22: A sketch of the stripped area from the second site visit.

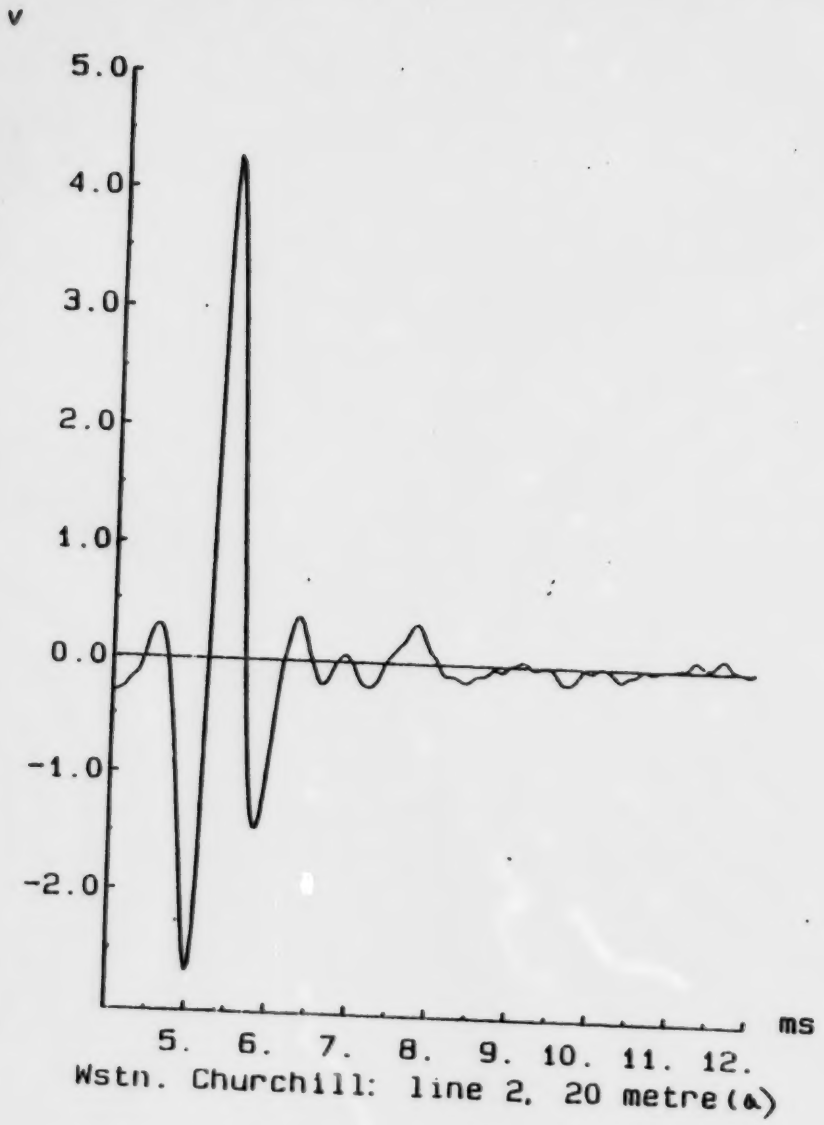

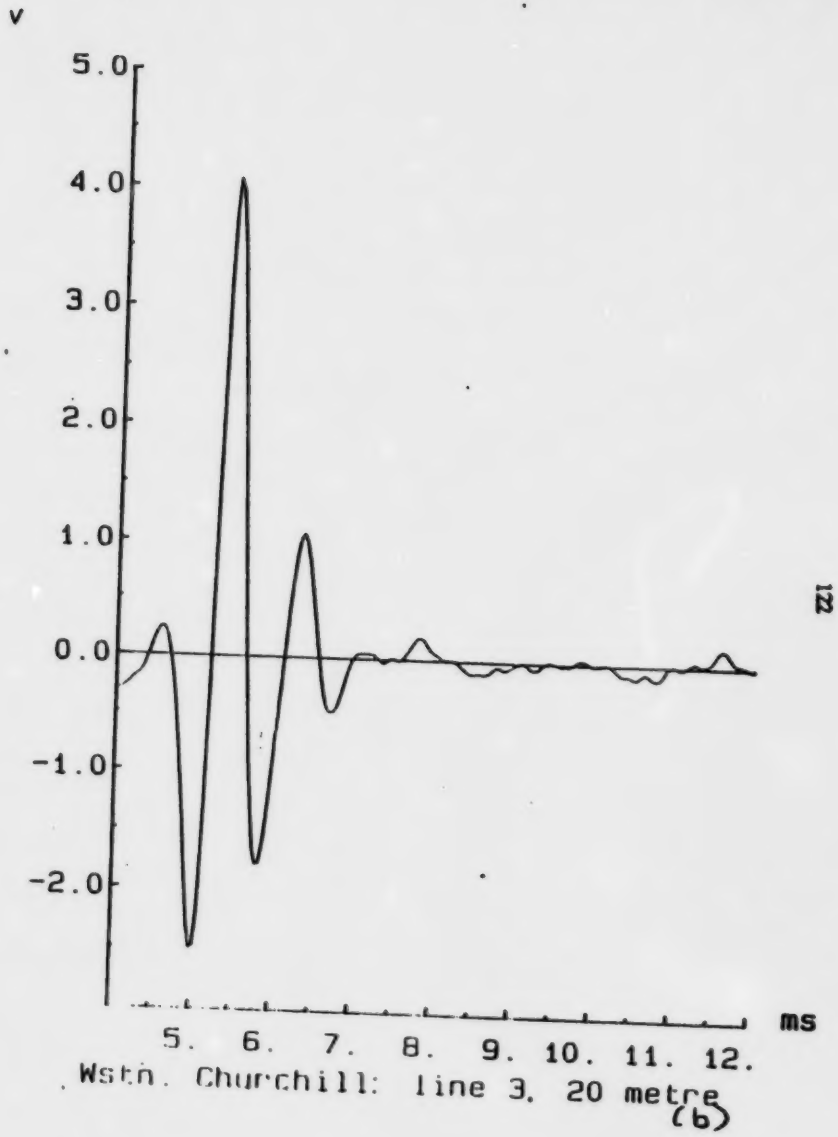

Fig. 5.23: (a) waveform from line 2 at 20m
(b) waveform from line 3 at 20m

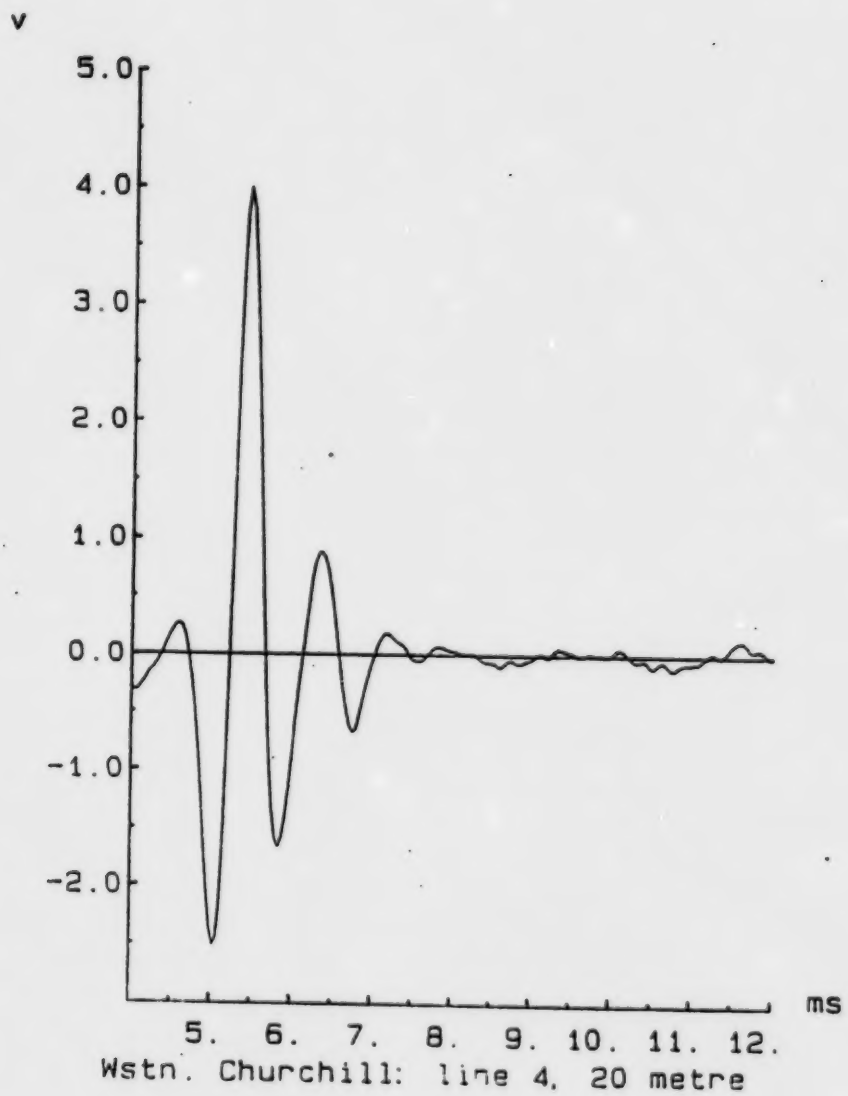

Fig. 5.23(c): waveform from line 4 at 20m.

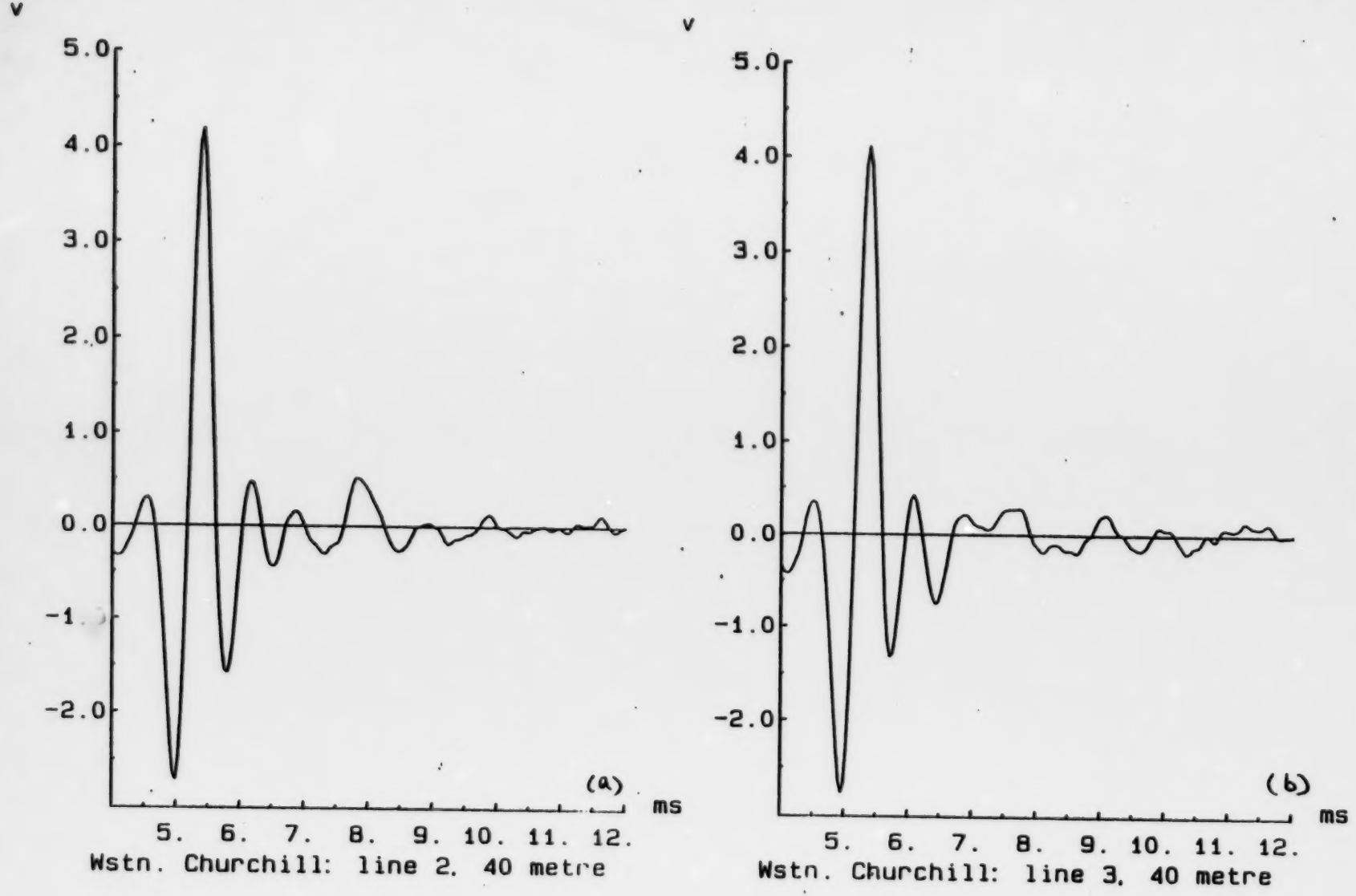

Fig. 5.24: (a) waveform from line 2 at 40m
(b) waveform from line 3 at 40m.

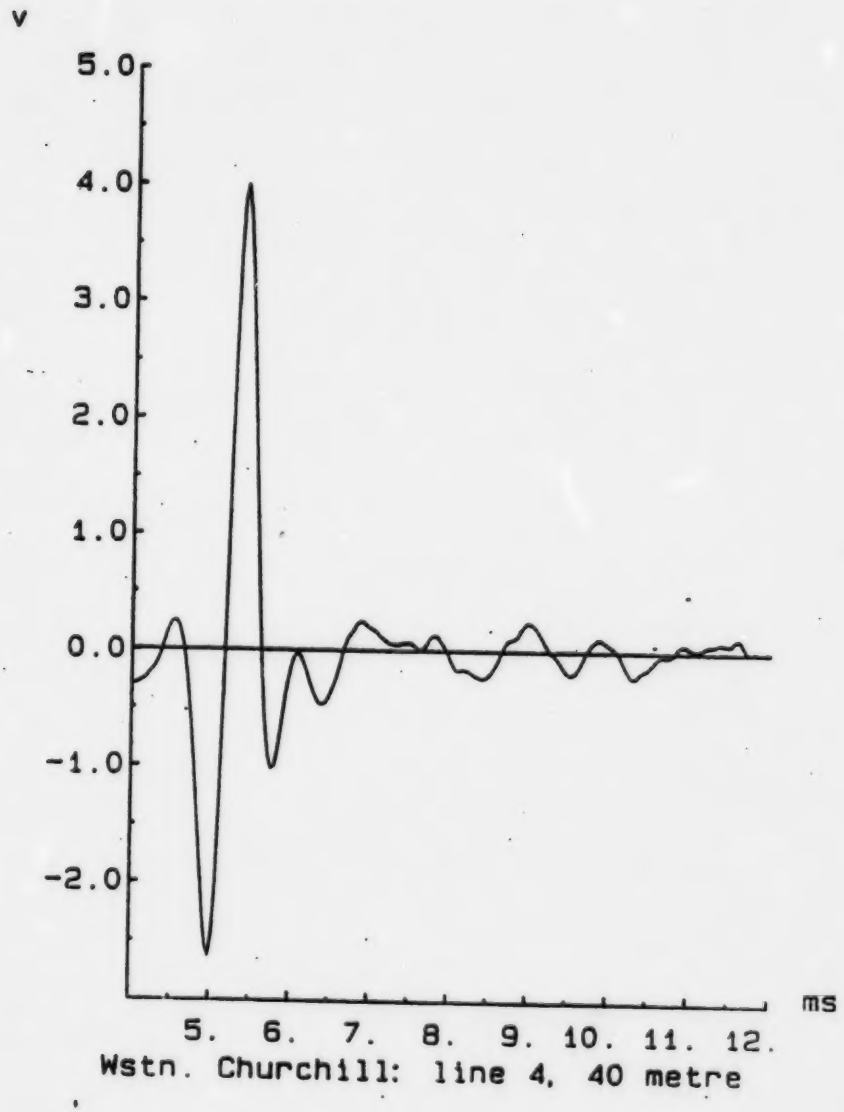

Fig. 5.24(c): waveform from line 4 at 40m

5.2.4/ Summary

In this analysis, bridge deck assessment was first performed by computer survey. A second site visit was then scheduled in order to verify the results. At the site, two locations were selected for intensive examination. We have shown that there is a good correlation of the computer findings with the field observations.

5.3/ Processing of Bloor Street Via Duct Data

Data from Bloor Street Via Duct were collected in late-May of 1987. The bridge deck covers a total length of 447 m. There are three driving lanes for each direction (East-West) of traffic. Six lines were recorded on each side covering the two outermost lanes each way. The site plan is given in Fig. 5.25. It is also noted that along the bridge deck there are numerous metal joints beneath the asphalt surface.

5.3.1/ Core Sample

A core sample was obtained from line 3 at about the 180 m location. A photograph of this core sample is shown in Fig. 2.14 We see that the asphalt layer was actually composed of three different layers of material. The composition of the first layer of asphalt is mainly tar and fine sand. The second layer contains tar, gravel and stone. The bottom layer also contains tar, gravel and stone but of a larger size than the middle layer. The individual layer of asphalt from top to bottom have thickness of 26, 44 and 60 mm respectively. The overall thickness is 130 mm.

In Fig. 5.26, the radar signature from the core sample location is provided. Except for the surface echo reflection (peak A), direct interpretation of the reflections, namely, peak 1, peak 2 and peak 3 is rather difficult. However, with the information obtained from the core sample, the asphalt-concrete interface layer can be located.

We have given that the total thickness of core sample as 130 mm. In order to determine the asphalt-concrete interface from the waveform in Fig. 5.26, we need to calculate the dielectric constant of asphalt. The amplitude of the surface echo of Fig. 5.26 is 3.8 V (5.6 ms) and the amplitude of the metal plate reflection at the core sample location is measured to be 9.7 V.

From the procedures given in Section 2, the dielectric constant of asphalt is calculated to be 5.23. Once the thickness and the dielectric constant of asphalt are available, the asphalt-concrete interface peak can be identified easily. According to eq. (3.1), the asphalt-concrete interface peak is

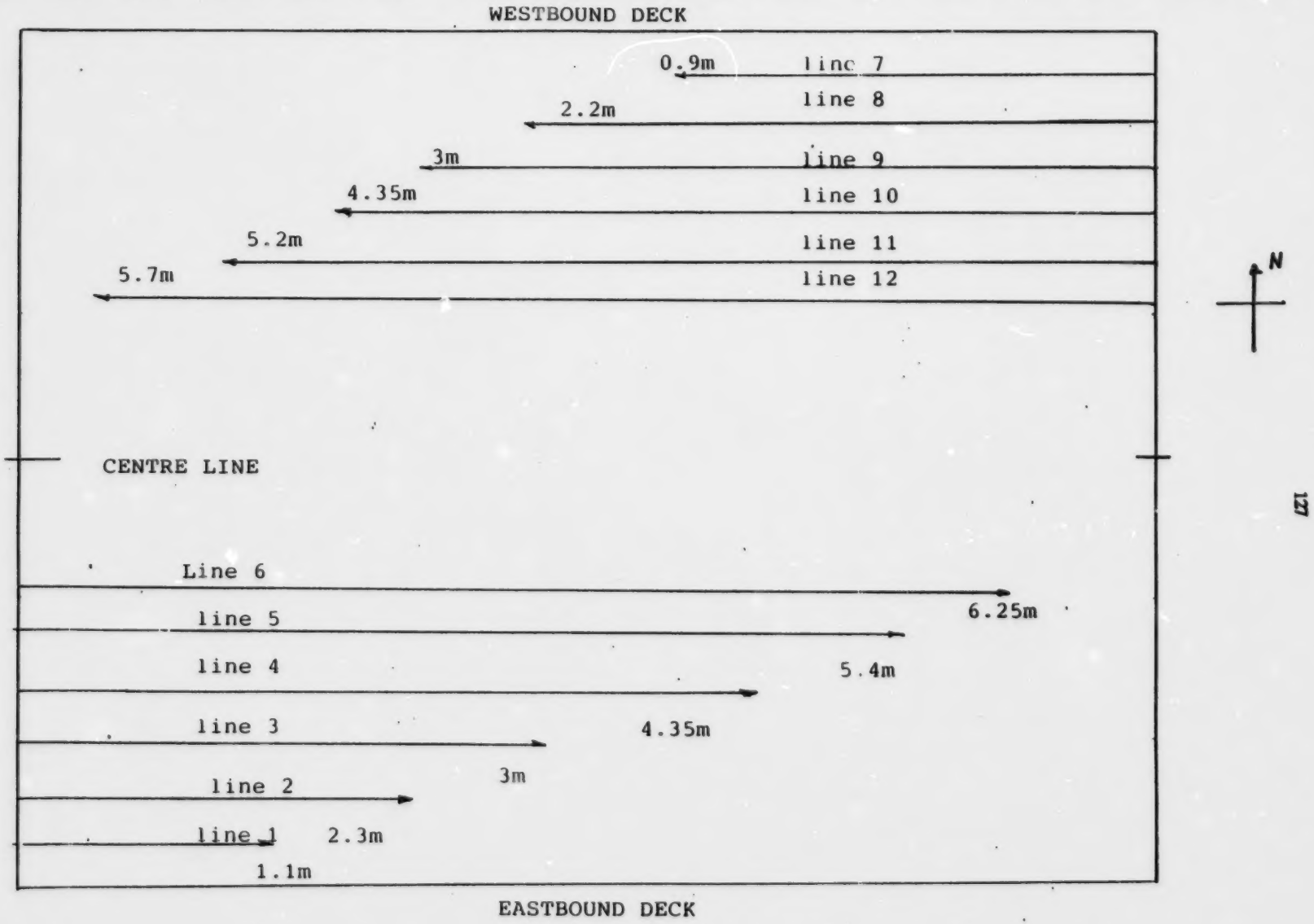

Fig. 5.25: A skectched site plan of Bloor Viaduct deck.

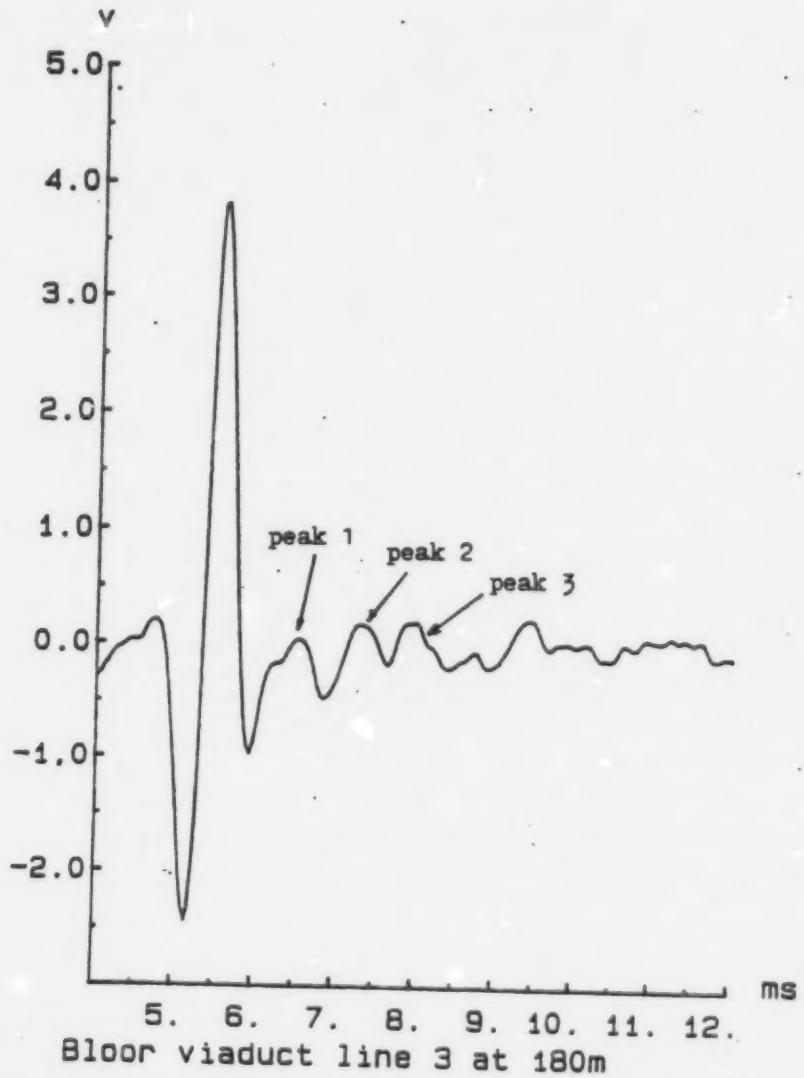

Fig. 5.26: Radar signature from the core sample.

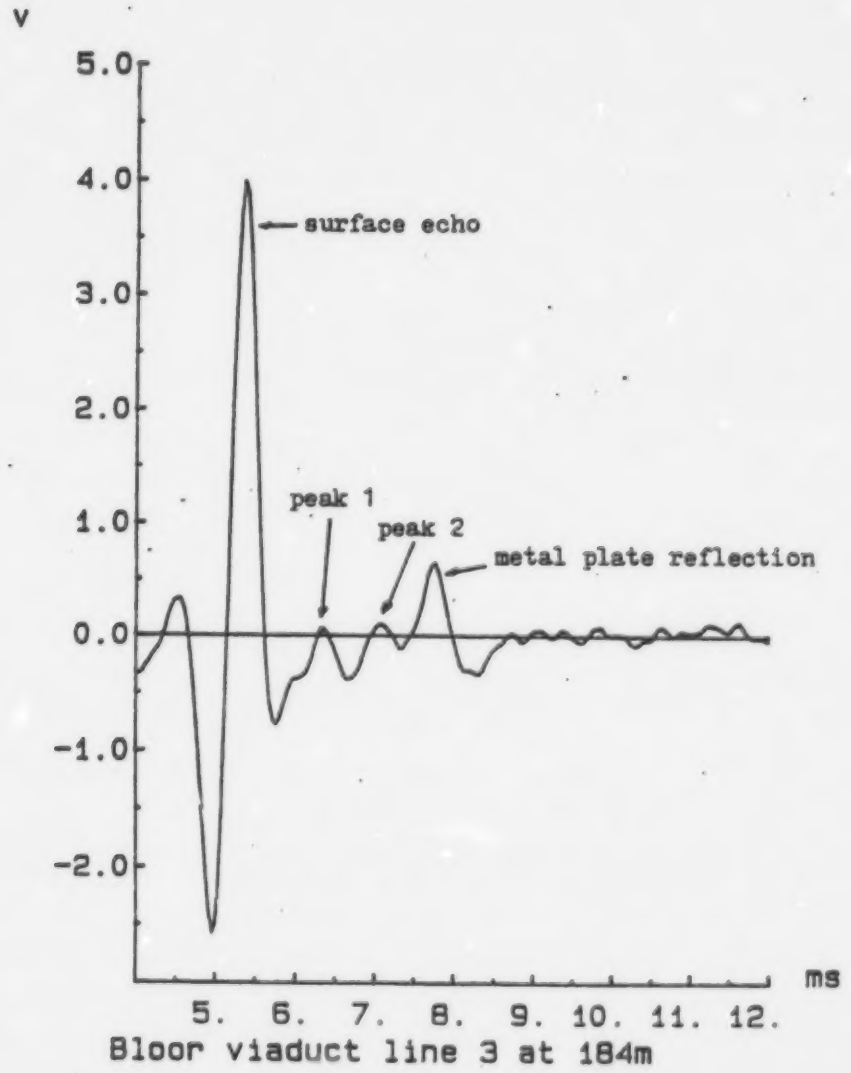

Fig. 5.27: Reflected signal from a metal joint under the asphalt surface.

estimated at 7.58 ms. From the waveform, we see that peak 3 (8 ms) is the nearest peak which can be identified.

It is necessary to estimate the magnitude of error in determining the asphalt thickness. We note that from our calculation the asphalt-interface peak is at 7.58 ms but the waveform indicates that the peak is actually at 8 ms. The time difference affects the thickness measurement. By calculating the time difference between the surface echo (5.6 ms)and the asphalt- concrete interface peak (8 ms) and knowing that the dielectric constant is 5.23, we can determine the asphalt thickness. The result yields 157 mm. In comparing this result with the physical measurement from the core sample the percentage of error is about 20%.

This error is due to the fact that the dielectric constant we have obtained does not reflect the actual character of the multi-layer asphalt. It is only the value of the first layer of asphalt.

For multi-layer asphalt each having significantly different dielectric constants, an averaged value of the dielectric constant is a better approximation. In the present case, we know that there are metal joints under the asphalt surface at numerous locations along the bridge deck. This arrangement is identical to the method we employed in measuring the dielectric constant of asphalt in Section 3. The same procedures can then be applied here again.

In Fig. 5.27, a sample waveform is obtained from a metal joint location (this is line 3 at about 184 m). We note that the metal joint provides significant reflection at 7.75 ms. By comparing this reflection with peak 3 in Fig. 5.26, we can determined that peak 3 is the asphalt-concrete reflection. The reflections at peak 1 and peak 2 (Fig. 5.27) are from the boundaries between each layer of asphalt. The averaged dielectric constant of the three layer asphalt is thus calculated to be about 6.92 at the given location. If we assume that the value of dielectric constant does not vary significant for each bridge deck, we can then re-calculate the asphalt thickness of the waveform given in Fig. 5.26. The result is 137 mm which agrees closely with the core sample. However, in order to achieve more accurate measurement, it is desirable to calculate the dielectric constant of each individual layer of asphalt.

Having determined the asphalt-concrete interface peak, the next reflection we want to identify is the reflection from rebars. By referring back to Fig. 5.26, we note that there is a well defined characteristic W after the asphalt-concrete interface peak for a deck in good condition. The rebar reflection is identified at about 9.5 ms. With the dielectric constant of concrete estimated as 8.22 (see Section 3), the concrete cover is measured to be 78 mm.

This further demonstrates the importance of taking core samples from each bridge deck. Without core sample information, radar reflection waveforms can be mis-interpreted. For example, it is not difficult to identify peak 1 from Fig. 5.26 as the asphalt-concrete interface peak and peak 2 as the rebar reflection. As a result the waveform is declared delaminated. Furthermore, it is possible that deterioration may occur between different layers of asphalt. This situation produces multiple reflections which interfere with the asphalt-concrete interface reflection. Waveform interpretation becomes more difficult to interpret.

5.3.2/ Waveforms Comparison

Waveforms obtained from Ninth Line and Winston Churchill data are compared with those from the Bloor Street Via Duct. These three sets of waveform represents three different classifications of bridge deck. For convenience, waveforms from Ninth Line and Winston Churchill are reproduced in Fig. 5.28 and Fig. 5.29, respectively.

Data collected from Ninth Line indicate that the bridge deck is in very good condition. The asphalt surface may have two lifts. Usually in this case, the top layer is quite thin. Underneath the asphalt surface there is a layer of waterproofing membrane. The changes in material produce a reflection at the boundary. The asphalt-membrane interface is indicated as point M on the averaged waveform in Fig. 5.28. The membrane-concrete interface is denoted by peak C and the rebar is given by peak D.

For Winston Churchill, the site inspection indicated that the bridge deck has asphalt overlay with thickness of about 55 mm and the concrete cover is around 40 mm. All interface peaks are identified and denoted in Fig. 5.29.

In the software, a search window for the asphalt-concrete interface peak is set according to the asphalt thickness obtained from one or more core samples. The window is tailored in such a way that it will not confuse the transient peak from the asphalt- membrane interface as the reflection from the membrane-concrete interface. As long as peak C is identified, the program will set a different window to locate the rebar reflection. This is usually the next well-defined peak after the asphalt-concrete (or membrane-concrete) interface. The software package MTC87 can handle both bridge deck types.

In Fig. 5.30, a set of waveform obtained from Bloor Via Duct is presented. The data is from the section between 47.2 and 52 m of line 2. From the waveforms we note that sometimes peak 2 has a magnitude which is comparable with the asphalt-concrete interface peak. Also the transient

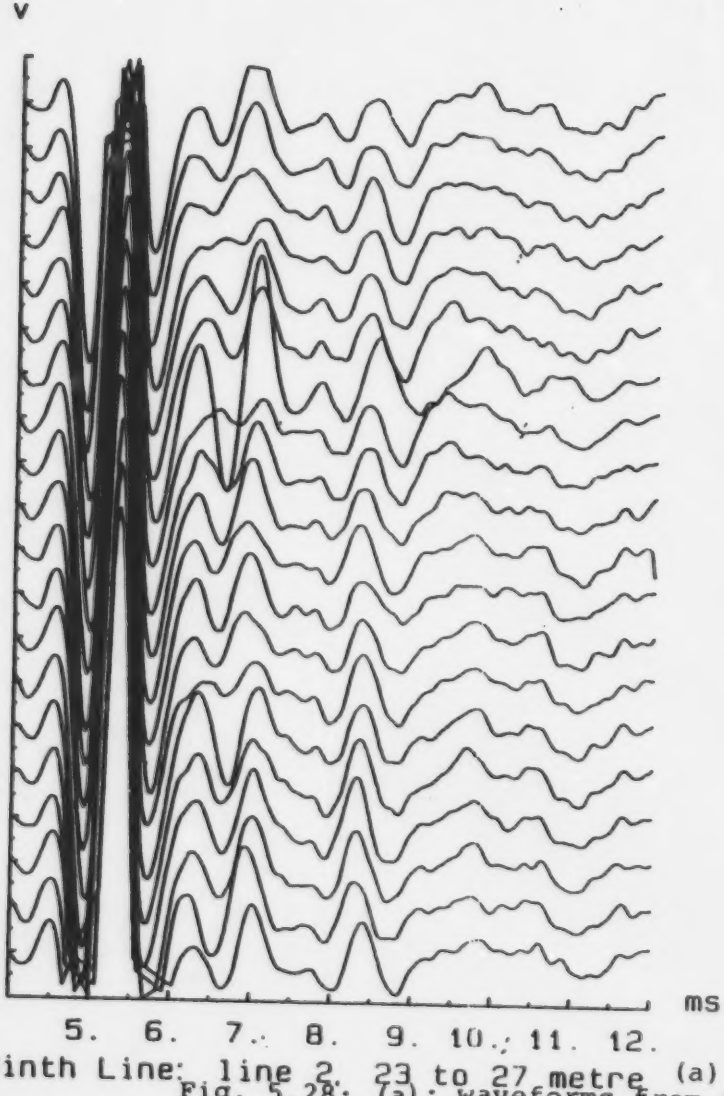

Ninth Line: line 2, 23 to 27 metre (a)

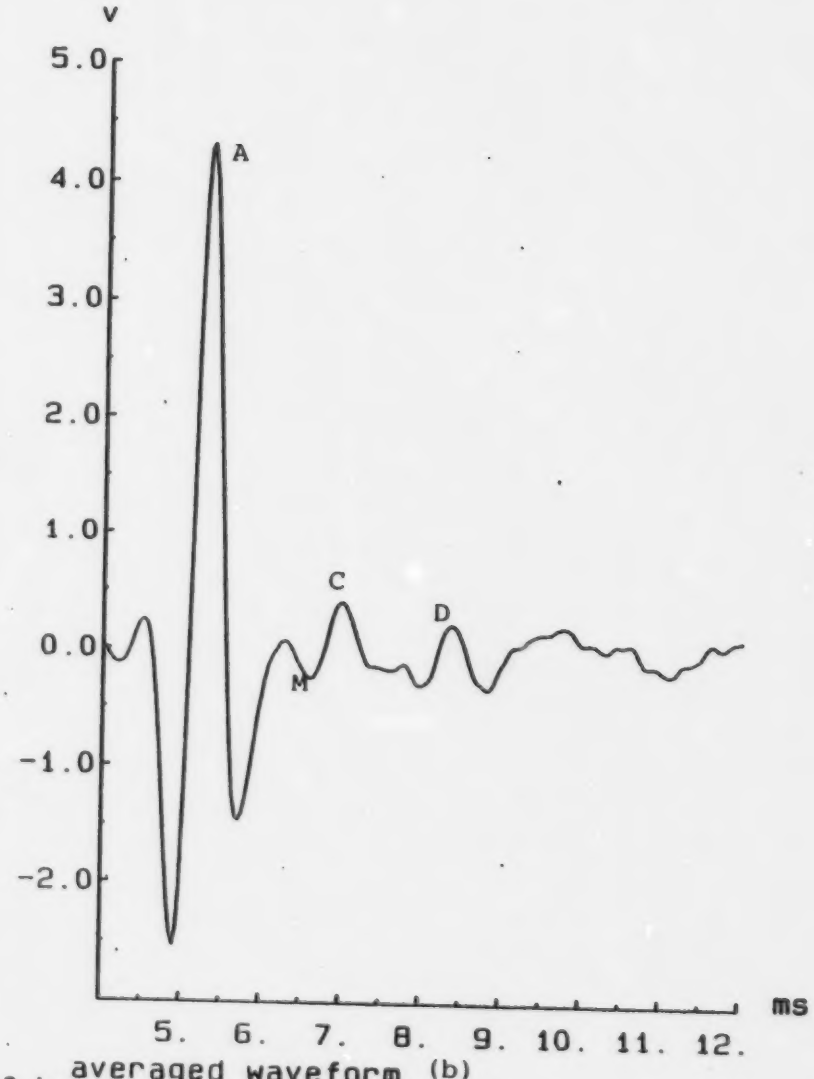

averaged waveform (b)

Fig. 5.28: (a): waveforms from line 2 betwen 23 to 27 m on NinthLine
(b) averaged waveform of (a)

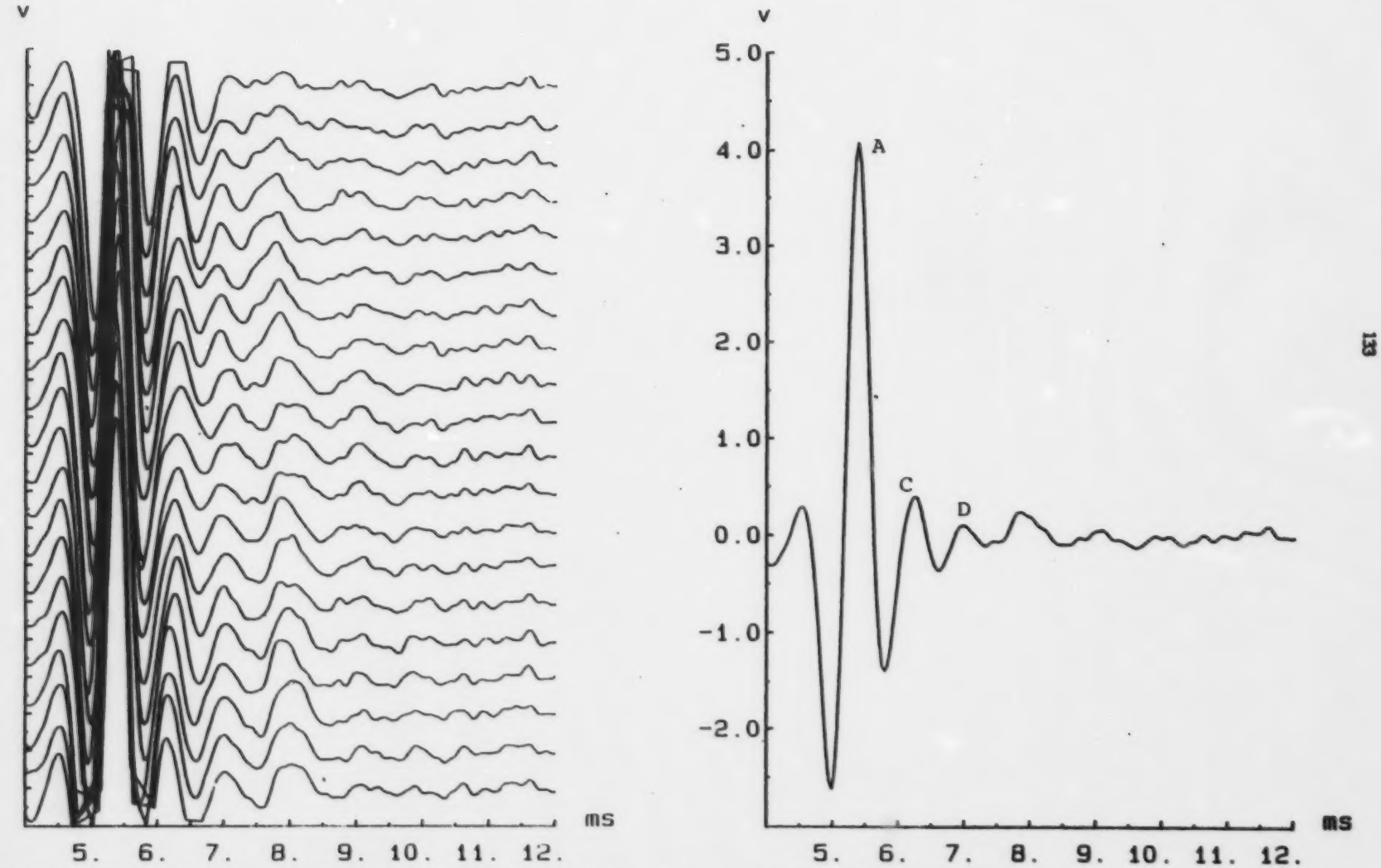

Fig. 5.29: (a) waveforms from line 2 between 16.2 to 21m on Winston Churchill
(b) averaged waveform of (a)

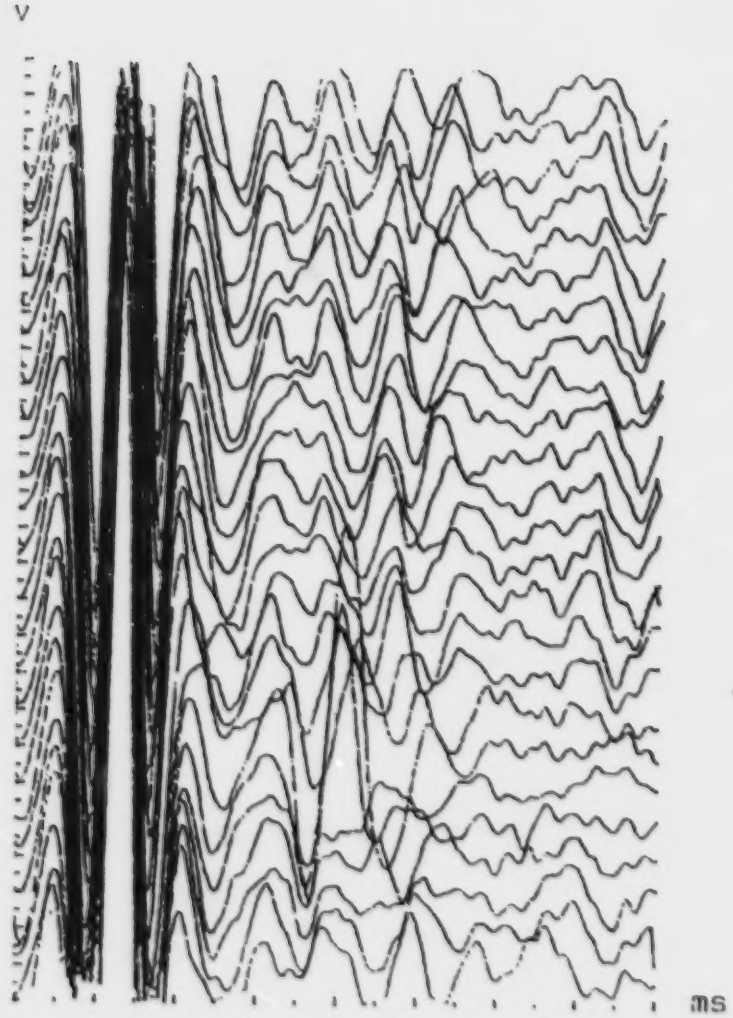

bvd2 (2): 47to 52 m (a)

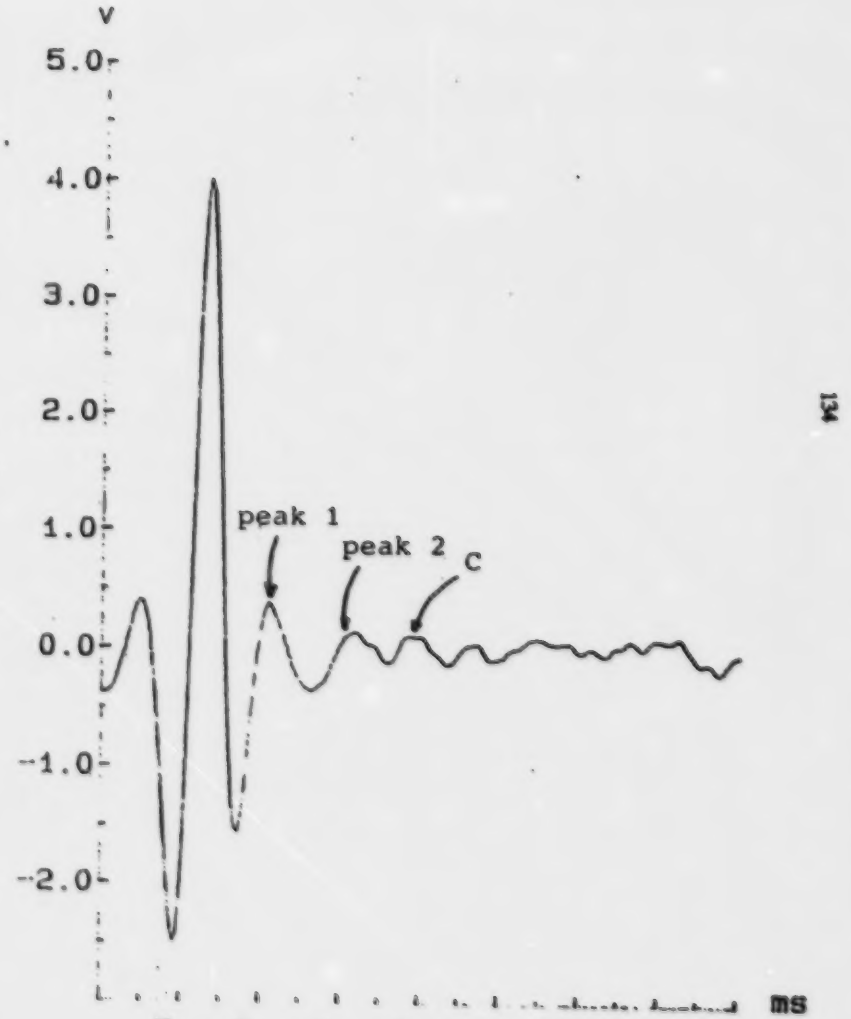

averaged waveform (b)

Fig. 5.30: (a) waveforms from line 2 at 46.2 to 52m on Bloor Viaduct
(b) averaged waveform of (a)

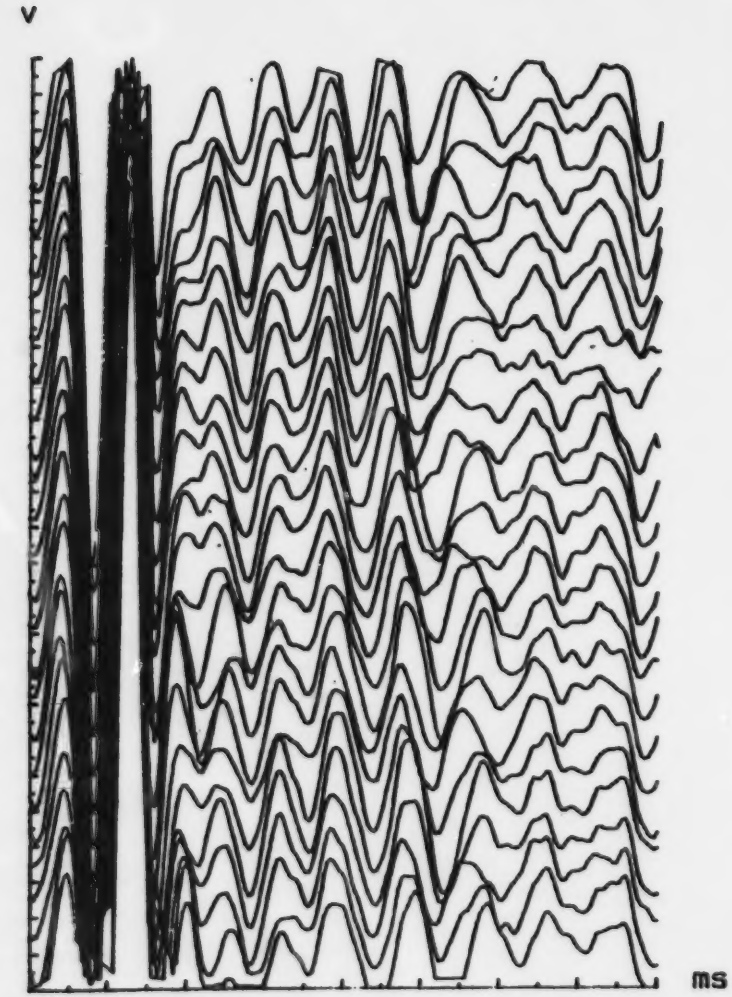

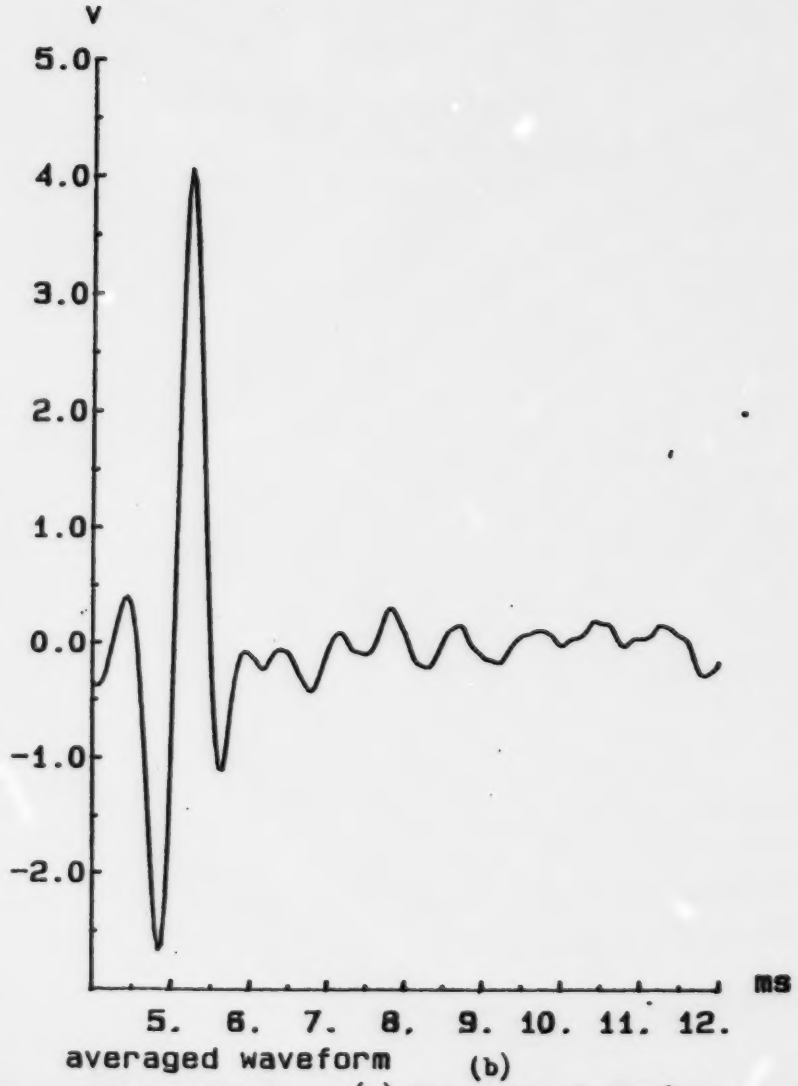

Fig. 5.31: (a) waveforms from line 8 between 65 to 70m on Bloor viaduct and (b) the averaged waveform.

between peak 2 and the interface peak is so short in time that it requires a narrower search window to alleviate the ambiguity. This situation does not occur for Ninth Line where the transient time between the asphalt-membrane and membrane-concrete interface is relatively longer and the magnitude of the membrane-concrete reflection is always well- defined. For Winston Churchill data, the asphalt-concrete peak is the only peak after the surface echo so there is no other peaks to be compared with.

In locating the rebar reflection from Bloor Via Duct data, attention is also required in setting the search window. From Figs. 5.30 and 5.31 (line 8 section 65.2 to 70 m), we see that some of the waveforms (marked asterisk) have magnitude in their characteristic W peak comparable with the rebar reflection. Therefore, the search window for rebar reflection has to be set further down the time frame in order to avoid wrong selection. This situation does not applied to both Ninth Line and Winston Churchill since the rebar reflections are always well defined after the asphalt (or membrane)-concrete interface peak.

With the above minor adjustment, bridge deck assessment for Bloor Via Duct can be proceed.

5.3.3/ Data Processing Speed

The total bridge length of Bloor Via Duct is 447 m. Since this is a relatively long bridge deck, it is interesting to know the time required for processing one completed line.

The software is designed to sample waveform at every 20 cm distance. For every five waveforms, the average is performed in order to produce results at every 1 m interval mark. A total of 2235 waveforms are sampled for every line recorded. This is equivalent to 2.3 Mbyte of computer memory. (One waveform occupies 1 byte of memory storage). The processing time for one waveform is estimated 2s, in which a large percentage of the time is consumed by system overhead, i.e. data transfer between computer memory and hard disk file. For processing one completed line of Bloor Via Duct data, a total of 1.25 hours is needed.

5.3.4/ Data Analysis Of Eastbound Deck

Six lines are analysed for the eastbound data (line 1 to 6). Three lines are recorded along the right (slow) lane and the other three lines are on the middle (driving) lane. One line is recorded on the left (passing) lane but the data are not processed.

In the current study, the software is not equipped with the capability of determining the averaged dielectric constant of multi-layer asphalt. The dielectric constant of asphalt is measured using the reflection coefficient method, i.e. with the dielectric constant of the first layer of asphalt provided we estimate the overall asphalt thickness.

Sampled waveforms from location 47.2 to 52 m are plotted for line 2 (Fig. 5.30), line 3 (Fig. 5.32), line 4 (Fig. 5.33) and line 5 (Fig. 5.34). The purpose of selecting these sets of waveforms is that metal joint can be detected at about 48 m. Reflection from the metal joint can be used as a bench-mark for indicating asphalt-concrete boundary. From the waveforms we note that the depth of the metal joint under the asphalt surface of line 2 and 3 (and line 1) is different from that beneath line 4 and 5 (and line 6). In the former case, the reflection from the metal joint is located at about 8 ms and in the latter case the reflection is found at 8.5 ms. It is suspected that, line 4, 5, and 6 must have thicker asphalt overlay than line 1, 2 and 3. The magnitude of difference is estimated to be 30 mm.

We have shown (section 5.3.1) that with the given core sample from Bloor Street Via Duct, the computer finding (in this particular case) is different from the actual measurement by 20%. Therefore, in order to set a proper search window for the asphalt-concrete reflection, the 20% error is included in the software as the input to the core sample thickness i.e. 156 mm. (If instead 130 mm is used, the search window may be locked at the wrong peak). This input only applied to lines 1 to 3. From the previous discussion, we mentioned that there was a depth difference of about 30 mm between the data from lines 1 to 3 and lines 4 to 6. Therefore, it is suitable to use 186 mm for the core sample thickness in processing lines 4, 5, and 6.

The averaged depth of asphalt and concrete cover, over 1 m intervals, for the eastbound deck are presented in Table 5.7. It is necessary to check the accuracy of the measurement. The most valid test is to compared the computer result with the core sample. From Table 5.7, line 3 at 180 m has 159 mm asphalt thickness and 84 mm concrete cover. (These results are obtained from averaging over five waveforms from 179.2 to 180 m). Since our measurement already compensated for the 20% error calculated from the given core sample asphalt thickness, this error is removed and the real asphalt thickness becomes 127 mm which is about 2.3% different from the core sample. This is within the error bound discussed in section 2.5.5.

The averaged waveforms from Fig. 5.30 to 5.33 can also be exploited in checking the computer results. In Table 5.8, the averaged thickness of both asphalt and concrete cover for the section 47.2 to 52 m of line 2 to line 5 are provided. The results are obtained by averaging the corresponding measurements from Table 5.7. Using these averaged depth measurements, we can estimate the

Bloor viaduct (EASTbound): line 1 (south curb) to line 6 (6.
AVEraged THICKness SUMMARY

[AVEraged THICKness (mm)]
line number

metre	1	2	3	4	5	6
1	156 (73)	159 (76)	147 (85)	169 (69)	190 (78)	188 (77)
2	157 (74)	155 (71)	150 (70)	184 (57)	203 (68)	188 (73)
3	163 (75)	163 (82)	156 (72)	176 (67)	188 (78)	175 (89)
4	142 (66)	160 (74)	147 (78)	164 (71)	179 (82)	171 (82)
5	138 (84)	161 (81)	146 (85)	177 (75)	183 (73)	170 (80)
6	134 (87)	153 (86)	145 (78)	174 (77)	171 (87)	165 (80)
7	133 (78)	166 (61)	152 (80)	171 (81)	182 (81)	178 (79)
8	156 (85)	179 (70)	162 (84)	182 (76)	196 (71)	179 (82)
9	162 (74)	175 (69)	163 (81)	185 (76)	201 (69)	189 (79)
10	162 (68)	177 (79)	160 (75)	176 (83)	191 (75)	175 (84)
11	176 (67)	188 (73)	164 (79)	182 (77)	182 (79)	172 (82)
12	184 (54)	204 (77)	177 (81)	167 (88)	186 (70)	164 (83)
13	179 (60)	157 (44)	174 (82)	169 (85)	179 (79)	164 (74)
14	173 (81)	171 (70)	172 (84)	172 (89)	179 (90)	172 (82)
15	177 (79)	195 (74)	176 (84)	172 (90)	183 (85)	185 (80)
16	164 (78)	198 (80)	186 (85)	179 (86)	203 (78)	183 (88)
17	159 (82)	201 (80)	157 (65)	188 (81)	197 (83)	195 (81)
18	167 (80)	196 (87)	161 (89)	196 (82)	202 (69)	197 (74)
19	167 (80)	179 (68)	157 (81)	198 (77)	187 (53)	201 (66)
20	163 (85)	165 (61)	145 (80)	196 (76)	165 (54)	199 (69)
21	163 (81)	157 (62)	141 (90)	203 (77)	171 (47)	201 (75)
22	159 (84)	152 (70)	141 (76)	210 (79)	214 (70)	198 (81)
23	149 (86)	150 (62)	142 (85)	195 (84)	202 (80)	180 (85)
24	142 (76)	146 (71)	143 (83)	194 (83)	204 (77)	172 (87)
25	149 (78)	143 (60)	137 (82)	191 (88)	194 (75)	172 (82)
26	144 (63)	151 (62)	136 (75)	180 (92)	184 (81)	170 (78)
27	144 (74)	152 (63)	138 (89)	174 (89)	187 (78)	165 (86)
28	144 (68)	154 (64)	142 (88)	191 (84)	195 (72)	183 (89)
29	148 (63)	152 (65)	149 (91)	195 (92)	194 (75)	191 (73)
30	148 (80)	162 (80)	150 (81)	206 (85)	187 (77)	190 (87)
31	154 (78)	166 (77)	154 (78)	214 (86)	187 (77)	190 (94)
32	149 (79)	172 (77)	160 (91)	163 (40)	191 (79)	196 (90)
33	163 (88)	176 (77)	156 (82)	184 (90)	191 (86)	203 (81)
34	155 (85)	168 (74)	150 (77)	175 (88)	196 (81)	202 (81)
35	154 (93)	165 (68)	153 (81)	179 (90)	194 (87)	196 (84)
36	155 (86)	164 (74)	152 (78)	180 (90)	187 (83)	186 (76)
37	151 (51)	165 (75)	151 (72)	167 (80)	182 (81)	180 (84)
38	146 (58)	166 (69)	144 (74)	170 (83)	187 (91)	179 (85)
39	143 (70)	159 (79)	141 (68)	171 (81)	182 (87)	177 (81)
40	149 (70)	156 (85)	145 (70)	168 (104)	174 (90)	169 (83)
41	139 (67)	161 (75)	151 (72)	172 (91)	181 (84)	167 (90)
42	137 (65)	159 (67)	147 (65)	169 (79)	176 (90)	170 (89)
43	150 (88)	160 (68)	144 (64)	168 (95)	178 (91)	169 (89)
44	146 (67)	157 (68)	143 (63)	170 (87)	180 (87)	168 (84)
45	144 (71)	157 (76)	141 (80)	170 (91)	178 (88)	169 (87)
46	156 (64)	159 (73)	142 (87)	162 (74)	171 (84)	169 (92)
47	160 (85)	163 (78)	148 (82)	168 (88)	184 (84)	170 (87)
48	156 (88)	169 (72)	156 (76)	173 (80)	188 (84)	187 (68)
49	161 (69)	175 (68)	146 (70)	186 (77)	198 (66)	187 (74)
50	160 (68)	159 (76)	143 (86)	173 (36)	196 (82)	182 (81)
51	156 (74)	153 (82)	144 (87)	166 (36)	197 (80)	181 (84)
52	151 (73)	158 (81)	145 (81)	164 (83)	189 (80)	177 (87)
53	150 (65)	160 (80)	143 (83)	162 (85)	175 (94)	172 (90)
54	166 (80)	163 (78)	143 (79)	166 (82)	173 (79)	172 (87)
55	160 (83)	168 (80)	141 (75)	164 (85)	180 (85)	183 (78)
56	153 (72)	173 (68)	140 (73)	171 (76)	193 (75)	187 (66)
57	155 (75)	167 (77)	146 (75)	175 (82)	191 (81)	186 (73)
58	162 (77)	182 (78)	149 (84)	172 (86)	186 (85)	170 (83)
59	157 (72)	173 (83)	145 (83)	172 (90)	192 (80)	172 (79)
60	157 (74)	171 (81)	153 (86)	166 (90)	182 (88)	177 (79)
61	160 (73)	166 (83)	155 (80)	166 (85)	188 (83)	183 (81)
62	152 (79)	168 (85)	149 (82)	177 (83)	196 (81)	184 (80)
63	150 (65)	168 (82)	143 (85)	173 (87)	199 (84)	188 (82)
64	147 (75)	166 (80)	142 (82)	175 (83)	193 (69)	188 (73)
65	142 (70)	160 (81)	146 (85)	164 (85)	188 (68)	191 (78)
66	141 (76)	163 (73)	146 (82)	163 (87)	198 (78)	192 (80)
67	146 (74)	166 (80)	147 (79)	176 (77)	200 (79)	194 (81)
68	146 (68)	161 (76)	146 (74)	163 (83)	197 (79)	188 (85)
69	145 (66)	162 (77)	144 (72)	160 (80)	195 (75)	192 (80)
70	141 (76)	159 (76)	148 (69)	169 (69)	200 (70)	198 (75)
71	149 (73)	158 (76)	148 (73)	174 (71)	197 (74)	200 (69)
72	147 (77)	155 (82)	152 (79)	173 (72)	184 (49)	193 (54)

Table 5.7: averaged thickness of eastbound deck.

73	:	156 (61)	155 (67)	144 (69)	174 (62)	201 (58)	207 (65)
74	:	153 (60)	151 (66)	142 (70)	168 (67)	212 (63)	200 (64)
75	:	146 (61)	152 (59)	140 (61)	173 (65)	194 (61)	199 (66)
76	:	142 (70)	151 (60)	153 (46)	173 (63)	202 (71)	192 (75)
77	:	145 (63)	154 (63)	157 (42)	176 (58)	195 (68)	187 (59)
78	:	159 (54)	159 (59)	154 (57)	186 (66)	195 (76)	188 (51)
79	:	166 (73)	163 (56)	150 (61)	188 (69)	194 (66)	199 (75)
80	:	161 (76)	164 (67)	137 (67)	184 (69)	196 (73)	185 (73)
81	:	161 (83)	149 (75)	149 (60)	183 (77)	183 (75)	184 (62)
82	:	159 (71)	145 (82)	137 (68)	192 (71)	189 (76)	178 (54)
83	:	161 (59)	157 (72)	136 (75)	186 (71)	203 (68)	179 (64)
84	:	153 (73)	161 (74)	147 (76)	179 (73)	187 (69)	169 (61)
85	:	155 (64)	159 (57)	153 (67)	190 (64)	195 (60)	178 (78)
86	:	151 (63)	154 (65)	142 (71)	192 (68)	203 (72)	196 (75)
87	:	156 (61)	154 (71)	144 (76)	184 (77)	210 (75)	198 (71)
88	:	148 (73)	153 (78)	143 (82)	189 (69)	208 (72)	205 (73)
89	:	148 (72)	155 (83)	142 (86)	189 (72)	207 (71)	199 (74)
90	:	152 (72)	157 (73)	148 (86)	182 (77)	202 (76)	190 (79)
91	:	160 (60)	159 (56)	147 (66)	172 (71)	197 (69)	184 (71)
92	:	145 (67)	156 (62)	144 (67)	178 (75)	184 (75)	174 (81)
93	:	152 (67)	151 (72)	163 (73)	184 (76)	187 (74)	180 (77)
94	:	156 (69)	161 (70)	164 (70)	178 (71)	193 (74)	175 (74)
95	:	151 (63)	168 (70)	165 (64)	184 (63)	200 (67)	176 (72)
96	:	157 (62)	163 (76)	167 (66)	185 (67)	193 (74)	177 (60)
97	:	162 (69)	160 (68)	166 (56)	188 (61)	187 (67)	176 (70)
98	:	158 (68)	161 (63)	157 (58)	179 (61)	186 (73)	177 (80)
99	:	161 (60)	164 (66)	161 (63)	183 (60)	187 (74)	181 (76)
100	:	165 (67)	167 (67)	156 (62)	193 (55)	198 (71)	172 (83)
101	:	158 (60)	168 (72)	158 (62)	181 (57)	206 (71)	181 (75)
102	:	162 (56)	169 (70)	150 (71)	175 (64)	200 (74)	184 (77)
103	:	159 (63)	167 (80)	146 (81)	174 (82)	202 (77)	181 (73)
104	:	165 (62)	161 (73)	148 (83)	174 (83)	203 (78)	183 (76)
105	:	156 (65)	167 (84)	151 (88)	181 (75)	206 (78)	194 (70)
106	:	157 (66)	167 (85)	158 (86)	174 (84)	196 (79)	195 (75)
107	:	154 (67)	171 (78)	157 (82)	178 (78)	183 (84)	187 (78)
108	:	154 (65)	159 (91)	143 (86)	174 (80)	174 (83)	164 (77)
109	:	151 (67)	151 (73)	144 (63)	169 (64)	162 (86)	154 (56)
110	:	148 (75)	150 (87)	138 (79)	168 (73)	176 (57)	174 (57)
111	:	134 (64)	162 (79)	151 (75)	174 (74)	159 (58)	188 (53)
112	:	171 (62)	167 (81)	168 (67)	174 (62)	189 (63)	207 (57)
113	:	163 (59)	177 (65)	157 (76)	150 (77)	164 (59)	173 (58)
114	:	150 (66)	158 (78)	149 (78)	173 (59)	189 (54)	194 (42)
115	:	152 (64)	155 (70)	154 (79)	158 (66)	186 (56)	190 (42)
116	:	146 (66)	169 (66)	157 (74)	175 (55)	196 (52)	184 (51)
117	:	140 (70)	156 (69)	144 (85)	175 (54)	181 (52)	196 (43)
118	:	148 (51)	150 (72)	148 (79)	167 (65)	156 (77)	179 (54)
119	:	148 (60)	157 (70)	140 (85)	158 (72)	165 (63)	164 (56)
120	:	139 (64)	153 (74)	137 (82)	170 (71)	167 (62)	154 (71)
121	:	149 (64)	153 (74)	141 (74)	176 (65)	171 (59)	168 (56)
122	:	159 (51)	152 (65)	160 (57)	182 (47)	187 (53)	193 (46)
123	:	152 (57)	135 (83)	157 (53)	174 (47)	181 (45)	191 (40)
124	:	133 (78)	143 (71)	140 (68)	173 (42)	181 (45)	165 (58)
125	:	145 (66)	150 (63)	139 (67)	168 (41)	182 (43)	156 (70)
126	:	139 (67)	134 (80)	144 (68)	171 (51)	166 (67)	160 (73)
127	:	161 (72)	151 (70)	142 (73)	149 (75)	172 (73)	164 (69)
128	:	143 (55)	156 (59)	159 (52)	170 (45)	170 (55)	174 (56)
129	:	140 (56)	149 (55)	151 (63)	164 (47)	172 (58)	171 (58)
130	:	149 (60)	154 (56)	153 (54)	167 (50)	161 (71)	168 (58)
131	:	152 (64)	148 (62)	154 (52)	155 (51)	157 (67)	153 (74)
132	:	153 (60)	148 (64)	140 (62)	149 (54)	170 (56)	162 (64)
133	:	149 (56)	152 (63)	141 (62)	161 (41)	179 (58)	161 (60)
134	:	149 (65)	151 (69)	153 (52)	176 (53)	192 (60)	171 (71)
135	:	141 (61)	158 (76)	154 (70)	173 (58)	189 (81)	169 (72)
137	:	142 (66)	139 (77)	163 (52)	173 (45)	203 (59)	170 (59)
138	:	152 (69)	158 (61)	165 (54)	184 (57)	179 (72)	177 (47)
139	:	144 (72)	157 (60)	166 (62)	159 (69)	183 (69)	165 (68)
140	:	143 (74)	161 (83)	164 (69)	179 (62)	183 (71)	169 (50)
141	:	130 (79)	154 (73)	144 (75)	174 (64)	186 (74)	168 (58)
142	:	134 (86)	143 (77)	139 (68)	174 (58)	180 (78)	178 (57)
143	:	129 (63)	145 (69)	147 (61)	178 (66)	183 (76)	171 (70)
144	:	122 (79)	148 (75)	141 (67)	176 (67)	186 (78)	173 (70)
145	:	131 (80)	150 (74)	156 (54)	184 (61)	185 (78)	165 (65)
146	:	133 (72)	155 (72)	156 (44)	179 (58)	169 (79)	169 (57)
147	:	129 (77)	155 (59)	151 (50)	180 (49)	185 (61)	168 (64)
148	:	138 (69)	154 (74)	141 (75)	177 (75)	180 (80)	176 (59)
149	:	136 (65)	162 (78)	145 (73)	182 (84)	183 (87)	164 (69)
150	:	146 (67)	168 (75)	151 (77)	176 (80)	186 (90)	161 (70)
151	:	161 (79)	174 (82)	153 (84)	171 (86)	186 (85)	171 (62)
152	:	175 (83)	167 (84)	153 (82)	159 (70)	177 (85)	160 (84)
153	:	166 (66)	171 (78)	158 (82)	166 (70)	177 (87)	163 (71)
154	:	148 (66)	164 (66)	156 (71)	162 (85)	185 (76)	153 (73)
155	:	144 (65)	175 (81)	155 (82)	167 (85)	176 (73)	160 (78)
156	:	160 (73)	173 (77)	154 (75)	171 (81)	178 (85)	177 (70)

Table 5.7(b)

157	: 174 (87)	174 (84)	161 (83)	170 (88)	183 (89)	171 (70)
158	: 155 (79)	174 (87)	156 (84)	173 (88)	189 (87)	172 (80)
159	: 168 (80)	169 (82)	156 (84)	163 (84)	181 (84)	175 (84)
160	: 176 (82)	176 (81)	158 (78)	168 (83)	186 (89)	183 (81)
161	: 169 (84)	141 (70)	158 (88)	177 (85)	204 (81)	189 (74)
162	: 172 (80)	162 (76)	158 (87)	183 (82)	203 (81)	185 (77)
163	: 159 (73)	146 (73)	158 (83)	190 (77)	184 (47)	193 (76)
164	: 161 (71)	180 (82)	159 (73)	183 (77)	218 (79)	182 (73)
165	: 157 (85)	173 (78)	156 (72)	180 (78)	195 (83)	171 (81)
166	: 163 (84)	168 (74)	148 (80)	181 (79)	187 (88)	176 (80)
167	: 173 (86)	166 (79)	145 (83)	178 (86)	188 (87)	176 (82)
168	: 167 (89)	173 (85)	146 (79)	180 (86)	195 (91)	182 (83)
169	: 158 (68)	172 (87)	148 (72)	184 (87)	186 (86)	187 (73)
170	: 157 (73)	172 (83)	148 (78)	188 (82)	180 (86)	174 (62)
171	: 157 (59)	168 (85)	149 (90)	189 (80)	187 (86)	169 (62)
172	: 144 (64)	160 (88)	145 (71)	190 (81)	185 (84)	170 (69)
173	: 164 (77)	162 (80)	144 (74)	186 (82)	185 (81)	176 (64)
174	: 151 (75)	159 (77)	144 (74)	187 (78)	182 (84)	166 (51)
175	: 155 (72)	161 (81)	144 (74)	176 (87)	181 (84)	158 (73)
176	: 151 (65)	165 (82)	151 (72)	173 (75)	179 (85)	173 (64)
177	: 146 (82)	171 (81)	153 (68)	170 (80)	180 (80)	179 (53)
178	: 157 (55)	163 (69)	146 (66)	173 (55)	180 (66)	153 (44)
179	: 150 (75)	156 (61)	136 (71)	165 (65)	171 (73)	171 (71)
180	: 153 (79)	169 (75)	159 (84)	158 (81)	172 (79)	169 (77)
181	: 147 (78)	183 (72)	166 (75)	171 (71)	175 (85)	171 (84)
182	: 159 (76)	178 (72)	159 (70)	165 (77)	171 (83)	168 (86)
183	: 151 (76)	170 (81)	155 (69)	167 (72)	169 (85)	170 (83)
184	: 173 (70)	172 (82)	158 (75)	155 (71)	167 (79)	166 (83)
185	: 158 (92)	181 (82)	163 (73)	156 (79)	163 (85)	170 (75)
186	: 156 (76)	187 (71)	155 (75)	156 (81)	161 (85)	157 (83)
187	: 157 (59)	178 (78)	152 (68)	166 (77)	165 (84)	170 (66)
188	: 157 (65)	173 (77)	151 (71)	162 (85)	171 (83)	169 (73)
189	: 164 (60)	166 (69)	152 (67)	162 (84)	157 (77)	170 (68)
190	: 156 (69)	159 (73)	148 (81)	163 (80)	175 (83)	168 (72)
191	: 149 (64)	159 (70)	144 (75)	161 (85)	176 (82)	163 (81)
192	: 152 (57)	157 (69)	148 (70)	165 (81)	170 (87)	167 (86)
193	: 157 (74)	148 (79)	149 (71)	171 (83)	179 (84)	173 (84)
194	: 151 (64)	159 (82)	156 (79)	173 (81)	189 (80)	192 (78)
195	: 149 (76)	159 (82)	152 (85)	185 (82)	196 (86)	191 (85)
196	: 152 (74)	157 (81)	153 (80)	195 (81)	156 (50)	187 (72)
197	: 147 (77)	158 (83)	153 (79)	202 (83)	158 (52)	199 (78)
198	: 148 (83)	161 (77)	158 (72)	204 (82)	177 (38)	193 (85)
199	: 156 (75)	173 (82)	164 (75)	207 (81)	211 (89)	198 (81)
200	: 164 (82)	173 (77)	164 (87)	211 (83)	207 (82)	198 (74)
201	: 162 (86)	186 (78)	178 (86)	195 (55)	159 (52)	182 (57)
202	: 158 (95)	191 (78)	182 (84)	181 (38)	161 (53)	196 (92)
203	: 154 (85)	193 (80)	190 (77)	167 (51)	160 (52)	198 (82)
204	: 156 (76)	185 (69)	181 (82)	217 (74)	164 (50)	201 (82)
205	: 152 (76)	176 (70)	183 (81)	211 (79)	165 (50)	169 (38)
206	: 152 (81)	188 (81)	182 (70)	212 (67)	175 (48)	169 (38)
207	: 152 (73)	157 (71)	172 (82)	194 (59)	174 (56)	197 (83)
208	: 148 (77)	153 (72)	183 (77)	214 (76)	168 (51)	201 (77)
209	: 147 (85)	185 (78)	179 (78)	209 (74)	162 (59)	170 (48)
210	: 155 (63)	168 (81)	175 (83)	192 (85)	183 (59)	189 (65)
211	: 155 (84)	170 (81)	153 (84)	188 (87)	199 (71)	192 (90)
212	: 144 (87)	164 (87)	153 (76)	183 (85)	192 (71)	187 (85)
213	: 152 (79)	162 (85)	154 (80)	183 (82)	183 (89)	180 (81)
214	: 147 (81)	159 (84)	147 (70)	185 (81)	185 (86)	177 (85)
215	: 149 (79)	155 (81)	145 (67)	188 (68)	192 (84)	182 (76)
216	: 151 (83)	158 (75)	157 (73)	191 (67)	199 (80)	184 (71)
217	: 143 (69)	162 (74)	154 (73)	183 (70)	189 (82)	177 (76)
218	: 152 (80)	160 (68)	146 (74)	182 (64)	182 (81)	182 (79)
219	: 141 (57)	152 (68)	161 (60)	173 (78)	191 (82)	183 (75)
220	: 141 (71)	153 (67)	180 (50)	177 (76)	191 (80)	180 (75)
221	: 144 (52)	160 (79)	144 (66)	181 (68)	185 (85)	183 (71)
222	: 138 (72)	162 (77)	154 (76)	174 (66)	179 (73)	175 (81)
223	: 142 (77)	153 (82)	147 (72)	164 (73)	177 (75)	175 (86)
224	: 143 (61)	153 (86)	149 (69)	161 (71)	175 (80)	173 (85)
225	: 141 (54)	155 (86)	148 (75)	158 (71)	178 (64)	172 (81)
226	: 134 (74)	154 (85)	149 (74)	169 (63)	178 (62)	167 (76)
227	: 132 (57)	155 (87)	147 (73)	158 (81)	173 (74)	163 (67)
228	: 130 (67)	159 (92)	148 (71)	159 (77)	167 (76)	167 (75)
229	: 134 (51)	169 (92)	150 (69)	172 (62)	171 (71)	164 (80)
230	: 133 (69)	170 (91)	153 (78)	178 (66)	175 (75)	169 (77)
231	: 136 (54)	182 (81)	154 (77)	171 (74)	175 (75)	172 (80)
232	: 148 (63)	172 (77)	159 (76)	180 (76)	174 (77)	179 (75)
233	: 144 (57)	177 (79)	160 (76)	180 (86)	182 (76)	181 (67)
234	: 146 (56)	152 (64)	161 (66)	181 (82)	187 (75)	177 (79)
235	: 148 (57)	182 (83)	153 (73)	178 (82)	181 (81)	174 (85)
236	: 154 (64)	182 (84)	149 (81)	174 (88)	180 (89)	176 (88)
237	: 143 (54)	171 (82)	174 (78)	172 (86)	183 (87)	179 (84)
238	: 169 (79)	176 (81)	156 (69)	174 (98)	186 (88)	179 (83)
239	: 146 (66)	176 (78)	161 (70)	176 (84)	181 (88)	175 (77)

table 5.7(c)

240	: 153 (63)	171 (85)	156 (79)	180 (83)	182 (85)	175 (82)
241	: 150 (67)	170 (83)	155 (81)	180 (75)	189 (75)	183 (79)
242	: 142 (69)	172 (84)	159 (76)	180 (80)	191 (76)	182 (84)
243	: 142 (67)	172 (86)	156 (78)	176 (73)	188 (81)	181 (81)
244	: 152 (64)	174 (84)	164 (72)	181 (67)	183 (84)	191 (79)
245	: 150 (55)	170 (81)	154 (83)	178 (83)	184 (86)	186 (76)
246	: 147 (71)	168 (81)	148 (78)	173 (83)	176 (80)	182 (78)
247	: 163 (74)	171 (77)	149 (76)	178 (76)	175 (79)	190 (86)
248	: 172 (78)	171 (78)	151 (75)	181 (73)	184 (85)	188 (86)
249	: 168 (77)	175 (77)	155 (73)	187 (71)	187 (77)	190 (82)
250	: 165 (79)	174 (79)	151 (80)	174 (74)	187 (77)	180 (84)
251	: 168 (80)	176 (74)	155 (87)	171 (71)	182 (83)	182 (82)
252	: 167 (75)	170 (79)	146 (82)	169 (70)	175 (81)	179 (78)
253	: 166 (82)	168 (84)	152 (74)	174 (81)	174 (77)	185 (79)
254	: 164 (79)	169 (66)	156 (74)	192 (78)	171 (80)	181 (81)
255	: 163 (84)	168 (79)	166 (66)	182 (83)	173 (74)	184 (73)
256	: 163 (84)	169 (73)	155 (77)	184 (83)	180 (70)	184 (82)
257	: 160 (79)	167 (77)	162 (75)	180 (75)	181 (83)	182 (88)
258	: 160 (76)	158 (81)	160 (70)	181 (75)	181 (76)	181 (87)
259	: 165 (55)	164 (75)	165 (77)	185 (83)	181 (90)	178 (86)
260	: 159 (83)	158 (76)	166 (78)	191 (80)	181 (79)	181 (83)
261	: 162 (74)	152 (84)	163 (77)	184 (76)	179 (79)	177 (82)
262	: 155 (78)	155 (78)	166 (76)	179 (84)	184 (85)	182 (78)
263	: 157 (76)	162 (77)	157 (81)	178 (84)	187 (84)	177 (65)
264	: 146 (57)	161 (80)	150 (73)	179 (86)	188 (89)	164 (78)
265	: 159 (78)	151 (70)	136 (71)	170 (84)	185 (83)	168 (70)
266	: 149 (78)	148 (79)	141 (69)	160 (68)	169 (61)	166 (64)
267	: 151 (74)	163 (84)	158 (86)	168 (74)	170 (76)	184 (73)
268	: 161 (72)	168 (76)	166 (84)	201 (76)	210 (74)	190 (71)
269	: 165 (77)	162 (76)	165 (85)	201 (81)	199 (74)	195 (68)
270	: 157 (76)	175 (85)	163 (88)	169 (73)	184 (76)	179 (59)
271	: 156 (73)	168 (82)	152 (74)	182 (71)	177 (87)	179 (70)
272	: 149 (70)	152 (75)	141 (73)	180 (80)	183 (82)	178 (68)
273	: 141 (69)	152 (77)	142 (79)	181 (72)	190 (81)	173 (69)
274	: 141 (69)	150 (69)	144 (69)	184 (65)	187 (83)	158 (69)
275	: 144 (69)	136 (76)	137 (68)	180 (68)	190 (73)	157 (72)
276	: 143 (71)	138 (76)	141 (67)	172 (73)	184 (70)	180 (50)
277	: 143 (70)	154 (54)	146 (71)	159 (71)	179 (63)	179 (50)
278	: 142 (70)	150 (56)	149 (71)	173 (62)	178 (59)	184 (52)
279	: 147 (67)	148 (67)	143 (78)	180 (53)	188 (56)	157 (77)
280	: 145 (68)	137 (74)	151 (71)	177 (48)	185 (71)	164 (69)
281	: 155 (68)	144 (66)	151 (73)	174 (59)	181 (54)	179 (54)
282	: 145 (66)	143 (68)	141 (78)	183 (57)	189 (53)	183 (58)
283	: 168 (50)	150 (60)	158 (61)	177 (60)	179 (58)	187 (66)
284	: 153 (62)	160 (50)	150 (69)	177 (57)	171 (70)	172 (76)
285	: 163 (51)	165 (52)	145 (66)	178 (63)	171 (67)	182 (60)
286	: 150 (67)	149 (66)	143 (80)	166 (75)	171 (71)	181 (62)
287	: 150 (72)	152 (70)	144 (80)	168 (77)	185 (73)	180 (65)
288	: 143 (75)	150 (81)	140 (81)	172 (69)	174 (70)	166 (72)
289	: 152 (72)	149 (84)	142 (71)	172 (60)	173 (72)	164 (71)
290	: 151 (70)	159 (70)	146 (74)	159 (74)	168 (69)	175 (60)
291	: 147 (68)	169 (57)	147 (67)	174 (63)	178 (67)	194 (46)
292	: 160 (58)	157 (61)	143 (68)	181 (50)	181 (61)	181 (60)
293	: 166 (52)	145 (71)	138 (81)	175 (60)	163 (74)	165 (73)
294	: 165 (52)	163 (60)	140 (69)	159 (75)	167 (74)	166 (71)
295	: 165 (59)	155 (61)	148 (60)	193 (43)	187 (64)	181 (59)
296	: 162 (56)	144 (69)	137 (70)	191 (45)	175 (67)	177 (50)
297	: 163 (55)	145 (73)	145 (67)	199 (45)	189 (50)	190 (51)
298	: 155 (61)	170 (54)	148 (54)	182 (48)	169 (61)	160 (73)
299	: 168 (68)	147 (67)	151 (54)	183 (45)	182 (62)	189 (49)
300	: 156 (64)	149 (66)	140 (64)	187 (45)	193 (59)	183 (57)
301	: 154 (61)	147 (73)	141 (65)	200 (45)	163 (66)	163 (73)
302	: 146 (68)	149 (74)	140 (63)	181 (63)	166 (78)	163 (79)
303	: 148 (81)	148 (76)	148 (63)	174 (64)	171 (78)	168 (77)
304	: 160 (76)	151 (76)	146 (70)	164 (74)	172 (77)	161 (76)
305	: 155 (77)	153 (83)	145 (65)	189 (54)	168 (75)	181 (58)
306	: 152 (83)	159 (83)	143 (67)	190 (47)	164 (71)	195 (45)
307	: 156 (87)	154 (83)	145 (64)	188 (43)	199 (46)	197 (46)
308	: 149 (83)	154 (83)	146 (62)	187 (44)	201 (44)	193 (47)
309	: 147 (77)	159 (75)	161 (55)	195 (46)	200 (46)	195 (74)
310	: 157 (76)	167 (66)	160 (62)	203 (70)	193 (54)	204 (62)
311	: 159 (84)	176 (51)	164 (47)	194 (48)	196 (75)	209 (49)
312	: 150 (68)	184 (55)	170 (51)	200 (44)	213 (43)	205 (45)
313	: 146 (72)	180 (58)	156 (52)	198 (39)	214 (49)	200 (45)
314	: 149 (74)	180 (71)	166 (50)	194 (49)	214 (61)	202 (56)
315	: 155 (69)	173 (54)	157 (67)	205 (53)	193 (67)	204 (45)
316	: 156 (67)	160 (64)	157 (69)	208 (44)	207 (51)	197 (44)
317	: 144 (76)	149 (77)	143 (74)	212 (46)	216 (45)	204 (50)
318	: 153 (79)	150 (75)	142 (72)	211 (43)	212 (51)	191 (57)
319	: 147 (78)	152 (75)	141 (72)	207 (48)	213 (48)	198 (45)
320	: 145 (83)	153 (81)	144 (79)	193 (56)	205 (50)	175 (51)
321	: 142 (82)	157 (79)	138 (71)	178 (63)	159 (66)	173 (48)
322	: 150 (80)	152 (78)	142 (71)	180 (59)	155 (63)	179 (46)
323						

Table 5.7(d)

324	151 (81)	153 (71)	132 (70)	195 (34)	182 (61)	178 (56)
325	146 (81)	163 (74)	140 (66)	204 (44)	218 (57)	198 (50)
326	143 (82)	168 (72)	154 (57)	210 (40)	222 (65)	184 (46)
327	146 (80)	166 (65)	160 (59)	203 (43)	202 (54)	183 (43)
328	163 (71)	160 (71)	151 (67)	210 (43)	209 (48)	178 (48)
329	174 (72)	157 (73)	157 (73)	187 (55)	206 (50)	195 (47)
330	173 (79)	157 (68)	163 (63)	175 (65)	174 (71)	194 (49)
331	163 (80)	160 (67)	154 (73)	159 (75)	163 (77)	175 (63)
332	162 (71)	159 (76)	152 (72)	157 (77)	164 (76)	159 (75)
333	158 (73)	168 (65)	148 (66)	158 (77)	167 (76)	163 (76)
334	157 (70)	169 (68)	150 (70)	166 (66)	164 (76)	171 (64)
335	151 (77)	167 (75)	149 (69)	160 (73)	173 (85)	176 (70)
336	155 (75)	168 (76)	152 (69)	170 (74)	174 (84)	160 (78)
337	156 (75)	163 (78)	153 (70)	163 (73)	183 (71)	161 (74)
338	157 (75)	161 (77)	152 (67)	160 (69)	172 (77)	162 (76)
339	150 (75)	160 (79)	153 (71)	173 (64)	169 (80)	161 (75)
340	156 (70)	158 (75)	152 (65)	166 (70)	172 (77)	159 (75)
341	152 (73)	158 (77)	150 (67)	164 (71)	175 (77)	156 (73)
342	145 (75)	162 (60)	152 (67)	169 (74)	172 (79)	173 (63)
343	145 (69)	154 (74)	157 (65)	171 (73)	173 (77)	179 (71)
344	146 (71)	153 (79)	150 (70)	167 (77)	182 (83)	169 (82)
345	145 (70)	152 (75)	149 (69)	157 (76)	181 (85)	172 (68)
346	145 (72)	151 (75)	153 (63)	170 (67)	176 (77)	163 (70)
347	144 (68)	150 (74)	146 (67)	174 (57)	165 (75)	159 (74)
348	140 (70)	154 (71)	144 (69)	166 (63)	165 (76)	162 (72)
349	151 (59)	152 (79)	143 (67)	157 (72)	166 (79)	170 (67)
350	150 (62)	152 (71)	150 (62)	170 (60)	165 (72)	178 (58)
351	147 (63)	149 (77)	180 (49)	171 (52)	182 (58)	183 (51)
352	154 (62)	146 (76)	183 (51)	188 (46)	182 (57)	192 (43)
353	166 (57)	142 (59)	150 (53)	172 (55)	198 (51)	154 (67)
354	163 (64)	162 (53)	162 (51)	169 (55)	159 (57)	199 (44)
355	160 (53)	166 (50)	182 (45)	214 (46)	189 (55)	211 (38)
356	160 (52)	143 (72)	191 (44)	206 (47)	208 (48)	160 (74)
357	155 (52)	163 (59)	182 (46)	197 (53)	170 (79)	159 (72)
358	163 (51)	163 (56)	156 (59)	192 (51)	164 (74)	159 (77)
359	170 (52)	153 (62)	161 (56)	159 (69)	165 (66)	164 (74)
360	140 (65)	152 (69)	152 (67)	161 (75)	168 (68)	174 (69)
361	136 (71)	155 (77)	143 (73)	160 (75)	169 (76)	161 (82)
362	136 (79)	156 (75)	148 (74)	175 (67)	168 (72)	167 (80)
363	138 (74)	153 (76)	149 (74)	171 (75)	180 (66)	183 (74)
364	139 (67)	181 (48)	157 (61)	171 (75)	165 (78)	178 (67)
365	147 (64)	169 (59)	180 (47)	170 (73)	167 (76)	177 (68)
366	148 (62)	157 (66)	151 (66)	171 (74)	169 (69)	181 (69)
367	152 (62)	149 (76)	145 (69)	169 (74)	170 (72)	185 (77)
368	145 (67)	145 (77)	142 (77)	173 (74)	172 (82)	178 (81)
369	144 (65)	142 (77)	157 (67)	171 (75)	185 (70)	179 (80)
370	158 (62)	156 (69)	144 (77)	175 (76)	179 (81)	180 (78)
371	153 (56)	151 (71)	156 (64)	192 (66)	176 (79)	181 (76)
372	166 (48)	157 (72)	162 (58)	183 (66)	186 (68)	177 (75)
373	144 (69)	148 (73)	154 (67)	170 (72)	186 (70)	175 (80)
374	149 (61)	150 (71)	147 (74)	166 (74)	179 (81)	176 (81)
375	139 (80)	155 (86)	148 (79)	178 (61)	178 (75)	173 (81)
376	164 (68)	155 (80)	149 (79)	174 (63)	180 (79)	173 (79)
377	149 (81)	154 (79)	154 (78)	178 (60)	184 (73)	175 (73)
378	145 (77)	156 (77)	155 (77)	161 (69)	172 (75)	170 (76)
379	143 (75)	154 (81)	155 (74)	159 (77)	173 (75)	169 (79)
380	143 (65)	157 (84)	159 (70)	160 (78)	174 (82)	170 (76)
381	147 (73)	158 (83)	158 (70)	168 (79)	175 (83)	176 (83)
382	152 (68)	157 (84)	158 (77)	175 (71)	175 (84)	179 (80)
383	151 (71)	165 (83)	162 (75)	173 (74)	183 (81)	178 (81)
384	149 (72)	161 (89)	164 (77)	175 (70)	185 (81)	182 (80)
385	152 (77)	162 (85)	163 (79)	176 (76)	189 (81)	185 (77)
386	155 (81)	164 (81)	158 (77)	173 (83)	194 (79)	185 (77)
387	151 (90)	165 (79)	161 (79)	176 (83)	191 (81)	189 (77)
388	153 (83)	160 (78)	158 (80)	178 (73)	191 (79)	181 (79)
389	151 (82)	164 (83)	160 (67)	177 (71)	179 (85)	180 (69)
390	154 (82)	162 (76)	166 (66)	178 (53)	188 (58)	185 (67)
391	148 (83)	166 (78)	163 (75)	172 (61)	181 (72)	176 (58)
392	151 (70)	165 (71)	161 (71)	191 (52)	185 (56)	197 (45)
393	161 (71)	166 (66)	166 (63)	206 (49)	208 (58)	181 (63)
394	157 (65)	159 (76)	156 (76)	194 (50)	184 (55)	184 (65)
395	148 (66)	161 (68)	186 (65)	195 (57)	220 (57)	191 (70)
396	148 (69)	160 (57)	178 (62)	185 (66)	205 (66)	193 (73)
397	155 (74)	159 (77)	150 (70)	208 (47)	192 (64)	179 (67)
398	157 (78)	159 (73)	151 (68)	187 (56)	174 (79)	178 (63)
399	158 (73)	153 (81)	149 (74)	171 (60)	173 (74)	178 (64)
400	150 (73)	154 (81)	148 (81)	163 (74)	185 (68)	175 (65)
401	148 (72)	157 (80)	150 (82)	173 (63)	176 (69)	171 (57)
402	148 (71)	153 (86)	152 (77)	177 (60)	178 (65)	167 (59)
403	152 (65)	152 (82)	149 (71)	170 (59)	176 (67)	158 (70)
404	145 (73)	149 (72)	145 (72)	175 (56)	173 (65)	171 (64)
405	148 (77)	150 (73)	145 (73)	171 (54)	178 (70)	174 (62)

Table 5.7(e)

407	:	149	(79)	151	(72)	153	(61)	185	(49)	182	(61)	176	(56)
409	:	146	(79)	155	(71)	143	(73)	180	(54)	165	(69)	205	(36)
410	:	140	(79)	153	(69)	175	(47)	175	(49)	203	(42)	175	(59)
411	:	148	(60)	162	(66)	179	(42)	187	(43)	201	(44)	164	(73)
412	:	140	(63)	150	(68)	160	(50)	181	(42)	203	(50)	208	(45)
413	:	151	(65)	156	(68)	165	(50)	184	(48)	203	(47)	176	(63)
414	:	143	(64)	151	(65)	161	(53)	195	(44)	193	(54)	183	(58)
415	:	150	(60)	179	(48)	156	(55)	202	(40)	198	(55)	194	(43)
416	:	147	(61)	160	(58)	157	(49)	195	(45)	204	(53)	199	(38)
417	:	143	(65)	139	(75)	166	(46)	195	(45)	207	(45)	207	(39)
418	:	146	(64)	153	(61)	157	(61)	195	(44)	210	(60)	178	(63)
419	:	146	(58)	153	(64)	166	(50)	198	(44)	195	(64)	174	(51)
420	:	142	(58)	152	(73)	145	(77)	180	(63)	177	(55)	178	(58)
421	:	148	(73)	150	(57)	138	(73)	170	(78)	183	(59)	160	(57)
422	:	138	(73)	154	(80)	147	(85)	162	(54)	167	(54)	168	(70)
423	:	140	(76)	157	(74)	168	(75)	179	(77)	166	(63)	185	(65)
424	:	145	(74)	165	(56)	191	(43)	187	(66)	173	(78)	212	(54)
425	:	153	(85)	182	(44)	187	(46)	211	(46)	223	(46)	214	(41)
426	:	165	(54)	169	(48)	177	(49)	198	(43)	206	(51)	190	(40)
427	:	159	(53)	163	(53)	172	(49)	189	(43)	194	(66)	186	(38)
428	:	152	(56)	179	(44)	176	(50)	184	(48)	200	(73)	178	(45)
429	:	145	(59)	170	(44)	169	(62)	185	(48)	185	(46)	188	(43)
430	:	145	(64)	162	(60)	174	(48)	188	(42)	184	(55)	186	(48)
431	:	144	(62)	153	(61)	180	(45)	182	(45)	185	(54)	196	(46)
432	:	150	(56)	141	(78)	181	(45)	188	(48)	191	(74)	195	(57)
433	:	149	(63)	148	(66)	174	(46)	179	(47)	196	(62)	192	(50)
434	:	155	(62)	150	(64)	168	(49)	178	(42)	191	(57)	192	(48)
435	:	162	(53)	146	(66)	155	(48)	187	(53)	183	(44)	201	(61)
436	:	145	(71)	182	(43)	175	(47)	202	(63)	185	(45)	198	(52)
437	:	164	(53)	169	(45)	175	(44)	188	(47)	189	(56)	180	(42)
438	:	149	(59)	168	(46)	169	(49)	183	(46)	188	(45)	188	(47)
439	:	150	(51)	156	(50)	170	(48)	182	(48)	188	(58)	203	(70)
440	:	147	(53)	152	(44)	168	(49)	183	(42)	181	(45)	207	(61)
441	:	138	(60)	158	(42)	179	(57)	188	(44)	184	(44)	185	(45)
442	:	138	(59)	160	(50)	191	(67)	187	(44)	187	(54)	177	(46)
443	:	144	(64)	156	(43)	184	(60)	203	(57)	184	(47)	193	(47)
444	:	146	(69)	159	(46)	186	(62)	205	(54)	182	(48)	198	(45)
445	:	136	(67)	159	(43)	176	(62)	207	(56)	187	(50)	189	(43)
446	:	151	(56)	170	(73)	174	(58)	194	(58)	191	(45)	187	(40)
447	:	144	(63)	164	(65)	180	(67)	203	(62)	183	(44)	202	(58)

Table 5.7(f)

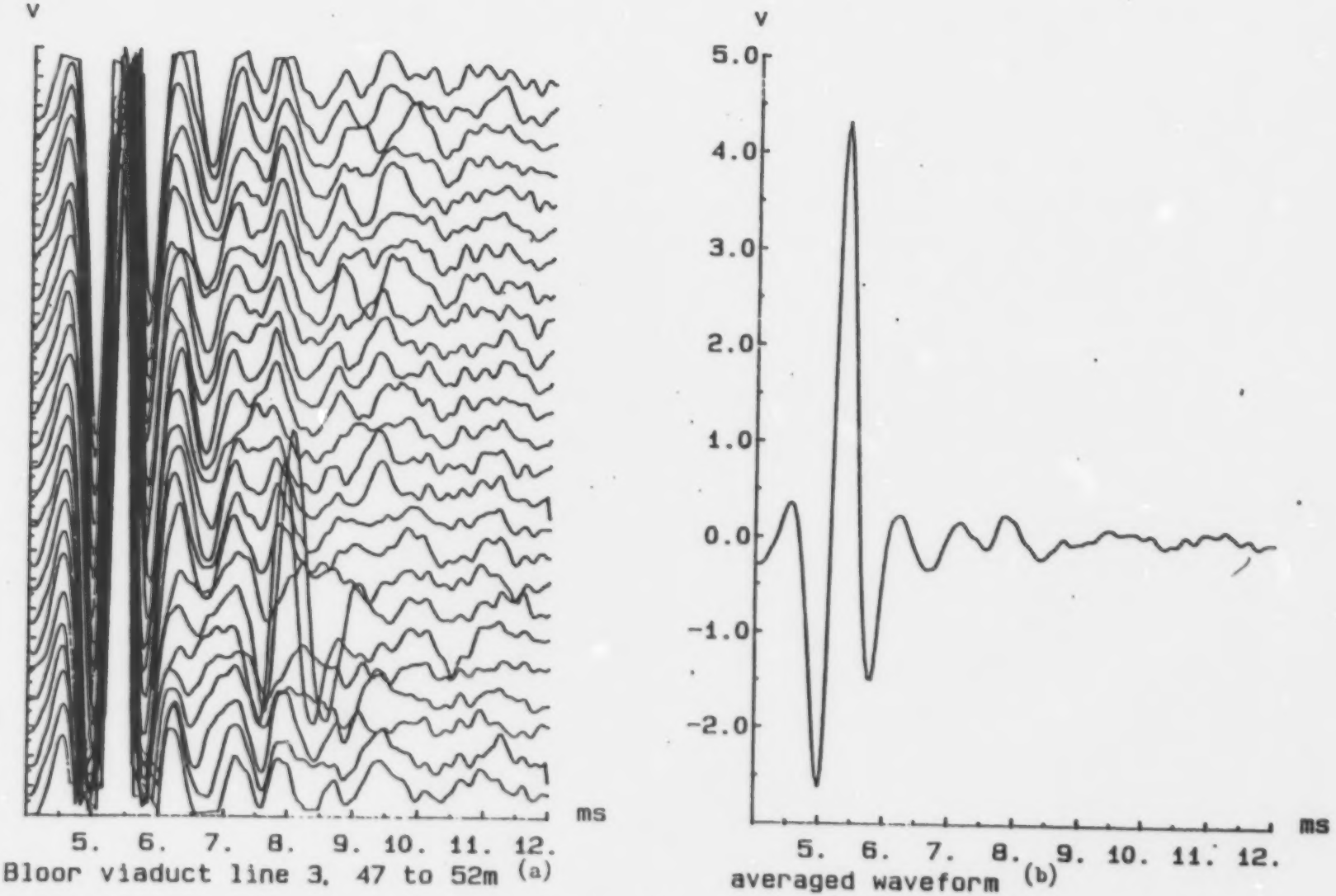

Fig. 5.32: (a) waveforms from line 3 between 47 to 52m and (b) the averaged waveform.

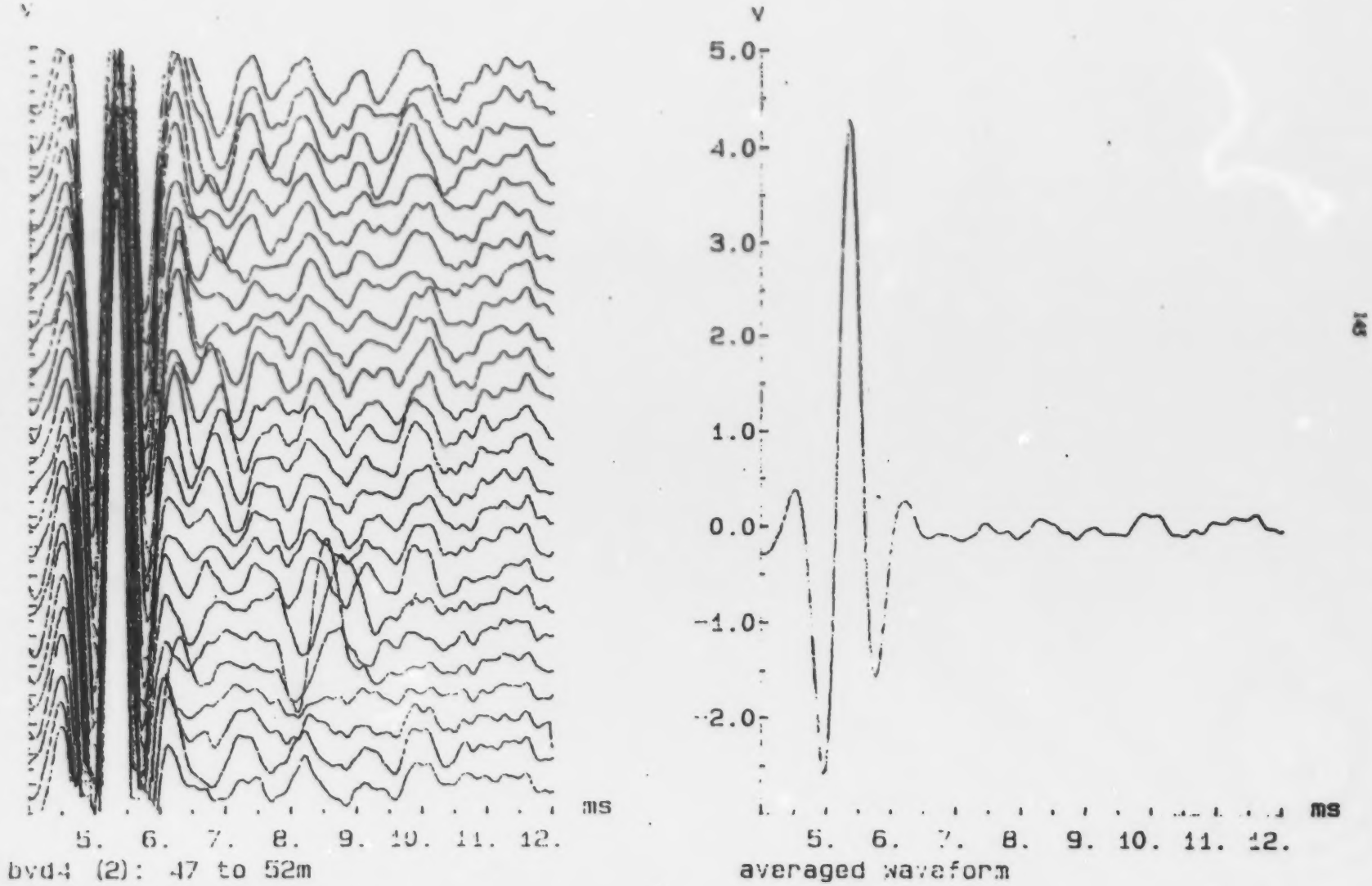

Fig. 5.33: (a) waveforms from line 4 between 46.2 to 52m
(b) averaged waveform of (a)

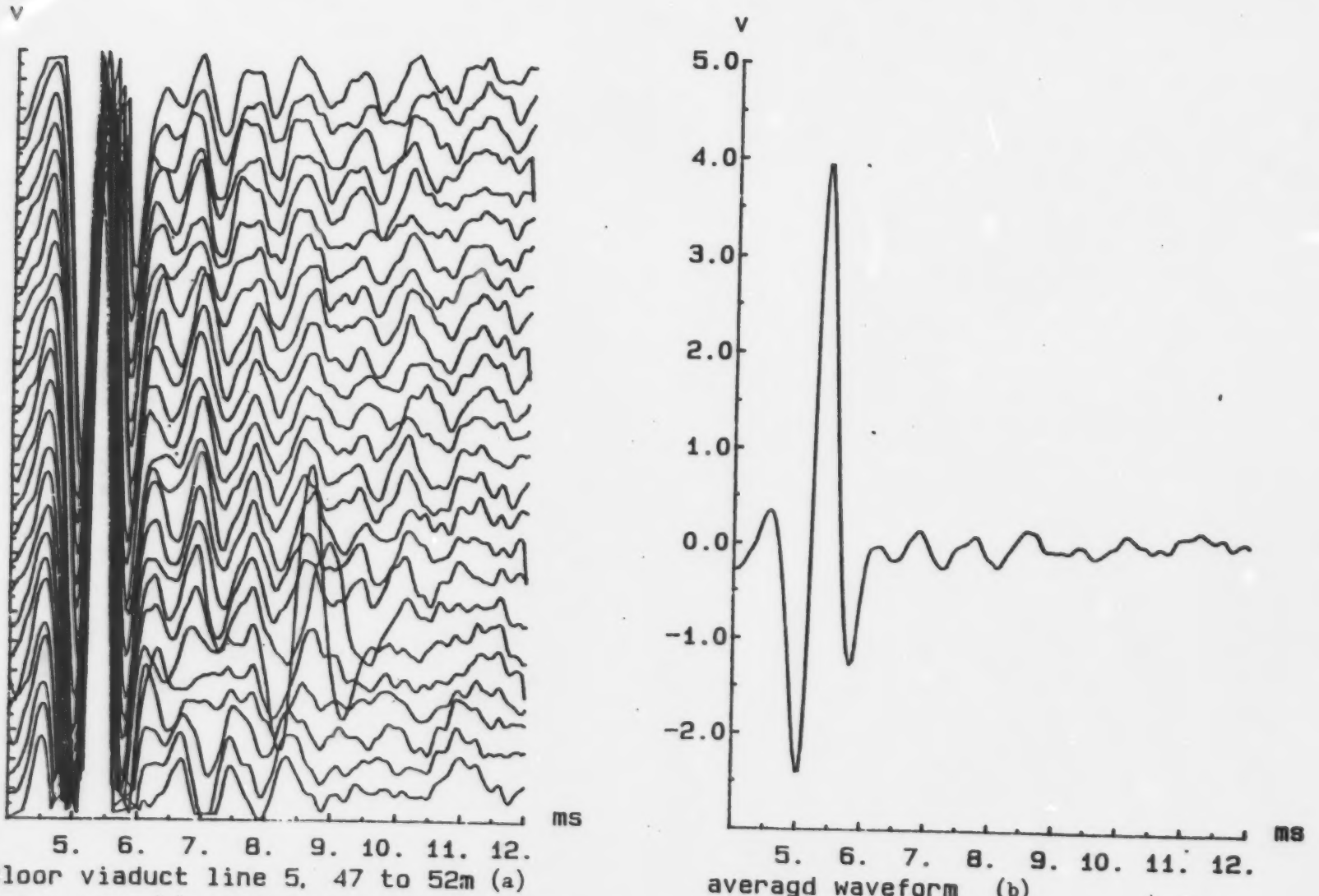

Fig. 5.34: (a) waveforms from line 5 between 47 to 52m and (b) the averaged waveform.

asphalt-concrete interface peak and the rebar location. The dielectric constant of asphalt used in the calculation is based on the averaged value obtained from each line. The results are applied to the averaged waveforms in order to check whether peaks do exist at the estimated locations.

Table 5.8/ Estimate boundary locations using computer results. Peak C defines the asphalt-concrete interface and peak D defines the rebar.

Figs	dielectric	asphalt	peak C	concrete	peak D
5.30	5.63	163 mm	7.85 ms	76 mm	9.30 ms
5.32	5.90	147	7.73	80	9.26
5.33	5.82	172	8.13	82	9.69
5.34	5.49	194	8.43	78	9.89

The time indications given in the above table compare quite well with the locations of the asphalt-concrete and rebar reflections from the waveform diagrams. This shows that the results are quite reliable.

A summary report is given in Table 5.9 for the analysis of the entire eastbound deck. It is reported that the overall asphalt thickness is 168 mm (this is about 134 mm with the 20% error removed as described above) and the concrete cover is on the averaged 70 mm. The deck is 81.23% good and 18.62% delaminated. Only a small portion of the structure is reported to have debonding and scaling.

In Fig. 5.35, the areas which are claimed delamination are indicated. We note that there is a considerable number of single- hits (i.e. single 'X' mark) which clutter the output. It is possible that most single-hits indication are false alarms. If they are filtered out from the map, the reliability of fault detection should be increased.

In the Fall of 1987, MTO conducted a selective survey on line 3. It is reported that the line is in good condition at the section 150 to 230 m. We refer to the map in Fig. 5.35(b) and (c), with the exception of single-hits scatter along the said section, there is only a small number of multiple-hit

```
Bloor viaduct (EASTBOUND): Line 1 (south curb) to line 6
BRIDGE deck CONDition SUMMARY

                [ ASPhalt AVERaged THICKness ]
                          line number
              1      2      3      4      5      6
.....
      mm    152    161    154    179    184    179
      in   5.98   6.34   6.06   7.05   7.24   7.05
ave dielect 6.32   5.63   5.90   5.82   5.49   5.81

              [ C/O REINFORCEment AVEraged THICKness ]
                          line number
              1      2      3      4      5      6
.....
      mm    70     73     71     69     71     69
      in   2.76   2.87   2.80   2.72   2.80   2.72

                [ LINE DISTRIBUTion (%) ]
                          line number
              1      2      3      4      5      6
.....
    GOOD   83.68  84.01  76.44  79.53  83.01  80.73
DEBONDed    .04    .32    .14    .04    .18    .00
  SCALEd    .04    .05    .00    .00    .00    .05
DELAMINATed 16.23  15.63  23.42  20.42  16.81  19.23
 BAD data    .00    .00    .00    .00    .00    .00
   TOTAL   100.00 100.00 100.00 100.00 100.00 100.00

          metal PLATE AMPlitude is: 10.169790 v

OVERALL AVEraged DIELECTric constant of asphalt is 5.8282

OVERALL AVERaged ASPhalt THICKness is 168 mm, [ 6.61 in ]

OVERALL AVEraged C/O REINFORCEment THICKness is  70 mm, [ 2.76 in ]

          [ OVERALL bridge deck CONDITION ]

              GOOD       81.23 %
            DEBONDED       .12 %
              SCALed       .02 %
          Delaminated    18.62 %
           BAD  data       .00 %
             Total      100.00 %
```

Table 5.9: Summarized reports of the eastbound deck.

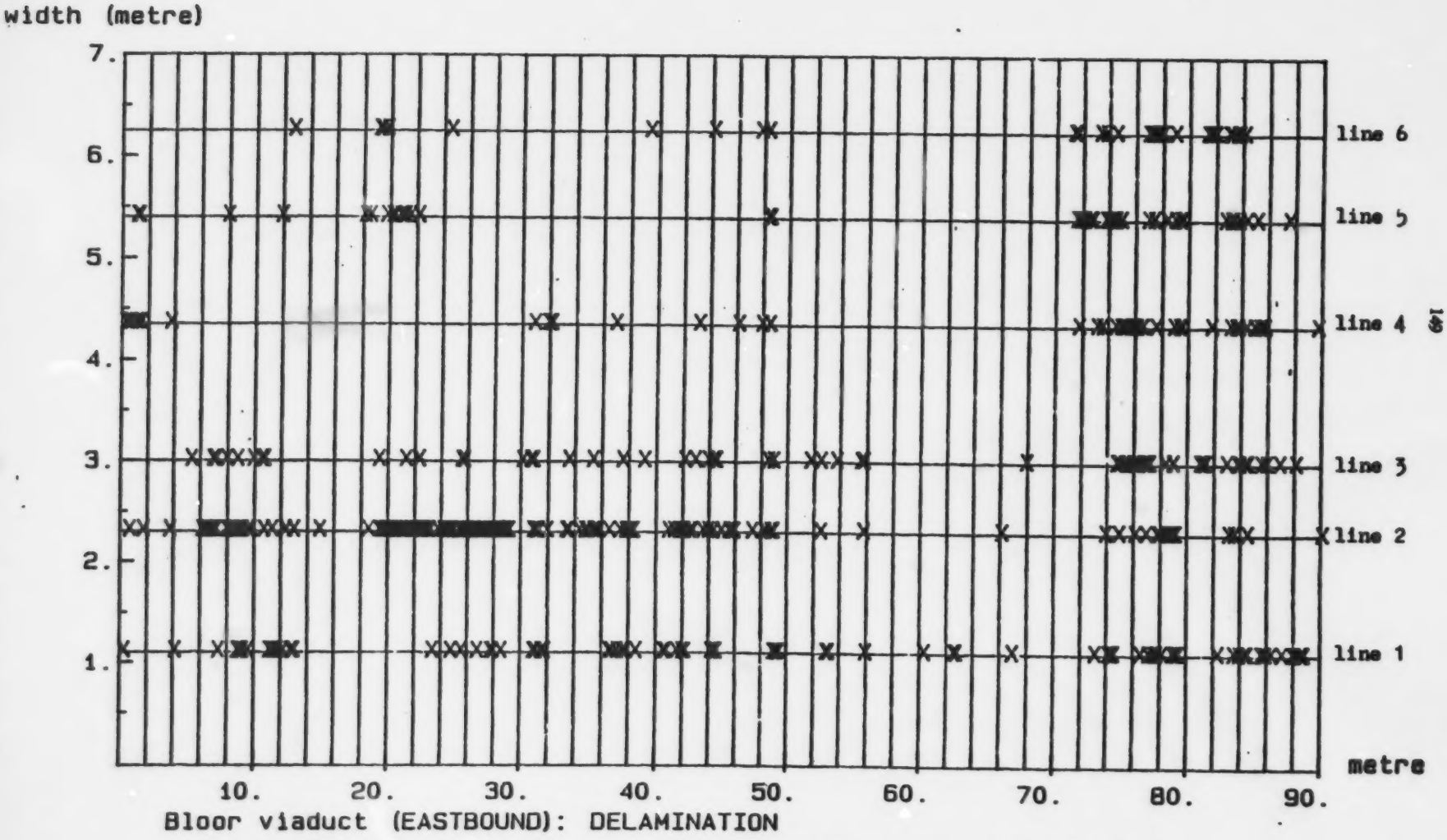

Fig. 5.35(a): Grid map indicates areas of delamination on eastbound deck between 0 to 90m.

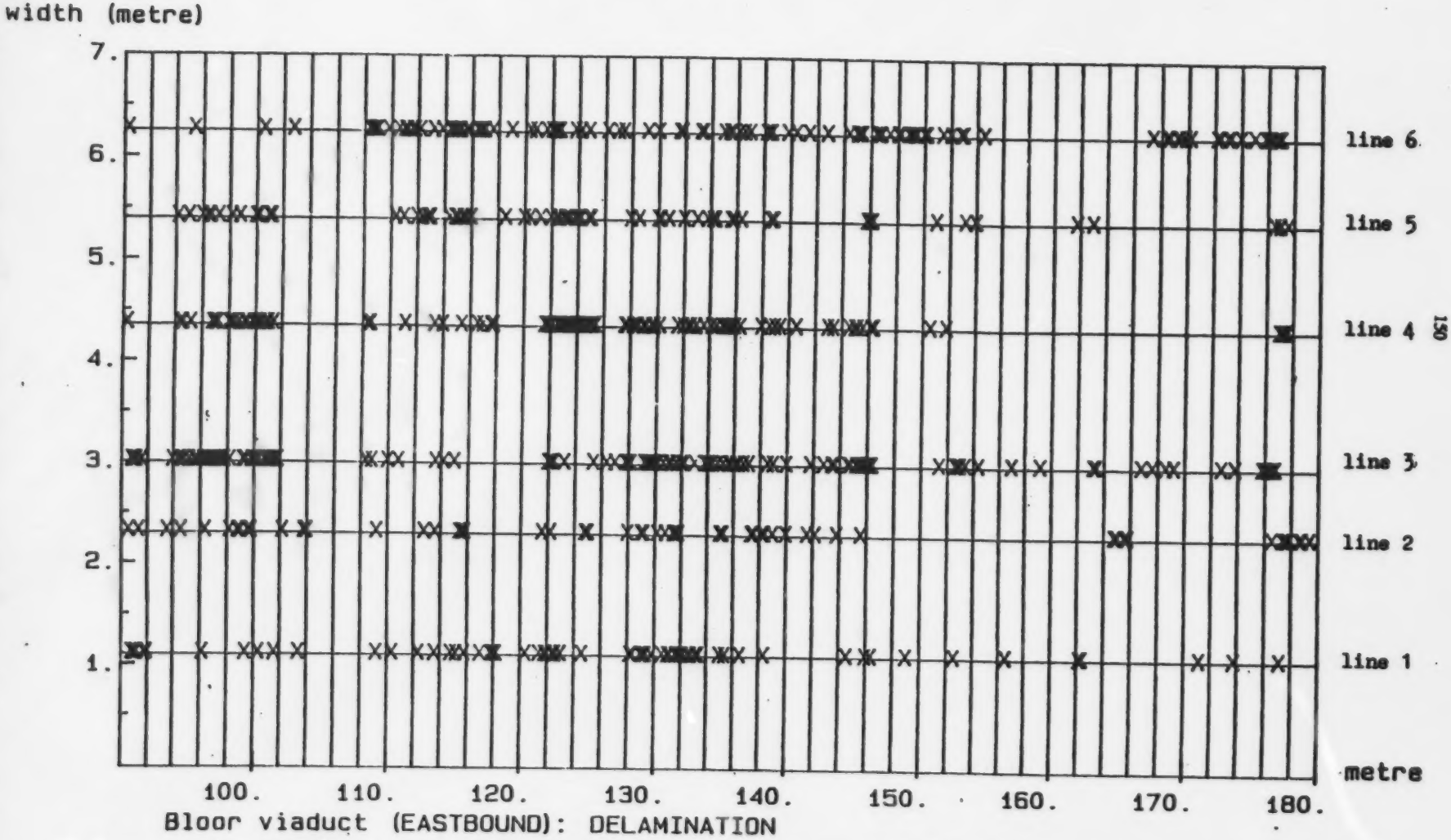

Fig. 5.35(b): Grid map indicates areas of delamination on eastbound deck between 90 to 180m.

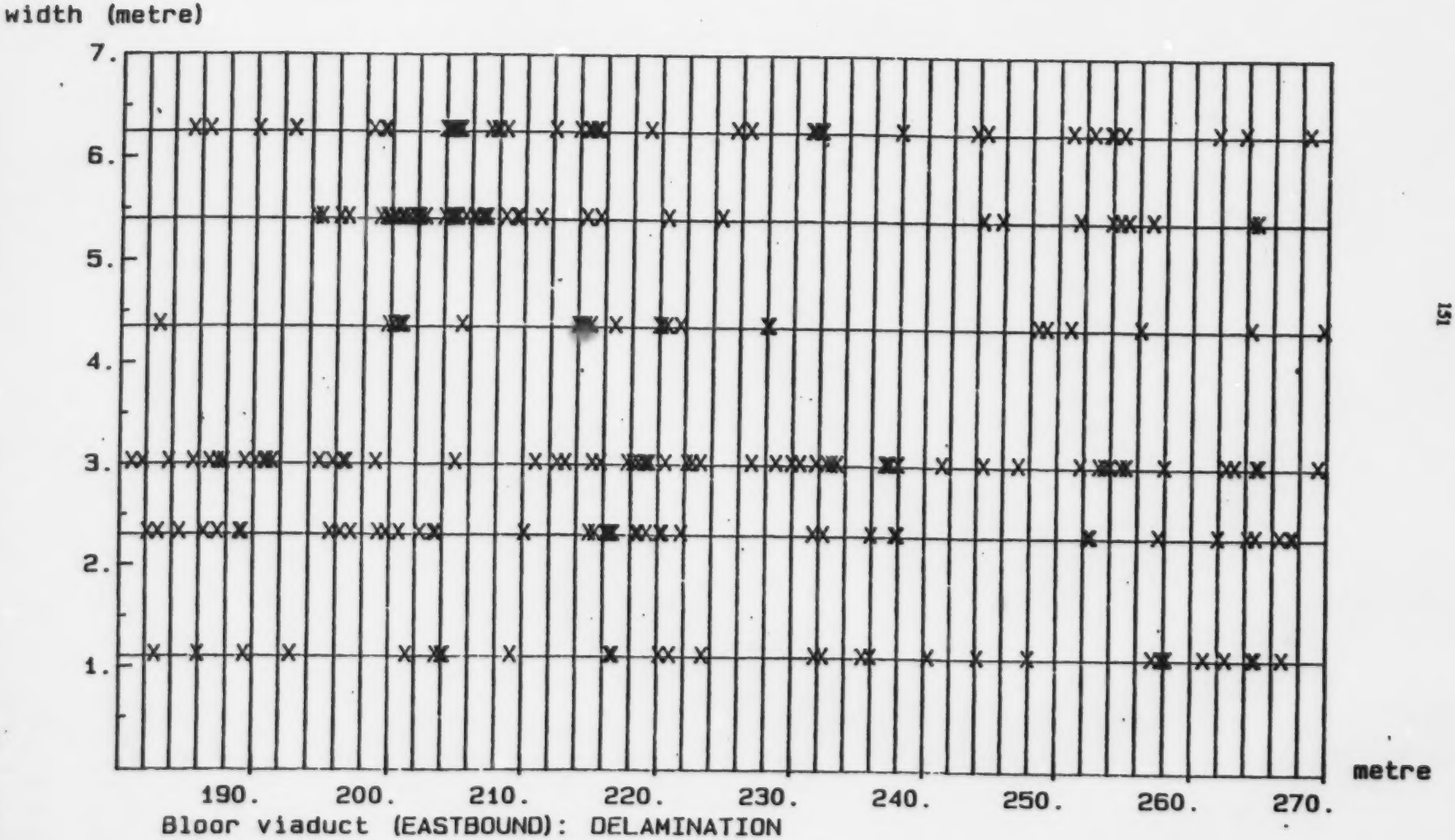

Fig. 5.35(o): areas of delamination between 180 to 270m

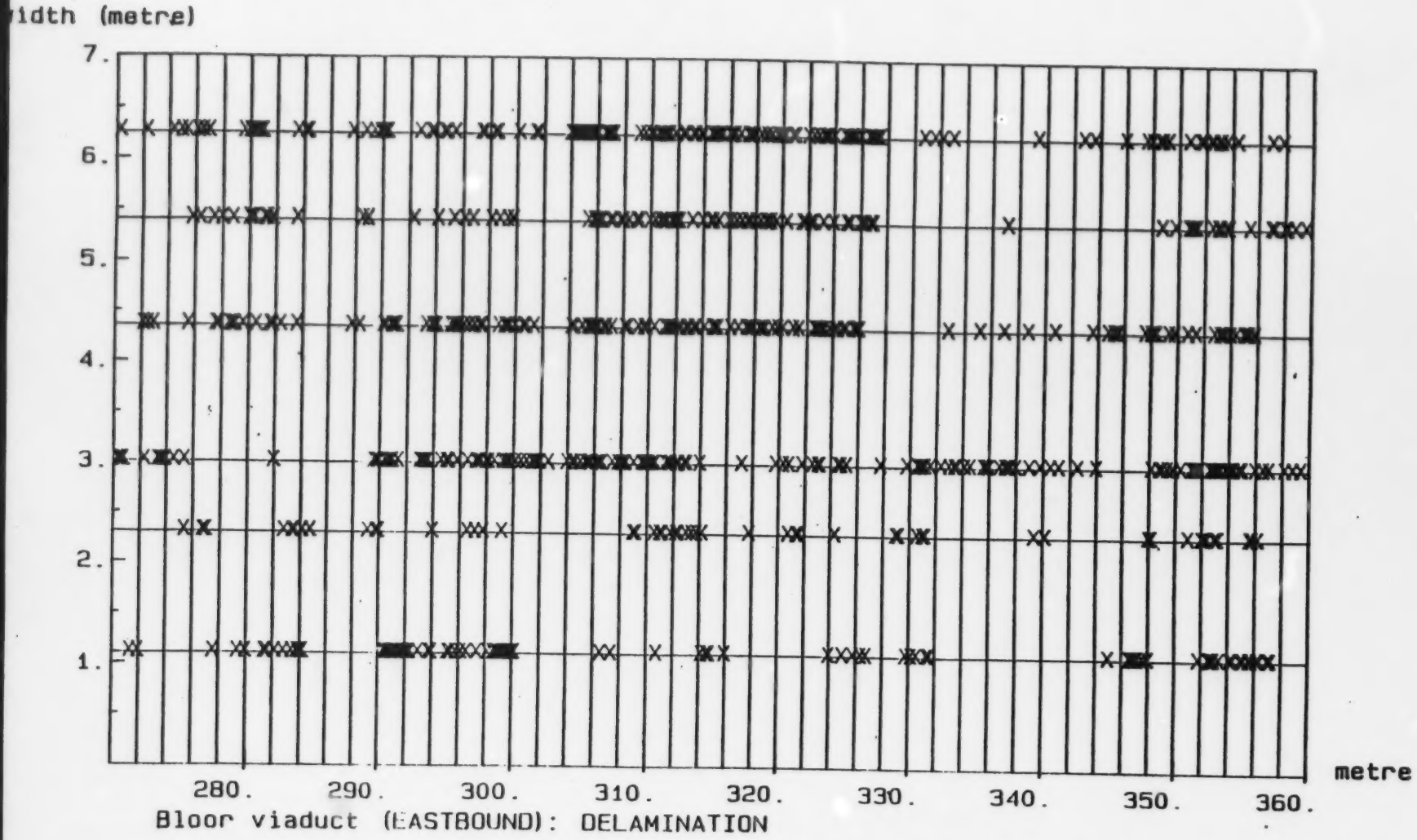

Fig. 5.35(d): areas of delamination between 270 to 360m.

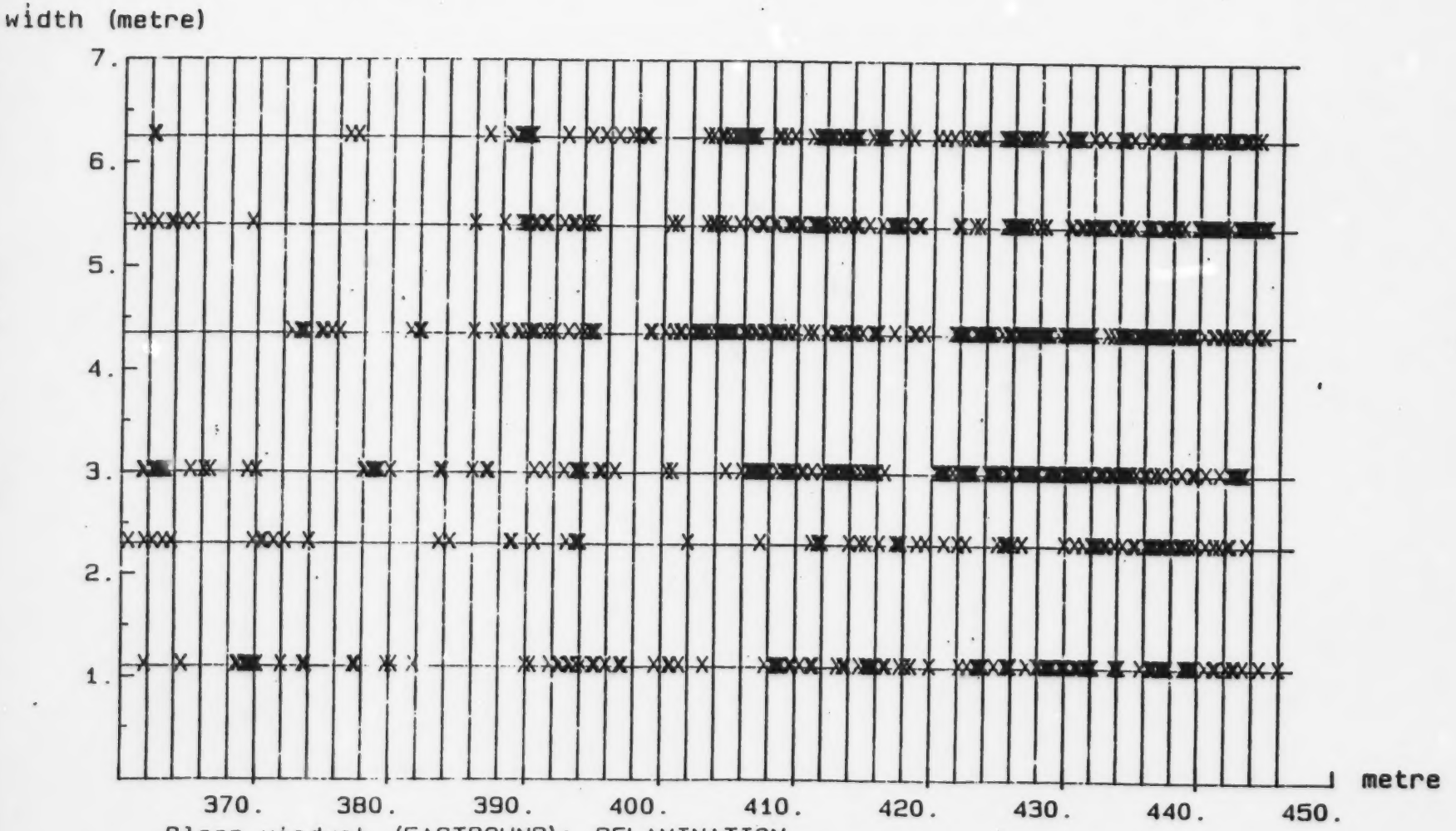

Bloor viaduct (EASTBOUND): DELAMINATION

Fig. 5.35(e): areas of delamination between 360 to 447m.

clusters together. The prominent location which has crowded indications is around 176 to 177 m. Sample waveforms are plotted from 175.2 to 180 m (Fig. 5.36) and 180.2 to 185 m (Fig. 5.37) respectively, in order to check for confirmation. The waveforms (Fig. 5.36) around 176 m do not contain the well-defined characteristic W pattern, which is a prime factor in determining delamination.

Areas which are declared debonded and scaled are given in Figs. 5.38 and 5.39 respectively. These locations coincide with the metal joint areas which are reported in Table 5.10,

Table 5.10/ Locations of metal joint under asphalt surface. Reverse for the westbound deck.

Eastbound:	48 m	to	54 m
	78		84
	109		110
	135		140
	178		182
	217		221
	265		centre line of another pier
	310		314
	352		centre line of another pier
	390		395
	420		joint

From previous experience, it is suggested that we should neglect any fault declaration near metal joint area. This is because the strong reflection from the metal plate disrupts the waveform analysis. In the present study, debonding and scaling are likely to be false alarms.

In Appendix D, we also present the statistical and histogram data for the eastbound deck.

5.3.5/ Data Analysis Of Westbound Deck

For the westbound data (line 7 to 12), three lines on the right lane and three lines on the middle lane are processed. Two lines were recorded from the left lane but the data are not analysed.

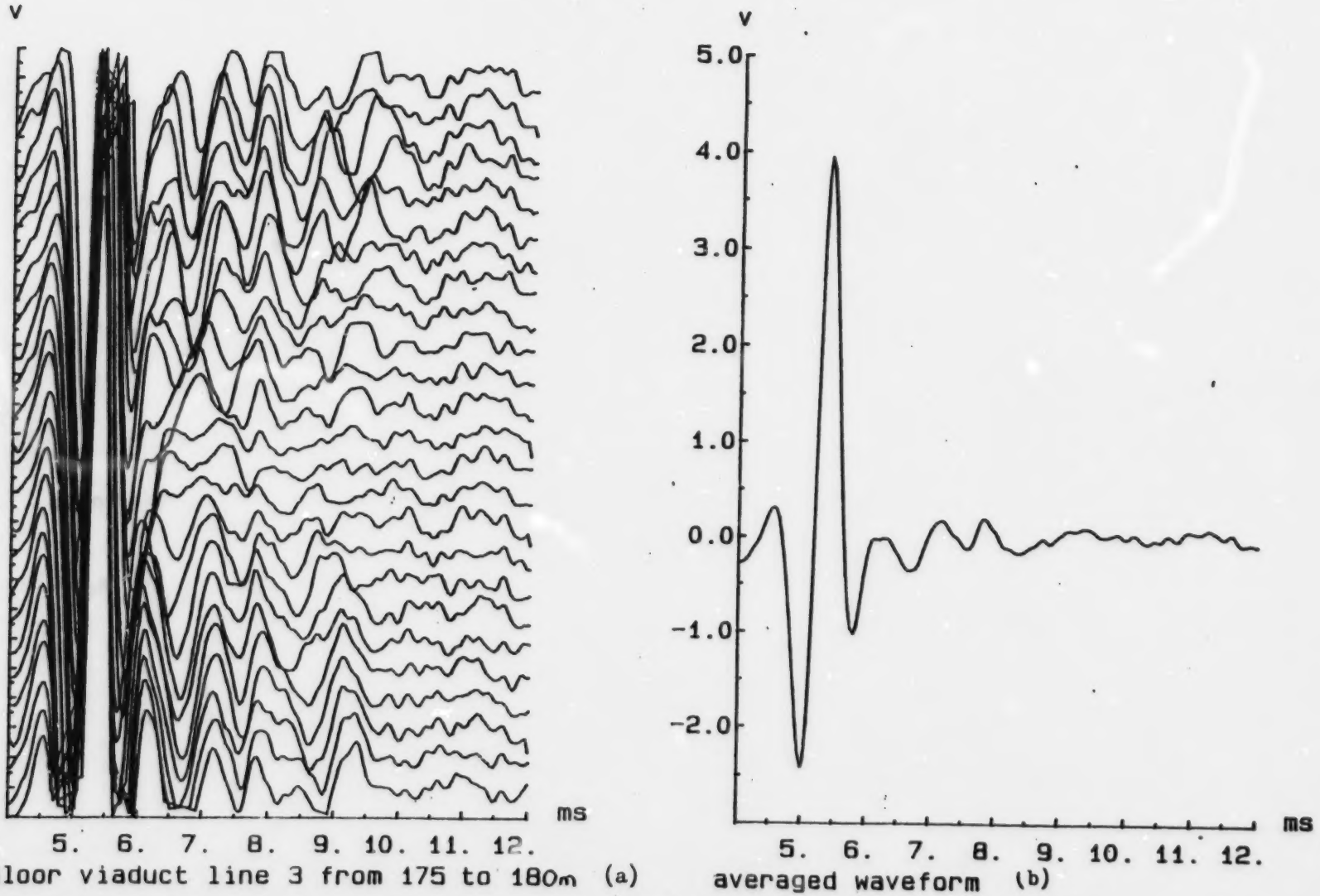

Fig. 5.36: (a) waveforms from line 3 between 175 to 180m and (b) the averaged waveform.

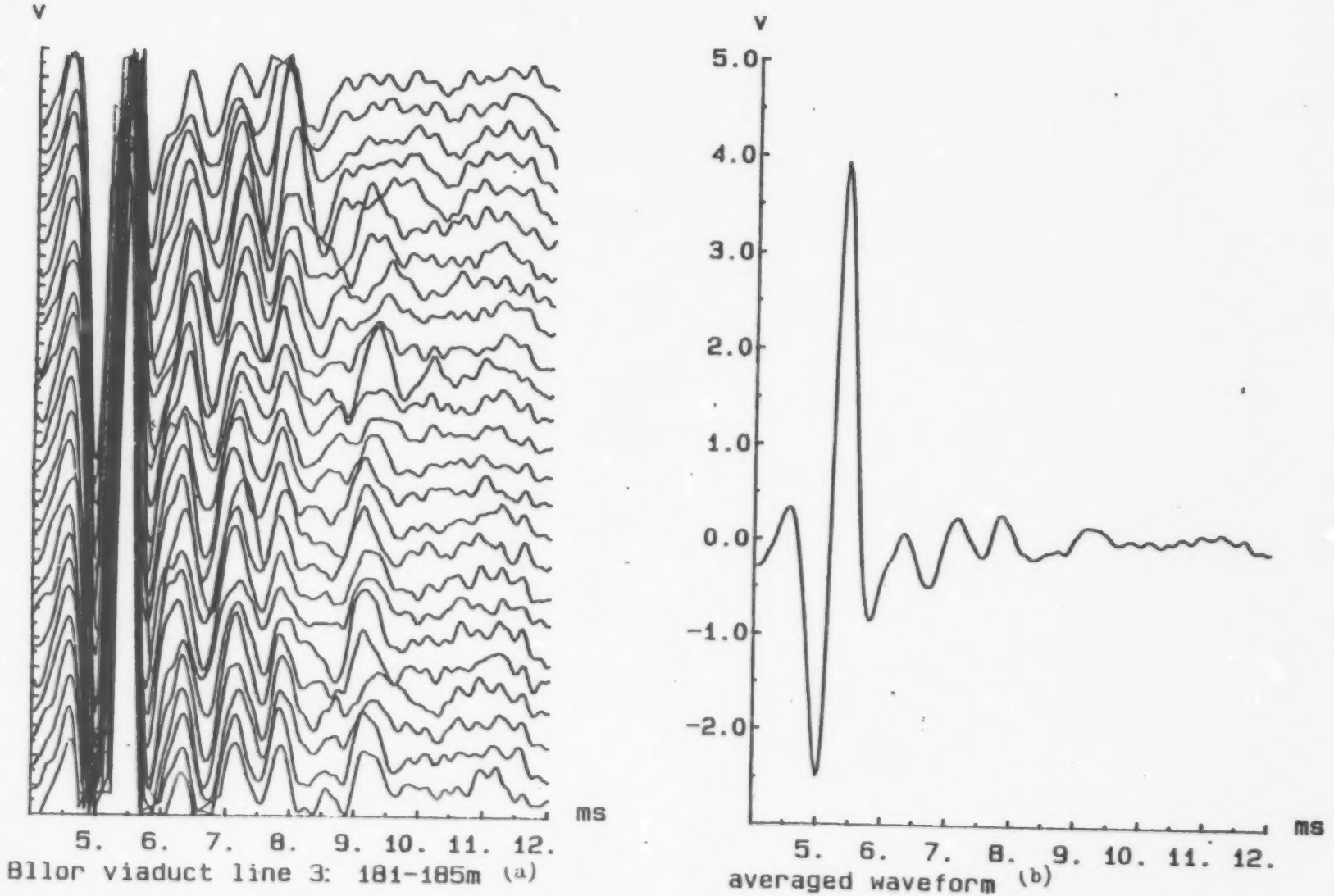

Fig. 5.5: (a) waveforms from line 3 between 181 to 185m and (b) the averaged waveform.

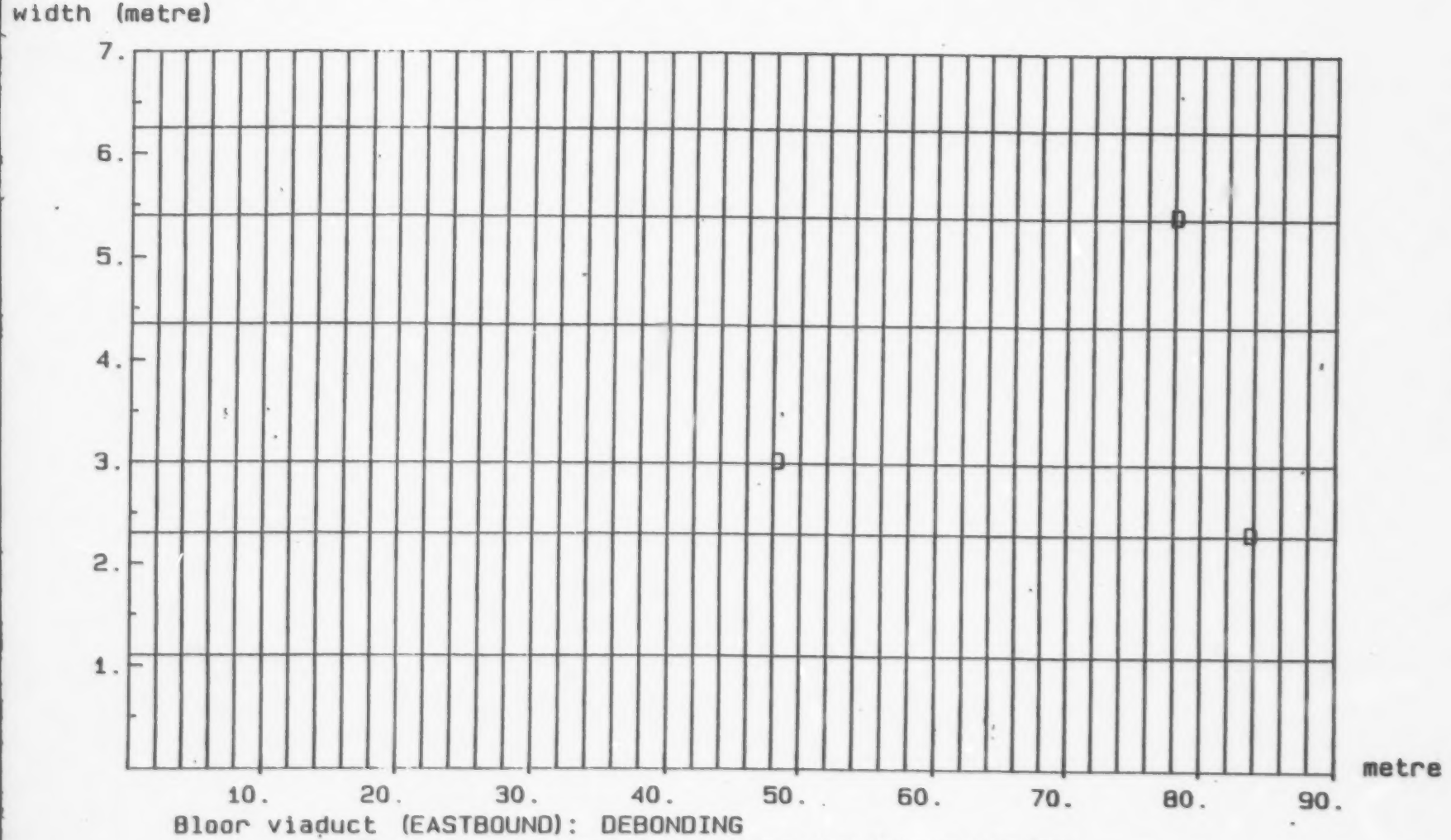

Fig. 5.38(a): areas of debonding on eastbound deck between 0 to 90m.

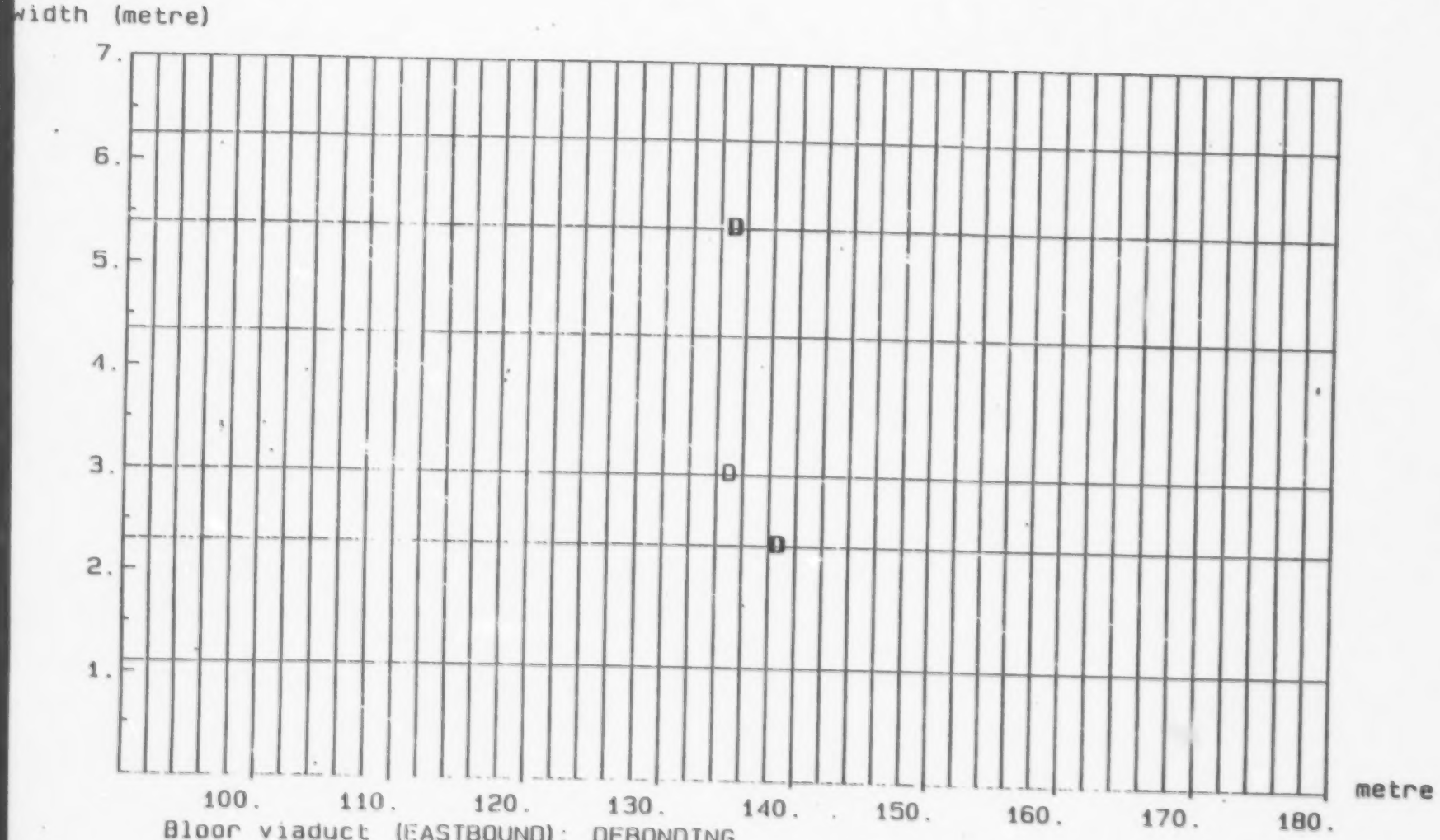

Fig. 5.38(b): areas of debonding between 90 to 180m.

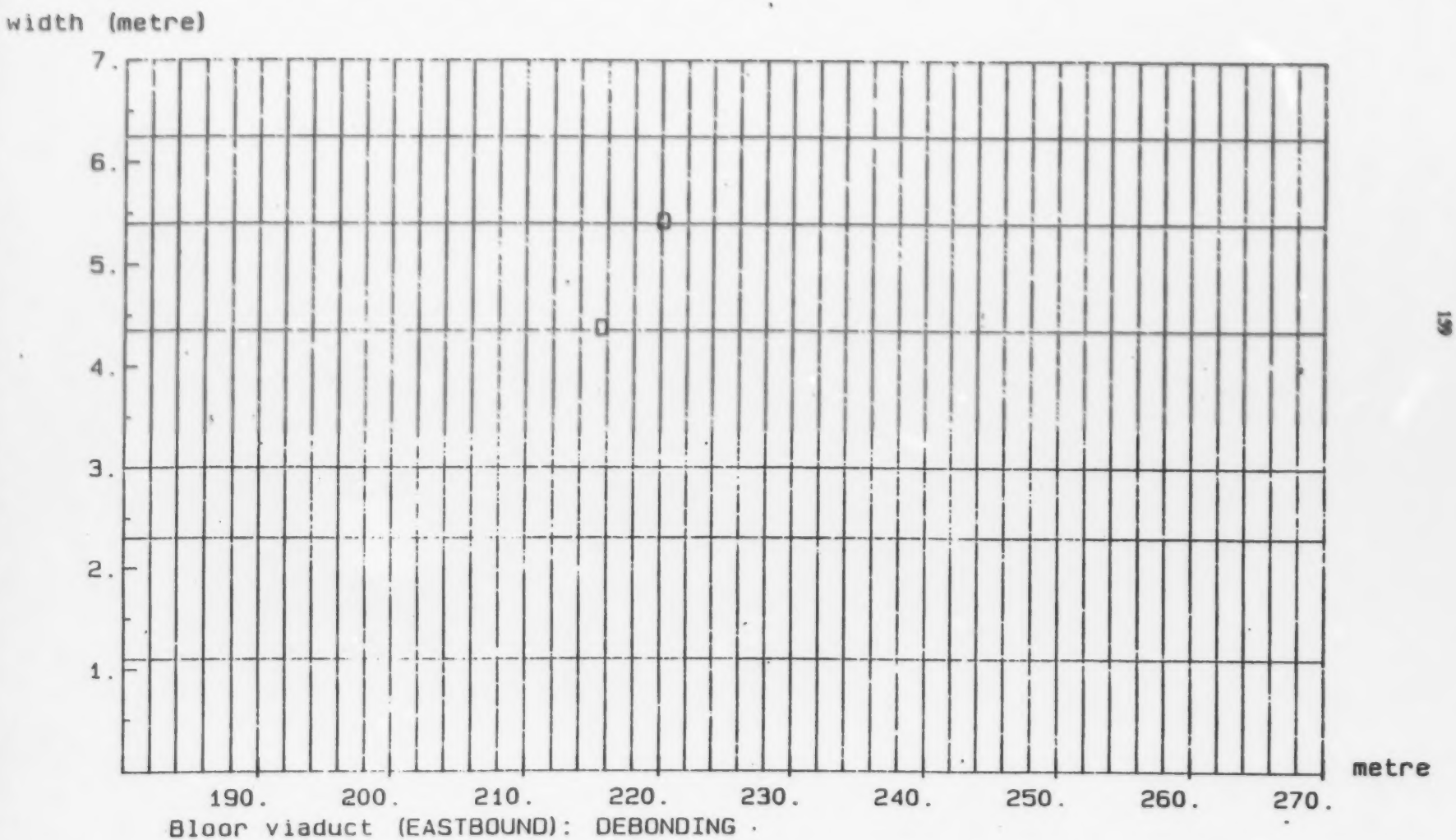

Fig. 5.38(c): areas of debonding between 180 to 270m.

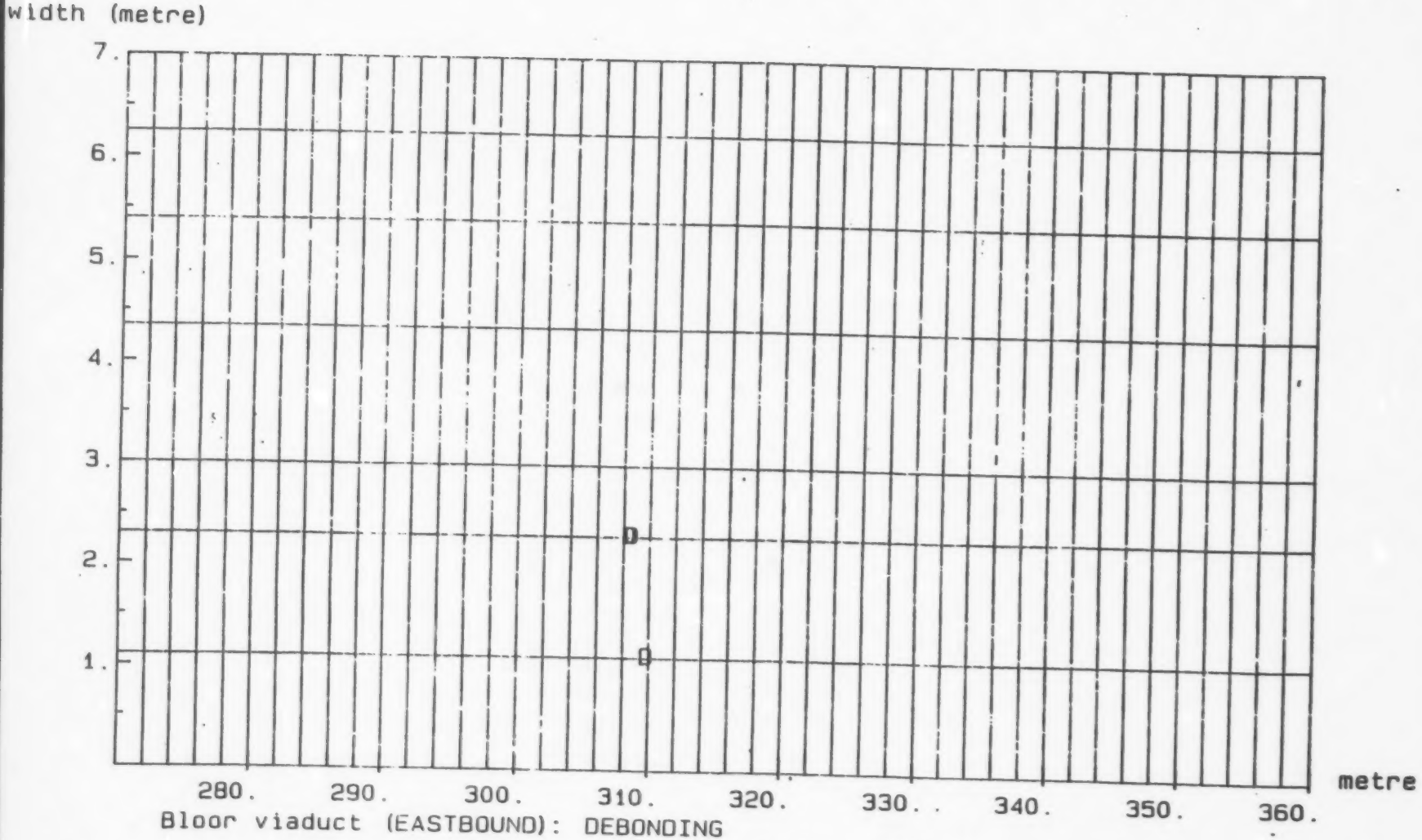

Fig. 4.38(d): areas of debonding between 270 to 360m.

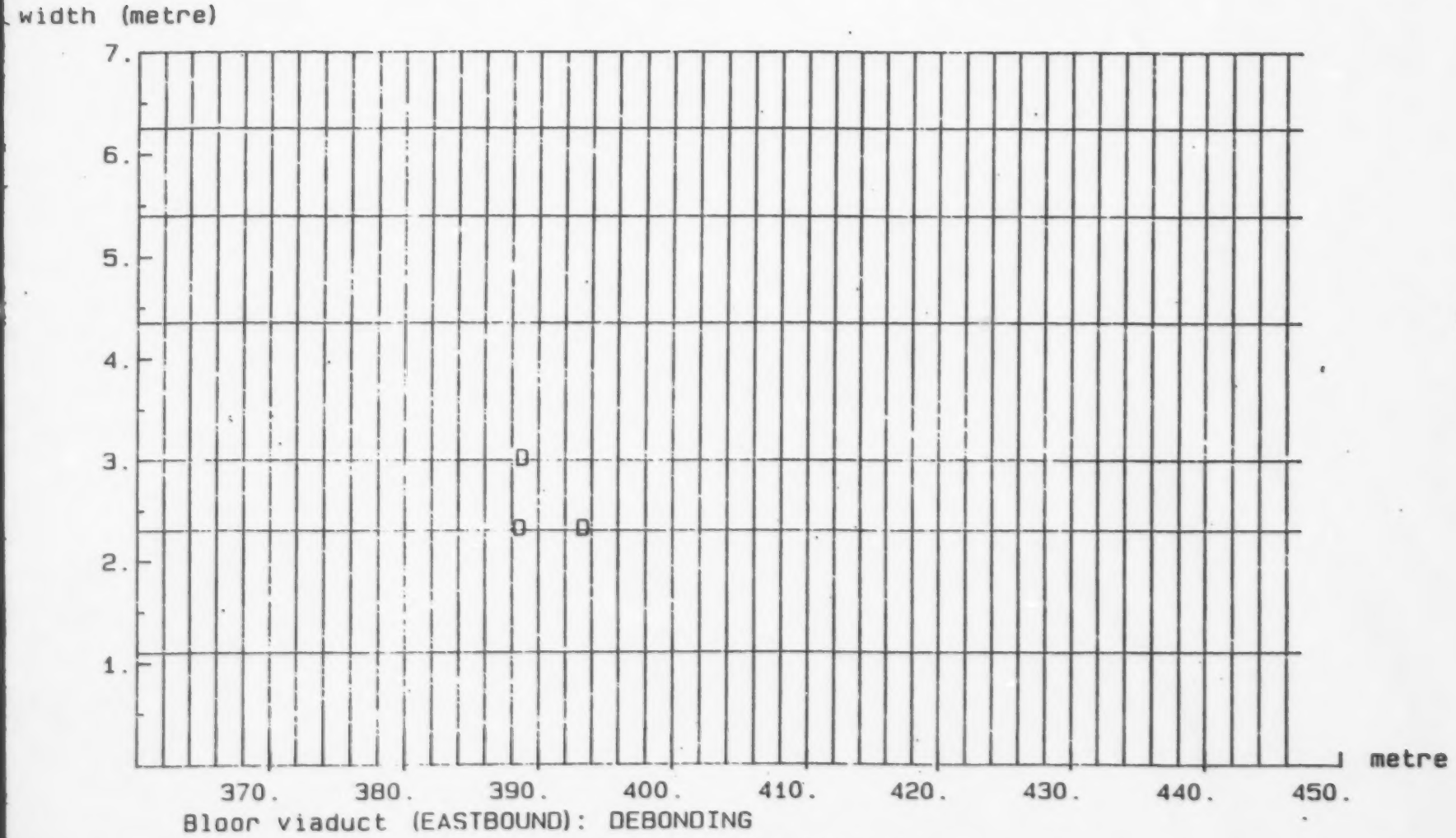

Fig. 5.38(e): areas of debonding between 360 to 447m.

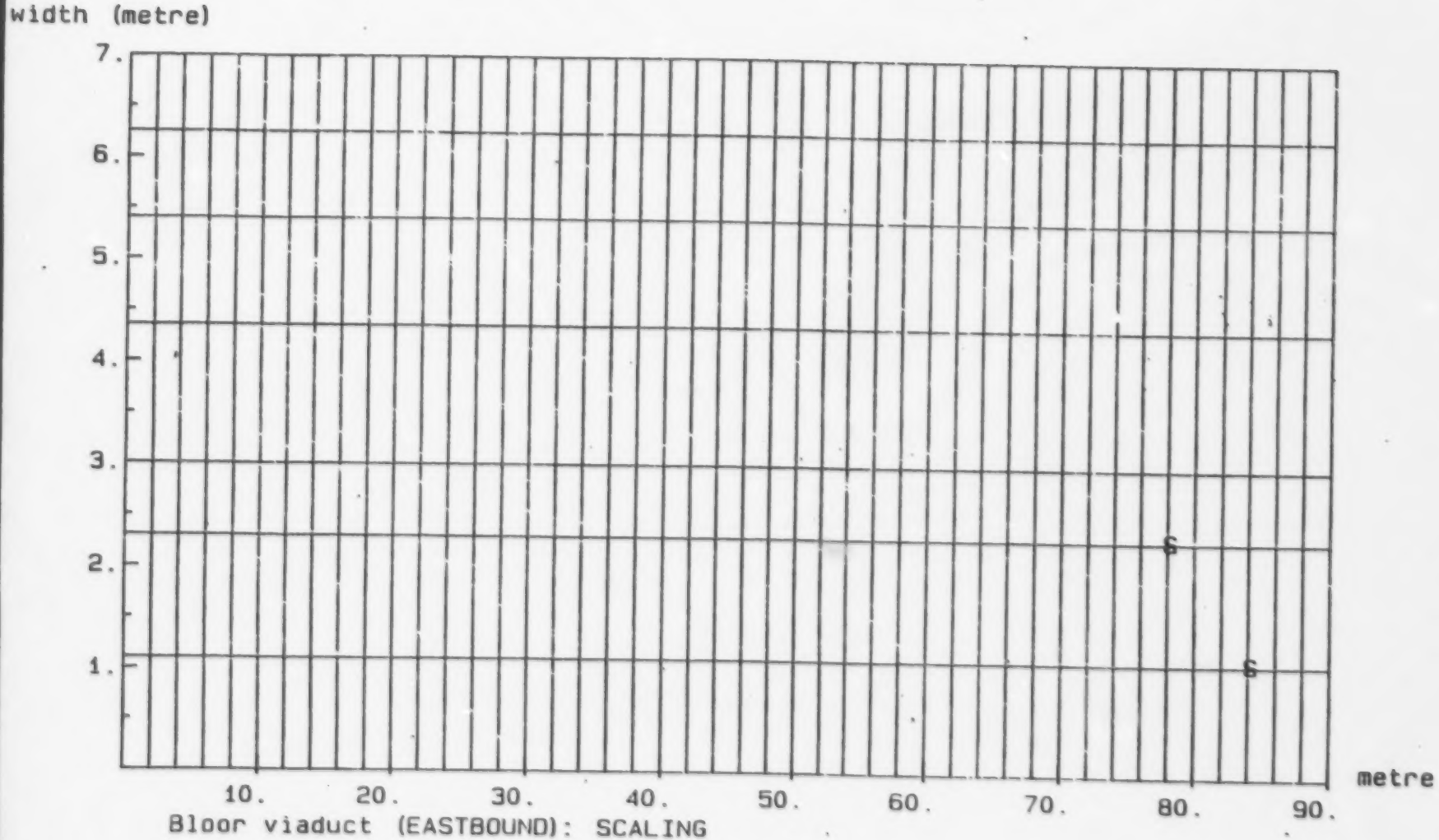

Fig. 5.39(a): areas of scaling between 0 to 90m.

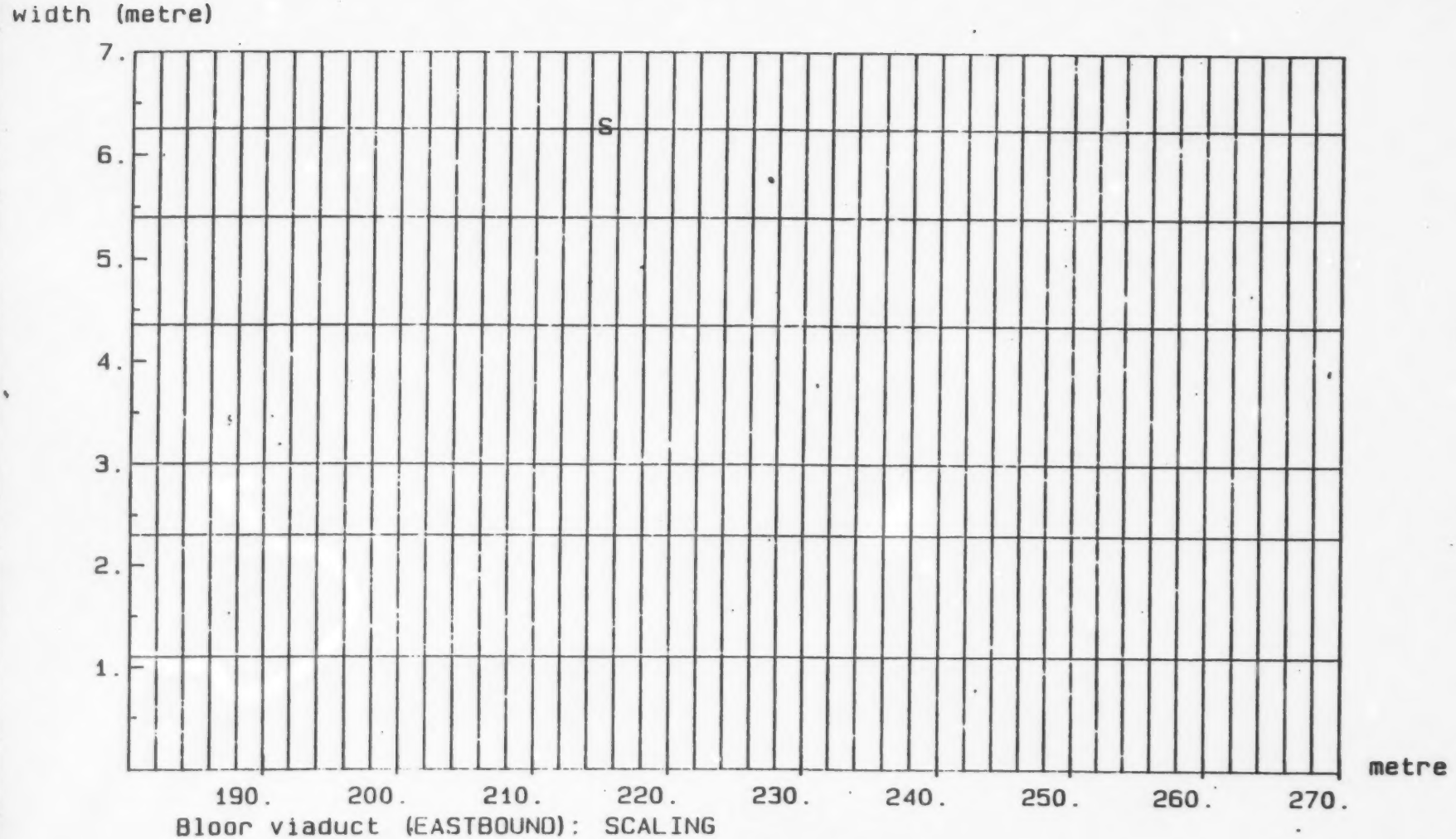

Fig. 5.39(b): areas of scaling between 180 to 270m.

Bloor viaDuct (WESTbound): line 7 (north curb) to line 12 (S
AVEraged THICKness SUMMARY

[AVEraged THICKness (mm)]
line number

metre	1	2	3	4	5	6
1	191 (58)	146 (85)	144 (75)	158 (78)	166 (68)	162 (65)
2	138 (64)	155 (80)	149 (79)	163 (68)	166 (70)	160 (66)
3	124 (67)	158 (80)	148 (79)	162 (69)	159 (72)	177 (68)
4	131 (61)	154 (79)	149 (77)	167 (69)	176 (70)	156 (72)
5	128 (63)	146 (76)	147 (76)	169 (65)	177 (68)	154 (69)
6	129 (60)	143 (77)	141 (75)	171 (70)	179 (70)	157 (71)
7	121 (61)	140 (76)	138 (72)	166 (73)	176 (71)	160 (72)
8	118 (61)	150 (69)	139 (75)	163 (69)	176 (74)	163 (67)
9	122 (51)	137 (77)	140 (76)	161 (70)	175 (69)	164 (69)
10	125 (62)	135 (77)	139 (78)	159 (74)	173 (79)	159 (66)
11	132 (56)	153 (60)	135 (76)	158 (73)	169 (73)	154 (72)
12	130 (54)	169 (46)	145 (69)	162 (75)	166 (75)	151 (75)
13	133 (53)	148 (68)	137 (75)	157 (69)	158 (77)	151 (69)
14	158 (47)	144 (74)	140 (83)	163 (73)	167 (70)	143 (71)
15	165 (42)	141 (76)	141 (82)	161 (81)	165 (76)	150 (79)
16	165 (48)	146 (81)	143 (81)	164 (73)	168 (74)	162 (77)
17	151 (48)	153 (61)	144 (82)	171 (65)	162 (76)	161 (79)
18	152 (54)	145 (72)	155 (71)	165 (66)	163 (75)	163 (75)
19	178 (56)	146 (76)	181 (48)	159 (68)	175 (76)	155 (75)
20	166 (53)	143 (69)	126 (67)	155 (71)	163 (74)	152 (74)
21	157 (55)	144 (80)	115 (77)	153 (70)	157 (75)	150 (68)
22	144 (72)	155 (73)	140 (75)	152 (68)	153 (73)	149 (63)
23	165 (67)	149 (72)	134 (77)	156 (75)	151 (75)	150 (65)
24	154 (75)	148 (70)	136 (79)	160 (81)	155 (81)	147 (70)
25	140 (83)	131 (68)	125 (73)	155 (81)	145 (80)	126 (74)
26	139 (75)	135 (70)	133 (82)	151 (77)	136 (76)	134 (64)
27	138 (74)	142 (61)	133 (63)	134 (69)	145 (75)	146 (68)
28	146 (72)	147 (62)	145 (68)	151 (82)	158 (80)	144 (75)
29	156 (59)	171 (70)	167 (71)	173 (80)	168 (56)	157 (59)
30	150 (52)	169 (63)	155 (66)	169 (75)	158 (89)	151 (60)
31	129 (64)	159 (74)	144 (68)	176 (66)	165 (87)	148 (80)
32	154 (60)	143 (65)	132 (80)	171 (68)	169 (79)	150 (86)
33	157 (63)	161 (60)	140 (77)	170 (72)	167 (79)	139 (78)
34	153 (68)	149 (78)	148 (76)	177 (76)	170 (76)	138 (79)
35	141 (77)	144 (66)	142 (83)	179 (75)	164 (75)	145 (86)
36	146 (76)	159 (63)	144 (83)	167 (73)	159 (78)	136 (64)
37	140 (76)	153 (62)	144 (76)	162 (76)	152 (85)	140 (70)
38	145 (67)	145 (77)	153 (67)	156 (85)	143 (82)	140 (84)
39	142 (71)	156 (68)	137 (77)	165 (71)	158 (73)	144 (84)
40	153 (63)	150 (76)	143 (81)	163 (69)	165 (69)	144 (78)
41	147 (75)	149 (77)	142 (83)	167 (67)	166 (69)	157 (76)
42	143 (76)	150 (67)	141 (79)	161 (77)	160 (72)	155 (69)
43	136 (84)	155 (69)	148 (78)	170 (77)	160 (68)	156 (68)
44	139 (82)	156 (76)	146 (82)	176 (69)	157 (54)	160 (68)
45	147 (81)	150 (70)	152 (79)	157 (76)	138 (48)	157 (80)
46	142 (82)	153 (80)	153 (74)	172 (75)	180 (74)	158 (86)
47	147 (81)	152 (69)	155 (70)	166 (77)	178 (81)	157 (88)
48	153 (77)	159 (84)	155 (72)	169 (75)	173 (90)	155 (92)
49	145 (75)	157 (79)	148 (75)	168 (73)	176 (78)	161 (86)
50	143 (75)	154 (68)	150 (73)	170 (72)	174 (76)	164 (74)
51	159 (72)	162 (66)	138 (78)	165 (72)	163 (66)	160 (73)
52	190 (76)	157 (67)	131 (78)	158 (77)	173 (79)	164 (77)
53	139 (71)	169 (66)	137 (73)	156 (82)	163 (88)	157 (83)
54	136 (66)	192 (62)	126 (73)	151 (90)	167 (82)	148 (83)
55	152 (56)	170 (68)	135 (73)	155 (87)	162 (84)	145 (84)
56	153 (63)	141 (71)	134 (66)	156 (69)	164 (65)	157 (72)
57	153 (50)	154 (57)	145 (75)	161 (80)	165 (74)	156 (86)
58	133 (51)	146 (74)	154 (74)	162 (79)	172 (78)	163 (72)
59	128 (48)	152 (74)	151 (75)	169 (81)	127 (82)	163 (64)
60	126 (51)	153 (72)	151 (81)	130 (78)	130 (58)	160 (72)
61	134 (47)	155 (61)	153 (80)	141 (51)	138 (49)	125 (84)
62	128 (54)	154 (74)	156 (77)	141 (51)	135 (55)	159 (79)
63	116 (55)	159 (75)	162 (77)	144 (91)	154 (58)	146 (83)
64	127 (56)	167 (80)	166 (77)	183 (82)	171 (84)	130 (87)
65	128 (66)	164 (87)	154 (87)	170 (87)	161 (83)	124 (86)
66	131 (78)	157 (77)	152 (87)	164 (92)	173 (75)	121 (86)
67	130 (79)	165 (80)	152 (89)	161 (77)	167 (72)	119 (81)
68	136 (81)	155 (82)	152 (79)	157 (80)	160 (67)	120 (77)
69	130 (75)	148 (74)	153 (81)	158 (92)	157 (70)	125 (72)
70	136 (67)	155 (81)	149 (77)	174 (83)	155 (75)	130 (91)
71	140 (73)	152 (69)	155 (76)	153 (82)	133 (65)	130 (69)
72	148 (77)	141 (70)	145 (90)	136 (101)	137 (56)	128 (48)
73	150 (87)	146 (74)	148 (83)	135 (89)	143 (55)	117 (57)

Table 5.11: Averaged thickness of the westbound deck.

74	152 (86)	150 (70)	156 (82)	141 (73)	150 (67)	125 (55)
75	154 (81)	148 (70)	153 (83)	143 (53)	175 (87)	136 (74)
76	157 (85)	147 (71)	160 (81)	190 (79)	172 (89)	142 (90)
77	153 (87)	149 (57)	160 (83)	153 (56)	145 (61)	129 (68)
78	146 (76)	145 (59)	149 (83)	139 (87)	138 (59)	117 (59)
79	148 (81)	139 (68)	143 (75)	148 (84)	152 (46)	127 (50)
80	152 (85)	135 (60)	148 (85)	148 (52)	150 (50)	123 (52)
81	150 (78)	144 (66)	151 (77)	154 (56)	135 (65)	131 (71)
82	150 (71)	144 (61)	148 (79)	144 (52)	134 (62)	123 (58)
83	143 (70)	149 (67)	141 (85)	156 (56)	132 (52)	138 (69)
84	151 (68)	144 (60)	151 (82)	141 (64)	147 (56)	139 (64)
85	138 (75)	142 (67)	141 (87)	143 (85)	145 (57)	158 (78)
86	168 (49)	140 (73)	142 (80)	136 (107)	144 (57)	136 (78)
87	165 (43)	136 (79)	148 (78)	157 (86)	142 (69)	127 (69)
88	164 (48)	141 (70)	148 (74)	165 (82)	135 (63)	129 (81)
89	157 (44)	144 (74)	150 (68)	147 (61)	149 (77)	162 (83)
90	151 (49)	148 (70)	152 (71)	186 (80)	171 (84)	159 (85)
91	151 (50)	157 (74)	142 (77)	159 (69)	175 (88)	154 (88)
92	152 (54)	149 (83)	143 (77)	179 (87)	174 (86)	152 (81)
93	128 (53)	127 (73)	119 (76)	155 (83)	168 (83)	137 (83)
94	128 (54)	122 (74)	111 (69)	132 (68)	155 (69)	123 (74)
95	128 (66)	142 (64)	118 (78)	150 (72)	150 (83)	134 (78)
96	131 (52)	156 (62)	140 (73)	165 (63)	167 (74)	144 (83)
97	142 (55)	150 (78)	138 (92)	163 (68)	166 (73)	141 (83)
98	156 (72)	143 (74)	125 (71)	163 (68)	167 (71)	149 (78)
99	125 (72)	155 (68)	131 (85)	172 (79)	169 (72)	142 (79)
100	129 (63)	163 (63)	135 (81)	181 (78)	180 (81)	153 (77)
101	141 (81)	168 (64)	118 (73)	178 (84)	180 (82)	145 (76)
102	139 (75)	162 (67)	122 (76)	171 (91)	170 (80)	147 (78)
103	138 (80)	156 (65)	138 (86)	158 (92)	166 (88)	134 (83)
104	151 (85)	152 (69)	141 (80)	156 (87)	158 (88)	130 (83)
105	159 (82)	153 (68)	143 (78)	150 (89)	151 (80)	125 (84)
106	163 (83)	157 (65)	138 (67)	145 (91)	149 (82)	130 (79)
107	163 (72)	157 (62)	139 (90)	146 (93)	147 (84)	124 (83)
108	172 (86)	152 (65)	138 (81)	147 (88)	147 (78)	117 (80)
109	133 (70)	156 (64)	131 (74)	151 (87)	149 (72)	125 (76)
110	143 (69)	153 (69)	131 (82)	150 (86)	149 (74)	128 (86)
111	154 (79)	154 (61)	132 (87)	152 (83)	150 (76)	137 (86)
112	159 (82)	153 (68)	129 (87)	148 (86)	151 (74)	139 (86)
113	152 (87)	150 (68)	135 (87)	148 (83)	153 (76)	137 (85)
114	156 (83)	149 (62)	147 (85)	144 (74)	152 (73)	133 (77)
115	155 (84)	150 (68)	147 (83)	147 (69)	150 (82)	136 (78)
116	150 (80)	157 (73)	145 (81)	151 (69)	157 (81)	136 (86)
117	143 (75)	154 (72)	149 (81)	152 (77)	152 (82)	121 (79)
118	129 (70)	149 (72)	146 (82)	157 (77)	159 (76)	122 (75)
119	139 (50)	151 (86)	144 (90)	153 (77)	154 (76)	132 (79)
120	170 (83)	151 (66)	152 (84)	154 (80)	151 (86)	134 (84)
121	155 (88)	148 (74)	150 (87)	159 (83)	159 (79)	141 (85)
122	153 (89)	150 (68)	154 (85)	161 (83)	163 (85)	146 (85)
123	150 (73)	148 (62)	154 (87)	157 (83)	167 (88)	145 (86)
124	152 (74)	148 (68)	151 (85)	160 (81)	172 (86)	131 (87)
125	160 (82)	151 (76)	152 (73)	155 (77)	168 (87)	141 (87)
126	146 (69)	152 (79)	151 (75)	153 (83)	162 (86)	124 (92)
127	143 (79)	150 (87)	150 (79)	155 (85)	174 (80)	147 (80)
128	135 (77)	153 (81)	144 (73)	160 (83)	161 (81)	161 (77)
129	134 (83)	155 (57)	142 (75)	156 (86)	140 (75)	145 (68)
130	138 (76)	145 (68)	134 (79)	159 (84)	150 (73)	127 (58)
131	137 (71)	147 (68)	148 (65)	164 (77)	147 (73)	160 (84)
132	133 (76)	151 (72)	134 (75)	170 (79)	176 (75)	161 (88)
133	138 (65)	136 (61)	129 (78)	166 (69)	180 (65)	160 (81)
134	145 (65)	158 (59)	144 (74)	165 (78)	169 (83)	143 (74)
135	135 (67)	157 (61)	127 (84)	159 (91)	171 (80)	153 (82)
137	134 (73)	170 (55)	142 (81)	166 (87)	177 (68)	155 (73)
138	137 (64)	160 (76)	142 (70)	160 (76)	161 (67)	156 (71)
139	133 (84)	164 (70)	148 (80)	153 (85)	171 (72)	144 (75)
140	138 (68)	161 (78)	150 (77)	159 (78)	163 (79)	138 (77)
141	145 (79)	153 (83)	152 (79)	164 (78)	164 (76)	134 (78)
142	143 (77)	154 (77)	160 (71)	164 (75)	160 (79)	139 (76)
143	135 (81)	156 (78)	161 (71)	161 (71)	162 (76)	141 (76)
144	134 (81)	147 (78)	158 (73)	168 (70)	163 (78)	146 (82)
145	135 (75)	135 (76)	163 (77)	172 (64)	162 (80)	147 (82)
146	130 (71)	139 (60)	172 (74)	154 (68)	149 (62)	151 (78)
147	139 (79)	147 (87)	168 (72)	169 (66)	163 (75)	152 (84)
148	136 (80)	146 (75)	162 (76)	155 (72)	129 (64)	150 (81)
149	140 (73)	144 (78)	155 (75)	166 (66)	164 (75)	150 (80)
150	137 (80)	149 (65)	153 (75)	163 (64)	154 (84)	148 (83)
151	130 (80)	147 (72)	150 (77)	169 (71)	146 (62)	139 (89)
152	125 (78)	150 (75)	150 (77)	139 (86)	127 (74)	143 (80)
153	122 (73)	154 (55)	155 (69)	161 (76)	124 (76)	134 (83)
154	143 (81)	146 (78)	152 (69)	167 (71)	164 (79)	134 (75)
155	132 (75)	135 (74)	153 (70)	166 (67)	166 (74)	127 (86)
156	127 (81)	140 (77)	167 (72)	142 (73)	129 (92)	128 (65)
157	126 (62)	136 (71)	164 (74)	135 (78)	140 (54)	125 (79)

Table 5.11(b)

158	134 (60)	142 (63)	154 (72)	138 (83)	134 (67)	157 (84)
159	131 (63)	145 (67)	156 (79)	136 (81)	145 (61)	153 (82)
160	128 (69)	148 (63)	151 (72)	139 (76)	126 (63)	152 (90)
161	128 (67)	159 (70)	158 (79)	169 (70)	142 (60)	156 (82)
162	133 (76)	156 (86)	148 (79)	147 (87)	143 (56)	150 (78)
163	126 (74)	153 (69)	152 (79)	174 (69)	136 (58)	150 (86)
164	132 (73)	141 (64)	156 (77)	142 (72)	137 (69)	147 (87)
165	141 (68)	141 (69)	163 (73)	139 (90)	141 (54)	117 (86)
166	130 (78)	149 (85)	156 (78)	149 (78)	128 (66)	122 (74)
167	137 (72)	147 (69)	154 (88)	161 (78)	131 (87)	127 (66)
168	145 (73)	161 (69)	157 (90)	167 (75)	138 (79)	122 (56)
169	151 (72)	161 (61)	160 (88)	172 (70)	143 (55)	125 (54)
170	146 (75)	160 (67)	154 (92)	174 (77)	144 (64)	134 (54)
171	146 (77)	162 (61)	161 (91)	170 (89)	142 (42)	134 (53)
172	148 (66)	150 (73)	162 (88)	137 (45)	140 (54)	138 (50)
173	144 (69)	141 (63)	161 (82)	141 (58)	142 (50)	140 (50)
174	145 (74)	146 (68)	147 (84)	170 (86)	141 (44)	137 (51)
175	148 (73)	156 (67)	146 (89)	153 (83)	129 (53)	137 (52)
176	148 (69)	155 (77)	145 (83)	169 (86)	129 (59)	131 (54)
177	148 (73)	151 (59)	141 (83)	153 (87)	136 (50)	131 (52)
178	154 (67)	151 (68)	137 (82)	158 (89)	137 (71)	124 (53)
179	158 (65)	151 (61)	139 (82)	164 (86)	170 (91)	137 (46)
180	161 (70)	150 (62)	151 (77)	166 (85)	166 (88)	144 (63)
181	163 (72)	141 (56)	142 (82)	151 (86)	139 (72)	122 (70)
182	151 (68)	141 (61)	126 (75)	141 (71)	145 (81)	136 (71)
183	143 (77)	165 (58)	126 (78)	148 (83)	151 (55)	156 (71)
184	163 (68)	161 (57)	135 (88)	165 (86)	161 (88)	162 (73)
185	164 (73)	166 (69)	152 (77)	155 (93)	155 (71)	156 (71)
186	156 (76)	158 (68)	149 (87)	155 (91)	150 (86)	149 (67)
187	155 (79)	150 (73)	144 (85)	145 (85)	144 (68)	146 (79)
188	151 (77)	153 (60)	144 (85)	143 (90)	149 (72)	145 (85)
189	150 (70)	153 (56)	143 (85)	149 (91)	145 (60)	151 (81)
190	152 (76)	153 (67)	150 (80)	152 (89)	148 (83)	146 (86)
191	154 (76)	161 (58)	147 (73)	156 (80)	155 (86)	153 (80)
192	151 (75)	159 (68)	153 (74)	158 (79)	158 (87)	157 (82)
193	147 (79)	177 (64)	146 (70)	153 (83)	158 (79)	149 (83)
194	139 (76)	168 (58)	144 (65)	157 (82)	158 (79)	151 (79)
195	147 (66)	155 (69)	140 (70)	161 (81)	166 (84)	151 (83)
196	146 (68)	153 (68)	131 (79)	159 (79)	163 (85)	154 (92)
197	140 (71)	158 (64)	152 (65)	158 (70)	162 (83)	161 (87)
198	135 (76)	158 (63)	133 (80)	156 (77)	167 (83)	155 (86)
199	142 (81)	166 (71)	148 (67)	155 (78)	164 (86)	156 (86)
200	146 (82)	163 (63)	150 (71)	159 (77)	167 (77)	153 (90)
201	149 (76)	166 (79)	150 (71)	156 (75)	158 (78)	149 (85)
202	144 (83)	164 (71)	149 (75)	154 (79)	156 (79)	140 (91)
203	157 (80)	160 (81)	146 (75)	149 (84)	159 (82)	144 (89)
204	153 (83)	158 (79)	157 (67)	150 (89)	155 (79)	128 (79)
205	154 (89)	146 (78)	151 (70)	147 (93)	158 (91)	146 (76)
206	157 (82)	155 (69)	150 (66)	158 (85)	158 (76)	143 (80)
207	143 (84)	169 (60)	151 (67)	151 (81)	155 (75)	146 (82)
208	141 (82)	220 (54)	144 (78)	148 (84)	157 (79)	145 (82)
209	137 (82)	167 (69)	152 (70)	151 (77)	155 (78)	142 (81)
210	139 (86)	161 (63)	151 (70)	152 (77)	159 (78)	140 (83)
211	140 (89)	163 (71)	152 (68)	155 (71)	160 (77)	146 (89)
212	142 (84)	153 (64)	140 (82)	161 (76)	167 (70)	139 (73)
213	139 (84)	153 (60)	143 (81)	158 (78)	167 (74)	129 (79)
214	133 (81)	162 (71)	148 (83)	154 (82)	167 (81)	126 (66)
215	150 (75)	158 (61)	151 (86)	161 (75)	174 (77)	133 (75)
216	145 (78)	158 (63)	152 (88)	163 (77)	167 (85)	136 (85)
217	132 (81)	157 (74)	152 (89)	160 (83)	163 (90)	116 (60)
218	136 (83)	151 (82)	151 (85)	163 (84)	173 (86)	116 (77)
219	146 (77)	148 (65)	150 (86)	169 (83)	135 (64)	131 (82)
220	146 (75)	144 (66)	149 (83)	166 (85)	176 (89)	140 (55)
221	141 (70)	144 (64)	150 (81)	162 (83)	170 (87)	168 (81)
222	149 (81)	140 (64)	140 (79)	161 (91)	172 (80)	139 (75)
223	137 (81)	142 (74)	141 (86)	154 (90)	168 (79)	157 (87)
224	136 (74)	141 (78)	147 (84)	164 (89)	163 (76)	156 (86)
225	139 (69)	143 (77)	150 (80)	151 (86)	156 (78)	153 (89)
226	142 (68)	161 (63)	139 (78)	147 (86)	146 (67)	144 (88)
227	144 (63)	152 (63)	154 (64)	146 (81)	153 (77)	154 (71)
228	129 (65)	151 (68)	151 (83)	152 (79)	157 (81)	139 (85)
229	132 (60)	148 (74)	148 (80)	149 (85)	157 (72)	140 (71)
230	131 (74)	149 (67)	148 (78)	149 (80)	156 (79)	136 (78)
231	129 (65)	143 (66)	144 (63)	152 (74)	160 (71)	149 (75)
232	132 (79)	139 (74)	150 (61)	146 (75)	150 (74)	144 (78)
233	130 (84)	152 (74)	146 (64)	146 (75)	154 (78)	153 (76)
234	137 (92)	152 (85)	145 (73)	151 (76)	160 (81)	159 (69)
235	141 (92)	145 (72)	145 (69)	153 (77)	162 (84)	148 (76)
236	142 (71)	151 (89)	148 (75)	153 (81)	161 (83)	143 (79)
237	135 (80)	151 (61)	141 (81)	145 (89)	163 (89)	147 (79)
238	139 (73)	149 (65)	144 (72)	150 (86)	161 (76)	148 (86)
239	131 (90)	149 (69)	141 (71)	150 (90)	164 (86)	154 (84)
240	130 (83)	157 (68)	147 (73)	154 (86)	163 (84)	157 (74)

Table 5.11(c)

241	141 (74)	147 (83)	143 (90)	155 (95)	162 (83)	160 (87)
242	130 (78)	157 (71)	148 (87)	154 (89)	160 (88)	149 (80)
243	141 (79)	157 (76)	150 (85)	156 (88)	156 (85)	153 (91)
244	140 (73)	163 (86)	149 (74)	155 (87)	149 (77)	156 (83)
245	141 (85)	169 (68)	153 (78)	159 (90)	150 (61)	139 (83)
246	134 (85)	169 (74)	151 (71)	161 (80)	173 (91)	133 (78)
247	130 (81)	158 (61)	147 (77)	163 (84)	171 (87)	157 (83)
248	130 (70)	156 (72)	146 (78)	157 (85)	172 (82)	157 (79)
249	130 (78)	157 (86)	147 (75)	158 (83)	168 (84)	141 (70)
250	128 (74)	145 (65)	150 (71)	159 (85)	162 (78)	145 (75)
251	126 (70)	144 (67)	148 (68)	157 (85)	167 (83)	154 (74)
252	122 (73)	162 (85)	147 (76)	158 (86)	156 (79)	148 (75)
253	126 (67)	159 (71)	141 (73)	156 (89)	140 (73)	132 (69)
254	128 (70)	164 (79)	143 (75)	159 (88)	130 (69)	120 (71)
255	128 (70)	166 (68)	141 (73)	151 (90)	167 (87)	122 (60)
256	124 (76)	159 (66)	148 (66)	147 (90)	147 (63)	125 (64)
257	117 (83)	152 (83)	145 (73)	158 (77)	131 (73)	122 (62)
258	119 (84)	150 (79)	142 (74)	160 (81)	127 (63)	127 (73)
259	121 (78)	158 (69)	142 (70)	153 (82)	143 (73)	132 (78)
260	123 (80)	162 (83)	144 (75)	157 (76)	138 (77)	127 (91)
261	127 (82)	161 (87)	145 (82)	153 (80)	146 (73)	131 (57)
262	135 (82)	160 (87)	148 (74)	132 (90)	135 (79)	124 (60)
263	131 (71)	156 (75)	142 (77)	159 (87)	127 (82)	126 (79)
264	130 (75)	158 (76)	140 (77)	157 (90)	132 (79)	122 (66)
265	136 (68)	157 (75)	144 (82)	152 (89)	169 (90)	123 (63)
266	134 (72)	160 (74)	145 (80)	147 (89)	168 (85)	128 (68)
267	146 (79)	158 (66)	147 (82)	142 (90)	160 (91)	152 (84)
268	143 (69)	151 (74)	146 (85)	149 (88)	158 (87)	148 (94)
269	157 (65)	133 (79)	139 (77)	145 (79)	161 (84)	136 (77)
270	130 (59)	129 (63)	137 (72)	142 (72)	151 (69)	134 (68)
271	137 (67)	151 (65)	139 (78)	148 (85)	162 (89)	133 (69)
273	146 (72)	165 (76)	147 (79)	163 (81)	147 (78)	124 (71)
274	144 (71)	159 (76)	148 (76)	162 (86)	127 (64)	119 (59)
275	136 (78)	156 (78)	143 (69)	151 (86)	128 (76)	118 (59)
276	135 (73)	156 (76)	144 (73)	153 (90)	135 (71)	111 (66)
277	135 (68)	154 (74)	146 (71)	153 (90)	126 (78)	117 (65)
278	136 (65)	158 (82)	146 (70)	143 (89)	130 (56)	112 (72)
279	137 (64)	157 (83)	150 (70)	150 (88)	132 (76)	108 (69)
280	144 (69)	159 (81)	151 (68)	149 (89)	132 (64)	114 (80)
281	152 (75)	154 (75)	149 (70)	150 (82)	137 (72)	110 (69)
282	140 (69)	147 (74)	139 (74)	152 (77)	133 (76)	113 (71)
283	142 (68)	138 (83)	141 (71)	151 (79)	134 (70)	117 (64)
284	136 (73)	150 (82)	139 (80)	150 (84)	138 (68)	116 (74)
285	146 (75)	154 (77)	140 (75)	153 (87)	137 (67)	125 (71)
286	145 (75)	154 (65)	146 (82)	145 (80)	137 (65)	118 (50)
287	142 (74)	155 (82)	146 (79)	151 (81)	124 (79)	126 (72)
288	142 (76)	158 (75)	146 (84)	145 (86)	125 (67)	129 (82)
289	158 (68)	161 (78)	146 (83)	150 (84)	146 (74)	130 (72)
290	153 (74)	161 (82)	148 (81)	154 (86)	155 (81)	131 (67)
291	163 (73)	163 (70)	147 (85)	158 (81)	141 (70)	131 (66)
292	145 (76)	162 (71)	145 (84)	144 (75)	156 (76)	131 (64)
293	133 (77)	163 (84)	148 (79)	155 (81)	165 (82)	127 (53)
294	132 (78)	160 (72)	143 (81)	151 (86)	158 (83)	123 (44)
295	130 (65)	162 (74)	146 (82)	149 (79)	154 (79)	122 (57)
296	136 (81)	163 (79)	147 (81)	159 (77)	124 (68)	136 (64)
297	137 (84)	146 (65)	142 (74)	158 (80)	137 (69)	134 (70)
298	132 (80)	151 (63)	143 (76)	160 (78)	139 (59)	129 (68)
299	128 (69)	153 (86)	138 (84)	158 (81)	137 (67)	127 (71)
300	131 (65)	154 (76)	135 (83)	158 (78)	127 (79)	128 (79)
301	128 (70)	153 (83)	138 (83)	151 (89)	133 (67)	132 (50)
302	125 (73)	154 (82)	141 (81)	151 (90)	131 (75)	124 (69)
303	123 (83)	156 (89)	140 (85)	153 (88)	162 (84)	123 (70)
304	129 (82)	155 (72)	141 (86)	147 (91)	159 (81)	115 (70)
305	135 (74)	154 (76)	141 (80)	149 (86)	162 (87)	118 (55)
306	140 (82)	158 (76)	143 (77)	153 (89)	154 (74)	117 (70)
307	148 (74)	156 (65)	140 (73)	150 (84)	159 (86)	115 (65)
308	151 (70)	157 (71)	143 (74)	146 (80)	161 (77)	112 (93)
309	153 (60)	160 (73)	146 (65)	154 (71)	136 (51)	118 (68)
310	153 (74)	159 (79)	144 (74)	156 (70)	145 (73)	132 (63)
311	162 (81)	161 (79)	147 (78)	157 (82)	145 (79)	133 (67)
312	133 (71)	156 (77)	148 (71)	162 (70)	135 (66)	118 (58)
313	133 (76)	178 (58)	149 (65)	151 (76)	136 (53)	115 (73)
314	146 (71)	163 (82)	150 (70)	133 (54)	139 (53)	116 (60)
315	146 (63)	154 (64)	143 (69)	140 (70)	147 (58)	118 (90)
316	131 (77)	153 (76)	147 (67)	160 (72)	156 (75)	147 (76)
317	139 (71)	153 (63)	140 (79)	166 (81)	155 (67)	121 (53)
318	128 (69)	148 (66)	143 (70)	161 (75)	160 (84)	119 (57)
319	124 (79)	151 (78)	135 (71)	154 (77)	155 (77)	123 (57)
320	134 (73)	151 (72)	142 (69)	154 (77)	161 (81)	125 (59)
321	136 (70)	158 (77)	145 (73)	156 (77)	161 (78)	121 (60)
322	141 (55)	155 (81)	138 (76)	152 (80)	161 (84)	125 (62)
323	133 (64)	156 (79)	145 (78)	149 (88)	162 (70)	127 (62)
324	124 (73)	157 (78)	143 (71)	153 (77)	158 (71)	122 (53)

Table 5.11(d)

325	: 125 (74)	159 (71)	148 (68)	156 (73)	161 (78)	128 (69)
326	: 126 (69)	154 (79)	143 (72)	162 (77)	167 (87)	155 (81)
327	: 125 (75)	148 (73)	137 (79)	160 (84)	160 (87)	115 (75)
328	: 125 (63)	147 (73)	137 (77)	155 (87)	170 (83)	115 (80)
329	: 123 (72)	144 (71)	140 (74)	159 (83)	145 (73)	113 (70)
330	: 120 (74)	148 (77)	148 (73)	154 (78)	134 (79)	125 (65)
331	: 129 (68)	146 (74)	140 (79)	156 (86)	142 (72)	129 (73)
332	: 126 (88)	152 (82)	145 (64)	160 (85)	136 (68)	117 (78)
333	: 133 (76)	160 (63)	148 (75)	158 (88)	135 (75)	124 (65)
334	: 136 (83)	158 (90)	145 (78)	164 (81)	131 (81)	112 (63)
335	: 136 (80)	161 (83)	144 (76)	163 (87)	166 (88)	112 (76)
336	: 150 (81)	154 (85)	141 (91)	156 (92)	163 (82)	112 (74)
337	: 155 (75)	138 (78)	121 (85)	150 (91)	145 (82)	127 (69)
338	: 144 (70)	147 (75)	128 (69)	142 (76)	147 (85)	140 (86)
339	: 146 (66)	155 (63)	140 (75)	143 (68)	150 (66)	140 (74)
340	: 156 (74)	166 (75)	135 (83)	144 (62)	150 (66)	140 (84)
341	: 149 (77)	161 (72)	149 (81)	148 (90)	156 (83)	142 (84)
342	: 142 (69)	155 (77)	142 (82)	147 (87)	150 (59)	140 (90)
343	: 133 (75)	152 (80)	141 (68)	141 (87)	147 (68)	142 (82)
344	: 134 (75)	152 (72)	137 (71)	144 (92)	153 (79)	132 (71)
345	: 142 (72)	153 (78)	141 (73)	149 (88)	166 (84)	146 (83)
346	: 133 (76)	153 (79)	147 (77)	156 (87)	153 (74)	148 (87)
347	: 130 (75)	148 (72)	146 (69)	155 (84)	167 (85)	150 (85)
348	: 134 (71)	150 (74)	143 (65)	157 (84)	165 (80)	147 (88)
349	: 134 (71)	149 (78)	144 (71)	154 (86)	165 (80)	144 (91)
350	: 133 (78)	149 (72)	142 (72)	146 (90)	172 (85)	147 (90)
351	: 136 (77)	149 (73)	141 (73)	143 (90)	164 (86)	148 (78)
352	: 141 (66)	151 (73)	141 (77)	149 (89)	152 (72)	149 (77)
353	: 141 (67)	152 (78)	143 (82)	155 (81)	135 (65)	152 (82)
354	: 143 (72)	151 (78)	141 (88)	156 (83)	134 (60)	151 (81)
355	: 141 (66)	154 (84)	147 (89)	156 (79)	144 (67)	147 (82)
356	: 145 (65)	156 (80)	155 (80)	152 (83)	131 (80)	146 (85)
357	: 145 (62)	154 (83)	155 (75)	162 (83)	134 (79)	119 (61)
358	: 142 (74)	167 (81)	159 (75)	168 (78)	142 (66)	149 (85)
359	: 138 (75)	166 (74)	161 (75)	158 (74)	156 (71)	148 (83)
360	: 146 (77)	168 (81)	163 (79)	159 (85)	167 (80)	148 (91)
361	: 145 (71)	169 (78)	158 (87)	153 (87)	164 (84)	142 (77)
362	: 154 (70)	163 (81)	155 (86)	144 (90)	155 (87)	144 (79)
363	: 146 (77)	167 (82)	149 (66)	152 (82)	159 (66)	146 (76)
364	: 164 (75)	173 (66)	154 (62)	148 (71)	141 (56)	131 (55)
365	: 164 (60)	169 (75)	154 (81)	147 (73)	165 (81)	116 (57)
366	: 165 (74)	165 (81)	154 (75)	148 (80)	163 (88)	121 (63)
367	: 158 (58)	167 (78)	153 (72)	149 (89)	165 (85)	124 (80)
368	: 153 (67)	158 (75)	149 (64)	153 (81)	142 (75)	115 (66)
369	: 163 (77)	168 (70)	152 (62)	159 (79)	139 (58)	128 (62)
370	: 162 (73)	167 (74)	148 (70)	124 (66)	145 (60)	127 (66)
371	: 160 (72)	165 (75)	150 (71)	163 (68)	138 (60)	116 (104)
372	: 163 (68)	167 (82)	139 (77)	156 (82)	144 (73)	144 (73)
373	: 163 (68)	155 (72)	144 (73)	161 (83)	129 (78)	137 (80)
374	: 156 (74)	160 (74)	143 (77)	162 (83)	145 (69)	115 (70)
375	: 153 (64)	163 (73)	142 (69)	159 (78)	148 (68)	118 (59)
376	: 143 (70)	158 (80)	142 (75)	159 (75)	144 (65)	116 (52)
377	: 141 (74)	156 (87)	142 (81)	158 (74)	132 (75)	124 (67)
378	: 144 (79)	159 (76)	144 (80)	156 (79)	170 (82)	153 (80)
379	: 146 (72)	159 (79)	142 (74)	151 (78)	140 (66)	124 (67)
380	: 149 (74)	155 (83)	145 (73)	154 (82)	166 (85)	129 (88)
381	: 147 (76)	154 (79)	139 (84)	150 (81)	153 (76)	132 (76)
382	: 149 (70)	156 (81)	139 (82)	147 (83)	139 (73)	131 (70)
383	: 145 (69)	155 (82)	148 (81)	147 (90)	139 (75)	114 (77)
384	: 149 (68)	156 (82)	152 (81)	155 (84)	161 (77)	116 (67)
385	: 141 (72)	154 (71)	150 (78)	158 (70)	140 (70)	119 (80)
386	: 138 (68)	156 (84)	151 (79)	145 (81)	135 (68)	119 (70)
387	: 141 (71)	156 (80)	147 (70)	150 (76)	136 (71)	121 (80)
388	: 138 (78)	155 (83)	145 (72)	157 (80)	163 (84)	114 (95)
389	: 139 (81)	157 (86)	145 (81)	148 (79)	166 (80)	141 (72)
390	: 141 (80)	153 (86)	142 (83)	149 (73)	165 (80)	146 (75)
391	: 140 (70)	153 (75)	142 (80)	147 (76)	164 (77)	143 (75)
392	: 140 (81)	155 (72)	144 (69)	146 (83)	155 (71)	134 (75)
393	: 149 (77)	154 (78)	143 (73)	139 (88)	156 (75)	135 (79)
394	: 148 (70)	151 (75)	146 (74)	151 (86)	142 (72)	141 (81)
395	: 155 (78)	155 (83)	142 (75)	148 (86)	154 (75)	146 (74)
396	: 150 (77)	159 (83)	150 (80)	156 (75)	162 (79)	153 (72)
397	: 142 (73)	154 (82)	150 (77)	151 (78)	132 (68)	118 (90)
398	: 142 (64)	158 (75)	150 (75)	141 (80)	136 (76)	121 (87)
399	: 131 (71)	160 (72)	150 (69)	142 (85)	136 (62)	132 (58)
400	: 154 (70)	156 (66)	145 (76)	133 (43)	145 (53)	134 (66)
401	: 165 (70)	153 (66)	144 (86)	157 (66)	140 (62)	125 (51)
402	: 154 (60)	153 (62)	147 (83)	140 (79)	138 (65)	124 (54)
403	: 142 (77)	156 (70)	139 (90)	156 (70)	135 (71)	121 (58)
404	: 141 (74)	154 (85)	139 (90)	141 (92)	133 (65)	120 (55)
405	: 139 (68)	151 (69)	137 (83)	152 (76)	133 (62)	126 (54)
406	: 132 (66)	147 (75)	134 (80)	147 (75)	139 (58)	121 (57)

Table 5.11(e)

409	144 (79)	148 (82)	138 (77)	146 (75)	130 (67)	118 (82)
410	140 (69)	148 (77)	133 (80)	145 (81)	154 (70)	114 (88)
411	144 (65)	145 (72)	134 (77)	146 (73)	138 (55)	112 (90)
412	130 (74)	148 (82)	141 (69)	145 (67)	143 (53)	115 (72)
413	136 (66)	151 (83)	141 (78)	152 (75)	149 (66)	142 (77)
414	142 (68)	158 (82)	141 (70)	150 (80)	171 (79)	135 (52)
415	141 (69)	156 (86)	146 (81)	157 (79)	135 (54)	133 (61)
416	144 (76)	148 (78)	144 (76)	167 (68)	137 (63)	128 (59)
417	148 (80)	154 (76)	134 (82)	158 (75)	136 (56)	126 (75)
418	153 (73)	150 (76)	137 (73)	156 (82)	148 (76)	116 (58)
419	152 (71)	148 (62)	136 (72)	155 (81)	131 (72)	122 (67)
420	146 (81)	154 (78)	141 (73)	162 (78)	127 (64)	122 (55)
421	147 (84)	152 (77)	147 (74)	158 (79)	137 (65)	123 (54)
422	148 (79)	151 (76)	142 (81)	159 (75)	138 (59)	123 (54)
423	145 (82)	151 (85)	137 (81)	135 (85)	136 (53)	122 (53)
424	143 (80)	152 (83)	143 (76)	163 (76)	133 (62)	137 (50)
425	143 (76)	152 (68)	147 (68)	130 (91)	136 (59)	138 (58)
426	150 (70)	157 (78)	144 (73)	125 (70)	134 (58)	136 (60)
427	141 (71)	153 (76)	145 (72)	121 (58)	133 (64)	140 (53)
428	138 (68)	152 (74)	141 (81)	120 (89)	133 (62)	133 (73)
429	142 (64)	160 (84)	143 (80)	164 (78)	134 (49)	137 (52)
430	140 (68)	170 (84)	142 (81)	161 (78)	130 (67)	133 (62)
431	138 (70)	167 (80)	145 (75)	134 (68)	131 (72)	133 (52)
432	136 (72)	159 (79)	147 (73)	140 (84)	132 (68)	134 (50)
433	155 (62)	158 (77)	142 (73)	125 (69)	131 (65)	135 (51)
434	154 (65)	160 (71)	145 (74)	122 (52)	135 (66)	135 (52)
435	149 (74)	163 (79)	138 (73)	124 (83)	137 (70)	138 (57)
436	168 (69)	159 (72)	138 (81)	125 (87)	138 (58)	138 (55)
437	185 (80)	164 (78)	144 (74)	142 (95)	135 (68)	138 (60)
438	183 (63)	157 (77)	142 (82)	158 (85)	155 (56)	136 (51)
439	182 (54)	158 (71)	142 (82)	160 (85)	169 (80)	139 (61)
440	171 (53)	152 (81)	140 (77)	153 (81)	167 (79)	135 (55)
441	149 (60)	162 (74)	147 (79)	153 (80)	167 (68)	129 (54)
442	160 (54)	156 (75)	145 (77)	154 (74)	136 (51)	137 (58)
443	149 (55)	146 (81)	145 (72)	149 (67)	132 (74)	136 (98)
444	147 (54)	155 (79)	146 (75)	150 (77)	143 (68)	133 (85)
445	134 (69)	162 (79)	145 (78)	149 (86)	135 (78)	135 (61)
446	133 (72)	159 (72)	145 (68)	156 (86)	126 (73)	138 (49)
447	128 (72)	146 (87)	148 (64)	157 (74)	138 (71)	142 (64)

Table 5.11(f)

Bloor viaduct (WESTBOUND): line 7 (north curb) to line 12
BRIDGE deck CONDition SUMMARY

[ASPhalt AVERaged THICKness]

	line number 1	2	3	4	5	6
mm	142	154	145	155	152	137
in	5.59	6.06	5.71	6.10	5.98	5.39
ave dielect	7.23	6.01	6.72	6.56	6.35	7.75

[C/O REINFORCEment AVEraged THICKness]

	line number 1	2	3	4	5	6
mm	72	73	77	79	73	73
in	2.83	2.87	3.03	3.11	2.87	2.87

[LINE DISTRIBUTion (%)]

	line number 1	2	3	4	5	6
GOOD	84.66	79.92	85.39	86.75	87.85	84.76
DEBONDed	.22	.32	.27	.09	.09	.22
SCALEd	.00	.05	.04	.04	.00	.00
DELAMINATed	15.07	19.72	14.29	9.65	12.02	14.97
BAD data	.04	.00	.00	3.46	.05	.04
TOTAL	100.00	100.00	100.00	100.00	100.00	100.00

metal PLATE AMPlitude is: 9.768392 v

OVERALL AVEraged DIELECTric constant of asphalt is 6.8040

OVERALL AVEraged ASPhalt THICKness is 147 mm, [5.79 in]

OVERALL AVEraged C/O REINFORCEment THICKness is 74 mm, [2.91 in]

[OVERALL bridge deck CONDITION]

GOOD	84.89 %
DEBONDED	.20 %
SCALed	.02 %
Delaminated	14.29 %
BAD data	.60 %
Total	100.00 %

Table 5.12: Summarized report of the westbound deck.

Sample waveforms from location 50.2 to 56 m are plotted for line 8 (Fig. 5.40), 9 (Fig. 5.41) and 10 (Fig. 5.42). Metal joint reflections can be detected from the waveforms at 50 and 55 m. (For eastbound deck, this is the 390 and 395 m location). From inspection of these waveforms, we note that the depth of the metal joint is quite constant across the westbound deck. The metal joint reflection occurs at about 7.75 ms and the surface echo peak is at about 5.4 ms. If we assume that the asphalt content is uniform on both decks, then the dielectric constant of asphalt (which is 6.92 from section 5.3.1) calculated from the core sample (line 3 at 180 m) given on the eastbound deck can be used to find the depth of the metal joint. The calculated depth is 134 mm. Again we know that there is 20% error in the measurement between the given core sample from Bloor Via Duct and the computer finding, the depth measurement is adjusted to 160 mm. Since on the westbound deck we do not obtain any core samples, 160 mm is used as the input to the software for core sample asphalt thickness.

The averaged depth of asphalt and concrete cover, over 1 m interval, for the westbound deck are provided in Table 5.11. A summary report is given in Table 5.12. It is reported that the overall asphalt thickness is 147 mm (this is about 117 mm with the 20% error removed as described above) and the concrete cover is on the average 74 mm thick. The deck is 84.89% good and 14.29% delaminated. Like the eastbound deck, the small percentage of debonding and scaling can be treated as false alarm.

The averaged waveforms given in Figs. 5.40 to 5.42 can be employed in evaluating the performance of the computer analysis. In Table 5.13, the averaged thickness of both asphalt and concrete cover for the section 50.2 to 55 m of line 8 to line 10 are measured. The results are obtained by averaging the corresponding measurements from Table 5.11. It is based on the averaged measurement that the locations of the asphalt-concrete (peak C) and rebar (peak D) boundaries are estimated.

Table 5.13/ Estimation of boundary locations using computer results. The values of dielectric constant of asphalt are from Table 5.12.

Figs	dielectric	asphalt	Peak C	concrete	peak D
5.40	6.01	166 mm	7.94 ms	67 mm	9.19 ms
5.41	6.72	132	7.57	73	8.94
5.42	6.56	155	7.97	81	9.5

The computer results are found to have strong agreement with the averaged waveforms.

In Fig. 5.43, the map shows delamination areas. Once again we see that there are a considerable number of single-hit indications. By eliminating these indications, the reliability of fault detection can be increased. The areas which are claimed to have debonding and scaling are given in Figs. 5.44 and 5.45. We note that these locations are near the metal joint areas which can give erroneous indications.

The statistical and histogram data for the westbound deck are attached in Appendix D.

5.3.6/ Summary

It is highly desirable to obtain a few core samples at a deck in order to ensure that the radar peaks are correctly identified. Measurement from the core sample can provide the software with a proper search window in locating the asphalt- concrete interface peak. Without this information, it is possible that reflections from radar waveform can be mis-interpreted. This error becomes acute when the analysis involves a multi-layer asphalt structure.

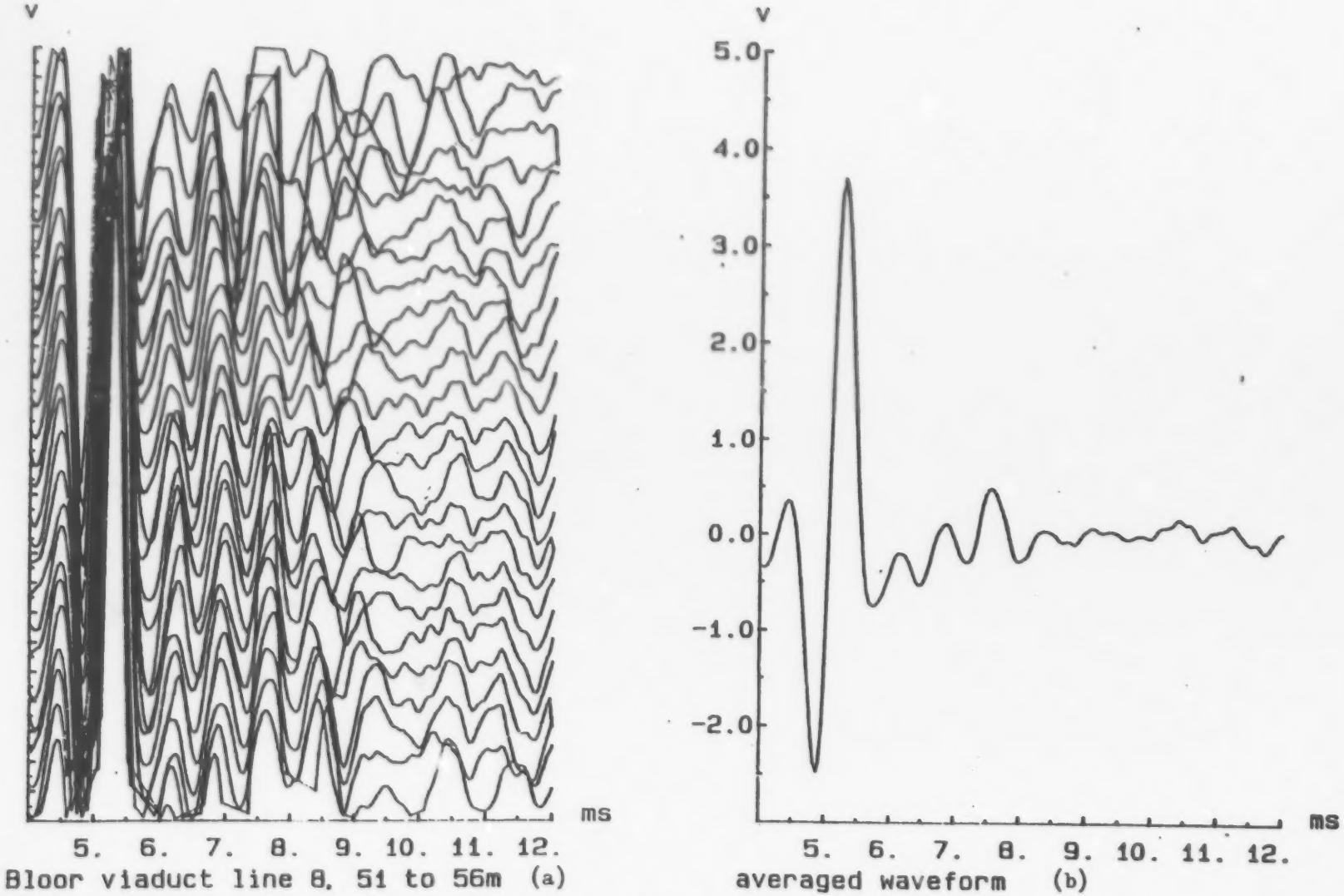

Fig. 5.40: (a) waveforms from line 8 between 51 to 56m and (b) the averaged waveform.

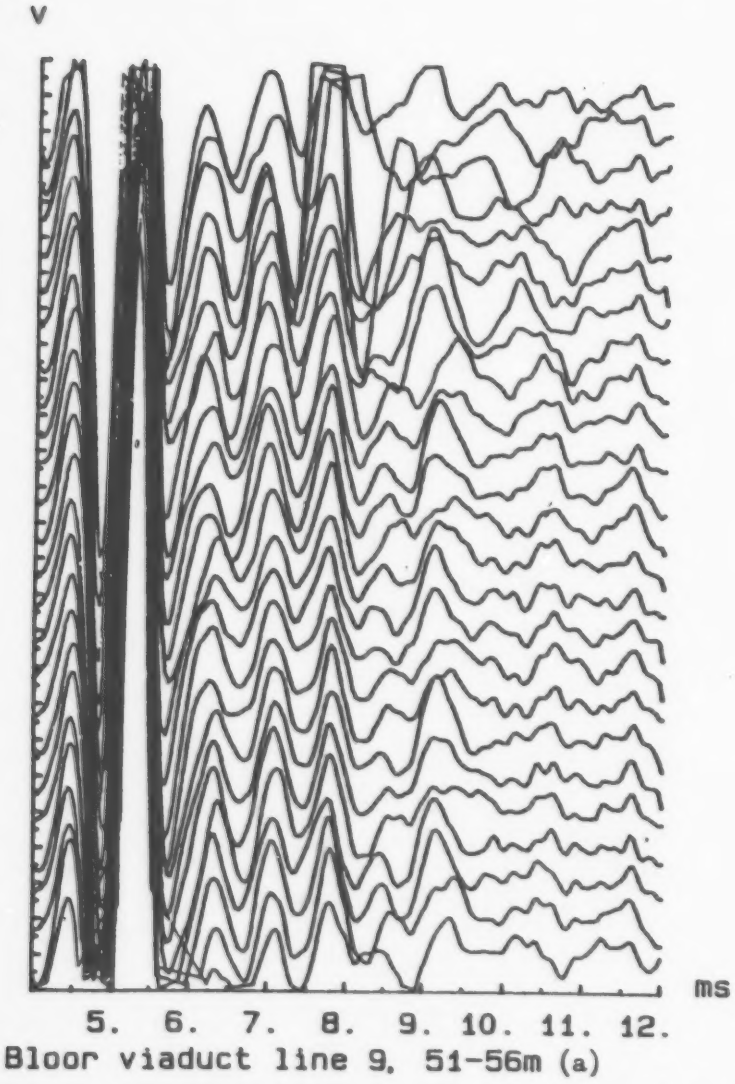

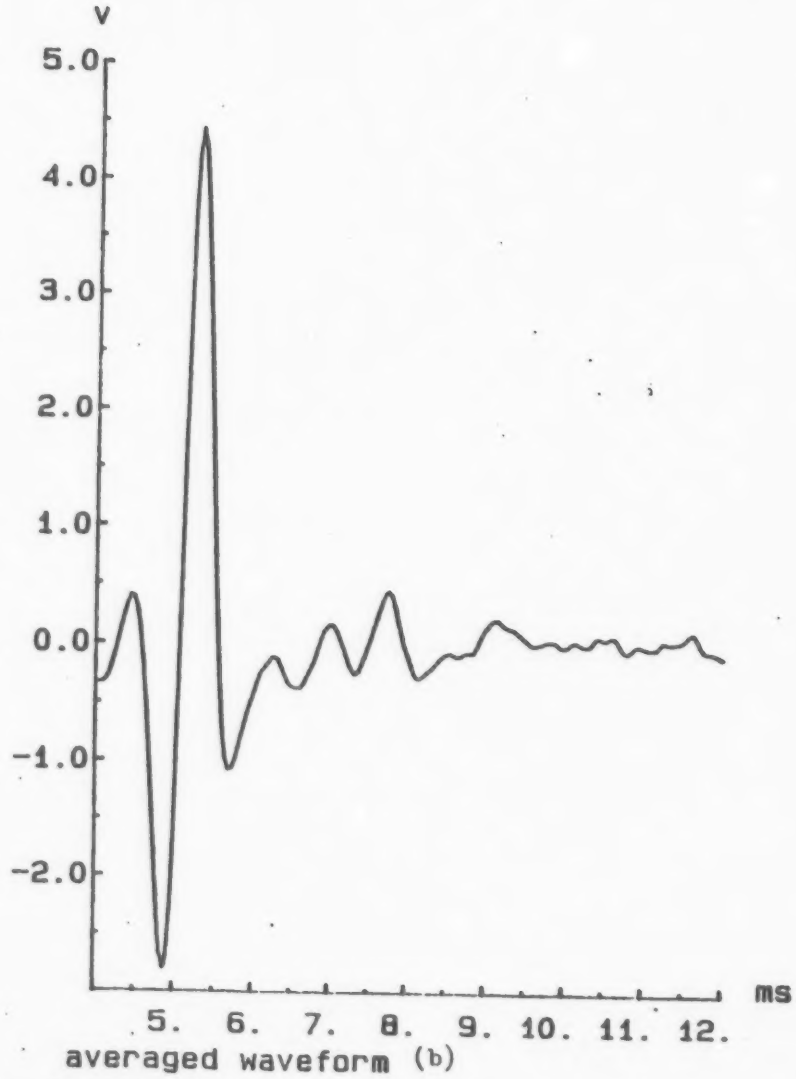

Fig. 5.41: (a) waveforms from line 9 between 51 to 56m and (b) the averaged waveform.

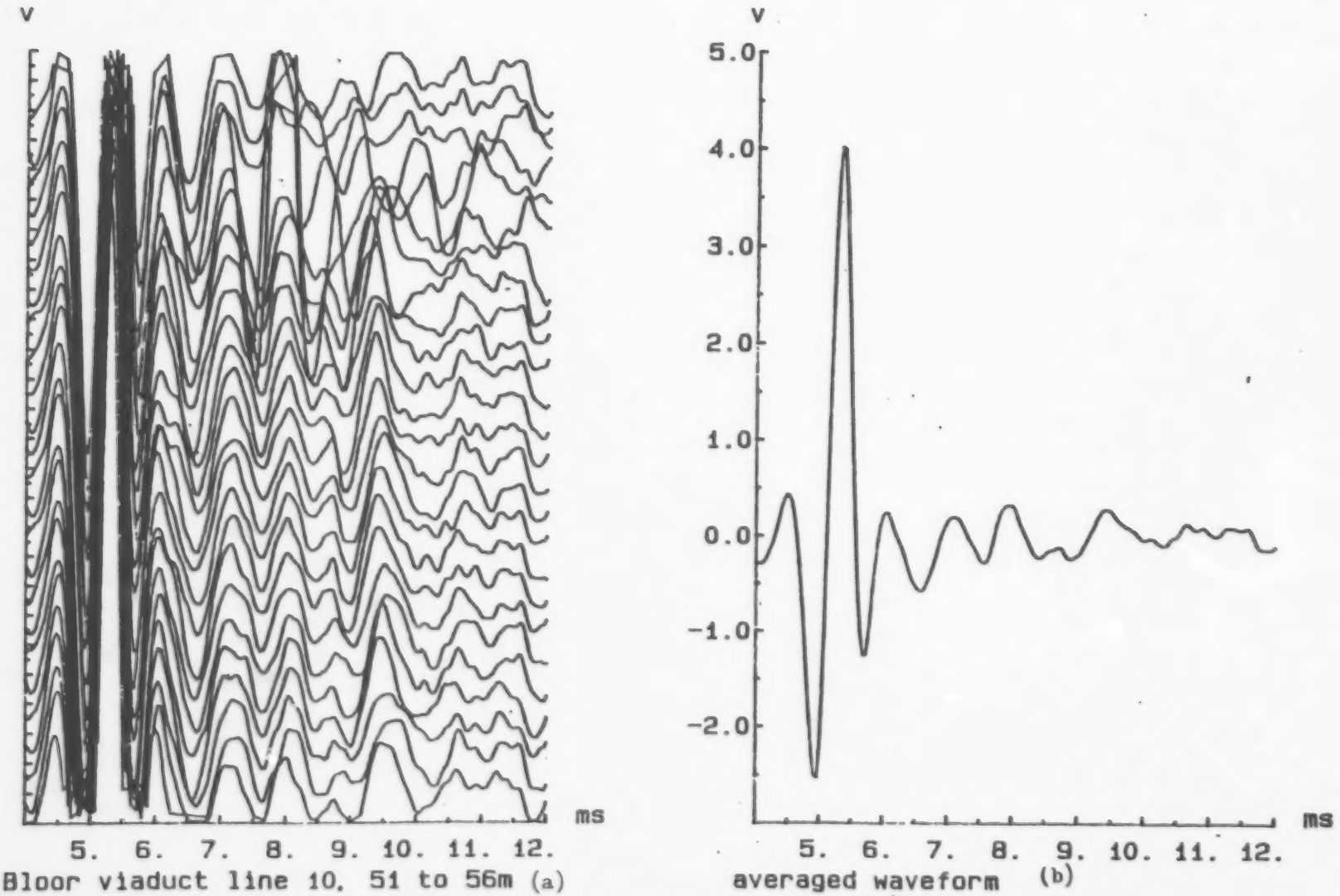

Fig. 5.42: (a) waveforms from line 10 between 51 to 56m and (b) the averaged waveform.

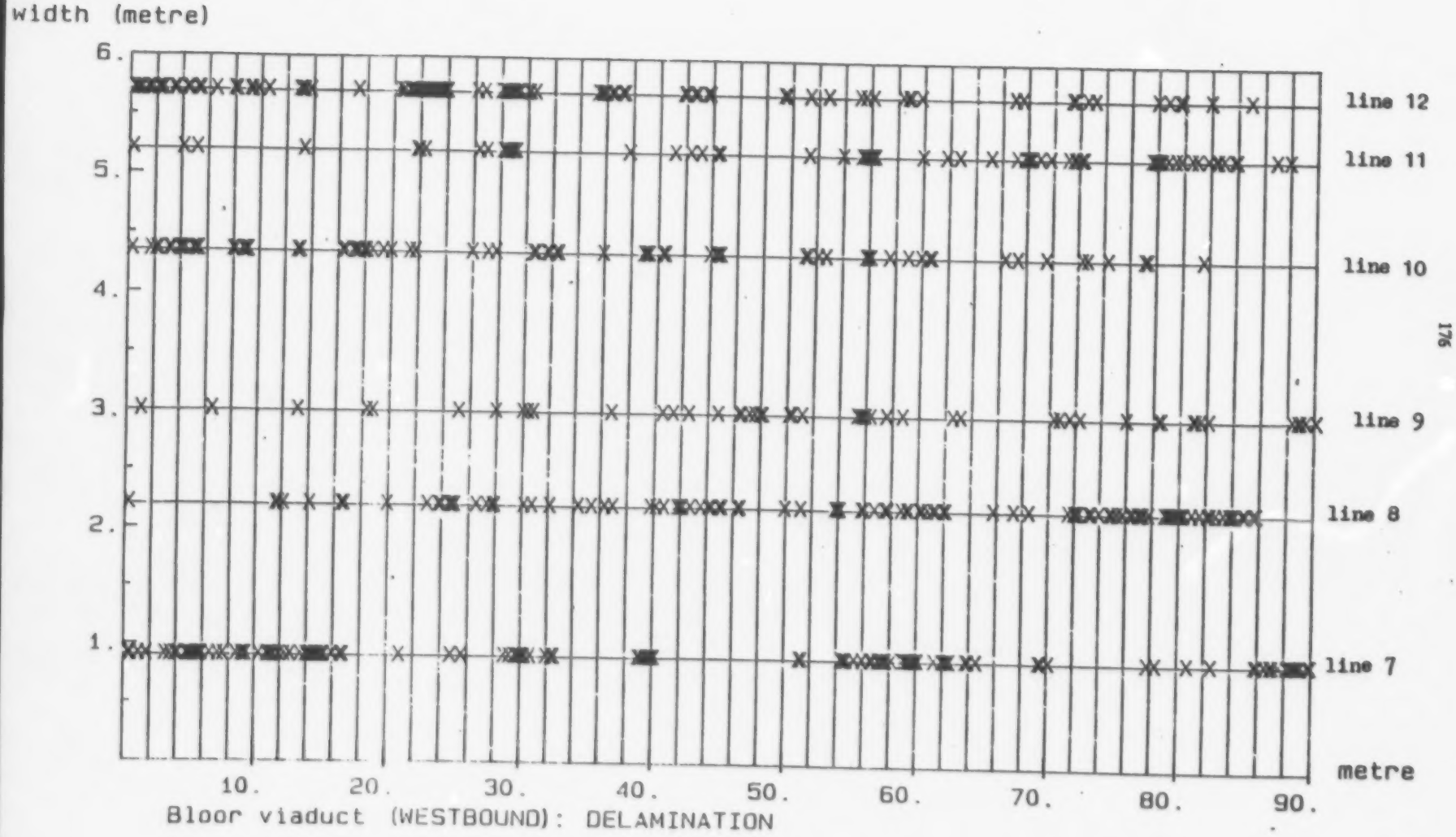

Fig. 5.43(a): areas of delamination between 0 to 90m on westbound deck,

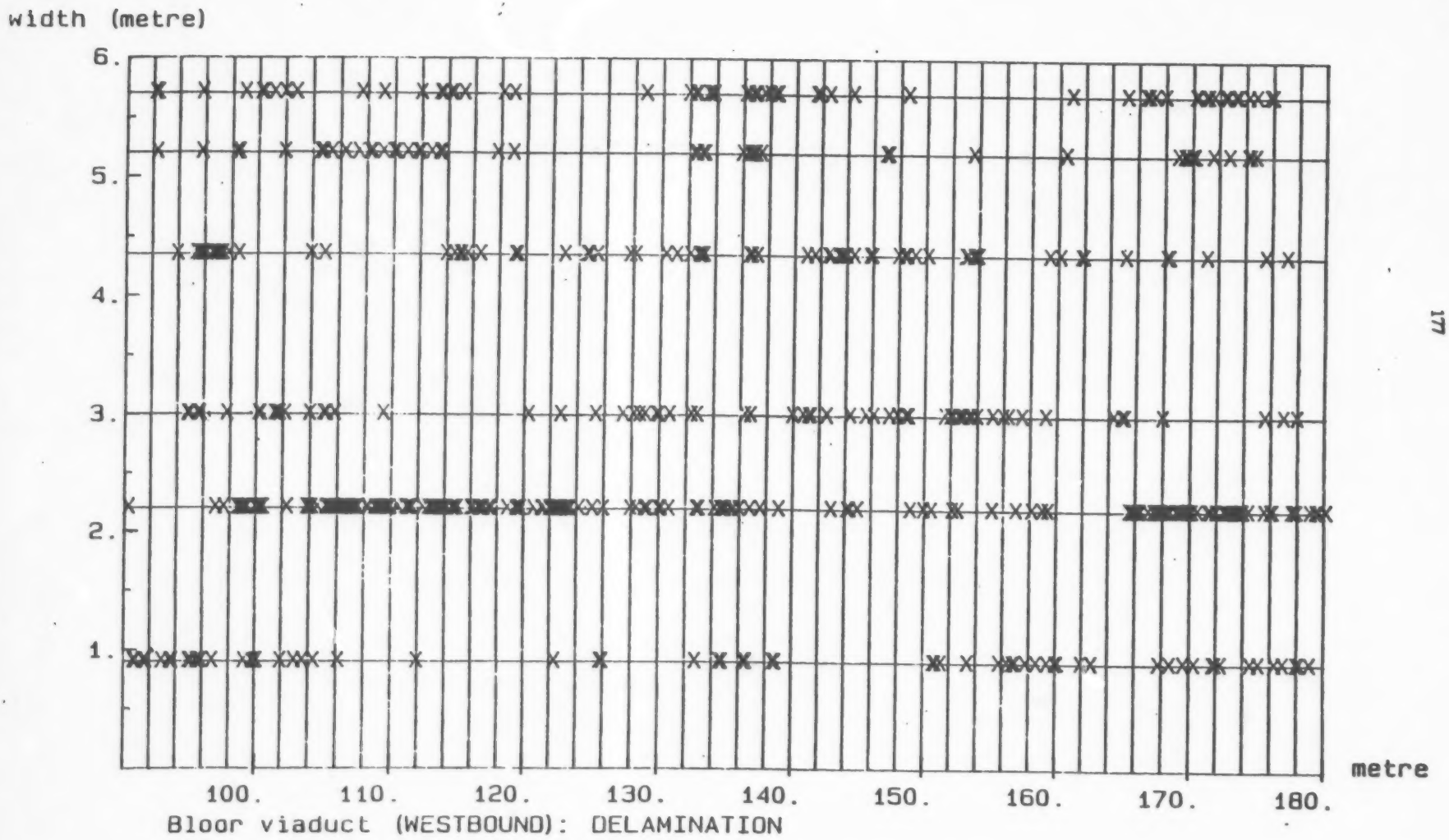

Fig. 5.43(b): areas of delamination between 90 to 180m.

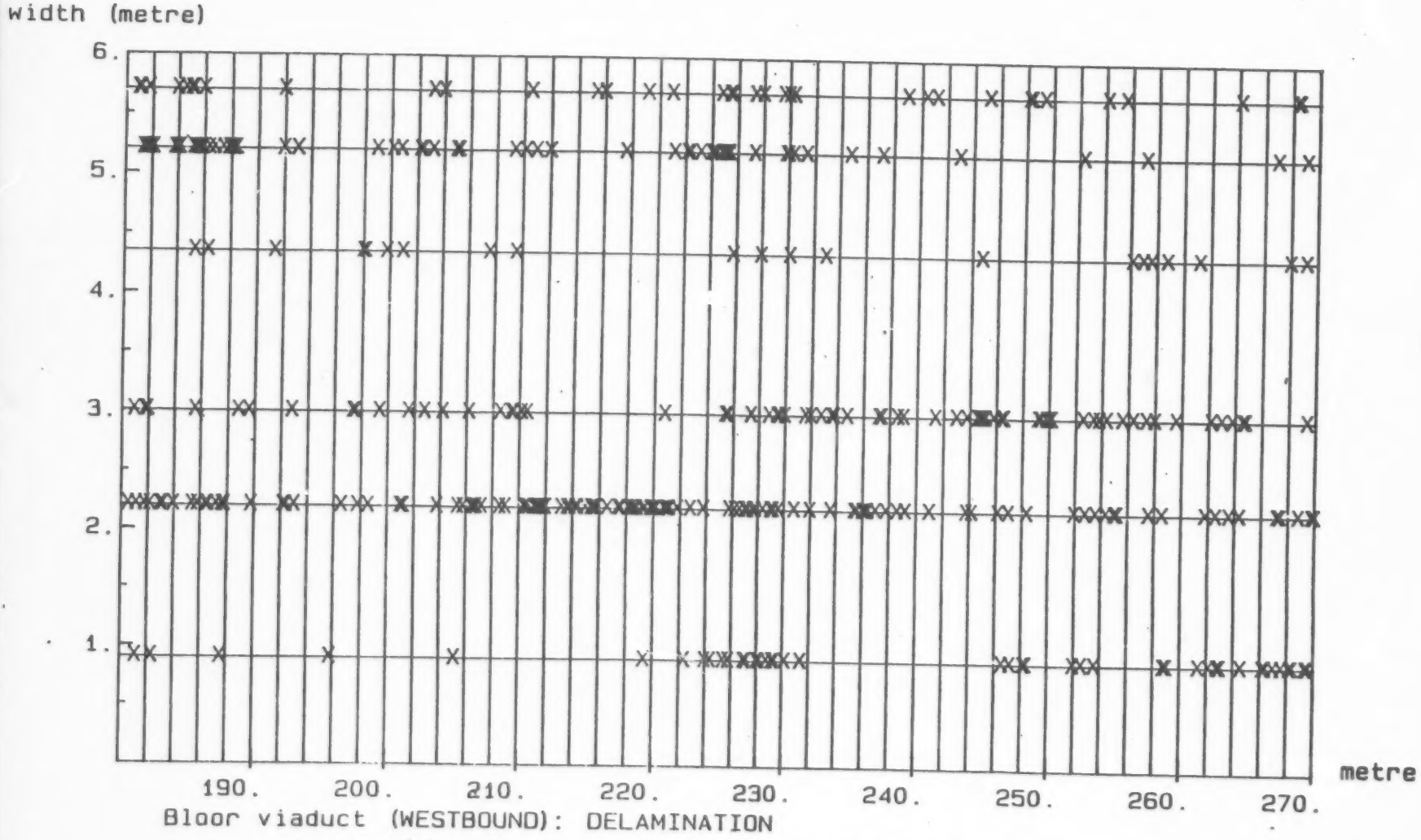

Fig. 5.43(c): areas of delamination between 180 to 270m.

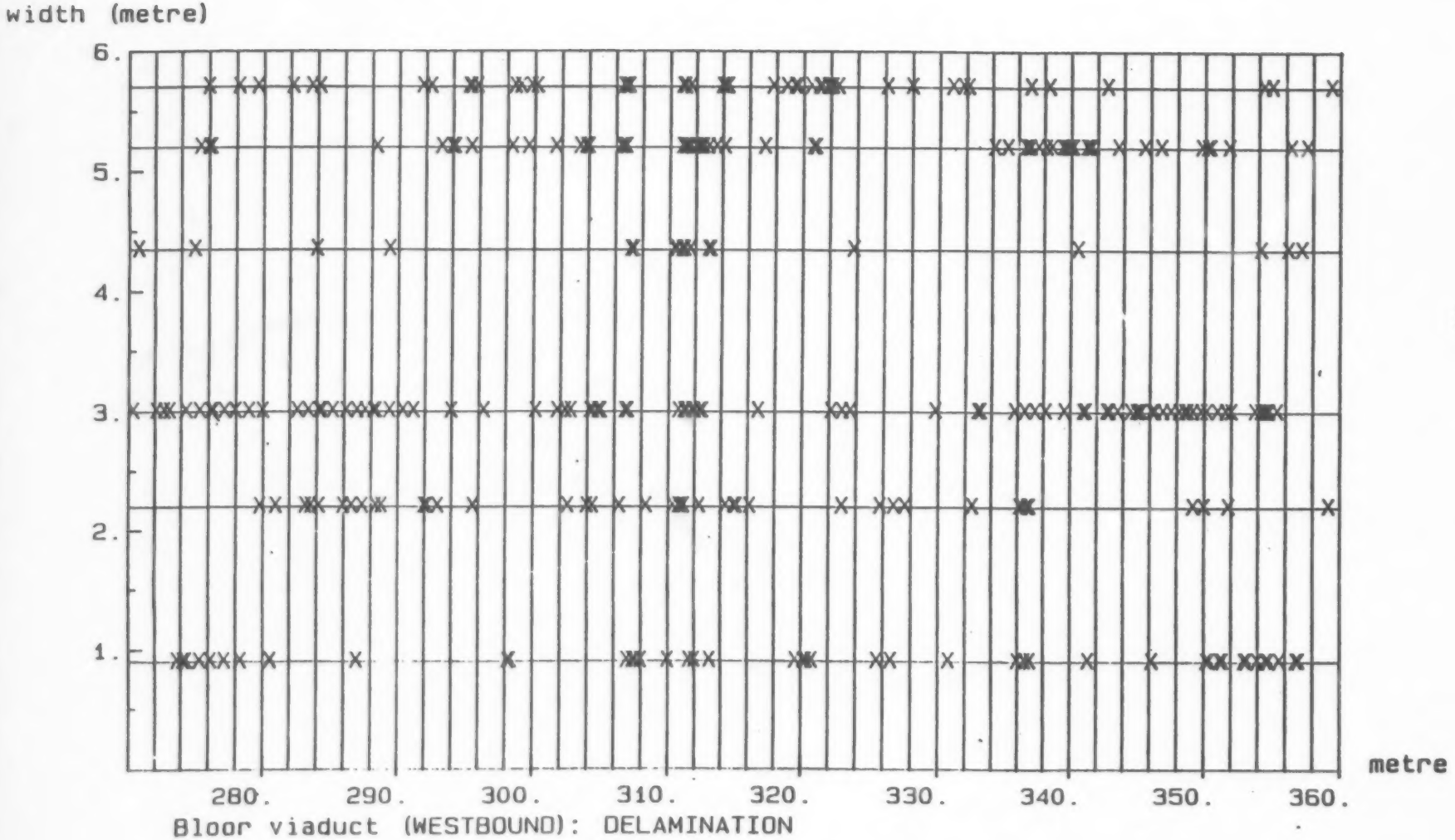

Fig. 5.13(d): areas of delamination between 270 to 360m.

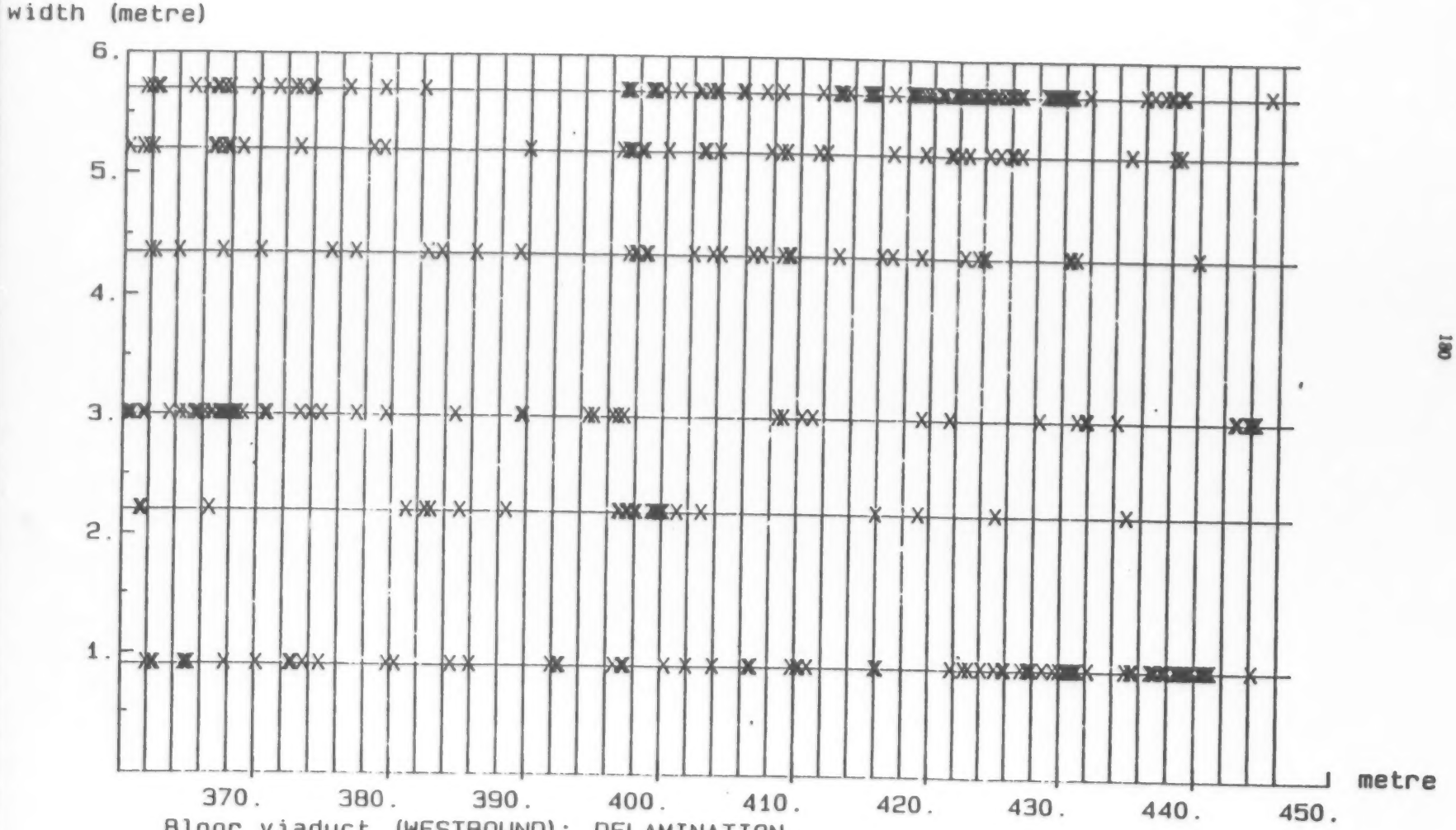

Bloor viaduct (WESTBOUND): DELAMINATION

Fig. 5.43(e): areas of delamination between 360 to 447m.

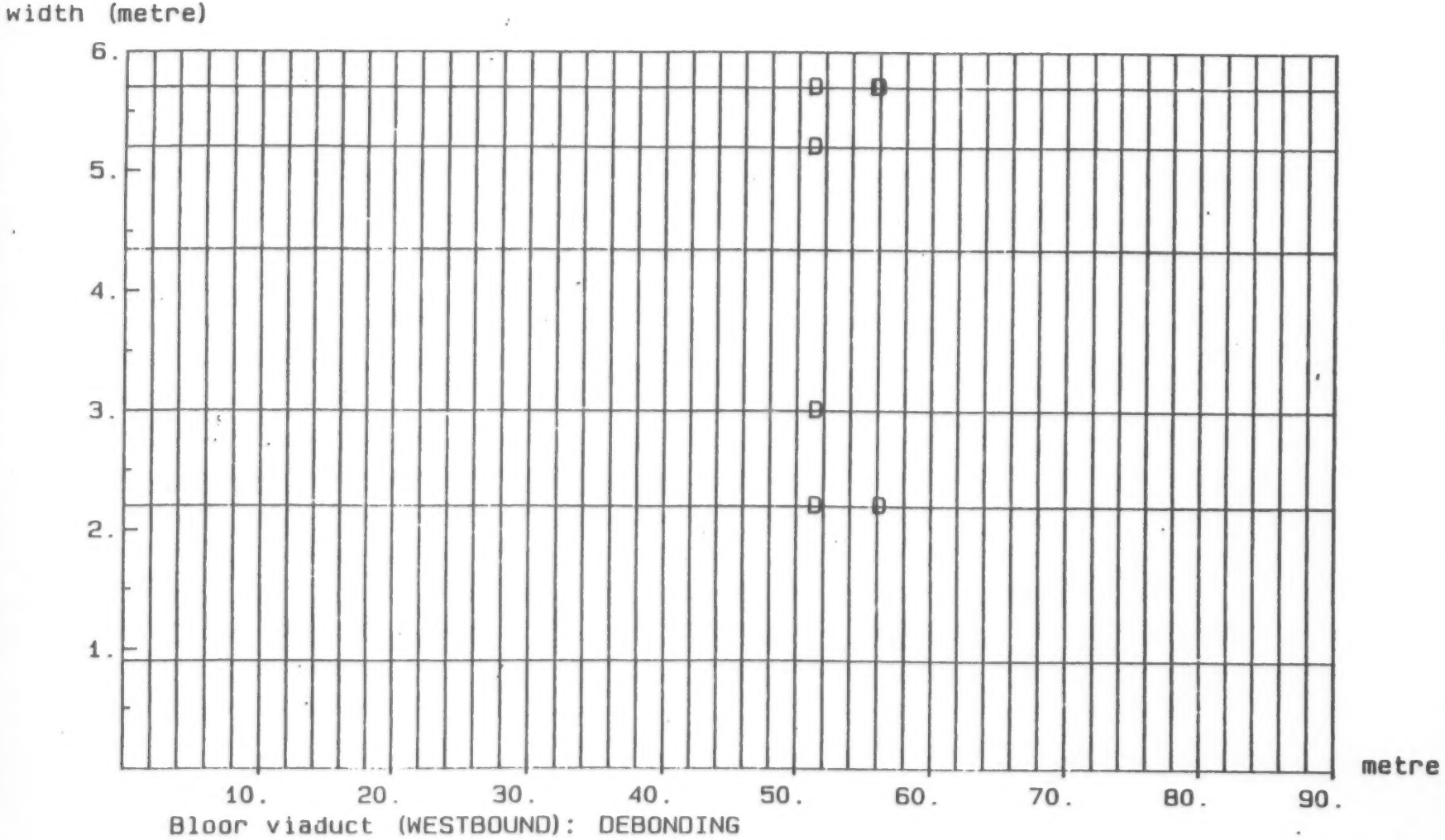

Fig. 5.44(a): areas of debonding between 0 to 90m.

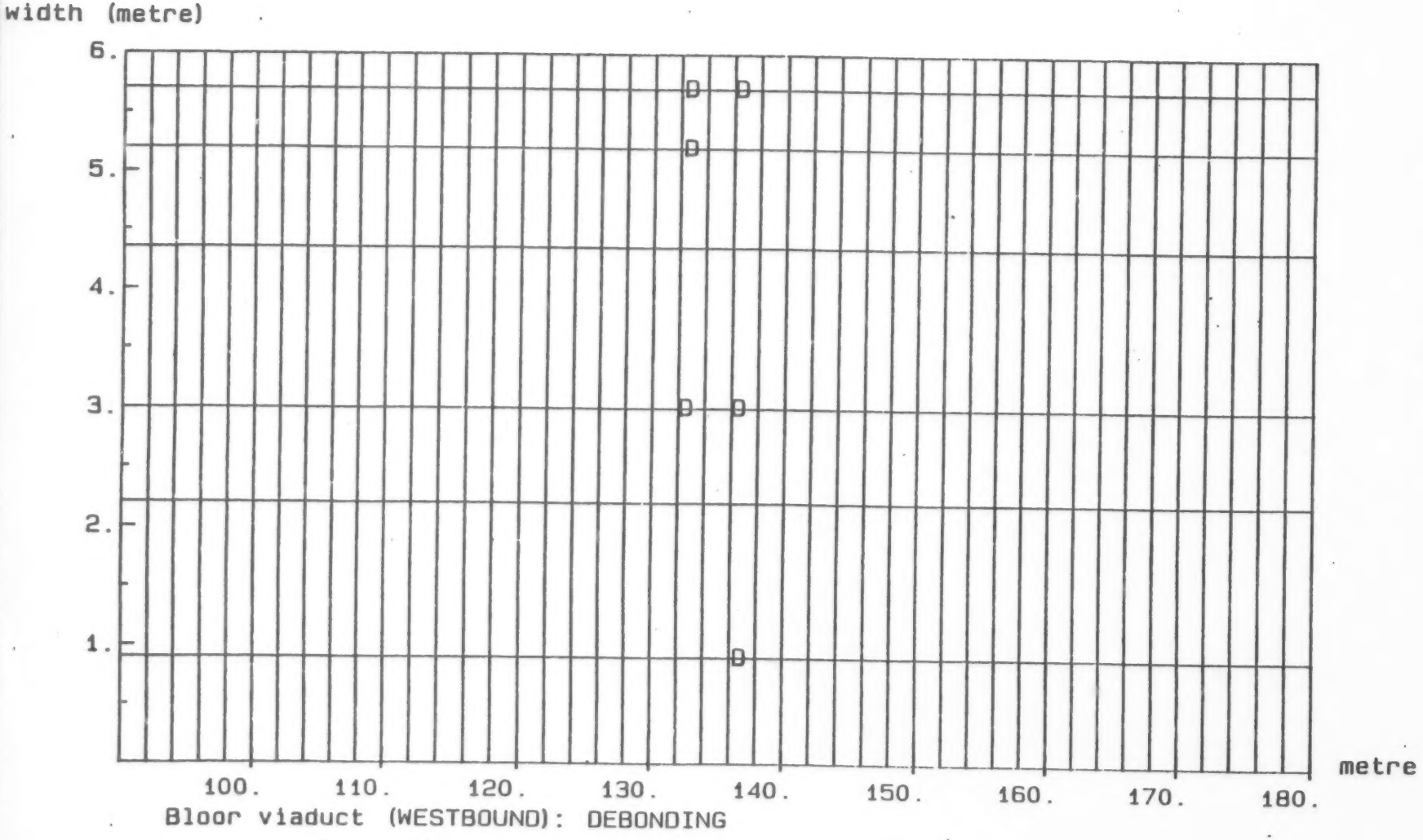

Fig. 5.44(b): areas of debonding between 90 to 180m.

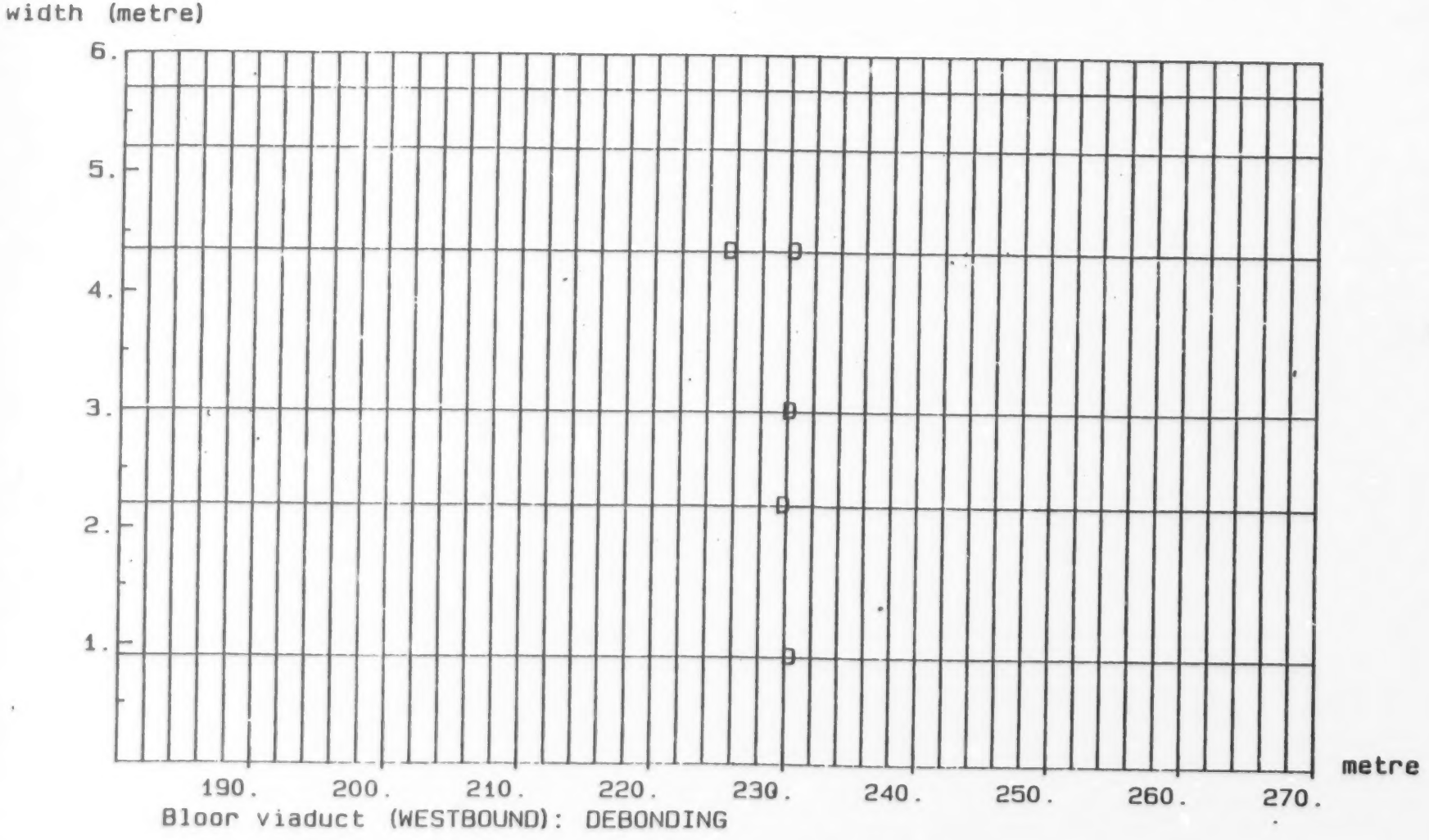

Fig. 5.44(c): areas of debonding between 180 to 270m.

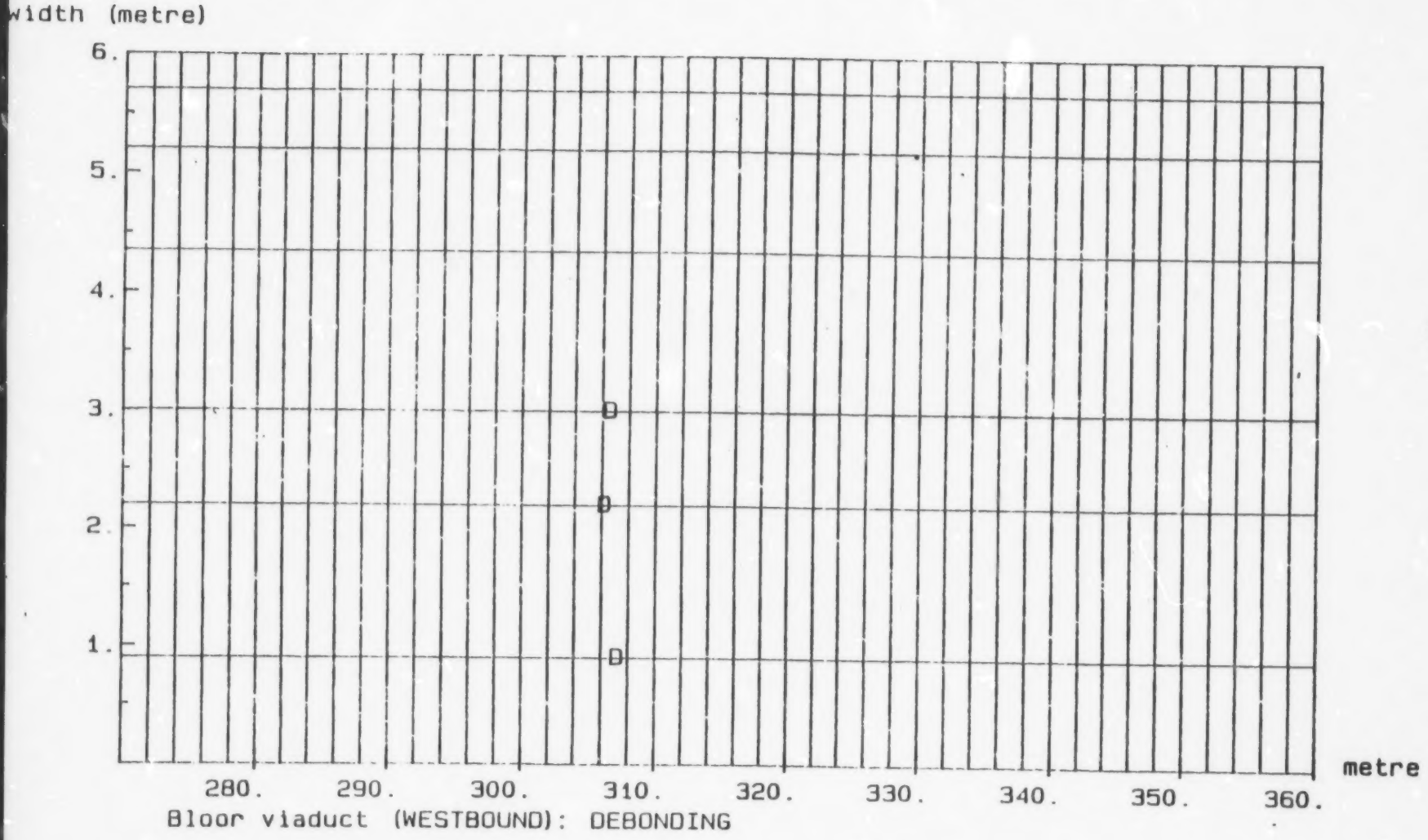

Fig. 5.44(d): areas of debonding between 270 to 360m.

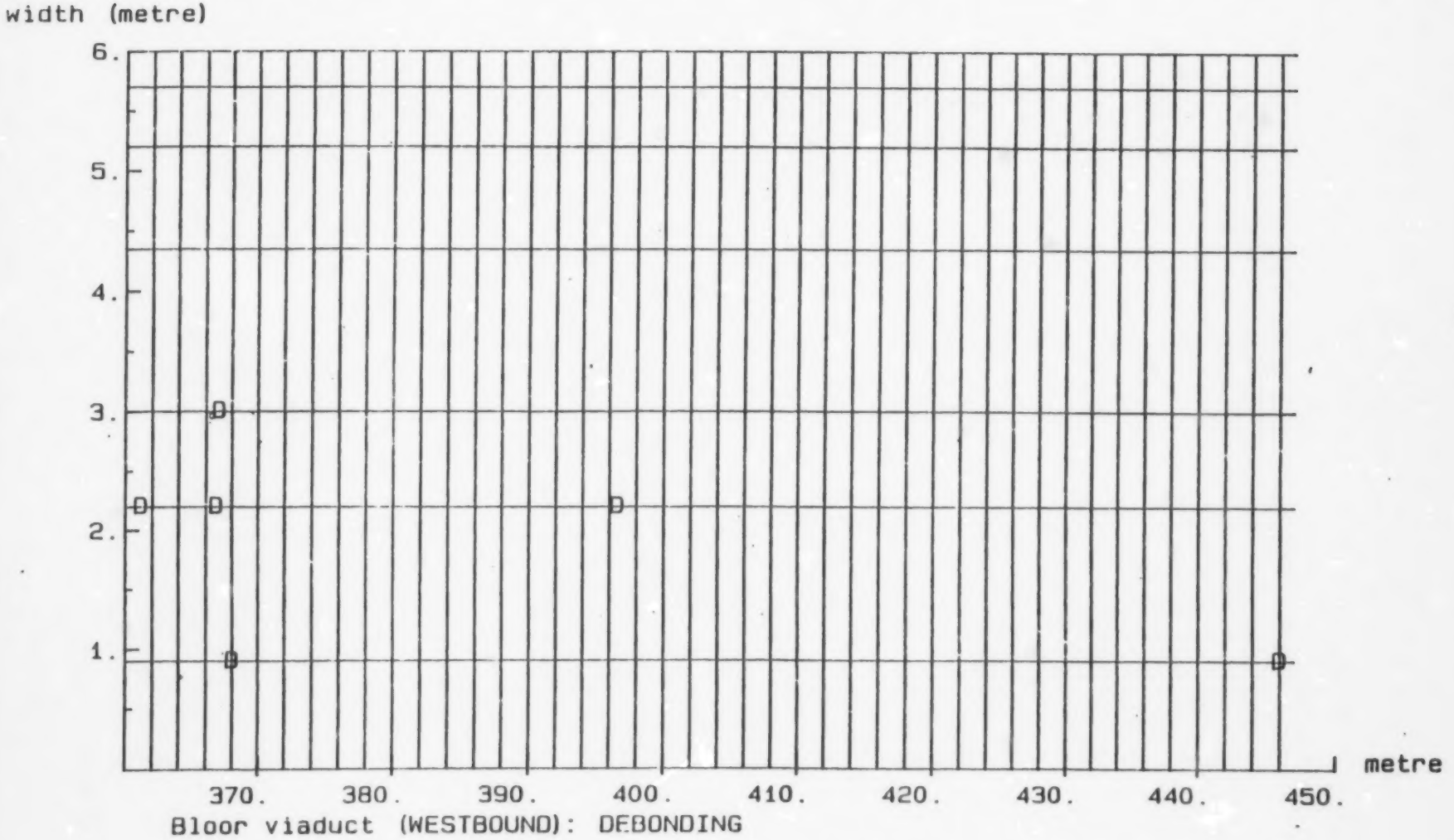

Fig. 5.44(e): areas of debonding between 360 to 447m.

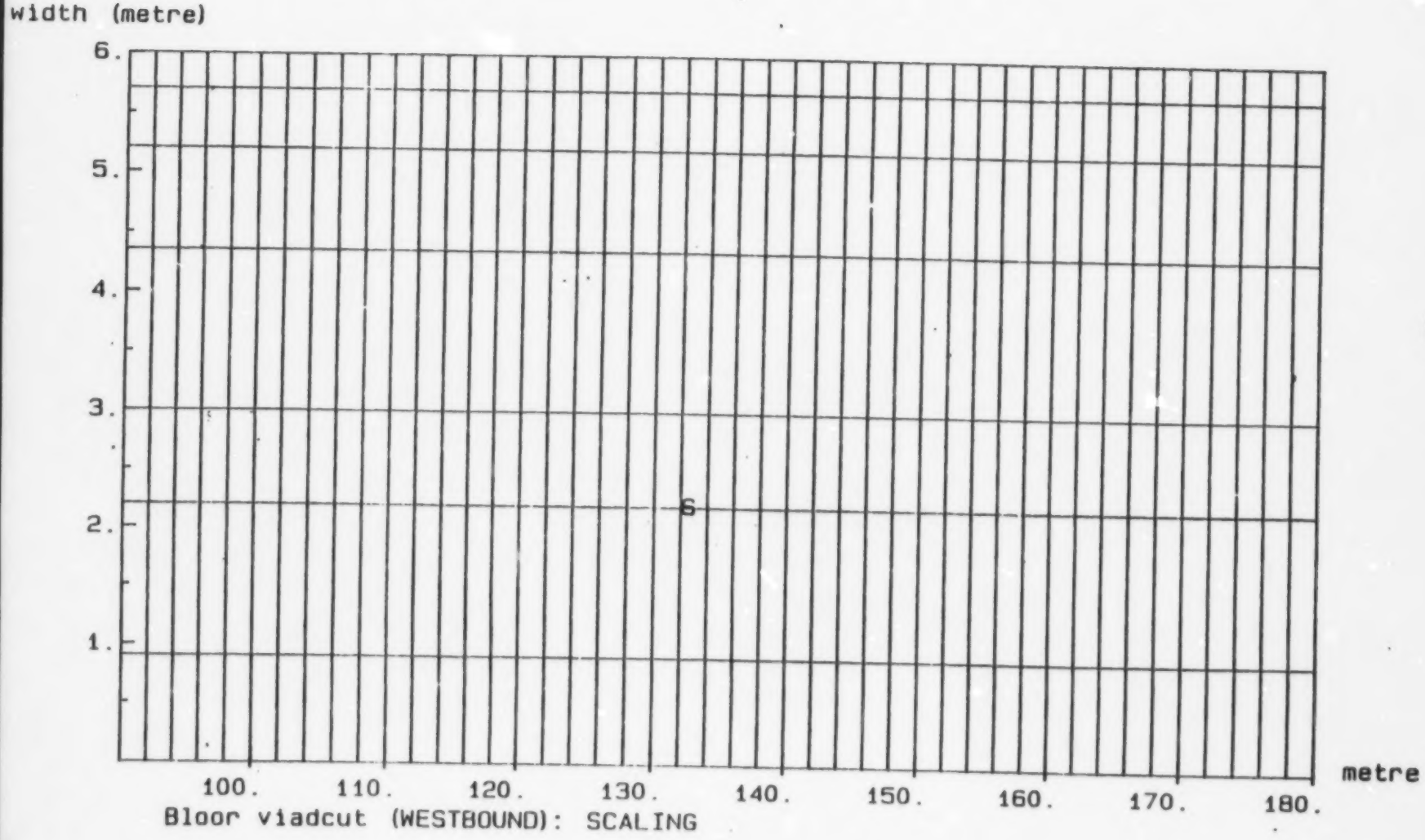

Fig. 5.45(a): areas of scaling between 90 to 180m.

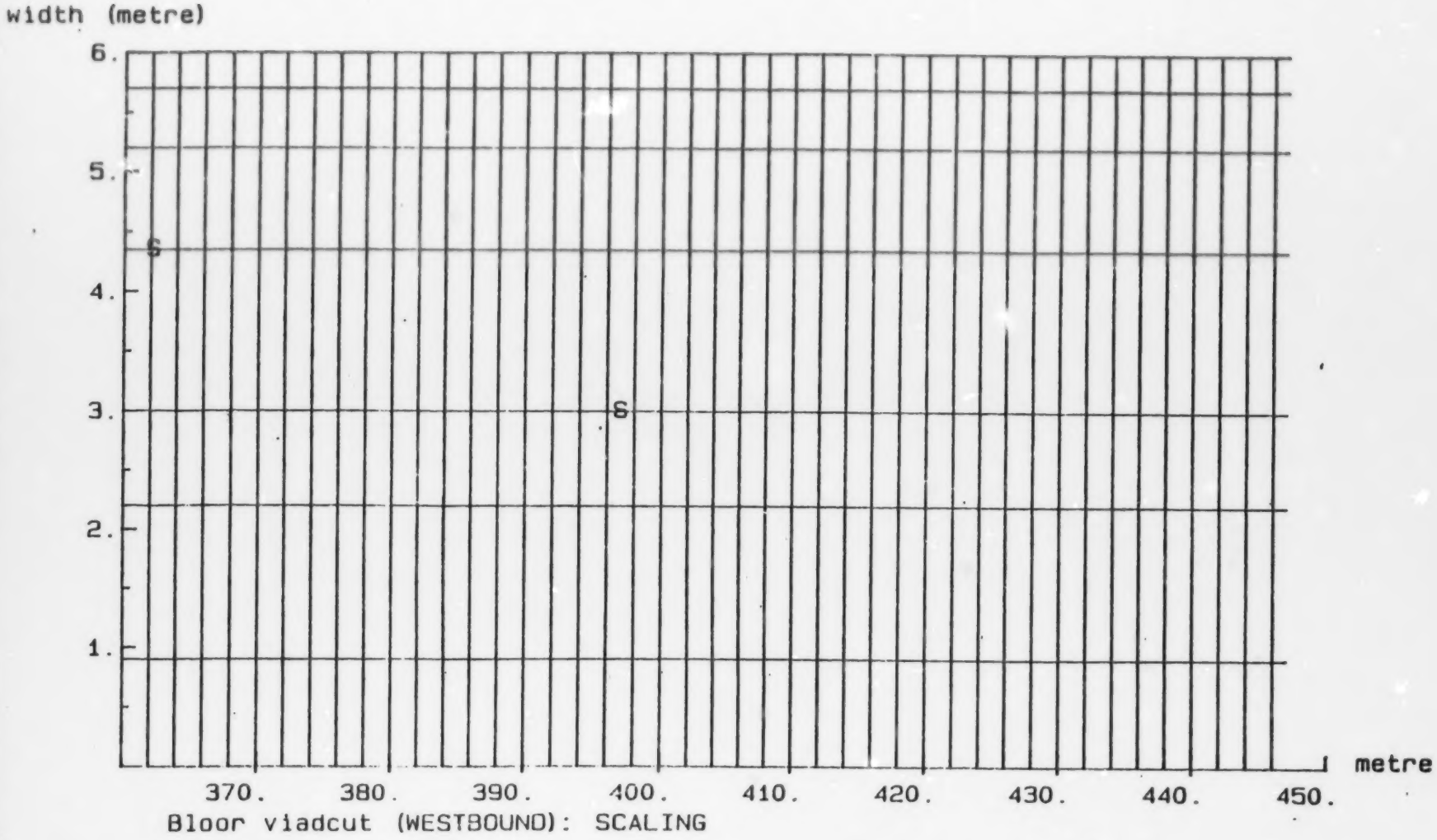

Fig. 5.45(b): areas of scaling between 360 to 447m.

6/ Conclusions and Recommendations for Further Research

6.1/ Conclusions

It is concluded that:

1) Signature of the antenna internal reflection waveform can be measured but these reflection are affected by the presence of the vehicle. Thus, any calibration can only be performed when the antenna is mounted.

2) The internal antenna reflections can be canceled to at least a first order approximation from the total reflected signal by means of computer subtraction. The resulting waveforms are seen to be much more closely related to the expected reflected waveforms.

3) System software has been recalibrated in order to take into account the canceled waveforms.

4) The problem of canceling surface reflections using subtraction of the transmitted waveform has also been solved. As a result, the separate reflections from each layer of asphalt can now be detected which is important for multi-layer asphalt decks..

5) The correlation technique does not provide feasible solutions in determining peak locations from signal waveforms.

6) An identification of the sources of error and an analysis of the precision with which the asphalt thickness can be determined has been provided.

7) In order to ensure the accuracy of the dielectric constant values, measurements on test slabs of asphalt of uniform mixture and the waterproofing membrane material have been made. Also the dielectric constant of concrete has been determined.

8) Software has been modified to provide measurements of the cover over reinforcement in the same tabular format used to present the thickness of asphalt.

9) Cluster analysis package has been added to the software. The package provides a statistical evaluation of the location of the peaks of the reflected signal.

10) The new software package has been tested and checked with real data taken from Ninth Line, Winston Churchill and Bloor Street Via Duct bridge decks.

11) In order to avoid problems in identifying the actual reflection from the asphalt-concrete interface, a policy of taking cores at one or more locations on the bridge decks has been implemented. These measurements are incorporated into the software package in order to maximize the information content.

12) Documentation on system design, software development and interfaces is completed.

6.2/ Recommendations for Further Research

It is recommended that:

1) Further studies be initiated to determine the accuracy limits to internal antenna reflection subtraction and surface reflection waveform subtraction. In particular, the effects of the presence of the vehicle should be more fully evaluated.

2) Methods be developed to determine the number of asphalt layers on a bridge deck, the existence of a membrane, the location of the concrete surface and the location of the top of rebars using a knowledge based system based on structure of the deck. For instance, it is known that asphalt thickness and cover over reinforcement does not usually vary more than a certain amount per metre distance. Thus, there should be heavy correlation along lines and from line to line across a lane which could be exploited.

3) For new bridge decks, a metal plate be installed at certain fixed locations under the asphalt surface in order to provide a self calibration feature for radar evaluation.

4) The software be upgraded to handle multi-layer asphalt covered bridge decks where the dielectric constant from layer to layer is considerably different (such as Bloor Street Via Duct).

5) The existing procedures for data processing can be enhanced by using more advanced techniques such as pattern recognition. Further, the establishment of decision boundaries in classifying the data is required in order to improve the reliability of the system.

6) A data base which includes a high percentage of the common types of waveforms is necessary. This provides an identification capability which is robust. The data base can be accomplished over a period of time as more decks are processed and the different anomalies resolved. To date, only new bridge decks exhibit the ideal waveform characteristics. Damaged decks have characteristics which are sometimes difficult to predict since many different changes can occur in the waveforms. It is expected that development of a data base would help resolve these difficulties.

7) Software be written to provide a computer system which can more easily interact with the operator in order to provide expert advice. In particular, at remote sites, it is essential for the operator to determine an estimate of the condition of the bridge deck and deduce whether the time consuming and expensive process of coring is required. Whenever anomalies arise, it is important to be able to call on an expert (contained in the computer) in order to instruct the operator as to how to proceed.

7/ References

1. Manning D.G. and Holt F.B., "Detecting Delamination In Concrete Bridge Decks", Concrete International, Nov 1980, pp. 34-41.

2. Manning D.G. and Holt F.B., "Detecting Deterioration In Asphalt Covered Bridge Decks", Transportation Research Record No. 899, 1983, pp. 10-20.

3. Chung T., Carter C.R., Manning D.G. and Holt F.B., "Signature Analysis Of Radar Waveforms Taken On Asphalt Covered Bridge Decks", Ontario Ministry Of Transportation And Communications, Report ME-84-01, 1984.

4. Cantor T.R. and Kneeter C.P., "Radar And Acoustic Emission Applied To The Study Of Bridge Decks, Suspension Cables and A Masonry Tunnel", Port Authority Of New York And New Jersey, Report No.77-13, 1977.

5. Carter C.R., Amorosi R. and Chung T., "Calibration Of Computer Program For Radar Waveform Analysis", Ontario Ministry Of Transportation And Communications, Report ME-86-03, 1986.

6. Carter C.R., Chung T., Holt F.B. and Manning D.G., "An Automated Signal Processing System For The Signature Analysis Of Radar Waveforms From Bridge Decks", Canadian Electrical Engineering Journal, Vol-11, No.3, 1986, pp. 128-137.

7. Skolnik M.I., Introduction To Radar Systems, McGraw-Hill, New York, 1962, Ch. 9.

Appendix A

The Data Acquisition System for the DART System using Impulse Radar

A.1/ System Configuration

A block diagram given in Fig. A.1 illustrates the configuration of the data acquisition system for the DART system using impulse radar. The equipment includes:

- TEAC 7-channel model R-81 cassette data recorder with remote control unit
- TECMAR Lab-Master interface cards
- IBM-XT computer system
- custom designed filter circuits for radar high video signals and fifth wheel pulses
- custom designed interface circuit for automatic control of the tape recorder
- HP model 7475A graphic plotter
- EPSON model RX-80 dot matrix line printer
- TEKTRONIX model 2213A 60 MHz oscilloscope

A.2/ General Descriptions of the Data Acquisition System

A.2.1/ The Tape Recorder

In the field, the DART equipped MTC van is driven across the bridge decks with several passes per lane. The radar signals and distance pulses are collected and recorded on the cassette data recorder. The tape recorder has 7 channels which are assigned to record the following informations:

- channel 1 - radar main trigger pulse
- channel 2 - radar pre-trigger pulse
- channel 3 - radar high video pulse

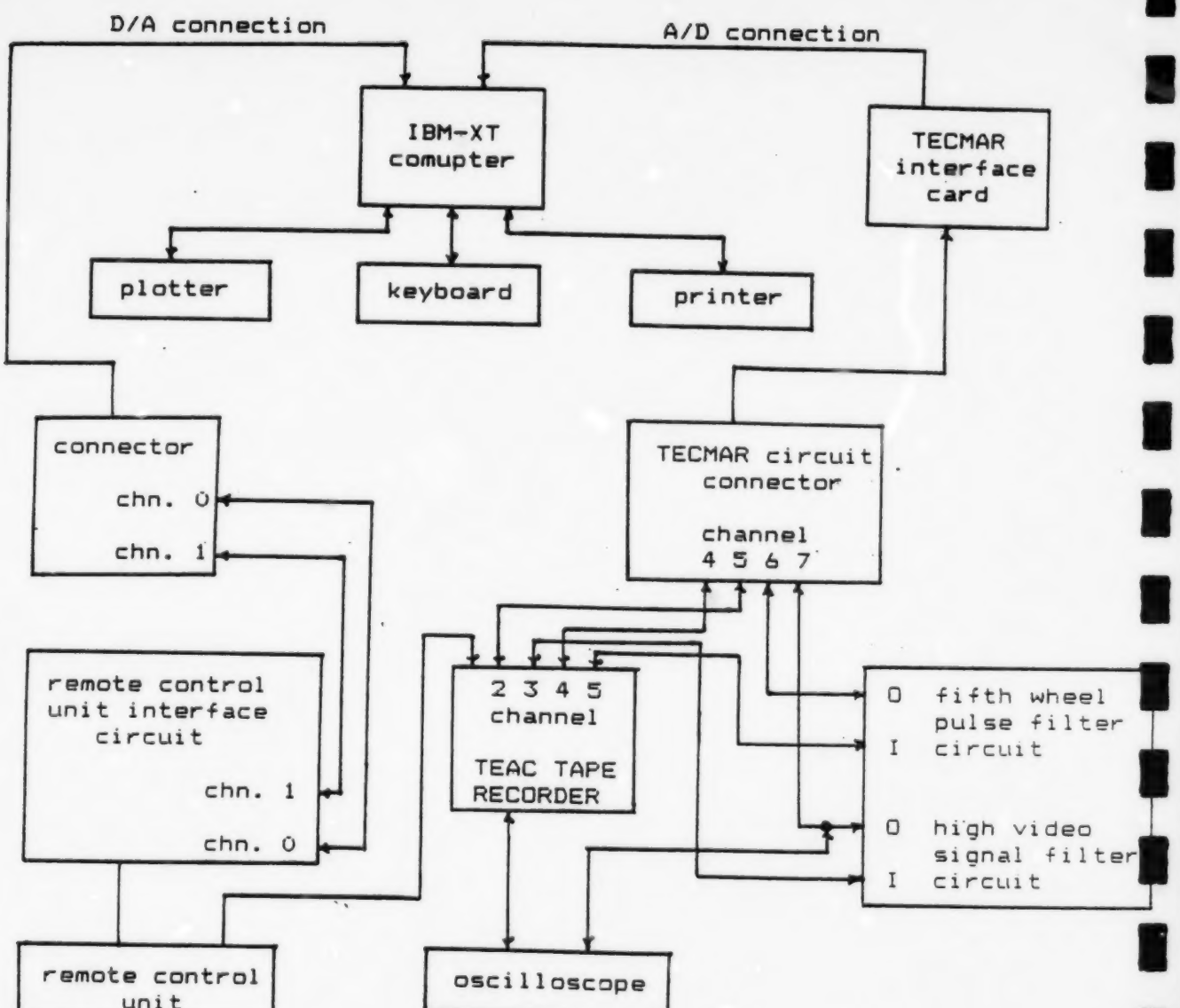

Fig. A.1: Configuration of the data acquisition system

- channel 4 - control track (or bridge line sync)
- channel 5 - 10 cm fifth wheel pulse
- channel 6 - 1 m fifth wheel pulse
- channel 7 - 10 m fifth wheel pulse

The radar main trigger pulse, pre-trigger pulse and high video signal are the standard video outputs from the radar. The bridge line sync is a control track which is used to monitor the beginning and ending of a line. The set of three fifth wheel pulses provides a coded set of waveforms which can be used to locate the position along any passes (or runs).

The radar high video signal and fifth wheel pulses are input to a custom designed filter circuit which improves the signal-to-noise ratio performance.

A.2.2/ The TECMAR Interface System

The actual data acquisition functions are performed by the TECMAR Lab-Master interface cards. The Lab-Master comprises two printed circuit boards: the mother board and the daughter board.

The mother board is a single full-size IBM board which can be plugged into any available expansion slot in the computer. It contains all the circuitry that controls the analog-to-digital (A/D) converter, the timer and the digital-to-analog (D/A) converter.

The daughter board is contained in a metal enclosure. The major function of this board is to perform the actual conversion from analog data to digital data. A 50-pin ribbon cable is used to carry signals between the mother board and the daughter board.

The Lab-Master has 8 A/D channels (channel 0 to 7) and 2 D/A channels (channel 0 and 1). Both converters provide 12-bit resolution and jumper selectable input/output bipolar voltage ranges. The A/D converter carry a 30 KHz conversion rate. The installation manual and user guide of the Lab-Master give detailed information about the interface cards.

Four of the A/D channels of the Lab-Master are used and assigned to have the following inputs:

channel 4 - control track signal

channel 5 - radar trigger pulse (usually pre-trigger)

channel 6 - fifth wheel pulse (usually 10 cm fifth wheel)

channel 7 - radar high video signal

The 2 D/A channels of the interface system are programmed to control the START and STOP functions of the tape recorder.

A.2.3/ The Microcomputer System

Digitization of radar waveforms is done at a sampling rate of 25000 samples per second. With the Lab-Master installed, the recorded radar data are played back into the computer for data processing.

The computer system has the following specifications:

- MS-DOS version 2.11 IBM-XT or compatible
- 640K computer memory
- 16-bit 8088 microprocessor
- 8087 arithmetic coprocessor
- 10 megabyte hard disk

In order to handle the high speed requirement of data sampling, a low level software program using 8088 assembly language is written to perform the task. It is due to the data volume involved and the limit of the computer memory, only a portion of the data set can be sampled into the computer memory buffer. The assembly language program is designed to sample up to 225 K byte of data. When this limit is reach, the D/A channel is activated and the tape recorder is commanded to stop. The sampled data in the memory buffer are off-loaded onto a hard disk file and the data are ready for analysis. The process can then be repeated by starting (which is also controlled by the

status of the D/A channels) the tape recorder again and so on until the whole bridge deck has been sampled and assessed.

Appendix B

Details of Interfaces for DART

B.1/ Fifth Wheel Filter Interface

The signal from the fifth wheel filter consists of logic 0V and 5V pulses which vary in frequency depending on the speed of the vehicle. Unfortunately, there are also spurious pulses of unknown nature which are capable of producing erratic behaviour in the counter circuits which are used to gate the data into the computer every 10 cm. The filter, shown in FIg. B.1 is a simple RC lowpass with a nominal 3 dB bandwidth of 160 Hz.

B.2/ Fifth Wheel Counter Circuit Interface

The fifth wheel counter circuit, shown in Fig. B.2, is used to convert the pulses from the fifth wheel to a more suitable format for entry into the computer. The pulses from the fifth wheel are generated once every centimetre and these are counted in the counter to produce a pulse every 10 cm. The main feature of the counter is the use of a standard decade counter fed by a digital Schist trigger in order to accommodate the slow rising edge from the filter circuit. The circuit has its own +5V power supply.

B.3/ Input Filter for High Video Interface

The input filter for the high video is a standard 3 pole Butterworth lowpass with a bandwidth of 2900 Hz. The circuit, shown in Fig. B.3, features an active circuit implementation with feedback. The input uses a buffer amplifier with gain set at 2.4 to feed the unity gain first stage of the filter. The second stage of the filter has normal gain of 2.

B.4/ Tape Recorder/Computer Control Interface

In order to control the tape recorder from the computer, it is necessary to automatically apply pulses to the tape recorder interface. These pulses, from the two TECMAR interface D/A converters, consist of a START pulse and a STOP pulse. The circuits, illustrated in Fig. B4, are simply digital inverters and gating circuits. Essentially, the computer sends a START pulse to inverter no. 1 which then feeds the start input of the tape recorder. when the computer has loaded sufficient data into memory, then a STOP pulse is sent to the gate which feeds the stop input of the recorder. Inverter no. 2 feeding the gate simply prohibits simultaneous inputs to the two recorder inputs.

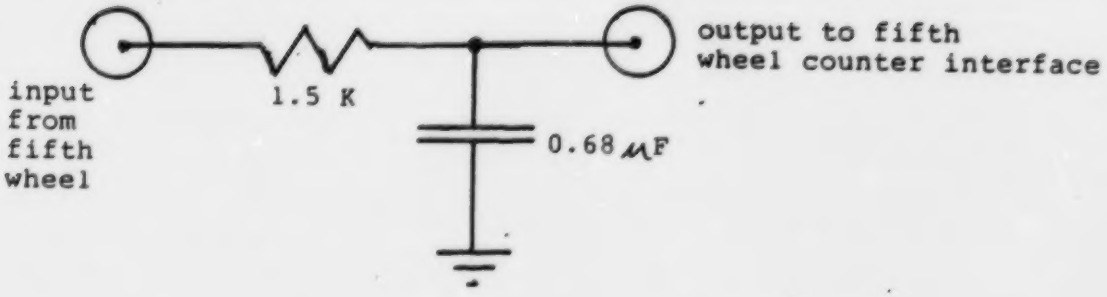

Fig. B.1 Fifth wheel filter interface.

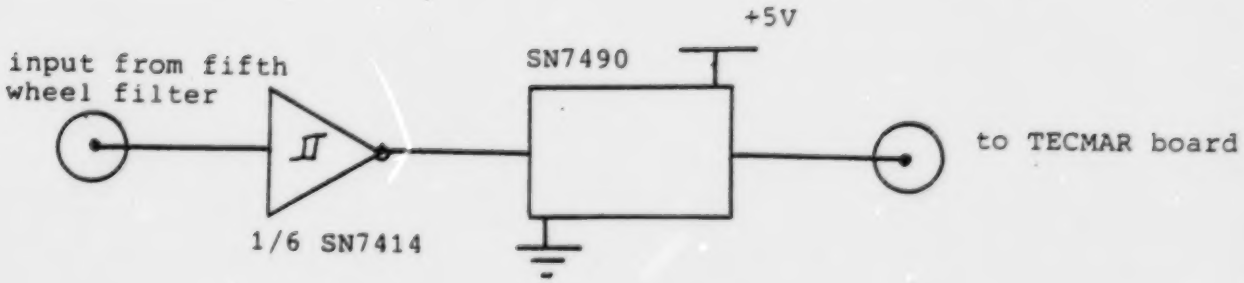

Fig. B.2 Fifth wheel counter circuit interface.

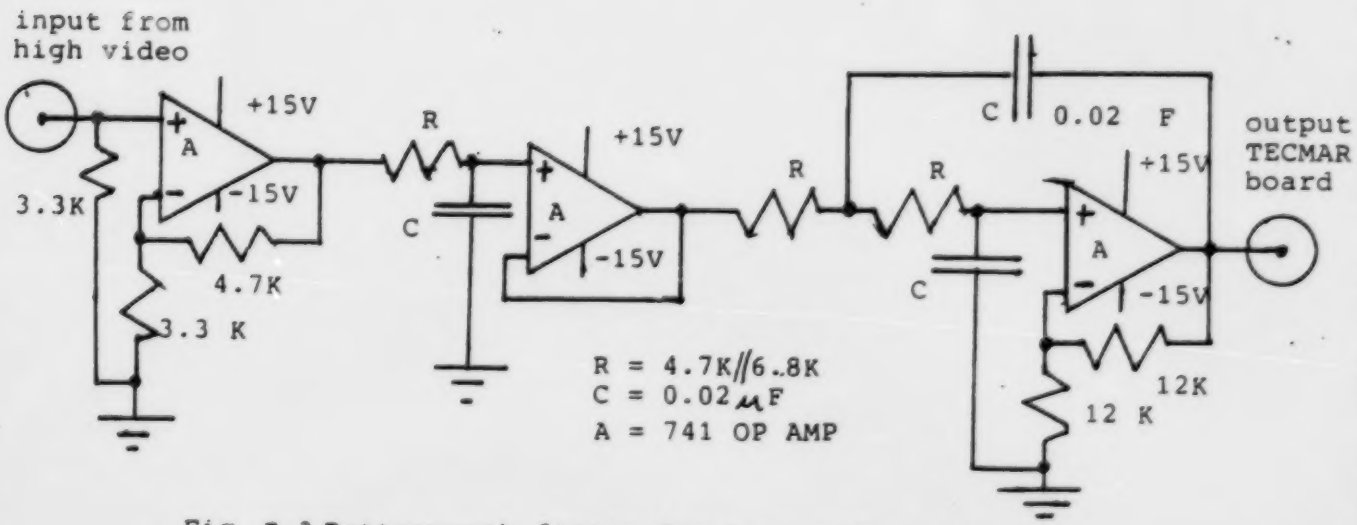

Fig. B.3 Butterworth filter for high video interface

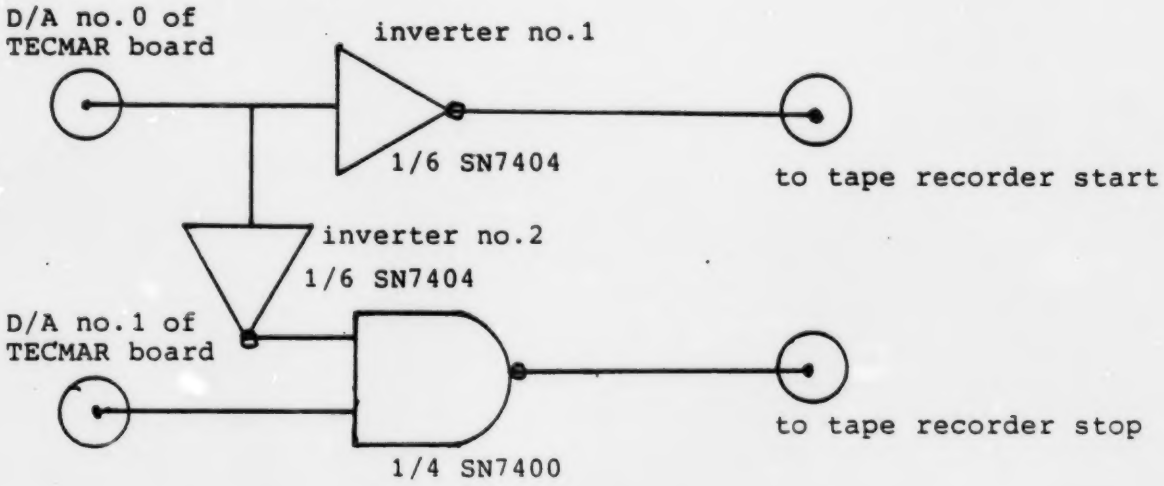

Fig. B.4 Tape recorder/computer control interface.

Appendix C

The Signal Processing Software

C.1/ General Descriptions of the Software Algorithms

Two software packages have been developed for the DART system using impulse radar. The first package - MTC87 performs all processing functions such as data acquisition, thickness measurement and fault detection. The second package - DECK87 plots areas of deterioration on a grid-formatted layout which represents the actual bridge deck. The main features of each of the software packages are detailed in the following sections.

C.2/ MTC87 Package

MTC87 was written in MS-Fortran 77 language. The software requires the following inputs from the operator:

- title (up to 60 characters)
- fifth wheel information
- asphalt thickness from core sample
- number of bridge lines (maximum 12)

There are nine separated program modules in the MTC87 package. These subroutines are: FPADC; FPVOLT; RESDUE; DIGSIG; SIGPRO; CONDIT; AVETHK; HISGAM and TABPRN. Each of the sub- programs performs a specific task, such as: data conversion; measure metal plate reflection; calibration of waveform; identify interfacing layers; thickness measurement; fault identification and cluster analysis. Figure C.1 is the flow graph of program MTC87. All of the subprograms are written in MS-Fortran 77 language with the exception of the subroutines FPADC and DIGSIG which are written in 8088 assembly language. The functions of each of the program modules are discussed next.

C.2.1/ Subroutine FPADC

FPADC implies 'Flat Plate A/D Conversion'. The primary function of this subroutine is to digitize metal plate signal. Each digitized waveform is 1024 bytes or 512 samples. The flow graph is given in Fig. C.2. Some of the features of FPADC include:

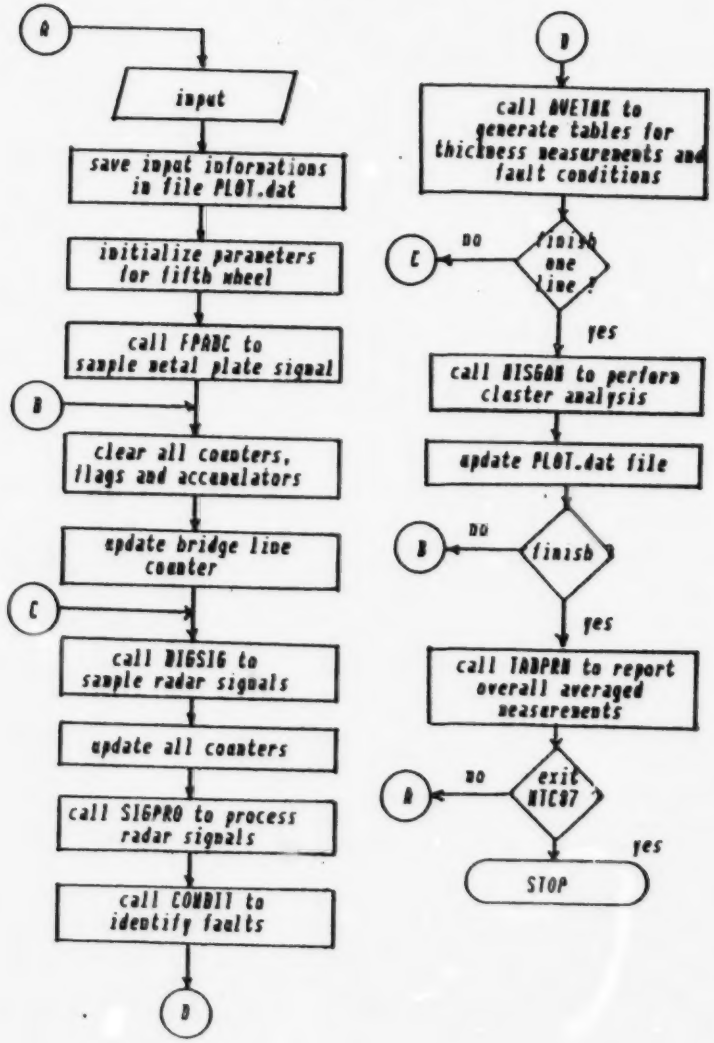

Fig. C.1: Main program MIC87 (flow graph)

•.program the Lab-Master D/A converter, A/D converter and 9513 timer

• determine the sampling rate

• enable the D/A and A/D conversions

• start the tape recorder when the system is ready

• use channel 5 of the Lab-Master card for radar pre-trigger pulse

• use channel 7 of the Lab-Master card for radar high video signal

• if channels 5 and 7 are ready, then perform 64 K bytes analog-to-digital conversion of metal plate signal

• write sampled data into memory buffer

• stop the tape recorder after sampling is finished

• transfer a total of 64 radar traces from memory buffer to data file FPLATE.bin

• return to MTC87

C.2.2/ Subroutine FPVOLT

FPVOLT implies 'Flat Plate amplitude in VOLTage'. The primary functions of the subroutine are to calibrate metal plate signal by removing the antenna internal reflections and measure the amplitude of surface echo. An averaged value (from 64 radar waveforms) of the amplitude is calculated. The flow graph is given in Fig. C.3. Some of the features of FPVOLT are:

• read a record of antenna internal reflections waveform from data file INTRF.dat

• read 64 metal plate radar waveforms from file FPLATE.dat

• locate a reference sample point which is common to both waveforms

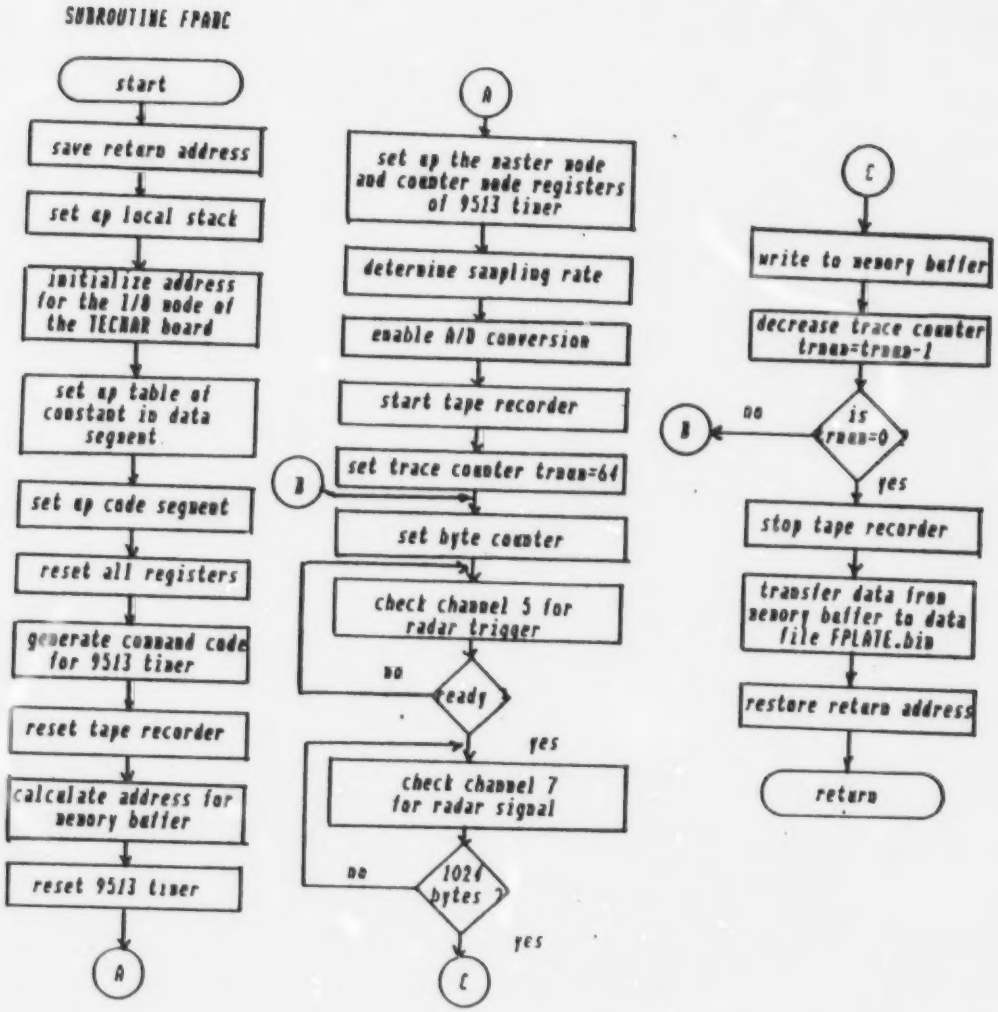

Fig. C.2: Subroutine FPABC (flow graph)

- call subroutine RESDUE to obtain the true radar signal (also referred as the residue waveform) by subtracting antenna internal reflections signal from the metal plate signal

- measure the amplitude of surface echo from each residue waveform

- calculate the averaged amplitude of the surface echo

- return to MTC87

C.2.3/ Subroutine RESDUE

RESDUE implies 'calculate RESIDUE waveform'. This subroutine is called from two modules: FPVOLT and SIGPRO, respectively. The function of this sub-program is to calculate the true radar reflection by subtracting antenna internal reflections. Figure C.4 is the flow graph of the subroutine. Some of the features of RESDUE are:

- align antenna internal reflections waveform and radar signal with respect to reference sample point

- subtract antenna internal reflection waveform from each radar signal

- calculate the residue magnitude over 112 samples

- repeat the subtraction by shifting the radar signal 1 sample to the RIGHT with respect to the reference point and calculate the residue magnitude

- repeat the subtraction by shifting the radar signal 1 sample to the LEFT with respect to the reference point and calculate the residue magnitude

- the three residue waveforms are compared

- the desired radar signal is the residue waveform with minimum residue magnitude

- measure the amplitude of the surface echo reflection from each residue waveform

- return to MTC87

SUBROUTINE FPVOLT

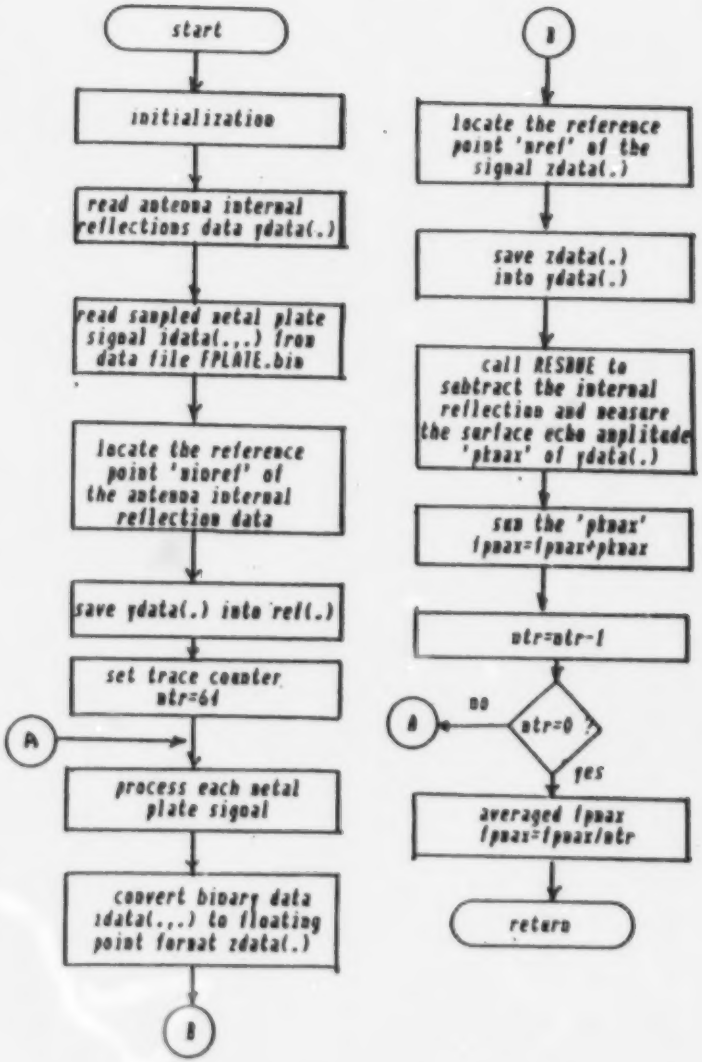
start
initialization
read antenna internal reflections data ydata(.)
read sampled metal plate signal idata(,,.) from data file fPLATE.bin
locate the reference point 'nioref' of the antenna internal reflection data
save ydata(.) into ref(.)
set trace counter ntr=64
A
process each metal plate signal
convert binary data idata(,,.) to floating point format zdata(.)
B
B
locate the reference point 'nref' of the signal zdata(.)
save zdata(.) into ydata(.)
call RESUBE to subtract the internal reflection and measure the surface echo amplitude 'ptmax' of ydata(.)
sum the 'ptmax' fpmax=fpmax+ptmax
ntr=ntr-1
ntr=0 ?
no
A
yes
averaged fpmax fpmax=fpmax/ntr
return

fig. C.3: Subroutine FPVOLT (flow graph)

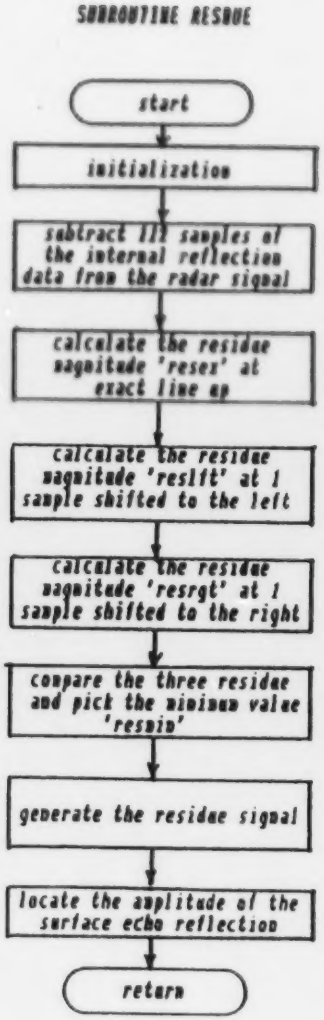
SUBROUTINE RESDUE
start
initialization
subtract III samples of the internal reflection data from the radar signal
calculate the residue magnitude 'resex' at exact line up
calculate the residue magnitude 'reslft' at 1 sample shifted to the left
calculate the residue magnitude 'resrgt' at 1 sample shifted to the right
compare the three residue and pick the minimum value 'resmin'
generate the residue signal
locate the amplitude of the surface echo reflection
return

Fig. C.4: Subroutine RESDUE (flow graph)

C.2.4/ Subroutine DIGSIG

DIGSIG implies ' DIGitization of radar SIGNALs'. Figure C.5 is the flow graph of the subroutine. Some of the features of DIGSIG are:

- assign a doubleword pointer to each of the parameters passed from MTC87 to DIGSIG
- reserve 225K bytes memory buffer space
- program the Lab-Master D/A converter, A/D converter and 9513 timer
- determine the sampling rate
- enable the A/D and D/A converters
- start the tape recorder when the system is ready
- check channel 4 of the A/D converter for the control track signal
- check channel 6 of the A/D converter for the fifth wheel pulse
- check channel 5 of the A/D converter for the radar pre-trigger pulse
- check channel 7 of the A/D converter for the radar high video signal
- if channels 4, 5, 6 and 7 are ready, then perform analog-to-digital conversion on radar high video signal
- discard every second waveform to simulate a 20 cm fifth wheel gating when actually a 10 cm gating is used
- sample up to 225 K bytes of data into memory buffer
- stop the tape recorder when sampling is done

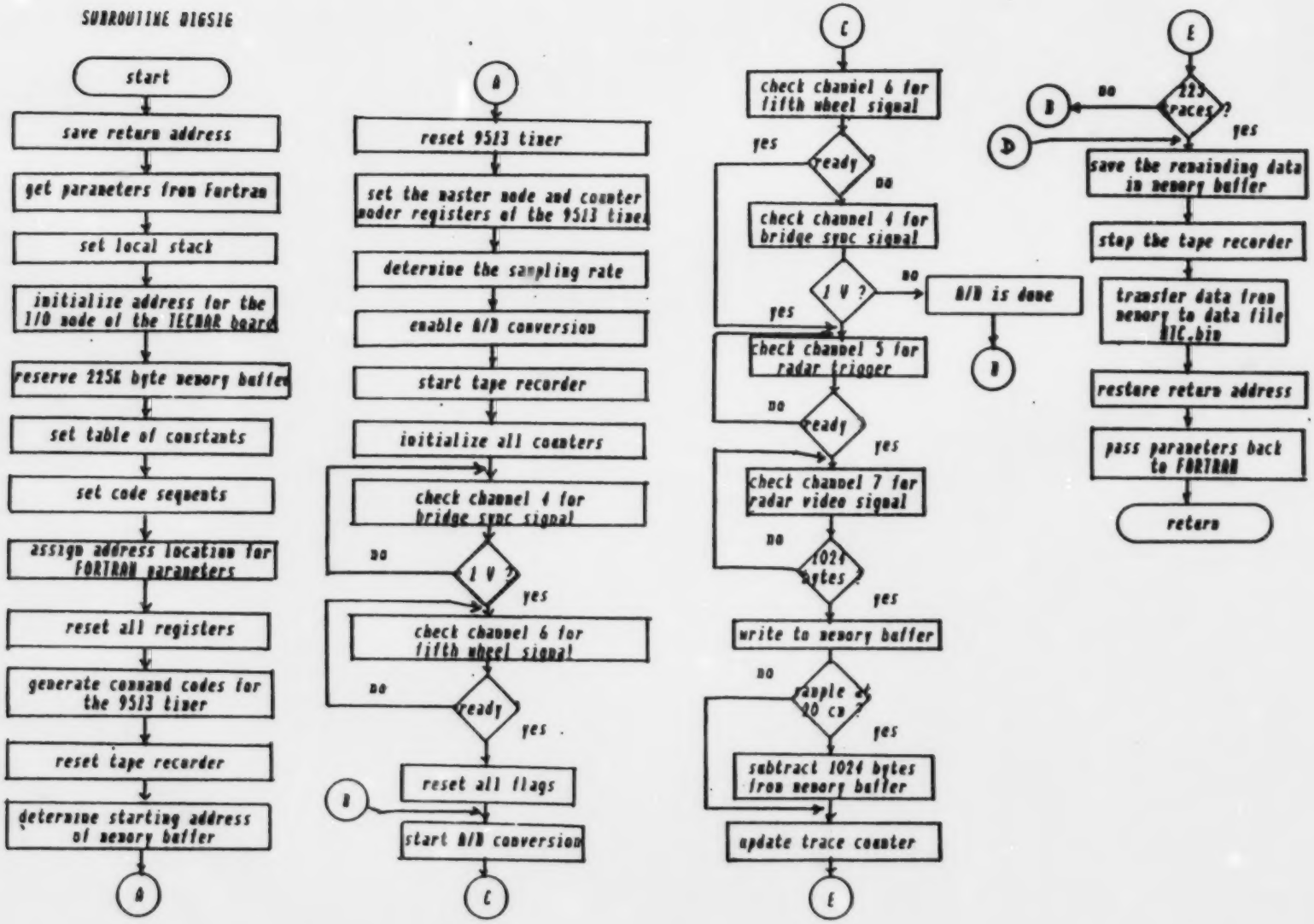

Fig. C.5: Subroutine BIGSIG (flow graph)

- transfer data from memory buffer to data file MTC.bin
- restore the addresses of each of the parameters which have to be returned to MTC87
- return to MTC87

C.2.5/ Subroutine SIGPRO

SIGPRO implies 'SIGnal PROcessing'. Figure C.6 shows the program flow graph. Some of the features of SIGPRO are:

- read a record of antenna internal reflections data from file INTRF.dat
- restore raw radar data from file MTC.bin
- find a reference sample point common to both waveforms
- call subroutine RESDUE to obtain the true radar signal by subtracting antenna internal reflections from the radar signal
- locate the surface echo reflections from the residue waveform and label it as 'peak A'
- search for the first negative going peak after peak A and label it as 'peak B'
- calculate the ratio of magnitude at peak B to magnitude at peak A. This is labeled as the 'R1 ratio'
- set a search window for asphalt-concrete interface using the asphalt thickness information from core sample
- locate the reflection at the asphalt-concrete interface and label it as 'peak C'
- locate the reflection at the first layer of rebars and label it as 'peak D'

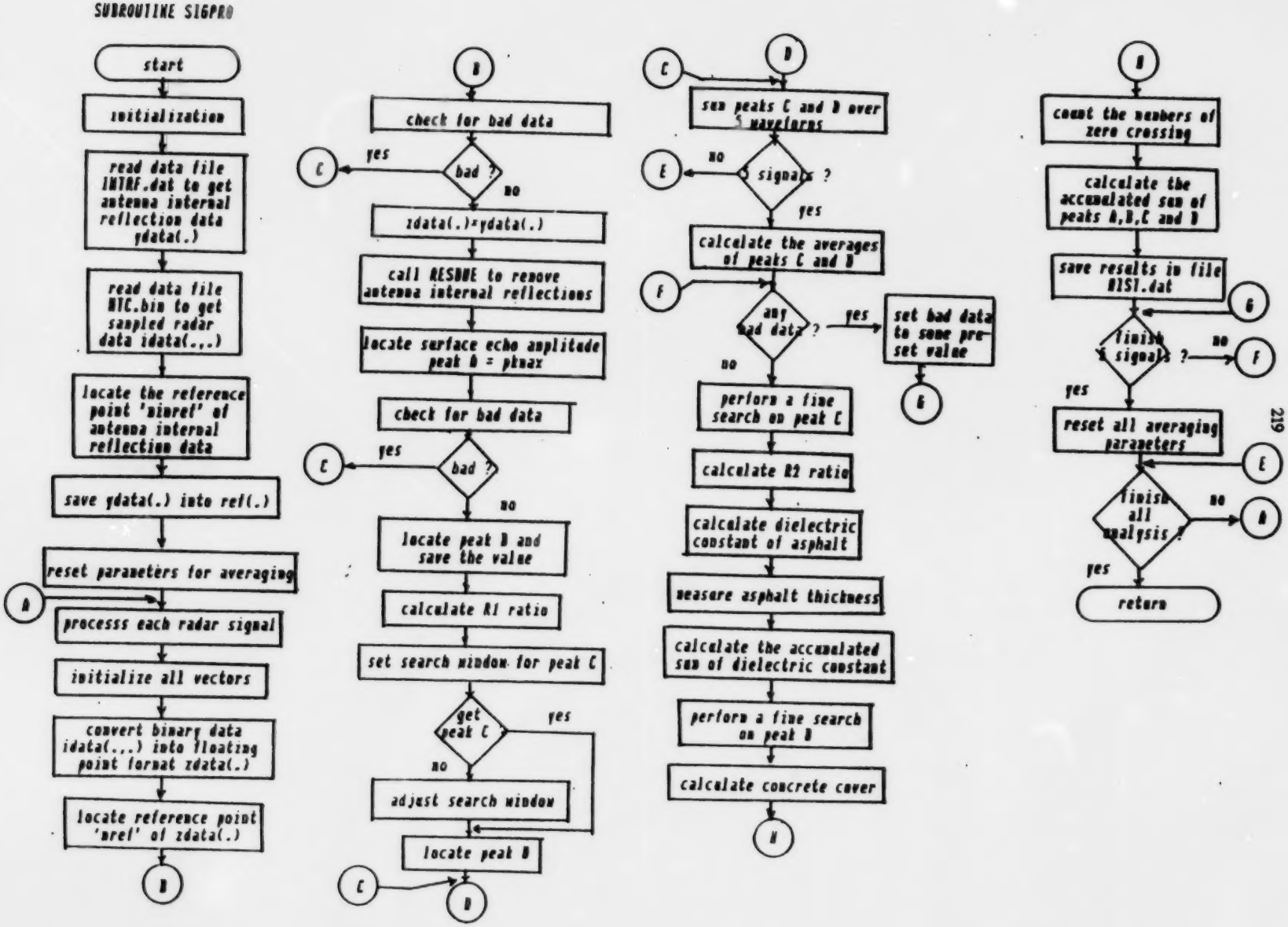
SUBROUTINE SIGPRO
start
initialization
read data file INTRF.dat to get antenna internal reflection data ydata(.)
read data file MIC.bin to get sampled radar data idata(...)
locate the reference point 'ninref' of antenna internal reflection data
save ydata(.) into ref(.)
reset parameters for averaging
processs each radar signal
initialize all vectors
convert binary data idata(...) into floating point format zdata(.)
locate reference point 'nref' of zdata(.)
check for bad data
bad ?
yes
no
idata(.)=ydata(.)
call RESBUE to remove antenna internal reflections
locate surface echo amplitude peak A = pmax
check for bad data
bad ?
yes
no
locate peak B and save the value
calculate R1 ratio
set search window for peak C
get peak C ?
yes
no
adjust search window
locate peak B
sum peaks C and B over 5 waveforms
signals ?
no
yes
calculate the averages of peaks C and B
any bad data ?
yes
set bad data to some pre-set value
no
perform a fine search on peak C
calculate R2 ratio
calculate dielectric constant of asphalt
measure asphalt thickness
calculate the accumulated sum of dielectric constant
perform a fine search on peak B
calculate concrete cover
count the numbers of zero crossing
calculate the accumulated sum of peaks A,B,C and D
save results in file RESI.dat
finish 5 signals ?
no
yes
reset all averaging parameters
finish all analysis ?
no
yes
return

Fig. C.6: Subroutine SIGPRO (flow graph)

- calculate the averaged value of peak C and peak D over every 5 waveforms
- based on the averaged value of peaks C and D, perform a fine search of peaks C and D on each of the 5 waveforms
- calculate the ratio of magnitude at peak C to magnitude at peak A. This is labeled as the 'R2 ratio'
- calculate the dielectric constant of asphalt
- calculate the thickness of asphalt layer
- calculate the thickness of concrete cover over reinforcement bars
- count the number of slope sign changes between peaks C and D
- calculate the accumulated sum of the values of peaks A, B,C and D
- save the values of peaks A,B,C,D and thickness measurement of each waveform in data file HIST.dat
- return to MTC87

C.2.6/ Subroutine CONDIT

CONDIT implies 'identify bridge deck CONDITions'. The flow graph is given in Fig. C.7. Some of the features of CONDIT are:

- identify the types of deterioration from waveform analysis
- if radar signal is not sampled properly, the waveform is declared 'BAD'
- if the R1 ratio exceeds 0.4 and R2 ratio exceeds 0.28, the waveform is declared 'SCALED'

SUBROUTINE CONDII

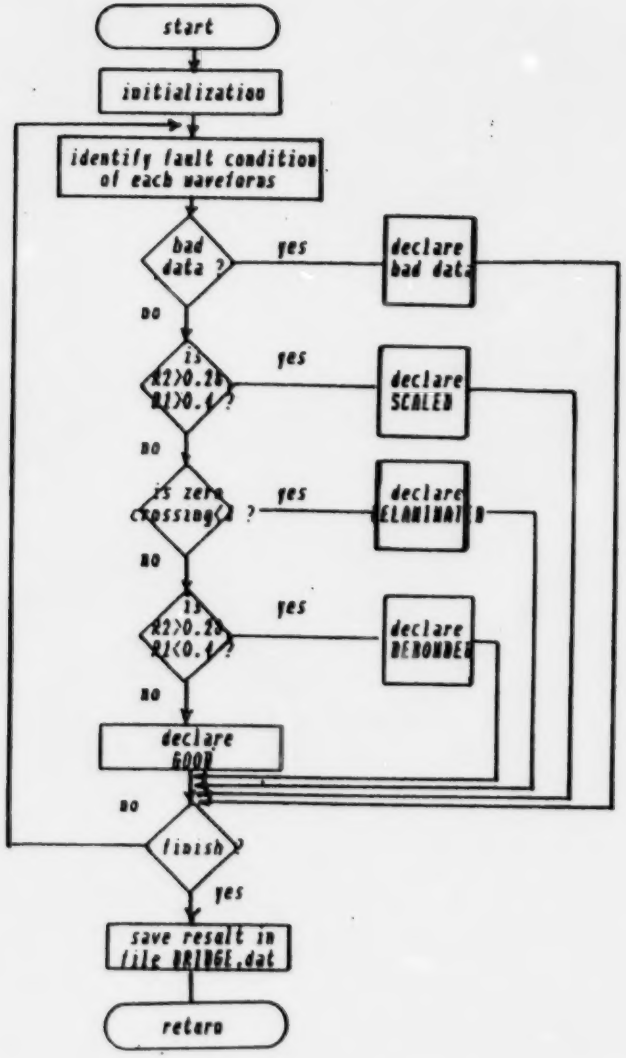

Fig. C.7: Subroutine CONDII (flow graph)

SUBROUTINE AVETHK

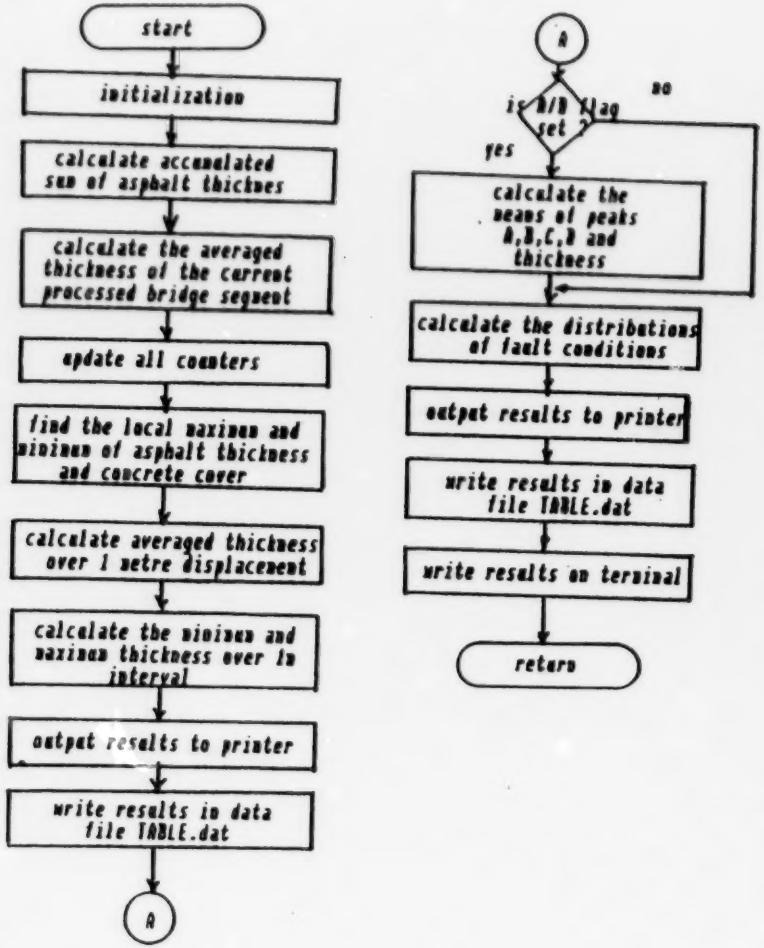
start
initialization
calculate accumulated sum of asphalt thicknes
calculate the averaged thickness of the current processed bridge segment
update all counters
find the local maximum and minimum of asphalt thickness and concrete cover
calculate averaged thickness over 1 metre displacement
calculate the minimum and maximum thickness over 1m interval
output results to printer
write results in data file TABLE.dat
A
A
is A/D flag set ?
no
yes
calculate the means of peaks A,B,C,D and thickness
calculate the distributions of fault conditions
output results to printer
write results in data file TABLE.dat
write results on terminal
return

Fig. C.8: Subroutine AVETHK (flow graph)

- if the number of slope sign changes (or zero crossing) is less than 3, the waveform is declared 'DELAMINATED'. Otherwise, it is declared 'GOOD'

- if the R1 ratio is at least 0.4 and R2 ratio exceeds 0.28, the waveform is declared 'DEBONDED'

- save the results in data file BRIDGE.dat

- return to MTC87

C.2.7/ Subroutine AVETHK

AVETHK implies 'measure AVEraged THicKness'. The flow graph is given in Fig. C.8. Some of the features of AVETHK are:

- measure the averaged thickness of asphalt layer over 1 m displacement

- measure the averaged thickness of concrete cover over reinforcement bars over 1 m displacement

- calculate the mean values of peaks A,B,C and D; asphalt thickness and concrete cover over a completed line

- calculate the distribution of faults over a completed line

- save results in data file TABLE.dat

- return to MTC87

C.2.8/ Subroutine HISGAM

HISGAM implies 'generate the HIStoGRAM'. The flow graph is given in Fig. C.9. Some of the features of HISGAM are:

- read data file HIST.dat to retrieve the values of peaks A,B,C,D and thickness measurements of each waveform

- calculate the variance, standard deviation and percentage of variations of the parameters
- generate histograms for peaks A,B,C,D and thickness measurements
- output the results on printer
- return to MTC87

C.2.9/ Subroutine TABPRN

TABPRN implies 'TABulate results and PRiNt them out'. The flow graph is given in Fig. C.10. Some of the features of TABPRN are:

- calculate the average value for the dielectric constant of asphalt
- measure the averaged length of the bridge deck
- read data file TABLE.dat to retrieve data one thickness measurements and fault distribution of each line
- tabulate the results
- calculate the overall average value of asphalt thickness
- calculate the overall average value of concrete cover
- output the results on printer
- save the results in data file AVER.dat
- return to MTC87

C.3/ DECK87 Package

The functions of DECK87 package are (1) to plot the bridge deck layout and (2) to indicate the area of deterioration. The plotting routines employ the software library (PLOTMS.LIB) from

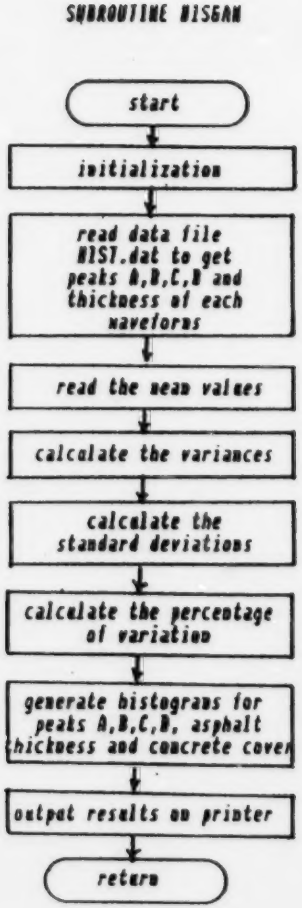

Fig. C.9: Subroutine HISGAN (flow graph)

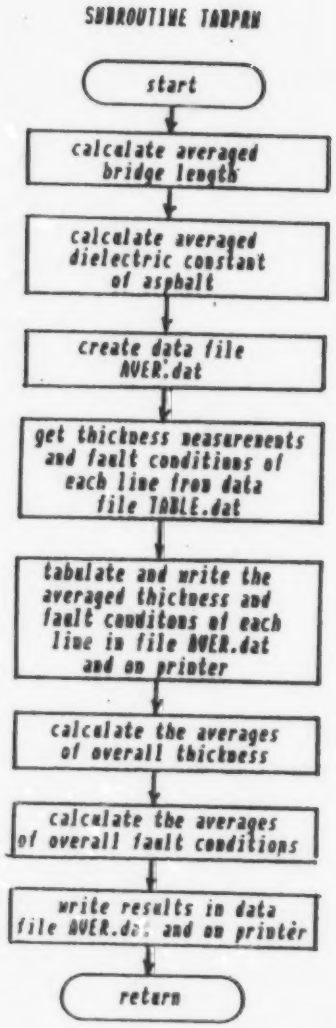
SUBROUTINE TABPRN
start
calculate averaged bridge length
calculate averaged dielectric constant of asphalt
create data file AVER.dat
get thickness measurements and fault conditions of each line from data file TABLE.dat
tabulate and write the averaged thickness and fault conditons of each line in file AVER.dat and on printer
calculate the averages of overall thickness
calculate the averages of overall fault conditions
write results in data file AVER.dat and on printer
return

Fig. C.10: Subroutine TABPRN (flow graph)

PLOTMATIC package. PLOTMATIC is a comprehensive pen-plotter package which is designed to interface with program written in MS-Fortran. Figure C.11 is the flow graph of DECK87. The functions of the program are:

- read the data file PLOT.dat to obtain the number of bridge lines and radar traces
- request operator to input the displacement of each line
- report the length and width of the deck layout
- read the data file BRIDGE.dat to obtain the types of fault at each location
- plot the bridge deck layout using PLOTMS.LIB software
- assign character 'X' for delamination
- assign character 'D' for debonding
- assign character 'S' for scaling
- plot the characters on a grid-formatted bridge deck layout

PROGRAM DECK87

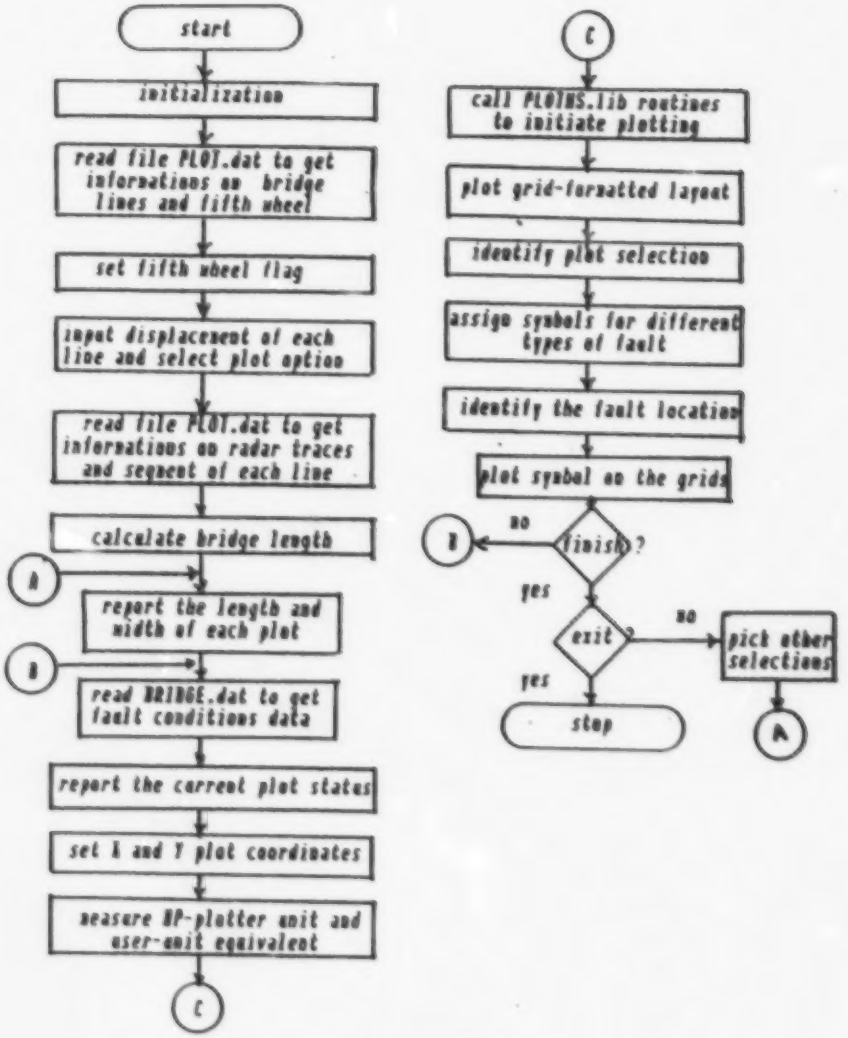

Fig. C.11: Program DECK87 (flow graph)

Appendix D

Cluster Analysis Results

D.1 NINTH LINE DATA

The statistical data and histograms for line 1 to line 8 of the Ninth Line bridge deck are provided in Figs. D.1 to D.8 respectively.

Ninth Line
LINE : 1, CLUSTER ANALYSIS REPORT

*** MEAN values ***

A(133 4.245839) B(143 -1.460505) C(177 .494328) D(217 .223913) THR(107) COR(81)

*** VARiances ***

A(.7 .045760) B(.7 .013106) C(14.9 .112556) D(14.1 .007441) THR(114) COR(58)

*** STanDard DEViations ***

A(.8 .213916) B(.8 .114483) C(3.9 .335494) D(3.8 .086264) THR(10) COR(7)

*** I of VARIATions ***

A(.61 5.04) B(.58 7.84) C(2.18 67.87) D(1.73 38.53) THR(9.35) COR(8.64)

*** HISTogram (PEAKs) ***

[PoinT SAMPle]	Numbers of WAVEform at PEAK A	B	C	D
100 to 105 :	0.	0.	0.	0.
105 to 110 :	0.	0.	0.	0.
110 to 115 :	0.	0.	0.	0.
115 to 120 :	0.	0.	0.	0.
120 to 125 :	0.	0.	0.	0.
125 to 130 :	0.	0.	0.	0.
130 to 135 :	307.	0.	0.	0.
135 to 140 :	16.	0.	0.	0.
140 to 145 :	0.	305.	0.	0.
145 to 150 :	0.	18.	0.	0.
150 to 155 :	0.	0.	0.	0.
155 to 160 :	0.	0.	0.	0.
160 to 165 :	0.	0.	0.	0.
165 to 170 :	0.	0.	2.	0.
170 to 175 :	0.	0.	64.	0.
175 to 180 :	0.	0.	168.	0.
180 to 185 :	0.	0.	76.	0.
185 to 190 :	0.	0.	11.	0.
190 to 195 :	0.	0.	2.	0.
195 to 200 :	0.	0.	0.	0.
200 to 205 :	0.	0.	0.	0.
205 to 210 :	0.	0.	0.	0.
210 to 215 :	0.	0.	0.	112.
215 to 220 :	0.	0.	0.	146.
220 to 225 :	0.	0.	0.	50.
225 to 230 :	0.	0.	0.	15.
230 to 235 :	0.	0.	0.	0.
235 to 240 :	0.	0.	0.	0.
240 to 245 :	0.	0.	0.	0.
245 to 250 :	0.	0.	0.	0.

*** HISTogram (THICKness) ***

[THICKness)	Nos. of WAVEform asphalt	C/o RIFsent
0 to 10 :	0.	0.
10 to 20 :	0.	0.
20 to 30 :	0.	0.
30 to 40 :	0.	0.
40 to 50 :	0.	1.
50 to 60 :	0.	0.
60 to 70 :	2.	18.
70 to 80 :	1.	113.
80 to 90 :	5.	151.
90 to 100 :	71.	37.
100 to 110 :	85.	3.
110 to 120 :	135.	0.
120 to 130 :	14.	0.
130 to 140 :	9.	0.
140 to 150 :	0.	0.
150 to 160 :	1.	0.
160 to 170 :	0.	0.
170 to 180 :	0.	0.
180 to 190 :	0.	0.
190 to 200 :	0.	0.
200 to 210 :	0.	0.
210 to 220 :	0.	0.
220 to 230 :	0.	0.
230 to 240 :	0.	0.
240 to 250 :	0.	0.
250 to 260 :	0.	0.
260 to 270 :	0.	0.
270 to 280 :	0.	0.
280 to 290 :	0.	0.
290 to 300 :	0.	0.

Fig. D.1: Ninth Line-line 1 cluster analysis report

Ninth Line
LINE : 2, CLUSTER ANALYSIS REPORT

*** MEAN values ***

A(133	4.320403)	B(143	-1.476318)	C(174	.784546)	D(211	.414782)	THK(97)	COR(76)

*** VARIances ***

A(.7	.050327)	B(.8	.011303)	C(0.8	.093513)	D(11.6	.020542)	THK(66)	COR(41)

*** STandard DEViations ***

A(.8	.241510)	B(.9	.106315)	C(1.0	.305799)	D(3.4	.143326)	THK(8)	COR(6)

*** % of VARIATions ***

A(.63	5.58)	B(.63	7.20)	C(1.70	38.98)	D(1.61	34.55)	THK(0.25)	COR(7.89)

*** HISTogram (PEAKs) ***

	Numbers of NAMEform at PEAK			
(Point SAMPle)	A	B	C	D
100 to 105 :	0.	0.	0.	0.
105 to 110 :	0.	0.	0.	0.
110 to 115 :	0.	0.	0.	0.
115 to 120 :	0.	0.	0.	0.
120 to 125 :	0.	0.	0.	0.
125 to 130 :	0.	0.	0.	0.
130 to 135 :	306.	0.	0.	0.
135 to 140 :	17.	0.	0.	0.
140 to 145 :	0.	302.	0.	0.
145 to 150 :	0.	21.	0.	0.
150 to 155 :	0.	0.	0.	0.
155 to 160 :	0.	0.	0.	0.
160 to 165 :	0.	0.	0.	0.
165 to 170 :	0.	0.	4.	0.
170 to 175 :	0.	0.	174.	0.
175 to 180 :	0.	0.	121.	0.
180 to 185 :	0.	0.	18.	0.
185 to 190 :	0.	0.	6.	0.
190 to 195 :	0.	0.	0.	0.
195 to 200 :	0.	0.	0.	0.
200 to 205 :	0.	0.	0.	2.
205 to 210 :	0.	0.	0.	88.
210 to 215 :	0.	0.	0.	191.
215 to 220 :	0.	0.	0.	38.
220 to 225 :	0.	0.	0.	3.
225 to 230 :	0.	0.	0.	1.
230 to 235 :	0.	0.	0.	0.
235 to 240 :	0.	0.	0.	0.
240 to 245 :	0.	0.	0.	0.
245 to 250 :	0.	0.	0.	0.

*** HISTogram (THICKness) ***

	Nos. of NAMEform	
(THICKness)	asphalt	C/o-RIFgeot
0 to 10 :	0.	0.
10 to 20 :	0.	0.
20 to 30 :	0.	0.
30 to 40 :	0.	0.
40 to 50 :	0.	3.
50 to 60 :	1.	0.
60 to 70 :	2.	33.
70 to 80 :	2.	195.
80 to 90 :	9.	89.
90 to 100 :	212.	3.
100 to 110 :	77.	0.
110 to 120 :	11.	0.
120 to 130 :	9.	0.
130 to 140 :	0.	0.
140 to 150 :	0.	0.
150 to 160 :	0.	0.
160 to 170 :	0.	0.
170 to 180 :	0.	0.
180 to 190 :	0.	0.
190 to 200 :	0.	0.
200 to 210 :	0.	0.
210 to 220 :	0.	0.
220 to 230 :	0.	0.
230 to 240 :	0.	0.
240 to 250 :	0.	0.
250 to 260 :	0.	0.
260 to 270 :	0.	0.
270 to 280 :	0.	0.
280 to 290 :	0.	0.
290 to 300 :	0.	0.

Fig. D.2: Ninth Line-line 2 cluster analysis report

Ninth Line
LINE : 3, CLUSTER ANALYSIS REPORT

*** MEAN values ***

A(132 4.380720) B(143 -1.525069) C(175 .725953) D(208 .359362) THK(97) COR(70)

*** VARIances ***

A(1.7 .039025) B(1.0 .010078) C(8.3 .114713) D(14.6 .014417) THK(58) COR(43)

*** STandard DEViations ***

A(1.3 .197547) B(1.0 .100391) C(2.9 .338692) D(3.8 .120073) THK(7) COR(6)

*** I of VARIATions ***

A(.98 4.51) B(.68 6.58) C(1.64 46.65) D(1.84 33.41) THK(7.22) COR(8.57)

*** HISTogram (PEAKs) ***

[Point SAMPle]	Numbers of HOVEfore at PEAK A	B	C	D
100 to 105 :	0.	0.	0.	0.
105 to 110 :	0.	0.	0.	0.
110 to 115 :	0.	0.	0.	0.
115 to 120 :	0.	0.	0.	0.
120 to 125 :	0.	0.	0.	0.
125 to 130 :	0.	0.	0.	0.
130 to 135 :	306.	0.	0.	0.
135 to 140 :	15.	0.	0.	0.
140 to 145 :	0.	300.	0.	0.
145 to 150 :	0.	21.	0.	0.
150 to 155 :	0.	0.	0.	0.
155 to 160 :	0.	0.	0.	0.
160 to 165 :	0.	0.	0.	0.
165 to 170 :	0.	0.	4.	0.
170 to 175 :	0.	0.	138.	0.
175 to 180 :	0.	0.	152.	0.
180 to 185 :	0.	0.	26.	0.
185 to 190 :	0.	0.	1.	0.
190 to 195 :	0.	0.	0.	0.
195 to 200 :	0.	0.	0.	2.
200 to 205 :	0.	0.	0.	25.
205 to 210 :	0.	0.	0.	160.
210 to 215 :	0.	0.	0.	116.
215 to 220 :	0.	0.	0.	18.
220 to 225 :	0.	0.	0.	0.
225 to 230 :	0.	0.	0.	0.
230 to 235 :	0.	0.	0.	0.
235 to 240 :	0.	0.	0.	0.
240 to 245 :	0.	0.	0.	0.
245 to 250 :	0.	0.	0.	0.

*** HISTogram (THICKness) ***

[THICKness]	Nos. of HOVEfore asphalt	C/a RIFseat
0 to 10 :	0.	0.
10 to 20 :	0.	0.
20 to 30 :	0.	0.
30 to 40 :	0.	1.
40 to 50 :	0.	0.
50 to 60 :	1.	21.
60 to 70 :	0.	116.
70 to 80 :	3.	173.
80 to 90 :	21.	9.
90 to 100 :	177.	1.
100 to 110 :	100.	0.
110 to 120 :	19.	0.
120 to 130 :	0.	0.
130 to 140 :	0.	0.
140 to 150 :	0.	0.
150 to 160 :	0.	0.
160 to 170 :	0.	0.
170 to 180 :	0.	0.
180 to 190 :	0.	0.
190 to 200 :	0.	0.
200 to 210 :	0.	0.
210 to 220 :	0.	0.
220 to 230 :	0.	0.
230 to 240 :	0.	0.
240 to 250 :	0.	0.
250 to 260 :	0.	0.
260 to 270 :	0.	0.
270 to 280 :	0.	0.
280 to 290 :	0.	0.
290 to 300 :	0.	0.

Fig. D.3: Ninth Line-line 3 cluster analysis report

Ninth Line
LINE : 4 CLUSTER ANALYSIS REPORT

*** MEAN values ***

A(133	4.336439)	B(143	-1.532383)	C(175	.746978)	D(219	.105367)	THR(99)	COR(92)

*** VARiances ***

A(1.1	.050114)	B(1.1	.016602)	C(8.7	.113175)	D(61.6	.007264)	THR(66)	COR(265)

*** STandard DEViations ***

A(1.0	.223862)	B(1.1	.128849)	C(3.0	.336414)	D(7.8	.085227)	THR(8)	COR(16)

*** % of VARIATions ***

A(.77	5.16)	B(.75	8.41)	C(1.69	45.04)	D(3.58	80.89)	THR(8.00)	COR(17.58)

*** HISTogram (PEAKs) ***

[PoinT SAMPle]	Numbers of WAVEform at PEAK A	B	C	D
100 to 105 :	0.	0.	0.	0.
105 to 110 :	0.	0.	0.	0.
110 to 115 :	0.	0.	0.	0.
115 to 120 :	0.	0.	0.	0.
120 to 125 :	0.	0.	0.	0.
125 to 130 :	0.	0.	0.	0.
130 to 135 :	306.	0.	0.	0.
135 to 140 :	15.	0.	0.	0.
140 to 145 :	0.	305.	0.	0.
145 to 150 :	0.	15.	0.	0.
150 to 155 :	0.	1.	0.	0.
155 to 160 :	0.	0.	0.	0.
160 to 165 :	0.	0.	0.	0.
165 to 170 :	0.	0.	1.	0.
170 to 175 :	0.	0.	155.	0.
175 to 180 :	0.	0.	128.	0.
180 to 185 :	0.	0.	36.	0.
185 to 190 :	0.	0.	1.	0.
190 to 195 :	0.	0.	0.	0.
195 to 200 :	0.	0.	0.	2.
200 to 205 :	0.	0.	0.	1.
205 to 210 :	0.	0.	0.	24.
210 to 215 :	0.	0.	0.	93.
215 to 220 :	0.	0.	0.	86.
220 to 225 :	0.	0.	0.	27.
225 to 230 :	0.	0.	0.	18.
230 to 235 :	0.	0.	0.	37.
235 to 240 :	0.	0.	0.	3.
240 to 245 :	0.	0.	0.	0.
245 to 250 :	0.	0.	0.	0.

*** HISTogram (THICKness) ***

[THICKness]	Nos. of WAVEform asphalt	C/a RIFmnt
0 to 10 :	0.	0.
10 to 20 :	0.	0.
20 to 30 :	0.	1.
30 to 40 :	0.	2.
40 to 50 :	0.	1.
50 to 60 :	2.	1.
60 to 70 :	0.	8.
70 to 80 :	2.	48.
80 to 90 :	6.	108.
90 to 100 :	169.	79.
100 to 110 :	104.	19.
110 to 120 :	37.	28.
120 to 130 :	1.	25.
130 to 140 :	0.	1.
140 to 150 :	0.	0.
150 to 160 :	0.	0.
160 to 170 :	0.	0.
170 to 180 :	0.	0.
180 to 190 :	0.	0.
190 to 200 :	0.	0.
200 to 210 :	0.	0.
210 to 220 :	0.	0.
220 to 230 :	0.	0.
230 to 240 :	0.	0.
240 to 250 :	0.	0.
250 to 260 :	0.	0.
260 to 270 :	0.	0.
270 to 280 :	0.	0.
280 to 290 :	0.	0.
290 to 300 :	0.	0.

Fig. D.4: Ninth Line-line 4 cluster analysis report

Ninth Line
LINE : 5 CLUSTER ANALYSIS REPORT

*** MEAN values ***

A(131 4.280299) B(141 -1.495157) C(170 .945063) D(220 .087286) THR(92) COR(104)

*** VARiances ***

A(1.9 .040951) B(2.1 .009599) C(14.0 .073927) D(32.4 .004066) THR(70) COR(144)

*** STanDard DEViations ***

A(1.4 .202364) B(1.4 .097975) C(3.7 .271895) D(5.7 .063762) THR(8) COR(12)

*** I of VARIATions ***

A(1.04 4.73) B(1.02 6.55) C(2.20 28.77) D(2.59 73.05) THR(8.70) COR(11.54)

*** HISTogram (PEAKs) ***

[Point SAMPle]	NUMbers of WAVEform at PEAK A	B	C	D
100 to 105 :	0.	0.	0.	0.
105 to 110 :	0.	0.	0.	0.
110 to 115 :	0.	0.	0.	0.
115 to 120 :	0.	0.	0.	0.
120 to 125 :	0.	0.	0.	0.
125 to 130 :	1.	0.	0.	0.
130 to 135 :	310.	0.	0.	0.
135 to 140 :	10.	0.	0.	0.
140 to 145 :	0.	308.	0.	0.
145 to 150 :	0.	13.	0.	0.
150 to 155 :	0.	0.	0.	0.
155 to 160 :	0.	0.	0.	0.
160 to 165 :	0.	0.	4.	0.
165 to 170 :	0.	0.	139.	0.
170 to 175 :	0.	0.	128.	0.
175 to 180 :	0.	0.	42.	0.
180 to 185 :	0.	0.	7.	0.
185 to 190 :	0.	0.	1.	0.
190 to 195 :	0.	0.	0.	0.
195 to 200 :	0.	0.	0.	0.
200 to 205 :	0.	0.	0.	1.
205 to 210 :	0.	0.	0.	2.
210 to 215 :	0.	0.	0.	46.
215 to 220 :	0.	0.	0.	139.
220 to 225 :	0.	0.	0.	39.
225 to 230 :	0.	0.	0.	78.
230 to 235 :	0.	0.	0.	12.
235 to 240 :	0.	0.	0.	4.
240 to 245 :	0.	0.	0.	0.
245 to 250 :	0.	0.	0.	0.

*** HISTogram (THICKness) ***

[THICKness]	Nos. of WAVEform asphalt	C/o RIFsent
0 to 10 :	0.	0.
10 to 20 :	0.	0.
20 to 30 :	0.	0.
30 to 40 :	0.	1.
40 to 50 :	0.	1.
50 to 60 :	1.	0.
60 to 70 :	1.	1.
70 to 80 :	5.	3.
80 to 90 :	117.	5.
90 to 100 :	140.	79.
100 to 110 :	41.	161.
110 to 120 :	16.	41.
120 to 130 :	0.	17.
130 to 140 :	0.	8.
140 to 150 :	0.	4.
150 to 160 :	0.	0.
160 to 170 :	0.	0.
170 to 180 :	0.	0.
180 to 190 :	0.	0.
190 to 200 :	0.	0.
200 to 210 :	0.	0.
210 to 220 :	0.	0.
220 to 230 :	0.	0.
230 to 240 :	0.	0.
240 to 250 :	0.	0.
250 to 260 :	0.	0.
260 to 270 :	0.	0.
270 to 280 :	0.	0.
280 to 290 :	0.	0.
290 to 300 :	0.	0.

Fig. D.5: Ninth Line-line 5 cluster analysis report

Ninth Line
LINE : 6 CLUSTER ANALYSIS REPORT

*** MEAN values ***

A(135 4.135907) B(145 -1.493320) C(173 .547604) D(223 .096955) THK(95) COR(103)

*** VARiances ***

A(.7 .049706) B(.7 .011494) C(19.9 .115898) D(66.1 .006667) THK(119) COR(453)

*** STandard DEViations ***

A(.8 .222950) B(.9 .107209) C(4.5 .340438) D(8.1 .081654) THK(10) COR(21)

*** I of VARIATions ***

A(.60 5.39) B(.60 7.18) C(2.58 62.17) D(3.65 84.22) THK(10.53) COR(20.39)

*** HISTogram (PEAKs) ***

[PoinT SAMPle]	NUMbers of HAVEform at PEAK A	B	C	D
100 to 105 :	0.	0.	0.	0.
105 to 110 :	0.	0.	0.	0.
110 to 115 :	0.	0.	0.	0.
115 to 120 :	0.	0.	0.	0.
120 to 125 :	0.	0.	0.	0.
125 to 130 :	0.	0.	0.	0.
130 to 135 :	69.	0.	0.	0.
135 to 140 :	252.	0.	0.	0.
140 to 145 :	0.	43.	0.	0.
145 to 150 :	0.	278.	0.	0.
150 to 155 :	0.	0.	0.	0.
155 to 160 :	0.	0.	0.	0.
160 to 165 :	0.	0.	6.	0.
165 to 170 :	0.	0.	164.	0.
170 to 175 :	0.	0.	83.	0.
175 to 180 :	0.	0.	35.	0.
180 to 185 :	0.	0.	4.	0.
185 to 190 :	0.	0.	0.	0.
190 to 195 :	0.	0.	0.	0.
195 to 200 :	0.	0.	0.	3.
200 to 205 :	0.	0.	0.	0.
205 to 210 :	0.	0.	0.	10.
210 to 215 :	0.	0.	0.	49.
215 to 220 :	0.	0.	0.	57.
220 to 225 :	0.	0.	0.	21.
225 to 230 :	0.	0.	0.	127.
230 to 235 :	0.	0.	0.	34.
235 to 240 :	0.	0.	0.	19.
240 to 245 :	0.	0.	0.	1.
245 to 250 :	0.	0.	0.	0.

*** HISTogram (THICKness) ***

[THICKness]	Nos. of HAVEform asphalt	C/o RIFsent
0 to 10 :	0.	0.
10 to 20 :	0.	0.
20 to 30 :	0.	0.
30 to 40 :	0.	2.
40 to 50 :	0.	1.
50 to 60 :	2.	3.
60 to 70 :	6.	10.
70 to 80 :	9.	39.
80 to 90 :	64.	48.
90 to 100 :	141.	33.
100 to 110 :	61.	17.
110 to 120 :	33.	90.
120 to 130 :	5.	57.
130 to 140 :	0.	17.
140 to 150 :	0.	4.
150 to 160 :	0.	0.
160 to 170 :	0.	0.
170 to 180 :	0.	0.
180 to 190 :	0.	0.
190 to 200 :	0.	0.
200 to 210 :	0.	0.
210 to 220 :	0.	0.
220 to 230 :	0.	0.
230 to 240 :	0.	0.
240 to 250 :	0.	0.
250 to 260 :	0.	0.
260 to 270 :	0.	0.
270 to 280 :	0.	0.
280 to 290 :	0.	0.
290 to 300 :	0.	0.

Fig. D.6: Ninth Line-line 6 cluster analysis report

Ninth Line
LINE : 7 CLUSTER ANALYSIS REPORT

*** MEAN values ***

A(135	4.151509)	B(145	-1.507321)	C(177	.264528)	D(211	.307143)	THK(103)		COR(72)	

*** VARiances ***

A(1.0	.019271)	B(1.4	.007210)	C(24.6	.026889)	D(9.9	.019655)	THK(153)		COR(162)	

*** STandard DEViations ***

A(1.0	.138821)	B(1.2	.084914)	C(5.0	.163979)	D(3.1	.140196)	THK(12)		COR(12)	

*** % of VARIATions ***

A(.75	3.34)	B(.81	5.63)	C(2.80	61.99)	D(1.49	45.65)	THK(11.65)		COR(16.67)	

*** HISTogram (PEAKs) ***

[Point SAMPle]	NUMbers of WAVEform at PEAK A	B	C	D
100 to 105 :	0.	0.	0.	0.
105 to 110 :	0.	0.	0.	0.
110 to 115 :	0.	0.	0.	0.
115 to 120 :	0.	0.	0.	0.
120 to 125 :	0.	0.	0.	0.
125 to 130 :	0.	0.	0.	0.
130 to 135 :	76.	0.	0.	0.
135 to 140 :	201.	0.	0.	0.
140 to 145 :	2.	35.	0.	0.
145 to 150 :	0.	241.	0.	0.
150 to 155 :	0.	3.	0.	0.
155 to 160 :	0.	0.	0.	0.
160 to 165 :	0.	0.	10.	0.
165 to 170 :	0.	0.	26.	0.
170 to 175 :	0.	0.	15.	0.
175 to 180 :	0.	0.	137.	0.
180 to 185 :	0.	0.	85.	0.
185 to 190 :	0.	0.	6.	0.
190 to 195 :	0.	0.	0.	0.
195 to 200 :	0.	0.	0.	0.
200 to 205 :	0.	0.	0.	1.
205 to 210 :	0.	0.	0.	69.
210 to 215 :	0.	0.	0.	179.
215 to 220 :	0.	0.	0.	30.
220 to 225 :	0.	0.	0.	0.
225 to 230 :	0.	0.	0.	0.
230 to 235 :	0.	0.	0.	0.
235 to 240 :	0.	0.	0.	0.
240 to 245 :	0.	0.	0.	0.
245 to 250 :	0.	0.	0.	0.

*** HISTogram (THICKness) ***

[THICKness]	Nos. of WAVEform asphalt	C/e RIFmnt
0 to 10 :	0.	0.
10 to 20 :	0.	0.
20 to 30 :	0.	0.
30 to 40 :	0.	1.
40 to 50 :	0.	1.
50 to 60 :	0.	28.
60 to 70 :	5.	105.
70 to 80 :	23.	87.
80 to 90 :	15.	22.
90 to 100 :	26.	22.
100 to 110 :	115.	13.
110 to 120 :	89.	0.
120 to 130 :	6.	0.
130 to 140 :	0.	0.
140 to 150 :	0.	0.
150 to 160 :	0.	0.
160 to 170 :	0.	0.
170 to 180 :	0.	0.
180 to 190 :	0.	0.
190 to 200 :	0.	0.
200 to 210 :	0.	0.
210 to 220 :	0.	0.
220 to 230 :	0.	0.
230 to 240 :	0.	0.
240 to 250 :	0.	0.
250 to 260 :	0.	0.
260 to 270 :	0.	0.
270 to 280 :	0.	0.
280 to 290 :	0.	0.
290 to 300 :	0.	0.

Fig. D.7: Ninth Line-line 7 cluster analysis report

Ninth Line
LINE : 8 CLUSTER ANALYSIS REPORT

*** MEAN values ***

A(132 4.247790) B(142 -1.515815) C(178 .414097) D(214 .197519) THK(109) COR(74)

*** VARiances ***

A(1.3 .043426) B(1.6 .011826) C(8.0 .016474) D(18.5 .007238) THK(66) COR(59)

*** STandard DEViations ***

A(1.1 .208390) B(1.3 .108748) C(2.8 .128350) D(4.3 .085076) THK(8) COR(7)

*** % of VARIATions ***

A(.87 4.91) B(.89 7.77) C(1.59 31.00) D(2.01 43.07) THK(7.34) COR(9.46)

*** HISTogram (PEAKs) ***

[Point SAMPle]	Numbers of WAVEform at PEAK A	B	C	D
100 to 105 :	0.	0.	0.	0.
105 to 110 :	0.	0.	0.	0.
110 to 115 :	0.	0.	0.	0.
115 to 120 :	0.	0.	0.	0.
120 to 125 :	0.	0.	0.	0.
125 to 130 :	0.	0.	0.	0.
130 to 135 :	309.	0.	0.	0.
135 to 140 :	12.	0.	0.	0.
140 to 145 :	0.	303.	0.	0.
145 to 150 :	0.	18.	0.	0.
150 to 155 :	0.	0.	0.	0.
155 to 160 :	0.	0.	0.	0.
160 to 165 :	0.	0.	0.	0.
165 to 170 :	0.	0.	7.	0.
170 to 175 :	0.	0.	17.	0.
175 to 180 :	0.	0.	201.	0.
180 to 185 :	0.	0.	93.	0.
185 to 190 :	0.	0.	3.	0.
190 to 195 :	0.	0.	0.	0.
195 to 200 :	0.	0.	0.	0.
200 to 205 :	0.	0.	0.	6.
205 to 210 :	0.	0.	0.	40.
210 to 215 :	0.	0.	0.	138.
215 to 220 :	0.	0.	0.	115.
220 to 225 :	0.	0.	0.	20.
225 to 230 :	0.	0.	0.	2.
230 to 235 :	0.	0.	0.	0.
235 to 240 :	0.	0.	0.	0.
240 to 245 :	0.	0.	0.	0.
245 to 250 :	0.	0.	0.	0.

*** HISTogram (THICKness) ***

[THICKness]	Nos. of WAVEform asphalt	C/o RIFvent
0 to 10 :	0.	0.
10 to 20 :	0.	0.
20 to 30 :	0.	0.
30 to 40 :	0.	1.
40 to 50 :	0.	1.
50 to 60 :	1.	2.
60 to 70 :	0.	75.
70 to 80 :	3.	166.
80 to 90 :	8.	69.
90 to 100 :	13.	6.
100 to 110 :	93.	1.
110 to 120 :	190.	0.
120 to 130 :	13.	0.
130 to 140 :	0.	0.
140 to 150 :	0.	0.
150 to 160 :	0.	0.
160 to 170 :	0.	0.
170 to 180 :	0.	0.
180 to 190 :	0.	0.
190 to 200 :	0.	0.
200 to 210 :	0.	0.
210 to 220 :	0.	0.
220 to 230 :	0.	0.
230 to 240 :	0.	0.
240 to 250 :	0.	0.
250 to 260 :	0.	0.
260 to 270 :	0.	0.
270 to 280 :	0.	0.
280 to 290 :	0.	0.
290 to 300 :	0.	0.

Fig. D.8: Ninth Line-line 8 cluster analysis report

D.2 WINSTON CHURCHILL DATA

The cluster analysis results for Winston Churchill Overpass data are presented in Figs. D.9 to D.15 respectively.

Winston Churchill
LINE : 1, CLUSTER ANALYSIS REPORT

*** MEAN values ***

A(136 5.147407) B(146 -1.827527) C(163 .275143) D(186 .152288) TOT(51) COR(48)

*** VARiances ***

A(6.8 .462126) B(7.2 .230936) C(245.1 .034850) D(215.8 .009255) TOT(1260) COR(158)

*** STandard DEViations ***

A(2.6 .679799) B(2.7 .480588) C(15.7 .186681) D(14.7 .096202) TOT(35) COR(12)

*** % of VARIATions ***

A(1.91 13.21) B(1.84 26.30) C(9.60 67.85) D(7.90 63.17) TOT(68.63) COR(25.00)

*** HISTogram (PEAKs) ***

[Point SAMPle]	NUMbers of HAVEform at PEAK A	B	C	D
100 to 105 :	0.	0.	0.	0.
105 to 110 :	0.	0.	0.	0.
110 to 115 :	0.	0.	0.	0.
115 to 120 :	0.	0.	0.	0.
120 to 125 :	0.	0.	0.	0.
125 to 130 :	0.	0.	0.	0.
130 to 135 :	100.	0.	0.	0.
135 to 140 :	248.	0.	0.	0.
140 to 145 :	30.	86.	0.	0.
145 to 150 :	4.	255.	0.	0.
150 to 155 :	0.	35.	1.	0.
155 to 160 :	0.	6.	93.	0.
160 to 165 :	0.	0.	118.	0.
165 to 170 :	0.	0.	99.	0.
170 to 175 :	0.	0.	44.	11.
175 to 180 :	0.	0.	18.	29.
180 to 185 :	0.	0.	5.	58.
185 to 190 :	0.	0.	1.	144.
190 to 195 :	0.	0.	0.	41.
195 to 200 :	0.	0.	0.	91.
200 to 205 :	0.	0.	0.	5.
205 to 210 :	0.	0.	0.	0.
210 to 215 :	0.	0.	0.	0.
215 to 220 :	0.	0.	0.	0.
220 to 225 :	0.	0.	0.	0.
225 to 230 :	0.	0.	0.	0.
230 to 235 :	0.	0.	0.	0.
235 to 240 :	0.	0.	0.	0.
240 to 245 :	0.	0.	0.	0.
245 to 250 :	0.	0.	0.	0.

*** HISTogram (THICKness) ***

[THICKness]	Nos. of HAVEform asphalt	C/o RIFseat
0 to 10 :	0.	1.
10 to 20 :	1.	2.
20 to 30 :	20.	14.
30 to 40 :	50.	72.
40 to 50 :	122.	143.
50 to 60 :	41.	107.
60 to 70 :	43.	13.
70 to 80 :	71.	18.
80 to 90 :	23.	12.
90 to 100 :	6.	0.
100 to 110 :	1.	0.
110 to 120 :	0.	0.
120 to 130 :	0.	0.
130 to 140 :	0.	0.
140 to 150 :	0.	0.
150 to 160 :	0.	0.
160 to 170 :	0.	0.
170 to 180 :	0.	0.
180 to 190 :	0.	0.
190 to 200 :	0.	0.
200 to 210 :	0.	0.
210 to 220 :	0.	0.
220 to 230 :	0.	0.
230 to 240 :	0.	0.
240 to 250 :	0.	0.
250 to 260 :	0.	0.
260 to 270 :	0.	0.
270 to 280 :	0.	0.
280 to 290 :	0.	0.
290 to 300 :	0.	0.

Fig. D.9: Winston Churchill - line 1 cluster analysis report

Winston Churchill
LINE : 2, CLUSTER ANALYSIS REPORT

*** MEAN values ***

A(134 4.218768) B(144 -1.484732) C(157 .465973) D(179 .176092) THK(54) COR(46)

*** VARiances ***

A(5.7 .078390) B(6.5 .070079) C(32.3 .043879) D(80.6 .015698) THK(203) COR(239)

*** STandard DEViations ***

A(2.4 .279982) B(2.6 .264724) C(5.7 .209473) D(9.0 .124491) THK(14) COR(15)

*** % of VARIATions ***

A(1.78 6.64) B(1.77 17.83) C(3.62 44.95) D(5.01 70.70) THK(25.93) COR(32.61)

*** HISTogram (PEAKs) ***

[Point SAMPle]	Numbers of WAVEform at PEAK A	B	C	D
100 to 105 :	0.	0.	0.	0.
105 to 110 :	0.	0.	0.	0.
110 to 115 :	0.	0.	0.	0.
115 to 120 :	0.	0.	0.	0.
120 to 125 :	0.	0.	0.	0.
125 to 130 :	2.	0.	0.	0.
130 to 135 :	198.	0.	0.	0.
135 to 140 :	166.	2.	0.	0.
140 to 145 :	12.	188.	0.	0.
145 to 150 :	5.	175.	2.	0.
150 to 155 :	0.	12.	133.	0.
155 to 160 :	0.	6.	172.	0.
160 to 165 :	0.	0.	23.	1.
165 to 170 :	0.	0.	26.	23.
170 to 175 :	0.	0.	24.	123.
175 to 180 :	0.	0.	3.	85.
180 to 185 :	0.	0.	0.	27.
185 to 190 :	0.	0.	0.	53.
190 to 195 :	0.	0.	0.	23.
195 to 200 :	0.	0.	0.	45.
200 to 205 :	0.	0.	0.	3.
205 to 210 :	0.	0.	0.	0.
210 to 215 :	0.	0.	0.	0.
215 to 220 :	0.	0.	0.	0.
220 to 225 :	0.	0.	0.	0.
225 to 230 :	0.	0.	0.	0.
230 to 235 :	0.	0.	0.	0.
235 to 240 :	0.	0.	0.	0.
240 to 245 :	0.	0.	0.	0.
245 to 250 :	0.	0.	0.	0.

*** HISTogram (THICKness) ***

[THICKness]	Nos. of WAVEform asphalt	C/o RIFvent
0 to 10 :	0.	0.
10 to 20 :	0.	1.
20 to 30 :	1.	12.
30 to 40 :	1.	147.
40 to 50 :	178.	129.
50 to 60 :	129.	36.
60 to 70 :	10.	15.
70 to 80 :	26.	13.
80 to 90 :	22.	23.
90 to 100 :	11.	7.
100 to 110 :	5.	0.
110 to 120 :	0.	0.
120 to 130 :	0.	0.
130 to 140 :	0.	0.
140 to 150 :	0.	0.
150 to 160 :	0.	0.
160 to 170 :	0.	0.
170 to 180 :	0.	0.
180 to 190 :	0.	0.
190 to 200 :	0.	0.
200 to 210 :	0.	0.
210 to 220 :	0.	0.
220 to 230 :	0.	0.
230 to 240 :	0.	0.
240 to 250 :	0.	0.
250 to 260 :	0.	0.
260 to 270 :	0.	0.
270 to 280 :	0.	0.
280 to 290 :	0.	0.
290 to 300 :	0.	0.

Fig. D.10: Winston Churchill - line 2 cluster analysis report

Winston Churchill
LINE : 3, CLUSTER ANALYSIS REPORT

*** MEAN values ***

A(133 4.016101) B(143 -1.288800) C(155 .466972) D(177 .191100) THR(54) COR(44)

*** VARiances ***

A(3.7 .121440) B(5.0 .178314) C(42.0 .097434) D(43.3 .011284) THR(232) COR(109)

*** STandard DEViations ***

A(1.9 .348493) B(2.2 .422273) C(6.5 .312144) D(6.6 .106228) THR(15) COR(10)

*** % of VARIATions ***

A(1.46 8.68) B(1.56 32.76) C(4.18 66.84) D(3.72 55.59) THR(27.78) COR(22.73)

*** HISTogram (PEAKs) ***

[Point SAMPle]	Numbers of WAVEform at PEAK A	B	C	D
100 to 105 :	0.	0.	0.	0.
105 to 110 :	0.	0.	0.	0.
110 to 115 :	0.	0.	0.	0.
115 to 120 :	0.	0.	0.	0.
120 to 125 :	0.	0.	0.	0.
125 to 130 :	1.	0.	0.	0.
130 to 135 :	324.	0.	0.	0.
135 to 140 :	47.	1.	0.	0.
140 to 145 :	11.	318.	0.	0.
145 to 150 :	0.	52.	38.	0.
150 to 155 :	0.	12.	196.	0.
155 to 160 :	0.	0.	77.	0.
160 to 165 :	0.	0.	21.	1.
165 to 170 :	0.	0.	36.	33.
170 to 175 :	0.	0.	11.	115.
175 to 180 :	0.	0.	2.	124.
180 to 185 :	0.	0.	1.	50.
185 to 190 :	0.	0.	1.	42.
190 to 195 :	0.	0.	0.	4.
195 to 200 :	0.	0.	0.	13.
200 to 205 :	0.	0.	0.	0.
205 to 210 :	0.	0.	0.	1.
210 to 215 :	0.	0.	0.	0.
215 to 220 :	0.	0.	0.	0.
220 to 225 :	0.	0.	0.	0.
225 to 230 :	0.	0.	0.	0.
230 to 235 :	0.	0.	0.	0.
235 to 240 :	0.	0.	0.	0.
240 to 245 :	0.	0.	0.	0.
245 to 250 :	0.	0.	0.	0.

*** HISTogram (THICKness) ***

[THICKness]	Nos. of WAVEform asphalt	C/o RIFcent
0 to 10 :	0.	0.
10 to 20 :	0.	1.
20 to 30 :	1.	20.
30 to 40 :	13.	105.
40 to 50 :	185.	151.
50 to 60 :	109.	58.
60 to 70 :	15.	45.
70 to 80 :	11.	2.
80 to 90 :	31.	1.
90 to 100 :	11.	0.
100 to 110 :	7.	0.
110 to 120 :	0.	0.
120 to 130 :	0.	0.
130 to 140 :	0.	0.
140 to 150 :	0.	0.
150 to 160 :	0.	0.
160 to 170 :	0.	0.
170 to 180 :	0.	0.
180 to 190 :	0.	0.
190 to 200 :	0.	0.
200 to 210 :	0.	0.
210 to 220 :	0.	0.
220 to 230 :	0.	0.
230 to 240 :	0.	0.
240 to 250 :	0.	0.
250 to 260 :	0.	0.
260 to 270 :	0.	0.
270 to 280 :	0.	0.
280 to 290 :	0.	0.
290 to 300 :	0.	0.

Fig. D.11: Winston Churchill - line 3 cluster analysis report

Winston Churchill
LINE : 4, CLUSTER ANALYSIS REPORT

*** MEAN values ***

A(	134	4.021481)	B(	144	-1.254416)	C(	157	.411286)	D(	181	.191049)	TRK(58)	COR(48)

*** VARiances ***

A(	3.4	.115845)	B(	5.0	.165050)	C(	57.4	.089356)	D(	77.9	.007375)	TRK(355)	COR(189)

*** STandard DEViations ***

A(	1.8	.340360)	B(	2.2	.406264)	C(	7.6	.298925)	D(	8.8	.085876)	TRK(18)	COR(13)

*** % of VARIATions ***

A(	1.37	8.46)	B(	1.55	32.39)	C(	4.83	72.68)	D(	4.88	44.95)	TRK(11.03)	COR(27.08)

*** HISTogram (PEAKs) ***

[Point SAMPle]	Numbers of WAVEform at PEAK A	B	C	D
100 to 105 :	0.	0.	0.	0.
105 to 110 :	0.	0.	0.	0.
110 to 115 :	0.	0.	0.	0.
115 to 120 :	0.	0.	0.	0.
120 to 125 :	0.	0.	0.	0.
125 to 130 :	1.	0.	0.	0.
130 to 135 :	228.	0.	0.	0.
135 to 140 :	143.	2.	0.	0.
140 to 145 :	10.	255.	2.	0.
145 to 150 :	1.	112.	16.	0.
150 to 155 :	0.	13.	144.	0.
155 to 160 :	0.	1.	113.	0.
160 to 165 :	0.	0.	40.	1.
165 to 170 :	0.	0.	25.	28.
170 to 175 :	0.	0.	18.	66.
175 to 180 :	0.	0.	25.	117.
180 to 185 :	0.	0.	0.	38.
185 to 190 :	0.	0.	0.	46.
190 to 195 :	0.	0.	0.	22.
195 to 200 :	0.	0.	0.	65.
200 to 205 :	0.	0.	0.	0.
205 to 210 :	0.	0.	0.	0.
210 to 215 :	0.	0.	0.	0.
215 to 220 :	0.	0.	0.	0.
220 to 225 :	0.	0.	0.	0.
225 to 230 :	0.	0.	0.	0.
230 to 235 :	0.	0.	0.	0.
235 to 240 :	0.	0.	0.	0.
240 to 245 :	0.	0.	0.	0.
245 to 250 :	0.	0.	0.	0.

*** HISTogram (THICKness) ***

[THICKness]	Nos. of WAVEform asphalt	C/o RIFsect
0 to 10 :	0.	0.
10 to 20 :	1.	1.
20 to 30 :	0.	9.
30 to 40 :	10.	84.
40 to 50 :	159.	160.
50 to 60 :	103.	69.
60 to 70 :	31.	17.
70 to 80 :	14.	19.
80 to 90 :	16.	23.
90 to 100 :	30.	1.
100 to 110 :	19.	0.
110 to 120 :	0.	0.
120 to 130 :	0.	0.
130 to 140 :	0.	0.
140 to 150 :	0.	0.
150 to 160 :	0.	0.
160 to 170 :	0.	0.
170 to 180 :	0.	0.
180 to 190 :	0.	0.
190 to 200 :	0.	0.
200 to 210 :	0.	0.
210 to 220 :	0.	0.
220 to 230 :	0.	0.
230 to 240 :	0.	0.
240 to 250 :	0.	0.
250 to 260 :	0.	0.
260 to 270 :	0.	0.
270 to 280 :	0.	0.
280 to 290 :	0.	0.
290 to 300 :	0.	0.

Fig. D.12: Winston Churchill - line 4 cluster analysis report

Winston Churchill
LINE : 5, CLUSTER ANALYSIS REPORT

*** MEAN values ***

A(135 3.960004) B(145 -1.261490) C(160 .437055) D(185 .151296) THK(63) COR(50)

*** VARIances ***

A(4.0 .090815) B(4.5 .118269) C(72.6 .064139) D(88.7 .006203) THK(494) COR(284)

*** STandard DEViations ***

A(2.0 .314349) B(2.1 .343902) C(8.5 .253256) D(9.4 .078760) THK(22) COR(16)

*** % of VARIATions ***

A(1.48 7.92) B(1.45 27.26) C(5.32 57.95) D(5.09 52.06) THK(34.92) COR(32.00)

*** HISTogram (PEAKs) ***

[Point SAMPle]	NUMbers of WAVEform at PEAK A	B	C	D
100 to 105 :	0.	0.	0.	0.
105 to 110 :	0.	0.	0.	0.
110 to 115 :	0.	0.	0.	0.
115 to 120 :	0.	0.	0.	0.
120 to 125 :	0.	0.	0.	0.
125 to 130 :	0.	0.	0.	0.
130 to 135 :	47.	0.	0.	0.
135 to 140 :	322.	0.	0.	0.
140 to 145 :	9.	96.	0.	0.
145 to 150 :	4.	271.	2.	0.
150 to 155 :	0.	8.	98.	0.
155 to 160 :	0.	7.	145.	0.
160 to 165 :	0.	0.	17.	0.
165 to 170 :	0.	0.	25.	5.
170 to 175 :	0.	0.	68.	77.
175 to 180 :	0.	0.	22.	56.
180 to 185 :	0.	0.	2.	22.
185 to 190 :	0.	0.	3.	75.
190 to 195 :	0.	0.	0.	21.
195 to 200 :	0.	0.	0.	121.
200 to 205 :	0.	0.	0.	2.
205 to 210 :	0.	0.	0.	3.
210 to 215 :	0.	0.	0.	0.
215 to 220 :	0.	0.	0.	0.
220 to 225 :	0.	0.	0.	0.
225 to 230 :	0.	0.	0.	0.
230 to 235 :	0.	0.	0.	0.
235 to 240 :	0.	0.	0.	0.
240 to 245 :	0.	0.	0.	0.
245 to 250 :	0.	0.	0.	0.

*** HISTogram (THICKness) ***

[THICKness]	Nos. of WAVEform asphalt	C/e RIFsent
0 to 10 :	0.	1.
10 to 20 :	1.	3.
20 to 30 :	0.	12.
30 to 40 :	2.	94.
40 to 50 :	134.	122.
50 to 60 :	113.	60.
60 to 70 :	20.	32.
70 to 80 :	8.	14.
80 to 90 :	10.	42.
90 to 100 :	66.	2.
100 to 110 :	20.	0.
110 to 120 :	4.	0.
120 to 130 :	3.	0.
130 to 140 :	1.	0.
140 to 150 :	0.	0.
150 to 160 :	0.	0.
160 to 170 :	0.	0.
170 to 180 :	0.	0.
180 to 190 :	0.	0.
190 to 200 :	0.	0.
200 to 210 :	0.	0.
210 to 220 :	0.	0.
220 to 230 :	0.	0.
230 to 240 :	0.	0.
240 to 250 :	0.	0.
250 to 260 :	0.	0.
260 to 270 :	0.	0.
270 to 280 :	0.	0.
280 to 290 :	0.	0.
290 to 300 :	0.	0.

Fig. D.13: Winston Churchill - line 5 cluster analysis report

Winston Churchill
LINE : 6, CLUSTER ANALYSIS REPORT

*** MEAN values ***

A(136 4.020952) B(145 -1.427403) C(159 .475911) D(179 .141799) THK(58) COR(42)

*** VARiances ***

A(5.7 .068144) B(7.2 .046290) C(39.5 .055329) D(64.6 .012479) THK(212) COR(103)

*** STandard DEViations ***

A(2.4 .261045) B(2.7 .215151) C(6.3 .235221) D(8.0 .111709) THK(14) COR(10)

*** % of VARIATions ***

A(1.75 6.49) B(1.86 15.07) C(3.95 49.43) D(4.49 78.78) THK(24.14) COR(23.81)

*** HISTogram (PEAKs) ***

[Point SAMPle]	Numbers of WAVEform at PEAK A	B	C	D
100 to 105 :	0.	0.	0.	0.
105 to 110 :	0.	0.	0.	0.
110 to 115 :	0.	0.	0.	0.
115 to 120 :	0.	0.	0.	0.
120 to 125 :	0.	0.	0.	0.
125 to 130 :	0.	0.	0.	0.
130 to 135 :	49.	0.	0.	0.
135 to 140 :	306.	0.	0.	0.
140 to 145 :	8.	53.	0.	0.
145 to 150 :	9.	101.	0.	0.
150 to 155 :	1.	9.	49.	0.
155 to 160 :	0.	8.	235.	0.
160 to 165 :	0.	2.	20.	0.
165 to 170 :	0.	0.	14.	23.
170 to 175 :	0.	0.	55.	91.
175 to 180 :	0.	0.	0.	101.
180 to 185 :	0.	0.	0.	36.
185 to 190 :	0.	0.	0.	73.
190 to 195 :	0.	0.	0.	15.
195 to 200 :	0.	0.	0.	31.
200 to 205 :	0.	0.	0.	3.
205 to 210 :	0.	0.	0.	0.
210 to 215 :	0.	0.	0.	0.
215 to 220 :	0.	0.	0.	0.
220 to 225 :	0.	0.	0.	0.
225 to 230 :	0.	0.	0.	0.
230 to 235 :	0.	0.	0.	0.
235 to 240 :	0.	0.	0.	0.
240 to 245 :	0.	0.	0.	0.
245 to 250 :	0.	0.	0.	0.

*** HISTogram (THICKness) ***

[THICKness]	Nos. of WAVEform asphalt	C/o RIFacet
0 to 10 :	0.	0.
10 to 20 :	1.	0.
20 to 30 :	0.	24.
30 to 40 :	1.	154.
40 to 50 :	81.	102.
50 to 60 :	205.	60.
60 to 70 :	26.	29.
70 to 80 :	7.	2.
80 to 90 :	13.	2.
90 to 100 :	38.	0.
100 to 110 :	1.	0.
110 to 120 :	0.	0.
120 to 130 :	0.	0.
130 to 140 :	0.	0.
140 to 150 :	0.	0.
150 to 160 :	0.	0.
160 to 170 :	0.	0.
170 to 180 :	0.	0.
180 to 190 :	0.	0.
190 to 200 :	0.	0.
200 to 210 :	0.	0.
210 to 220 :	0.	0.
220 to 230 :	0.	0.
230 to 240 :	0.	0.
240 to 250 :	0.	0.
250 to 260 :	0.	0.
260 to 270 :	0.	0.
270 to 280 :	0.	0.
280 to 290 :	0.	0.
290 to 300 :	0.	0.

Fig. D.14: Winston Churchill - line 6 cluster analysis report

Winston Churchill
LINE : 7, CLUSTER ANALYSIS REPORT

*** MEAN values ***

A(133 4.352026) B(143 -1.560533) C(156 .464460) D(175 .170103) THR(52) COR(40)

*** VARiances ***

A(2.7 .039195) B(3.4 .038122) C(25.1 .050365) D(42.1 .010037) THR(127) COR(71)

*** STandard DEViations ***

A(1.6 .243300) B(1.8 .195252) C(5.0 .224422) D(6.5 .100183) THR(11) COR(8)

*** I of VARIATions ***

A(1.22 5.59) B(1.29 12.51) C(3.21 48.32) D(3.71 58.90) THR(21.15) COR(20.00)

*** HISTogram (PEAKs) ***

[Point SAMPle]	Numbers of WAVEform at PEAK A	B	C	D
100 to 105 :	0.	0.	0.	0.
105 to 110 :	0.	0.	0.	0.
110 to 115 :	0.	0.	0.	0.
115 to 120 :	0.	0.	0.	0.
120 to 125 :	0.	0.	0.	0.
125 to 130 :	3.	0.	0.	0.
130 to 135 :	354.	0.	0.	0.
135 to 140 :	16.	3.	0.	0.
140 to 145 :	7.	318.	0.	0.
145 to 150 :	0.	52.	4.	0.
150 to 155 :	0.	7.	165.	0.
155 to 160 :	0.	0.	155.	0.
160 to 165 :	0.	0.	23.	11.
165 to 170 :	0.	0.	20.	47.
170 to 175 :	0.	0.	9.	121.
175 to 180 :	0.	0.	4.	117.
180 to 185 :	0.	0.	0.	42.
185 to 190 :	0.	0.	0.	30.
190 to 195 :	0.	0.	0.	3.
195 to 200 :	0.	0.	0.	9.
200 to 205 :	0.	0.	0.	0.
205 to 210 :	0.	0.	0.	0.
210 to 215 :	0.	0.	0.	0.
215 to 220 :	0.	0.	0.	0.
220 to 225 :	0.	0.	0.	0.
225 to 230 :	0.	0.	0.	0.
230 to 235 :	0.	0.	0.	0.
235 to 240 :	0.	0.	0.	0.
240 to 245 :	0.	0.	0.	0.
245 to 250 :	0.	0.	0.	0.

*** HISTogram (THICKness) ***

[THICKness]	Nos. of WAVEform asphalt	C/o RIFmnt
0 to 10 :	0.	0.
10 to 20 :	0.	1.
20 to 30 :	1.	37.
30 to 40 :	0.	153.
40 to 50 :	174.	124.
50 to 60 :	155.	57.
60 to 70 :	12.	1.
70 to 80 :	20.	0.
80 to 90 :	8.	0.
90 to 100 :	8.	0.
100 to 110 :	2.	0.
110 to 120 :	0.	0.
120 to 130 :	0.	0.
130 to 140 :	0.	0.
140 to 150 :	0.	0.
150 to 160 :	0.	0.
160 to 170 :	0.	0.
170 to 180 :	0.	0.
180 to 190 :	0.	0.
190 to 200 :	0.	0.
200 to 210 :	0.	0.
210 to 220 :	0.	0.
220 to 230 :	0.	0.
230 to 240 :	0.	0.
240 to 250 :	0.	0.
250 to 260 :	0.	0.
260 to 270 :	0.	0.
270 to 280 :	0.	0.
280 to 290 :	0.	0.
290 to 300 :	0.	0.

Fig. D.15: Winston Churchill - line 7 cluster analysis report

D.3 BLOOR VIADUCT DATA

The cluster analysis results for Bloor Viaduct bridge deck are given in Figs. D.16 to D.21 for the eastbound and Figs. D.22 to D.27 for the westbound.

Bloor Viaduct EASTbound
LINE : 1, CLUSTER ANALYSIS REPORT

*** MEAN values ***

A(134 4.414333) B(143 -1.675633) C(197 .164571) D(231 .111123) THR(152) COR(70)

*** VARiances ***

A(1.0 .042187) B(2.2 .058466) C(13.8 .018206) D(56.4 .003918) THR(119) COR(180)

*** STandard DEViations ***

A(1.0 .205395) B(1.5 .241797) C(3.7 .134931) D(7.5 .062592) THR(10) COR(13)

*** % of VARIATions ***

A(.75 4.65) B(1.03 14.43) C(1.89 81.99) D(3.25 56.33) THR(6.58) COR(10.57)

*** HISTogram (PEAKs) ***

[Point SAMPle]	Numbers of WAVEform at PEAK A	B	C	D
100 to 105 :	0.	0.	0.	0.
105 to 110 :	0.	0.	0.	0.
110 to 115 :	0.	0.	0.	0.
115 to 120 :	0.	0.	0.	0.
120 to 125 :	0.	0.	0.	0.
125 to 130 :	0.	0.	0.	0.
130 to 135 :	1632.	0.	0.	0.
135 to 140 :	595.	0.	0.	0.
140 to 145 :	3.	1639.	0.	0.
145 to 150 :	0.	585.	0.	0.
150 to 155 :	0.	6.	0.	0.
155 to 160 :	0.	0.	0.	0.
160 to 165 :	0.	0.	0.	0.
165 to 170 :	0.	0.	0.	0.
170 to 175 :	0.	0.	0.	0.
175 to 180 :	0.	0.	0.	0.
180 to 185 :	0.	0.	0.	0.
185 to 190 :	0.	0.	7.	0.
190 to 195 :	0.	0.	270.	3.
195 to 200 :	0.	0.	1241.	0.
200 to 205 :	0.	0.	503.	0.
205 to 210 :	0.	0.	207.	1.
210 to 215 :	0.	0.	2.	12.
215 to 220 :	0.	0.	0.	111.
220 to 225 :	0.	0.	0.	122.
225 to 230 :	0.	0.	0.	869.
230 to 235 :	0.	0.	0.	371.
235 to 240 :	0.	0.	0.	168.
240 to 245 :	0.	0.	0.	209.
245 to 250 :	0.	0.	0.	144.

*** HISTogram (THICKness) ***

[THICKness]	Nos. of WAVEform asphalt	C/o RIFmont
0 to 10 :	0.	0.
10 to 20 :	0.	0.
20 to 30 :	0.	0.
30 to 40 :	0.	23.
40 to 50 :	0.	94.
50 to 60 :	0.	300.
60 to 70 :	0.	713.
70 to 80 :	0.	474.
80 to 90 :	0.	491.
90 to 100 :	0.	116.
100 to 110 :	0.	12.
110 to 120 :	1.	6.
120 to 130 :	26.	1.
130 to 140 :	200.	0.
140 to 150 :	744.	0.
150 to 160 :	729.	0.
160 to 170 :	353.	0.
170 to 180 :	151.	0.
180 to 190 :	24.	0.
190 to 200 :	2.	0.
200 to 210 :	0.	0.
210 to 220 :	0.	0.
220 to 230 :	0.	0.
230 to 240 :	0.	0.
240 to 250 :	0.	0.
250 to 260 :	0.	0.
260 to 270 :	0.	0.
270 to 280 :	0.	0.
280 to 290 :	0.	0.
290 to 300 :	0.	0.

Fig. D.16: Bloor Viaduct Eastbound-line 1 cluster analysis report

Bloor Viaduct EASTbound
LINE : 2, CLUSTER ANALYSIS REPORT

*** MEAN values ***

A(132	4.1731666)	B(142	-1.400673)	C(196	.244676)	D(231	.223968)	THK(161)	COR(73)

*** VARIances ***

A(2.1	.027718)	B(1.5	.006956)	C(17.9	.031151)	D(52.9	.008326)	THK(145)	COR(157)

*** STandard DEViations ***

A(1.5	.166487)	B(1.2	.294884)	C(4.2	.176495)	D(7.3	.091245)	THK(12)	COR(12)

*** % of VARIATions ***

A(1.10	3.99)	B(.87	21.05)	C(2.16	72.13)	D(3.15	40.74)	THK(7.45)	COR(16.44)

*** HISTogram (PEAKs) ***

[Point SAMPle]	Numbers of WAVEform at PEAK A	B	C	D
100 to 105 :	0.	0.	0.	0.
105 to 110 :	0.	0.	0.	0.
110 to 115 :	0.	0.	0.	0.
115 to 120 :	0.	0.	0.	0.
120 to 125 :	0.	0.	0.	0.
125 to 130 :	3.	0.	0.	0.
130 to 135 :	2095.	0.	0.	0.
135 to 140 :	118.	5.	0.	0.
140 to 145 :	4.	2121.	0.	0.
145 to 150 :	0.	91.	0.	0.
150 to 155 :	0.	3.	0.	0.
155 to 160 :	0.	0.	0.	0.
160 to 165 :	0.	0.	0.	0.
165 to 170 :	0.	0.	0.	0.
170 to 175 :	0.	0.	0.	0.
175 to 180 :	0.	0.	0.	0.
180 to 185 :	0.	0.	0.	0.
185 to 190 :	0.	0.	64.	0.
190 to 195 :	0.	0.	676.	0.
195 to 200 :	0.	0.	877.	0.
200 to 205 :	0.	0.	428.	0.
205 to 210 :	0.	0.	171.	0.
210 to 215 :	0.	0.	4.	15.
215 to 220 :	0.	0.	0.	100.
220 to 225 :	0.	0.	0.	156.
225 to 230 :	0.	0.	0.	744.
230 to 235 :	0.	0.	0.	441.
235 to 240 :	0.	0.	0.	415.
240 to 245 :	0.	0.	0.	214.
245 to 250 :	0.	0.	0.	117.

*** HISTogram (THICKness) ***

[THICKness]	Nos. of WAVEform asphalt	C/o RIFpent
0 to 10 :	0.	0.
10 to 20 :	0.	0.
20 to 30 :	0.	0.
30 to 40 :	0.	12.
40 to 50 :	0.	102.
50 to 60 :	0.	199.
60 to 70 :	0.	494.
70 to 80 :	0.	613.
80 to 90 :	0.	689.
90 to 100 :	0.	107.
100 to 110 :	0.	3.
110 to 120 :	0.	1.
120 to 130 :	0.	0.
130 to 140 :	41.	0.
140 to 150 :	259.	0.
150 to 160 :	829.	0.
160 to 170 :	568.	0.
170 to 180 :	345.	0.
180 to 190 :	126.	0.
190 to 200 :	40.	0.
200 to 210 :	11.	0.
210 to 220 :	1.	0.
220 to 230 :	0.	0.
230 to 240 :	0.	0.
240 to 250 :	0.	0.
250 to 260 :	0.	0.
260 to 270 :	0.	0.
270 to 280 :	0.	0.
280 to 290 :	0.	0.
290 to 300 :	0.	0.

Fig. D.17: Bloor Viaduct Eastbound-line 2 cluster analysis report

Bloor Viaduct EASTbound
LINE : 3, CLUSTER ANALYSIS REPORT

*** MEAN values ***

A(134 4.272526) B(144 -1.200664) C(197 .195647) D(231 .200538) THK(154) CBR(71)

*** VARiances ***

A(2.0 .037462) B(1.9 .077687) C(17.7 .030033) D(44.6 .008190) THK(159) CBR(166)

*** STanDard DEViations ***

A(1.4 .193549) B(1.4 .278724) C(4.2 .173300) D(6.7 .090500) THK(12) CBR(12)

*** % of VARIATions ***

A(1.06 4.53) B(.95 23.21) C(2.13 88.58) D(2.89 43.40) THK(7.79) CBR(16.90)

*** HISTogram (PEAKs) ***

[Point SAMPle]	Numbers of WAVEform at PEAK A	B	C	D
100 to 105 :	0.	0.	0.	0.
105 to 110 :	0.	0.	0.	0.
110 to 115 :	0.	0.	0.	0.
115 to 120 :	0.	0.	0.	0.
120 to 125 :	0.	0.	0.	0.
125 to 130 :	0.	0.	0.	0.
130 to 135 :	696.	0.	0.	0.
135 to 140 :	1516.	0.	0.	0.
140 to 145 :	7.	1156.	0.	0.
145 to 150 :	1.	1054.	0.	0.
150 to 155 :	0.	9.	0.	0.
155 to 160 :	0.	1.	0.	0.
160 to 165 :	0.	0.	0.	0.
165 to 170 :	0.	0.	0.	0.
170 to 175 :	0.	0.	0.	0.
175 to 180 :	0.	0.	0.	0.
180 to 185 :	0.	0.	0.	0.
185 to 190 :	0.	0.	4.	0.
190 to 195 :	0.	0.	473.	0.
195 to 200 :	0.	0.	1151.	0.
200 to 205 :	0.	0.	342.	0.
205 to 210 :	0.	0.	231.	0.
210 to 215 :	0.	0.	17.	2.
215 to 220 :	0.	0.	2.	54.
220 to 225 :	0.	0.	0.	108.
225 to 230 :	0.	0.	0.	928.
230 to 235 :	0.	0.	0.	491.
235 to 240 :	0.	0.	0.	361.
240 to 245 :	0.	0.	0.	134.
245 to 250 :	0.	0.	0.	117.

*** HISTogram (THICKness) ***

[THICKness]	Nos. of WAVEform asphalt	C/a RIFsent
0 to 10 :	0.	0.
10 to 20 :	0.	0.
20 to 30 :	0.	0.
30 to 40 :	0.	19.
40 to 50 :	0.	132.
50 to 60 :	0.	216.
60 to 70 :	0.	622.
70 to 80 :	0.	607.
80 to 90 :	0.	511.
90 to 100 :	0.	109.
100 to 110 :	0.	2.
110 to 120 :	1.	2.
120 to 130 :	3.	0.
130 to 140 :	128.	0.
140 to 150 :	733.	0.
150 to 160 :	766.	0.
160 to 170 :	319.	0.
170 to 180 :	137.	0.
180 to 190 :	101.	0.
190 to 200 :	27.	0.
200 to 210 :	4.	0.
210 to 220 :	1.	0.
220 to 230 :	0.	0.
230 to 240 :	0.	0.
240 to 250 :	0.	0.
250 to 260 :	0.	0.
260 to 270 :	0.	0.
270 to 280 :	0.	0.
280 to 290 :	0.	0.
290 to 300 :	0.	0.

Fig. D.18: Bloor Viaduct Eastbound-line 3 cluster analysis report

Bloor Viaduct EASTbound
LINE : 4, CLUSTER ANALYSIS REPORT

*** MEAN values ***

A(134	4.153273)	B(143	-1.296643)	C(206	.087241)	D(239	.206326)	THR(179)	COR(69)

*** VARIances ***

A(1.7	.038520)	B(2.8	.111930)	C(20.4	.023702)	D(64.0	.006244)	THR(206)	COR(245)

*** STandard DEViations ***

A(1.3	.196264)	B(1.7	.334560)	C(4.5	.153955)	D(8.0	.079019)	THR(14)	COR(15)

*** % of VARIATions ***

A(.97	4.73)	B(1.16	25.80)	C(2.19	176.47)	D(3.35	38.30)	THR(7.82)	COR(21.74)

*** HISTogram (PEAKs) ***

[Point SAMPle]	Numbers of WAVEform at PEAK A	B	C	D
100 to 105 :	0.	0.	0.	0.
105 to 110 :	0.	0.	0.	0.
110 to 115 :	0.	0.	0.	0.
115 to 120 :	0.	0.	0.	0.
120 to 125 :	0.	0.	0.	0.
125 to 130 :	0.	0.	0.	0.
130 to 135 :	1112.	0.	0.	0.
135 to 140 :	1097.	0.	0.	0.
140 to 145 :	14.	1668.	0.	0.
145 to 150 :	0.	537.	0.	0.
150 to 155 :	0.	18.	0.	0.
155 to 160 :	0.	0.	0.	0.
160 to 165 :	0.	0.	0.	0.
165 to 170 :	0.	0.	0.	0.
170 to 175 :	0.	0.	0.	0.
175 to 180 :	0.	0.	0.	0.
180 to 185 :	0.	0.	0.	0.
185 to 190 :	0.	0.	0.	0.
190 to 195 :	0.	0.	0.	0.
195 to 200 :	0.	0.	97.	0.
200 to 205 :	0.	0.	505.	0.
205 to 210 :	0.	0.	1171.	0.
210 to 215 :	0.	0.	348.	0.
215 to 220 :	0.	0.	100.	2.
220 to 225 :	0.	0.	1.	34.
225 to 230 :	0.	0.	0.	179.
230 to 235 :	0.	0.	0.	357.
235 to 240 :	0.	0.	0.	624.
240 to 245 :	0.	0.	0.	262.
245 to 250 :	0.	0.	0.	458.

*** HISTogram (THICKness) ***

[THICKness]	Nos. of WAVEform asphalt	C/e RIFcent
0 to 10 :	0.	0.
10 to 20 :	0.	0.
20 to 30 :	0.	0.
30 to 40 :	0.	69.
40 to 50 :	0.	310.
50 to 60 :	0.	198.
60 to 70 :	0.	431.
70 to 80 :	0.	530.
80 to 90 :	0.	562.
90 to 100 :	0.	115.
100 to 110 :	0.	4.
110 to 120 :	0.	3.
120 to 130 :	0.	1.
130 to 140 :	0.	0.
140 to 150 :	9.	0.
150 to 160 :	122.	0.
160 to 170 :	396.	0.
170 to 180 :	764.	0.
180 to 190 :	486.	0.
190 to 200 :	202.	0.
200 to 210 :	146.	0.
210 to 220 :	80.	0.
220 to 230 :	17.	0.
230 to 240 :	1.	0.
240 to 250 :	0.	0.
250 to 260 :	0.	0.
260 to 270 :	0.	0.
270 to 280 :	0.	0.
280 to 290 :	0.	0.
290 to 300 :	0.	0.

Fig. D.19: Bloor Viaduct Eastbound-line 4 cluster analysis report

Bloor Viaduct EASTbound
LINE : 5, CLUSTER ANALYSIS REPORT

*** MEAN values ***

A(135 4.037404) B(144 -1.247714) C(207 .122612) D(241 .152455) THR(184) COR(71)

*** VARiances ***

A(1.3 .024859) B(2.1 .044724) C(24.1 .027611) D(74.2 .004884) THR(200) COR(235)

*** STandard DEViations ***

A(1.2 .157667) B(1.5 .258309) C(4.9 .166167) D(8.6 .069888) THR(14) COR(15)

*** % of VARIATions ***

A(.85 3.91) B(1.01 20.70) C(2.37 135.52) D(3.57 45.84) THR(7.61) COR(21.13)

*** HISTogram (PEAKs) ***

[Point SAMPle]	Numbers of WAVEform at PEAK A	B	C	D
100 to 105 :	0.	0.	0.	0.
105 to 110 :	0.	0.	0.	0.
110 to 115 :	0.	0.	0.	0.
115 to 120 :	0.	0.	0.	0.
120 to 125 :	0.	0.	0.	0.
125 to 130 :	0.	0.	0.	0.
130 to 135 :	549.	0.	0.	0.
135 to 140 :	1660.	0.	0.	0.
140 to 145 :	15.	1138.	0.	0.
145 to 150 :	1.	1074.	0.	0.
150 to 155 :	0.	12.	0.	0.
155 to 160 :	0.	1.	0.	0.
160 to 165 :	0.	0.	0.	0.
165 to 170 :	0.	0.	0.	0.
170 to 175 :	0.	0.	0.	0.
175 to 180 :	0.	0.	0.	0.
180 to 185 :	0.	0.	0.	0.
185 to 190 :	0.	0.	0.	0.
190 to 195 :	0.	0.	0.	0.
195 to 200 :	0.	0.	80.	0.
200 to 205 :	0.	0.	521.	0.
205 to 210 :	0.	0.	1010.	0.
210 to 215 :	0.	0.	476.	0.
215 to 220 :	0.	0.	135.	4.
220 to 225 :	0.	0.	2.	50.
225 to 230 :	0.	0.	1.	189.
230 to 235 :	0.	0.	0.	208.
235 to 240 :	0.	0.	0.	461.
240 to 245 :	0.	0.	0.	267.
245 to 250 :	0.	0.	0.	556.

*** HISTogram (THICKness) ***

[THICKness]	Nos. of WAVEform asphalt	C/o RIFmnt
0 to 10 :	0.	0.
10 to 20 :	0.	0.
20 to 30 :	0.	0.
30 to 40 :	0.	51.
40 to 50 :	0.	232.
50 to 60 :	0.	246.
60 to 70 :	0.	306.
70 to 80 :	0.	541.
80 to 90 :	0.	723.
90 to 100 :	0.	114.
100 to 110 :	0.	8.
110 to 120 :	0.	2.
120 to 130 :	0.	2.
130 to 140 :	0.	0.
140 to 150 :	2.	0.
150 to 160 :	45.	0.
160 to 170 :	254.	0.
170 to 180 :	551.	0.
180 to 190 :	680.	0.
190 to 200 :	348.	0.
200 to 210 :	209.	0.
210 to 220 :	106.	0.
220 to 230 :	30.	0.
230 to 240 :	0.	0.
240 to 250 :	0.	0.
250 to 260 :	0.	0.
260 to 270 :	0.	0.
270 to 280 :	0.	0.
280 to 290 :	0.	0.
290 to 300 :	0.	0.

Fig. D.20: Bloor Viaduct Eastbound-line 5 cluster analysis report

Bloor Viaduct EASTbound
LINE : 6, CLUSTER ANALYSIS REPORT

*** MEAN values ***

A(135 4.154051) B(145 -1.378803) C(207 .092928) D(241 .167410) THR(179) COR(69)

*** VARiances ***

A(1.6 .029360) B(1.7 .096766) C(23.4 .020557) D(71.1 .005160) THR(186) COR(251)

*** STanDard DEViations ***

A(1.3 .171347) B(1.3 .311072) C(4.8 .143376) D(8.4 .071831) THR(13) COR(15)

*** I of VARIATions ***

A(.94 4.12) B(.91 22.56) C(2.34 154.29) D(3.50 42.91) THR(7.26) COR(21.74)

*** HISTogram (PEAKs) ***

[Point SAMPle]	Numbers of WAVEform at PEAK A	B	C	D
100 to 105 :	0.	0.	0.	0.
105 to 110 :	0.	0.	0.	0.
110 to 115 :	0.	0.	0.	0.
115 to 120 :	0.	0.	0.	0.
120 to 125 :	0.	0.	0.	0.
125 to 130 :	0.	0.	0.	0.
130 to 135 :	285.	0.	0.	0.
135 to 140 :	1909.	0.	0.	0.
140 to 145 :	26.	803.	0.	0.
145 to 150 :	1.	1395.	0.	0.
150 to 155 :	0.	23.	0.	0.
155 to 160 :	0.	0.	0.	0.
160 to 165 :	0.	0.	0.	0.
165 to 170 :	0.	0.	0.	0.
170 to 175 :	0.	0.	0.	0.
175 to 180 :	0.	0.	0.	0.
180 to 185 :	0.	0.	0.	0.
185 to 190 :	0.	0.	0.	0.
190 to 195 :	0.	0.	0.	0.
195 to 200 :	0.	0.	54.	0.
200 to 205 :	0.	0.	355.	0.
205 to 210 :	0.	0.	1158.	0.
210 to 215 :	0.	0.	476.	0.
215 to 220 :	0.	0.	173.	0.
220 to 225 :	0.	0.	3.	28.
225 to 230 :	0.	0.	2.	175.
230 to 235 :	0.	0.	0.	268.
235 to 240 :	0.	0.	0.	538.
240 to 245 :	0.	0.	0.	264.
245 to 250 :	0.	0.	0.	483.

*** HISTogram (THICKness) ***

[THICKness]	Nos. of WAVEform asphalt	C/o RIFsent
0 to 10 :	0.	0.
10 to 20 :	0.	0.
20 to 30 :	0.	0.
30 to 40 :	0.	108.
40 to 50 :	0.	249.
50 to 60 :	0.	199.
60 to 70 :	0.	377.
70 to 80 :	0.	571.
80 to 90 :	0.	607.
90 to 100 :	0.	103.
100 to 110 :	0.	4.
110 to 120 :	0.	3.
120 to 130 :	0.	0.
130 to 140 :	2.	0.
140 to 150 :	6.	0.
150 to 160 :	94.	0.
160 to 170 :	391.	0.
170 to 180 :	695.	0.
180 to 190 :	519.	0.
190 to 200 :	296.	0.
200 to 210 :	167.	0.
210 to 220 :	45.	0.
220 to 230 :	4.	0.
230 to 240 :	2.	0.
240 to 250 :	0.	0.
250 to 260 :	0.	0.
260 to 270 :	0.	0.
270 to 280 :	0.	0.
280 to 290 :	0.	0.
290 to 300 :	0.	0.

Fig. D.21: Bloor Viaduct Eastbound-line 6 cluster analysis report

Bloor Viaduct WESTbound
LINE : 7, CLUSTER ANALYSIS REPORT

*** MEAN values ***

A(133 4.487285) B(143 -1.365497) C(197 .180916) D(232 .107398) THR(142) COR(72)

*** VARiances ***

A(1.4 .077242) B(2.0 .066868) C(15.2 .029374) D(42.6 .002854) THR(174) COR(151)

*** STandard DEViations ***

A(1.2 .277924) B(1.4 .294734) C(3.9 .171390) D(6.5 .053425) THR(13) COR(12)

*** % of VARIATions ***

A(.88 6.19) B(1.00 21.58) C(1.98 94.73) D(2.81 49.74) THR(9.15) COR(16.67)

*** HISTogram (PEAKs) ***

[Point SAMPle]	Numbers of WAVEform at PEAK A	B	C	D
100 to 105 :	0.	0.	0.	0.
105 to 110 :	0.	0.	0.	0.
110 to 115 :	0.	0.	0.	0.
115 to 120 :	0.	0.	0.	0.
120 to 125 :	0.	0.	0.	0.
125 to 130 :	7.	0.	0.	0.
130 to 135 :	1997.	0.	0.	0.
135 to 140 :	219.	0.	0.	0.
140 to 145 :	5.	1852.	0.	0.
145 to 150 :	0.	370.	0.	0.
150 to 155 :	0.	6.	0.	0.
155 to 160 :	0.	0.	0.	0.
160 to 165 :	0.	0.	0.	0.
165 to 170 :	0.	0.	0.	0.
170 to 175 :	0.	0.	0.	0.
175 to 180 :	0.	0.	0.	0.
180 to 185 :	0.	0.	0.	0.
185 to 190 :	0.	0.	0.	0.
190 to 195 :	0.	0.	417.	0.
195 to 200 :	0.	0.	1259.	0.
200 to 205 :	0.	0.	331.	0.
205 to 210 :	0.	0.	203.	0.
210 to 215 :	0.	0.	16.	15.
215 to 220 :	0.	0.	2.	75.
220 to 225 :	0.	0.	0.	65.
225 to 230 :	0.	0.	0.	804.
230 to 235 :	0.	0.	0.	555.
235 to 240 :	0.	0.	0.	497.
240 to 245 :	0.	0.	0.	83.
245 to 250 :	0.	0.	0.	106.

*** HISTogram (THICKness) ***

[THICKness]	Nos. of WAVEform asphalt	C/a RIFwent
0 to 10 :	0.	0.
10 to 20 :	0.	0.
20 to 30 :	0.	0.
30 to 40 :	0.	13.
40 to 50 :	0.	85.
50 to 60 :	0.	216.
60 to 70 :	0.	582.
70 to 80 :	0.	621.
80 to 90 :	0.	627.
90 to 100 :	0.	77.
100 to 110 :	0.	5.
110 to 120 :	28.	2.
120 to 130 :	297.	0.
130 to 140 :	635.	0.
140 to 150 :	655.	0.
150 to 160 :	380.	0.
160 to 170 :	160.	0.
170 to 180 :	49.	0.
180 to 190 :	14.	0.
190 to 200 :	7.	0.
200 to 210 :	2.	0.
210 to 220 :	1.	0.
220 to 230 :	0.	0.
230 to 240 :	0.	0.
240 to 250 :	0.	0.
250 to 260 :	0.	0.
260 to 270 :	0.	0.
270 to 280 :	0.	0.
280 to 290 :	0.	0.
290 to 300 :	0.	0.

Fig. D.22: Bloor Viaduct Westbound-line 7 cluster analysis report

Bloor Viaduct WESTbound
LINE : 8, CLUSTER ANALYSIS REPORT

*** MEAN values ***

A(131 4.127527) B(141 -1.055340) C(194 .249388) D(229 .162708) THR(154) COR(73)

*** VARiances ***

A(2.7 .040001) B(3.6 .087723) C(9.7 .048286) D(49.8 .007826) THR(107) COR(179)

*** STanDard DEViations ***

A(1.6 .200002) B(1.9 .292705) C(3.1 .219740) D(7.1 .088467) THR(10) COR(13)

*** I of VARIATions ***

A(1.25 4.85) B(1.34 27.74) C(1.61 88.11) D(3.08 54.37) THR(6.49) COR(17.81)

*** HISTogram (PEAKs) ***

[PoinT SAMPle]	Numbers of WAVEform at PEAK A	B	C	D
100 to 105 :	0.	0.	0.	0.
105 to 110 :	0.	0.	0.	0.
110 to 115 :	0.	0.	0.	0.
115 to 120 :	0.	0.	0.	0.
120 to 125 :	0.	0.	0.	0.
125 to 130 :	14.	0.	0.	0.
130 to 135 :	2176.	0.	0.	0.
135 to 140 :	30.	25.	0.	0.
140 to 145 :	0.	2114.	0.	0.
145 to 150 :	0.	77.	0.	0.
150 to 155 :	0.	4.	0.	0.
155 to 160 :	0.	0.	0.	0.
160 to 165 :	0.	0.	0.	0.
165 to 170 :	0.	0.	0.	0.
170 to 175 :	0.	0.	0.	0.
175 to 180 :	0.	0.	0.	0.
180 to 185 :	0.	0.	0.	0.
185 to 190 :	1.	0.	124.	0.
190 to 195 :	0.	0.	837.	0.
195 to 200 :	0.	1.	1132.	0.
200 to 205 :	0.	0.	97.	0.
205 to 210 :	0.	0.	24.	1.
210 to 215 :	0.	0.	7.	27.
215 to 220 :	0.	0.	0.	268.
220 to 225 :	0.	0.	0.	219.
225 to 230 :	0.	0.	0.	598.
230 to 235 :	0.	0.	0.	474.
235 to 240 :	0.	0.	0.	541.
240 to 245 :	0.	0.	0.	73.
245 to 250 :	0.	0.	0.	18.

*** HISTogram (THICKness) ***

[THICKness]	Nos. of WAVEform asphalt	C/o RIFsent
0 to 10 :	0.	0.
10 to 20 :	0.	0.
20 to 30 :	0.	0.
30 to 40 :	0.	6.
40 to 50 :	0.	71.
50 to 60 :	0.	343.
60 to 70 :	0.	418.
70 to 80 :	0.	457.
80 to 90 :	0.	813.
90 to 100 :	0.	101.
100 to 110 :	0.	9.
110 to 120 :	5.	3.
120 to 130 :	16.	0.
130 to 140 :	91.	0.
140 to 150 :	514.	0.
150 to 160 :	1045.	0.
160 to 170 :	444.	0.
170 to 180 :	75.	0.
180 to 190 :	17.	0.
190 to 200 :	1.	0.
200 to 210 :	0.	0.
210 to 220 :	2.	0.
220 to 230 :	3.	0.
230 to 240 :	0.	0.
240 to 250 :	0.	0.
250 to 260 :	0.	0.
260 to 270 :	0.	0.
270 to 280 :	0.	0.
280 to 290 :	0.	0.
290 to 300 :	0.	0.

Fig. D.23: Bloor Viaduct Westbound-line 8 cluster analysis report

Bloor Viaduct WESTbound
LINE : 9, CLUSTER ANALYSIS REPORT

*** MEAN values ***

A(132	4.220066)	B(141	-1.263356)	C(195	.259869)	D(232	.247336)	THR(145)	COR(77)

*** VARIances ***

A(1.3	.053327)	B(2.2	.123852)	C(9.7	.036060)	D(25.8	.009219)	THR(85)	COR(75)

*** STandard DEViations ***

A(1.2	.230926)	B(1.5	.351926)	C(3.1	.189967)	D(5.1	.096015)	THR(9)	COR(8)

*** % of VARIAtions ***

A(.38	5.47)	B(1.05	27.86)	C(1.60	73.09)	D(2.19	38.82)	THR(6.21)	COR(10.39)

*** HISTogram (PEAKs) ***

[Point SAMPle]	Numbers of WAVEform at PEAK A	B	C	D
100 to 105 :	0.	0.	0.	0.
105 to 110 :	0.	0.	0.	0.
110 to 115 :	0.	0.	0.	0.
115 to 120 :	0.	0.	0.	0.
120 to 125 :	0.	0.	0.	0.
125 to 130 :	7.	0.	0.	0.
130 to 135 :	2154.	0.	0.	0.
135 to 140 :	64.	13.	0.	0.
140 to 145 :	0.	2134.	0.	0.
145 to 150 :	0.	76.	0.	0.
150 to 155 :	0.	2.	0.	0.
155 to 160 :	0.	0.	0.	0.
160 to 165 :	0.	0.	0.	0.
165 to 170 :	0.	0.	0.	0.
170 to 175 :	0.	0.	0.	0.
175 to 180 :	0.	0.	0.	0.
180 to 185 :	0.	0.	0.	0.
185 to 190 :	0.	0.	72.	0.
190 to 195 :	0.	0.	864.	0.
195 to 200 :	0.	0.	992.	0.
200 to 205 :	0.	0.	277.	0.
205 to 210 :	0.	0.	17.	0.
210 to 215 :	0.	0.	3.	3.
215 to 220 :	0.	0.	0.	19.
220 to 225 :	0.	0.	0.	44.
225 to 230 :	0.	0.	0.	780.
230 to 235 :	0.	0.	0.	686.
235 to 240 :	0.	0.	0.	495.
240 to 245 :	0.	0.	0.	173.
245 to 250 :	0.	0.	0.	25.

*** HISTogram (THICKness) ***

[THICKness]	Nos. of WAVEform asphalt	C/o RIFsent
0 to 10 :	0.	0.
10 to 20 :	0.	0.
20 to 30 :	0.	0.
30 to 40 :	0.	1.
40 to 50 :	0.	7.
50 to 60 :	0.	36.
60 to 70 :	0.	410.
70 to 80 :	0.	817.
80 to 90 :	0.	835.
90 to 100 :	0.	115.
100 to 110 :	2.	3.
110 to 120 :	32.	1.
120 to 130 :	65.	0.
130 to 140 :	357.	0.
140 to 150 :	1063.	0.
150 to 160 :	591.	0.
160 to 170 :	93.	0.
170 to 180 :	18.	0.
180 to 190 :	4.	0.
190 to 200 :	0.	0.
200 to 210 :	0.	0.
210 to 220 :	0.	0.
220 to 230 :	0.	0.
230 to 240 :	0.	0.
240 to 250 :	0.	0.
250 to 260 :	0.	0.
260 to 270 :	0.	0.
270 to 280 :	0.	0.
280 to 290 :	0.	0.
290 to 300 :	0.	0.

Fig. D.24: Bloor Viaduct Westbound-line 9 cluster analysis report

Bloor Viaduct WESTbound
LINE : 10, CLUSTER ANALYSIS REPORT

*** MEAN values ***

A(133 4.340237) B(142 -1.632823) C(199 .201818) D(237 .249638) THK(155) COR(79)

*** VARiances ***

A(1.0 .041714) B(1.5 .078546) C(17.8 .035757) D(56.4 .011495) THK(125) COR(160)

*** STanDard DEViations ***

A(1.0 .204241) B(1.2 .280260) C(4.2 .189095) D(7.5 .107215) THK(11) COR(12)

*** % of VARIATions ***

A(.77 4.71) B(.88 17.16) C(2.12 93.70) D(3.17 42.95) THK(7.10) COR(15.19)

*** HISTogram (PEAKs) ***

[Point SAMPle]	Numbers of WAVEforms at PEAK A	B	C	D
100 to 105 :	0.	0.	0.	0.
105 to 110 :	0.	0.	0.	0.
110 to 115 :	0.	0.	0.	0.
115 to 120 :	0.	0.	0.	0.
120 to 125 :	0.	0.	0.	0.
125 to 130 :	2.	0.	0.	0.
130 to 135 :	2047.	0.	0.	0.
135 to 140 :	99.	5.	0.	0.
140 to 145 :	2.	2080.	0.	0.
145 to 150 :	0.	64.	0.	0.
150 to 155 :	0.	1.	0.	0.
155 to 160 :	0.	0.	0.	0.
160 to 165 :	0.	0.	0.	0.
165 to 170 :	0.	0.	0.	0.
170 to 175 :	0.	0.	0.	0.
175 to 180 :	0.	0.	0.	0.
180 to 185 :	0.	0.	0.	0.
185 to 190 :	0.	0.	62.	0.
190 to 195 :	0.	0.	206.	0.
195 to 200 :	0.	0.	638.	0.
200 to 205 :	0.	0.	936.	0.
205 to 210 :	0.	0.	307.	1.
210 to 215 :	0.	0.	1.	58.
215 to 220 :	0.	0.	0.	61.
220 to 225 :	0.	0.	0.	8.
225 to 230 :	0.	0.	0.	165.
230 to 235 :	0.	0.	0.	240.
235 to 240 :	0.	0.	0.	599.
240 to 245 :	0.	0.	0.	712.
245 to 250 :	0.	0.	0.	301.

*** HISTogram (THICKness) ***

[THICKness]	Nos. of WAVEforms asphalt	C/e RIFvent
0 to 10 :	0.	0.
10 to 20 :	0.	0.
20 to 30 :	0.	0.
30 to 40 :	0.	6.
40 to 50 :	0.	47.
50 to 60 :	0.	79.
60 to 70 :	0.	276.
70 to 80 :	0.	591.
80 to 90 :	0.	780.
90 to 100 :	0.	292.
100 to 110 :	0.	50.
110 to 120 :	2.	29.
120 to 130 :	39.	0.
130 to 140 :	124.	0.
140 to 150 :	439.	0.
150 to 160 :	835.	0.
160 to 170 :	516.	0.
170 to 180 :	165.	0.
180 to 190 :	25.	0.
190 to 200 :	5.	0.
200 to 210 :	0.	0.
210 to 220 :	0.	0.
220 to 230 :	0.	0.
230 to 240 :	0.	0.
240 to 250 :	0.	0.
250 to 260 :	0.	0.
260 to 270 :	0.	0.
270 to 280 :	0.	0.
280 to 290 :	0.	0.
290 to 300 :	0.	0.

Fig. D.25: Bloor Viaduct Westbound-line 10 cluster analysis report

Bloor Viaduct WESTbound
LINE : 11, CLUSTER ANALYSIS REPORT

*** MEAN values ***

A(133 4.170780) B(142 -1.417585) C(198 .155794) D(233 .136467) THK(152) COR(73)

*** VARiances ***

A(1.2 .026869) B(1.6 .067725) C(32.1 .046546) D(110.5 .000202) THK(234) COR(194)

*** STandard DEViations ***

A(1.1 .161458) B(1.2 .260240) C(5.7 .215746) D(10.5 .090564) THK(15) COR(13)

*** % of VARIATions ***

A(.61 3.87) B(.88 15.16) C(2.96 138.48) D(4.51 66.16) THK(9.87) COR(17.81)

*** HISTogram (PEAKs) ***

[Point SAMPle]	Numbers of OCCUrs at PEAK A	B	C	D
100 to 105 :	0.	0.	0.	0.
105 to 110 :	0.	0.	0.	0.
110 to 115 :	0.	0.	0.	0.
115 to 120 :	0.	0.	0.	0.
120 to 125 :	0.	0.	0.	0.
125 to 130 :	2.	0.	0.	0.
130 to 135 :	2095.	0.	0.	0.
135 to 140 :	118.	1.	0.	0.
140 to 145 :	6.	2146.	0.	0.
145 to 150 :	0.	70.	0.	0.
150 to 155 :	0.	2.	0.	0.
155 to 160 :	0.	0.	0.	0.
160 to 165 :	0.	0.	0.	0.
165 to 170 :	0.	0.	0.	0.
170 to 175 :	0.	0.	0.	0.
175 to 180 :	0.	0.	0.	0.
180 to 185 :	0.	0.	0.	0.
185 to 190 :	0.	0.	216.	0.
190 to 195 :	0.	0.	525.	0.
195 to 200 :	0.	0.	159.	0.
200 to 205 :	0.	0.	649.	0.
205 to 210 :	0.	0.	445.	7.
210 to 215 :	0.	0.	7.	127.
215 to 220 :	0.	0.	0.	148.
220 to 225 :	0.	0.	0.	65.
225 to 230 :	0.	0.	0.	631.
230 to 235 :	0.	0.	0.	142.
235 to 240 :	0.	0.	0.	244.
240 to 245 :	0.	0.	0.	360.
245 to 250 :	0.	0.	0.	440.

*** HISTogram (THICKness) ***

[THICKness]	Nos. of OCCUrs asphalt	C/o RIFpave
0 to 10 :	0.	0.
10 to 20 :	0.	0.
20 to 30 :	0.	0.
30 to 40 :	0.	26.
40 to 50 :	0.	103.
50 to 60 :	0.	239.
60 to 70 :	0.	390.
70 to 80 :	0.	552.
80 to 90 :	0.	740.
90 to 100 :	0.	161.
100 to 110 :	0.	13.
110 to 120 :	1.	7.
120 to 130 :	124.	0.
130 to 140 :	496.	0.
140 to 150 :	371.	0.
150 to 160 :	316.	0.
160 to 170 :	584.	0.
170 to 180 :	296.	0.
180 to 190 :	31.	0.
190 to 200 :	2.	0.
200 to 210 :	0.	0.
210 to 220 :	0.	0.
220 to 230 :	0.	0.
230 to 240 :	0.	0.
240 to 250 :	0.	0.
250 to 260 :	0.	0.
260 to 270 :	0.	0.
270 to 280 :	0.	0.
280 to 290 :	0.	0.
290 to 300 :	0.	0.

Fig. D.26: Bloor Viaduct Westbound-line 11 cluster analysis report

Bloor Viaduct WESTbound
LINE : 12, CLUSTER ANALYSIS REPORT

*** MEAN values ***

A(132 4.586448) B(141 -1.490091) C(196 .149114) D(231 .143370) THR(137) COR(73)

*** VARiances ***

A(1.3 .058188) B(2.1 .057752) C(26.4 .033344) D(112.6 .012213) THR(227) COR(270)

*** STandard DEViations ***

A(1.1 .241296) B(1.5 .240316) C(5.1 .182603) D(10.6 .110512) THR(15) COR(16)

*** % of VARIATions ***

A(.85 5.35) B(1.03 16.04) C(2.62 122.46) D(4.59 77.08) THR(10.95) COR(21.92)

*** HISTogram (PEAKs) ***

[Point SAMPle]	Numbers of WAVEform at PEAK A	B	C	D
100 to 105 :	0.	0.	0.	0.
105 to 110 :	0.	0.	0.	0.
110 to 115 :	0.	0.	0.	0.
115 to 120 :	0.	0.	0.	0.
120 to 125 :	0.	0.	0.	0.
125 to 130 :	11.	0.	0.	0.
130 to 135 :	2162.	0.	0.	0.
135 to 140 :	51.	19.	0.	0.
140 to 145 :	0.	2158.	0.	0.
145 to 150 :	0.	47.	0.	0.
150 to 155 :	0.	0.	0.	0.
155 to 160 :	0.	0.	0.	0.
160 to 165 :	0.	0.	0.	0.
165 to 170 :	0.	0.	0.	0.
170 to 175 :	0.	0.	0.	0.
175 to 180 :	0.	0.	0.	0.
180 to 185 :	0.	0.	0.	0.
185 to 190 :	0.	0.	306.	0.
190 to 195 :	0.	0.	634.	0.
195 to 200 :	0.	0.	492.	0.
200 to 205 :	0.	0.	581.	0.
205 to 210 :	0.	0.	209.	18.
210 to 215 :	0.	0.	2.	176.
215 to 220 :	0.	0.	0.	250.
220 to 225 :	0.	0.	0.	44.
225 to 230 :	0.	0.	0.	524.
230 to 235 :	0.	0.	0.	191.
235 to 240 :	0.	0.	0.	348.
240 to 245 :	0.	0.	0.	358.
245 to 250 :	0.	0.	0.	299.

*** HISTogram (THICKness) ***

[THICKness]	Nos. of WAVEform asphalt	C/o RIFsent
0 to 10 :	0.	0.
10 to 20 :	0.	0.
20 to 30 :	0.	0.
30 to 40 :	0.	31.
40 to 50 :	0.	110.
50 to 60 :	0.	347.
60 to 70 :	0.	343.
70 to 80 :	0.	502.
80 to 90 :	0.	608.
90 to 100 :	0.	182.
100 to 110 :	17.	55.
110 to 120 :	280.	43.
120 to 130 :	461.	3.
130 to 140 :	453.	0.
140 to 150 :	441.	0.
150 to 160 :	403.	0.
160 to 170 :	153.	0.
170 to 180 :	15.	0.
180 to 190 :	0.	0.
190 to 200 :	1.	0.
200 to 210 :	0.	0.
210 to 220 :	0.	0.
220 to 230 :	0.	0.
230 to 240 :	0.	0.
240 to 250 :	0.	0.
250 to 260 :	0.	0.
260 to 270 :	0.	0.
270 to 280 :	0.	0.
280 to 290 :	0.	0.
290 to 300 :	0.	0.

Fig. D.27: Bloor Viaduct Westbound-line 12 cluster analysis report